
VNIVERSITAT DE VALÈNCIA

# Precision Physics in Hadronic Tau Decays

Tesis Doctoral

Programa de Doctorado en Física de la Universitat de València

**Antonio Rodríguez Sánchez**

IFIC - Universitat de València - CSIC
Departament de Física Teòrica

Director: Antonio Pich Zardoya

Co-director: Martín González Alonso

Valencia, 07/2018

*A mis padres*

Antonio Pich Zardoya,
Catedrático de la Universitat de València, y
Martín González Alonso,
Investigador posdoctoral en el CERN,

CERTIFICAN:

Que la presente memoria "Precision Physics in Hadronic Tau Decays" ha sido realizada bajo su dirección en el Instituto de Física Corpuscular, centro mixto de la Universidad de Valencia y del CSIC, por Antonio Rodríguez Sánchez y constituye su Tesis para optar al grado de Doctor en Física.

Y para que así conste, en cumplimiento de la legislación vigente, presentan en el Departament de Física Teòrica de la Universitat de València la referida Tesis Doctoral, y firman el presente certificado.

Valencia, a 12 de julio de 2018.

Antonio Pich Zardoya  Martín González Alonso

# Contents

# Preface

The Standard Model of Particle Physics gives a very precise description of nature for an overwhelming amount of observables non-trivially related. In the last years, the LHC has carried out a huge number of measurements looking for new physics hints with negative results, which indicates that the Standard Model, proven before to precisely describe all interactions at $\sim 1-100\,\text{GeV}$, remains valid at least up to the $\sim$ TeV.

The Standard Model (SM) was built by looking for a self-consistent Quantum Field Theory framework that could accommodate all the experimental information at the energies explored at that time. Imposing the local symmetry $SU(3)_C \times SU(2)_L \times U(1)_Y$ and some building blocks plus the Spontaneous Symmetry Breaking (SSB) generated by the vacuum expectation value of a scalar boson, was the simplest way to unify weak, electromagnetic and strong interactions in a self-consistent way explaining all the available experimental data with a relatively small number of free parameters.

In principle, the SM might explain all interactions, except maybe dark matter, up to the Planck Scale ($\sim 10^{18}\,\text{GeV}$), where gravity enters into the game. However, every time new physics scales had been explored, new patterns, slightly different than predicted by the simplest possible models, had arisen, which indeed had helped to understand new aspects about physics at the previously studied scales. There were no strong reasons to think anything different was going to happen, since the SM does not give any answer about why in particular those symmetry realizations and building blocks should be everything we have. Nevertheless, probably for the first time in the history of physics, all the higher energy predictions have been confirmed and no Beyond the Standard Model (BSM) physics has been observed apart from the very tiny neutrino masses, which in principle could be accommodated by extending it without any significant additional changes.

Although this fact is certainly discouraging for new physics searches, as far as we lack satisfactory explanations of different aspects of the SM, such as why there should not be more building blocks or the nondemocratic hierarchy of the

free parameters, one would expect that new physics hints arise at higher energies, which may help us to improve our understanding of nature.

In order to try to discover new physics very different paths can be taken. One possibility consists in improving the experimental precision and the theoretical prediction of the SM for a set of observables larger than the number of free parameters of the theory. If they are incompatible, the SM does not hold up and new physics should be incorporated to explain that incompatibility. Sometimes, one focuses on observables whose theoretical dependence is dominated by one single parameter, either because the dependence on other parameters is very small or because they have been very precisely determined with other observables. Then the comparison becomes a determination of that parameter, which can be used to test other observables. This is the approach followed in the Chapters 2, 3 and 4.

Another possibility is looking for new physics in specific directions. There are many BSM models that incorporate more complex new physics scenarios, in principle more (or are least not less) theoretically justified than the SM, and which give different prediction for physics in different observables. One can compare the SM and BSM predictions and test if they are compatible with experimental data. Instead, one can also group many different possible directions, with some assumptions but without choosing a specific model, in order to see which directions can be ruled out or, at least, constrained with data. This path is taken for example by the Standard Model Effective Field Theory (SM-EFT) and is useful to see where new physics is more likely to arise, as well as to test models and build new ones without violating those constraints. The work in Chapter 5 is precisely in that direction.

Independently on the new physics at higher energies, the SM is far away from a simple mathematical algorithm in which one inserts the fundamental inputs and the desired observable to get an exact theoretical prediction. In fact, depending on the sector one is studying and on the energies that are involved, many different tools have been developed to obtain those predictions with different level of success. For example, perturbative QCD, extremely successful in making predictions at LHC scales, can not be used at scales of hundreds of MeV. If the SM is able to give a prediction for it, then it will be with different tools. The highly nontrivial and very exciting task of looking for those tools and applying them to understand the complex structure of nature that emerges at different high energy scales is known as Phenomenology of Particle Physics.

In this work we focus on the phenomenology of hadronic $\tau$ decays. Because of its mass, the $\tau$ is the only lepton that can decay into hadrons. On the one hand,

the decay occurs through the interaction of two weak charged currents mediated by the $W^-$ boson, so it becomes a very nice test of electroweak interactions.

On the other hand, because it emits a neutrino in the decay, a very rich hadronic continuum energy spectrum, generated unambiguously by the weak quark current, is observed, which allows to study strong interactions at different energy regimes. Then, the set of tools one applies depends on the regime one wants to study. Unfortunately, the best known description of strong interactions at some energy regimes is far from been derived from first principles and one needs extra assumptions more or less justified.

Within the very rich phenomenology of hadronic $\tau$ decays, we put our attention in some of those observables whose theoretical prediction becomes more precise. Although one can also get some precise predictions for some channel decays at very low energies by using Chiral Perturbation Theory (ChPT), and extend it with some extra assumptions through Resonance Chiral Theory (RChT), today the most precise predictions are reached, apart from the very clean single-hadron decays, for inclusive tau decays, where one can make use of analytical methods to relate low-energy experimental data with nearly perturbative QCD through dispersion relations. Most of this thesis is about the study of those inclusive observables.

In Chapter 1 we give an introduction to different theoretical common tools we use along the thesis. The first application is the study of the determination of physical observables associated to the different moments of the inclusive $V - A$ non-strange spectral function, which cancels in perturbative QCD and becomes specially interesting to test non-perturbative methods. Some of them can be related to Low-Energy Constants (LECs) of ChPT and others to vacuum condensates of dimensional operators. This study can be found in Chapter 2, while we study the determination of the strong coupling using inclusive non-strange tau decays in Chapter 3. Special attention is given to the different sources of non-perturbative uncertainties, trying to select the most efficient set of observables to reduce them. In Chapter 4, we revisit the determination of one of the dominant matrix elements responsible for direct CP violation ($\frac{\epsilon'}{\epsilon}$) in kaons, which through soft-meson methods can be related to the non-strange $V - A$ spectral function. Finally in Chapter 5 we make an extensive study about the potential of hadronic tau decays to obtain new physics constraints in a model independent way.

# Chapter 1

# Theoretical aspects in hadronic tau decays

## 1.1 The Standard Model Lagrangian

In this section we present a brief overview of the basics of the SM [1–4]. For a more detailed discussion we refer to the many reviews on the SM that can be found in the literature, for example [5, 6].

The Standard Model Lagrangian is the most general one that is renormalizable and invariant under local gauge transformations of the symmetry group $SU(3)_C \times SU(2)_L \times U(1)_Y$ (which requires $8+3+1$ gauge fields $G^a_\mu$, $W^b_\mu$ and $B_\mu$), given its building matter blocks that transform as the fundamental or trivial (singlet) representation of those symmetries. Taking Greek symbols for the color $SU(3)_C$ indices, capitalized letters for the family ones and writing the n-plets in the $SU(2)_L$ in explicit column form, the building matter blocks of the Standard Model are:

$$
\begin{aligned}
l_N = \begin{pmatrix} \nu_L \\ l_L \end{pmatrix}_N , \quad e_N = l_{R,\,N} , \quad \varphi = \begin{pmatrix} \phi^{(+)} \\ \phi^{(0)} \end{pmatrix} , \\
q_{\alpha N} = \begin{pmatrix} u_L \\ d_L \end{pmatrix}_{\alpha N} , d_{\alpha N} = d_{R,\,\alpha N} , \quad u_{\alpha N} = u_{R,\,\alpha N} ,
\end{aligned}
\tag{1.1}
$$

where $\alpha = 1,2,3$, $N = 1,2,3$, $\varphi$ is a scalar boson doublet and the rest are fermions. Their hypercharges are:

$$\begin{aligned} Y(l_N) = -\frac{1}{2}, \quad Y(e_n) = -1, \quad Y(\varphi) = -\frac{1}{2}\,, \\ Y(q_{\alpha N}) = -\frac{1}{6}, \quad Y(d_{\alpha N}) = -\frac{1}{3}, \quad Y(u_{\alpha N}) = \frac{2}{3}\,. \end{aligned} \tag{1.2}$$

The Lagrangian reads as

$$\mathcal{L} = \mathcal{L}_F + \mathcal{L}_B + \mathcal{L}_S + \mathcal{L}_Y\,, \tag{1.3}$$

where:

$$\mathcal{L}_F = \sum_N i(\bar{l}_N \not{D}\, l_N + \bar{q}_N \not{D}\, q_N + \bar{e}_N \not{D}\, e_N + \bar{d}_N \not{D}\, d_N + \bar{u}_N \not{D}\, u_N)\,, \tag{1.4}$$

with $q_N$, $d_N$ and $u_N$ color vectors and $D$ the covariant derivative:

$$D_\mu = I\partial_\mu + ig_s\frac{\lambda_a}{2}G^a_\mu + ig\frac{\sigma_b}{2}W^b_\mu + ig'B_\mu\,, \tag{1.5}$$

so that every term couples to a matter building block only if it is in the fundamental representation of the associated symmetry and

$$\mathcal{L}_B = -\frac{1}{4}G^a_{\mu\nu}G^{\mu\nu}_a - \frac{1}{4}W^b_{\mu\nu}W^{\mu\nu}_b - \frac{1}{4}B_{\mu\nu}B^{\mu\nu}\,, \tag{1.6}$$

where:

$$G^a_{\mu\nu} = \partial_\mu G^a_\nu - \partial_\nu G^a_\mu - g_s f^{abc}G^\mu_b G^\nu_c\,, \tag{1.7}$$

$$W^b_{\mu\nu} = \partial_\mu W^b_\nu - \partial_\nu W^b_\mu - g\epsilon^{abc}W^\mu_b W^\nu_c\,, \tag{1.8}$$

$$B_{\mu\nu} = \partial_\mu B_\nu - \partial_\nu B_\mu\,. \tag{1.9}$$

The scalar Lagrangian $\mathcal{L}_S$ reads as:

$$\mathcal{L}_S = (D_\mu\varphi)^\dagger(D^\mu\varphi) - \mu^2\varphi\varphi - \frac{1}{2}\lambda(\varphi^\dagger\varphi)^2\,, \tag{1.10}$$

and finally the Yukawa Lagrangian $\mathcal{L}_Y$ reads as

$$\mathcal{L}_Y = Y^1_N\; e_N\bar{l}_N\varphi + Y^2_N\; d_N\bar{q}_N\varphi + Y^3_{NM}\; u_M\bar{q}_N\hat{\varphi} + h.c.\,, \tag{1.11}$$

with $\hat{\varphi} = i\sigma_2\varphi$ and where we have diagonalized as many Yukawa matrices $Y^i$ as possible by making rotations in the family space, which leaves the rest of the Lagrangian invariant. Indeed, an extra rotation of $u$ allows to set $Y^3_{NM}$ as a unitary times a diagonal matrix without loss of generality, $Y^3_{NM} \equiv Y^3_M V^\dagger_{NM}$.

One last ingredient is needed to build the SM. If in $\mathcal{L}_S$ $\mu^2 < 0$ and $\lambda > 0$, the potential has a degenerate minimum in $|\langle\varphi\rangle| = \frac{v}{\sqrt{2}} \equiv \sqrt{\frac{-2\mu^2}{\lambda}}$. In the SM, the symmetry $SU(2)_L \times U(1)_Y$ is spontaneously broken to $U(1)_{em}$ by choosing

$$\langle\varphi\rangle = \frac{1}{\sqrt{2}} \begin{pmatrix} 0 \\ v \end{pmatrix}, \tag{1.12}$$

among them. Parameterizing perturbations from that minimum as

$$\varphi(x) = \frac{1}{\sqrt{2}} e^{\frac{i\sigma_i\theta_i(x)}{2}} \begin{pmatrix} 0 \\ v + H(x) \end{pmatrix}, \tag{1.13}$$

one can choose a local $SU(2)_L$ gauge transformation for $\varphi(x)$ such that $\theta(x)$ completely disappears from the Lagrangian, so we end up with only a new scalar boson $H(x)$.

The $SU(2)_L$ gauge bosons, necessarily massless before the symmetry breaking, acquire mass through the covariant derivative of the scalar boson $\varphi$. The charged gauge bosons $W^{\mp}_\mu \equiv \frac{W^\mu_1 \pm i W^\mu_2}{\sqrt{2}}$ are directly in diagonal form while the massless photon $A_\mu$ and the $Z_\mu$ boson are obtained by diagonalizing the $W^\mu_3 - B_\mu$ mass matrix.

The same happens with the fermions, which acquire their masses through the Yukawa Lagrangian. If we expand the mass part of Eq. (1.11) we have:

$$\mathcal{L}_Y = \frac{1}{\sqrt{2}} v \left( Y^2_N \, \bar{e}_{LN} e_{RN} + Y^1_N \, \bar{d}_{LN} d_{RN} + Y^3_M \, V^\dagger_{NM} \, \bar{u}_{LN} u_{RM} \right) + h.c. \tag{1.14}$$

If we want to write the Lagrangian in term of physical fields, we need an extra transformation to diagonalize the last mass matrix, $u_{LN} \to V^\dagger_{NM} u_{LM}$. The only contribution which changes under that transformation is the non-diagonal part of the covariant derivative in $iq^{(1)} \not{D} q^{(1)}$ (Eq. 1.4).[1] This term, together with the analogous leptonic one, corresponds to the charged current Lagrangian $\mathcal{L}_{CC}$,

[1] The fact that the diagonal one is invariant leads directly to the GIM mechanism.

which becomes central in this thesis, since it is responsible for the $\tau$ decay:

$$\mathcal{L}_{CC} = -\frac{g}{\sqrt{2}} W_\mu^\dagger \left( V_{NM}\, \bar{u}_{LN} \gamma^\mu d_{LM} + \bar{\nu}_{LN} \gamma^\mu e_{LN} \right) + h.c. \tag{1.15}$$

## 1.2 The hadronic decay of the tau

The decay of the tau into hadrons involves both terms of Eq. (1.15). The matrix element is trivial to compute using the Dyson series for the S-matrix with $\mathcal{L}_{CC}$ as the relevant part of the interaction Lagrangian, except for the fact that the final hadronic states, $\langle n|$, generated by the quark currents, are not fundamental particles of the high-energy theory. We end up with a total matrix element dependent on that nontrivial hadronic part:

$$\mathcal{M}_{\tau \to n\nu_\tau} = -\frac{g^2 V_{uD}^\dagger}{2} \frac{1}{q^2 - M_W^2} \bar{\nu}_L \gamma_\mu \tau_L \, \langle n(p_n) | L_\mu^{Du}(0) | 0 \rangle \,, \tag{1.16}$$

with $q = p_\tau - p_\nu$, $L_\mu^{Du} = \bar{D}_L \gamma_\mu u_L$ and $D = d$ or $D = s$. Since $s \equiv q^2 = m_\tau^2 - 2m_\tau |p_\nu^{cm}| < m_\tau^2 \ll M_w^2$, we can neglect $q^2$ in the propagator to obtain:

$$\mathcal{M}_{\tau \to n\nu_\tau} = \frac{g^2 V_{uD}^\dagger}{2} \frac{1}{M_W^2} \bar{\nu}_L \gamma_\mu \tau_L \, \langle n | L_\mu^{Du}(0) | 0 \rangle \,. \tag{1.17}$$

The same result would have been obtained with the Lagragian of the Fermi-Theory:

$$\mathcal{L}_{CC} = -2\sqrt{2} G_F (\bar{d}_{LN} V_{NM}^\dagger \gamma_\mu u_{LM} \quad \bar{\nu}_{LN} \gamma^\mu e_{LN}) + h.c. \,, \tag{1.18}$$

with $G_F = \frac{g^2}{4\sqrt{2} M_W^2}$, which can be obtained by integrating out the $W$ boson.

The hadronic invariant mass distribution $d\Gamma(s)$ for a final state $\langle n\nu_\tau|$ is then [7]:

$$d\Gamma(s) = \frac{G_F^2 |V_{uD}|^2 S_{ew}^h m_\tau^5}{4\pi} \frac{ds}{m_\tau^2} \left(1 - \frac{s}{m_\tau^2}\right)^2 \left\{ \left(1 + 2\frac{s}{m_\tau^2}\right) H^{(1)}(q^2) + H^{(0)}(q^2) \right\} , \tag{1.19}$$

where $S_{ew}^h$ represents radiative corrections and $H^{(i)}$ are defined as:

$$H^{\mu\nu}(q^2) = (-g^{\mu\nu} q^2 + q^\mu q^\nu) H^{(1)}(q^2) + q^\mu q^\nu H^{(0)}(q^2) \,, \tag{1.20}$$

with

$$H_{\mu\nu} \equiv (2\pi)^3 \int d\phi_n \, \delta^4(p_n - q) \, \langle n|L_\mu^{Du}(0)|0\rangle \, \langle 0|L_\nu^{Du\,\dagger}(0)|n\rangle \,, \tag{1.21}$$

where $\phi_n$ is the phase space of the $n$ final hadrons and $p_n$ its total momentum.

### 1.2.1 Decay into a single hadron

For one single hadron $H^-$ as final state, $\pi^-$ or $K^-$, there is only one possible Lorentz structure allowed:

$$\langle H^-|L_\mu^{Du}|0\rangle = \frac{i}{\sqrt{2}} \, p_\mu^H \, f_H \,. \tag{1.22}$$

Then:

$$H^{\mu\nu} = q^\mu q^\nu \, \frac{1}{2} \delta(s - m_H^2) \, f_H^2 \,. \tag{1.23}$$

So that we finally get:

$$\Gamma_{\tau\to H^-\nu_\tau} = \frac{G_F^2 |V_{uD}|^2 f_H^2 S_{ew}^h m_\tau^3}{8\pi} \left(1 - \frac{m_H^2}{m_\tau^2}\right)^2 \,. \tag{1.24}$$

### 1.2.2 Decay into two hadrons

Since there are two final particles in the final hadronic state, $H^-$ and $H'^0$, one has two possible invariant Lorentz structures for the hadronic matrix element:

$$\begin{aligned} \langle H^-(p)H'^0(p')|L_\mu^{Du}|0\rangle = \frac{C_{HH'}}{2} \Bigg\{ & \left(P^- - \frac{\Delta_{HH'}}{p^{+\,2}} P^+\right)^\mu F_V^{HH'}(P^{+\,2}) \\ & + \frac{\Delta_{HH'}}{P^{+\,2}} P^{-\,\mu} F_S^{HH'}(P^{+\,2}) \Bigg\} \,, \end{aligned} \tag{1.25}$$

where $\Delta_{HH'} = m_H^2 - m_{H'}^2$, $P^+ \equiv p + p'$ and $P^- \equiv p - p'$. The normalization coefficients $C_{HH'}$ are given by [7]:

$$\begin{aligned} & C_{\pi\pi} = \sqrt{2}, \quad C_{K\bar{K}} = -1, \quad C_{K\pi} = \frac{1}{\sqrt{2}}, \\ & C_{\pi\bar{K}} = -1, \quad C_{K\eta_8} = \sqrt{\frac{3}{2}}, \quad C_{\pi\eta'} = -\sqrt{2} \,. \end{aligned} \tag{1.26}$$

The Lorentz structure corresponds, respectively, to $J = 1$ and $J = 0$, so that inserting it into Eq. (1.21), one finds:

$$H^{(1)}(s) = \frac{(2\pi)^3\, C_{HH'}^2}{12 s^2} \lambda(s, m^2, m'^2) |F_V(s)|^2 \int d\phi_2\, \delta^4(s - P^{+\,2}) \,, \tag{1.27}$$

and

$$H^{(0)}(s) = \frac{(2\pi)^3 C_{HH'}^2}{4 s^2} |F_S(s)|^2 \int d\phi_2\, \delta^4(s - P^{+\,2}) \,. \tag{1.28}$$

Using now that:

$$\int d\phi_2\, \delta^4(s - P^{+\,2}) = \frac{\pi}{2} \frac{\lambda^{1/2}(s, m^2, m'^2)}{(2\pi)^6 s} \,, \tag{1.29}$$

one has:

$$\begin{aligned} \frac{d\Gamma_{\tau \to H^- H'^0 \nu_\tau}}{ds} = {} & \frac{G_F^2\, |V_{uD}^2|\, m_\tau^3}{768\, \pi^3\, s^3} S_{ew}^h\, C_{HH'}^2 \left(1 - \frac{s}{m_\tau}\right)^2 \\ & \times \left\{ \left(1 + 2\frac{s}{m_\tau}\right) \lambda^{3/2}(s, m^2, m'^2) |F_V^{HH'}(s)|^2 \right. \\ & \left. + 3\, \Delta_{HH'}^2 \lambda^{1/2}(s, m^2, m'^2) |F_S^{HH'}(s)|^2 \right\} . \end{aligned} \tag{1.30}$$

Obtaining a theoretical value for the form factors $F^{HH'}(s)$ is far from trivial and it involves non-perturbative methods. At very low energies one can make use of $\chi$PT, but for some channels, for example those involving kaons, even the threshold $s_{th} = (m_H + m_{H'})^2$ is close to the energies where $\chi$PT is not able to give precise predictions. Then one has to make use of theoretically motivated ansatzes, which one fits to data. They usually bring extra assumptions that can be relaxed when they do not fit well the precise experimental data by adding new parameters. Specially when the counting becomes unclear, this scenario is, unfortunately, far from the ideal one in which it is possible to make precise predictions from first principles. Since this problem becomes worse for more complex $\tau$ decays, they are beyond the scope of this thesis.

### 1.2.3 Inclusive $\tau$ decay

The well-defined strangeness of a final hadronic state $|n\rangle$ in a tau decay allows us to identify if it came from the strange current $J_S = \bar{s}_L \gamma_\mu u_L$, $|n_S\rangle$, or the non-strange one $J_{NS} = \bar{d}_L \gamma_\mu u_L$, $|n_{NS}\rangle$. Summing over all of them in Eq. (1.19), one

gets the inclusive strange (non-strange) hadronic mass-squared distribution:

$$d\Gamma_{S(NS)}(s) = \frac{G_F^2 |V_{uD}|^2 S_{ew}^h m_\tau^5}{16\pi} \frac{ds}{m_\tau^2} \left(1 - \frac{s}{m_\tau^2}\right)^2 \times \left\{ \left(1 + 2\frac{s}{m_\tau^2}\right) \rho^{(1)}_{V+A,\, S(NS)}(q^2) + \rho^{(0)}_{V+A,\, S(NS)}(q^2) \right\} , \qquad (1.31)$$

where $\rho^{(i)}_{V+A,\, S(NS)} \equiv 4 \sum_{S(NS)} H^{(i)}$. The interesting thing about performing those sums is that if we define the correlation function of two currents as:

$$\begin{aligned} \Pi^{\mu\nu}(q) &\equiv i \int d^4x \; e^{iqx} \; \langle 0 | \, T[J^\mu(x) J^{\nu\dagger}(0)] \, | 0 \rangle \\ &= \; (-g^{\mu\nu} q^2 + q^\mu q^\nu) \; \Pi_J^{(1)}(q^2) + q^\mu q^\nu \; \Pi_J^{(0)}(q^2) \, , \end{aligned} \qquad (1.32)$$

then it can be proven that (see for example Refs. [8, 9]):

$$\mathrm{Im}\Pi_{\mu\nu}(s) = \pi \sum_n (2\pi)^3 \int d\phi_n \, \delta^4(p_n - q) \, \langle n | J_\mu | 0 \rangle \; \langle 0 | J_\nu^\dagger | n \rangle \, , \qquad (1.33)$$

so that:

$$\rho^{(i)}_{V+A,\, S(NS)} = \frac{1}{\pi} \mathrm{Im}\Pi^{(i)}_{V+A,\, S(NS)}(s) \, , \qquad (1.34)$$

where the associated current is simply $J^\mu_{V+A\, S(NS)} = \bar{s}(\bar{d})\gamma^\mu u + \bar{s}(\bar{d})\gamma^\mu\gamma_5 u$.

Using symmetry arguments one can, in the non-strange sector, split final hadronic states into those ones that can not decay through axial currents, $|n_V\rangle$, and those ones that can not decay through vector ones, $|n_A\rangle$. Summing over them, one is able to extract $\rho_V^{(i)}(s) = \frac{1}{\pi}\mathrm{Im}\Pi_V^{(i)}(s)$ and $\rho_A^{(i)}(s) = \frac{1}{\pi}\mathrm{Im}\Pi_A^{(i)}(s)$. Exploiting our knowledge of $\Pi^{(i)}(s)$ to make very precise predictions is one of the main topics of this thesis.

## 1.3 The Operator Product Expansion

When dealing with non-local interactions, frequently one has to deal with the product of two operators, $\hat{A}(x)\hat{B}(y)$. In principle, singularities when performing the $y \to x$ limit would not allow to translate them into a local interaction. Wilson hypothesized [11], and Zimmermann proved [12] within perturbation theory, that those singularities could be reabsorbed into $c$-numbers $c_i'(x, y)$, so that an

Operator Product Expansion (OPE) can be defined as:

$$\hat{A}(x)\hat{B}(y) = \sum_i c_i'(x,y)\mathcal{O}_i(y)\,. \tag{1.35}$$

By dimensional analysis, up to logarithmic corrections, $c_i'(x,y) = \frac{c_i}{(x-y)^{d_A+d_B-d_{O_i}}}$, where $d_{O_i}$ becomes anomalous when quantum corrections are taken into account. Those operators with lower dimensions will dominate the sum when $y$ becomes close to $x$.

### 1.3.1 Integrating out a heavy field. A simple example of OPE

The OPE is explicitly made when integrating out a heavy field. For the sake of simplicity let us see this in a very naive example with a light scalar boson $\phi(x)$ with mass $m$ and a heavy one $\Phi(x)$ with mass $M$ with the Lagrangian [13, 14]:

$$\mathcal{L} = \frac{1}{2}\partial_\mu\phi(x)\partial^\mu\phi(x) + \frac{1}{2}\partial_\mu\Phi(x)\partial^\mu\Phi(x) - \frac{1}{2}m^2\phi(x)^2 - \frac{1}{2}M^2\Phi(x)^2 - \frac{1}{2}\kappa\phi(x)^2\Phi(x)\,. \tag{1.36}$$

Let us now define $J(x) \equiv -\frac{1}{2}\phi^2$. The generating functional is:

$$Z_i = \int d[\Phi]d[\phi]e^{i\int d^4x\mathcal{L}_\phi^{\text{free}}}e^{i\int d^4x\mathcal{L}_\Phi^{\text{free}}+\kappa J(x)\Phi(x)}\,. \tag{1.37}$$

In order to integrate out the heavy field $\Phi(x)$ we have to manipulate the part of the action that involves it:

$$\begin{aligned} S_\Phi &\equiv \int d^4x\left(\frac{1}{2}\partial_\mu\Phi(x)\partial^\mu\Phi(x) - \frac{1}{2}M^2\Phi(x)^2 + \kappa J(x)\Phi(x)\right) \\ &= \int d^4x\left[-\frac{1}{2}\Phi(x)(\Box + M^2)\Phi(x) + \kappa J(x)\Phi(x)\right]\,. \end{aligned} \tag{1.38}$$

Let us shift the field $\Phi(x) = \Phi_0(x) + \Phi'(x)$ [15], so that the functional form of $\Phi_0(x)$ is fixed by imposing that it satisfies the classical equation of motion:

$$(\Box + M^2)\Phi_0(x) = \kappa J(x)\,. \tag{1.39}$$

Then, we can rewrite Eq. (1.38) as:

$$S_\Phi = -\frac{1}{2}\int d^4x\,\left[\Phi'(x)[\Box + M^2]\Phi'(x) - \kappa J(x)\Phi_0(x)\right]\,. \tag{1.40}$$

Using now that the free Feynman propagator,

$$D_F(x) = \int \frac{d^4k}{(2\pi)^4} \frac{e^{-ikx}}{k^2 - M^2}\,, \tag{1.41}$$

satisfies

$$[\Box + M^2]D_F(x) = -\delta^4(x)\,, \tag{1.42}$$

one can rewrite the field $\Phi_0(x)$ as

$$\Phi_0(x) = -\int d^4x D_F(x-y)\kappa J(y)\,, \tag{1.43}$$

which allows us to split the action of Eq. (1.40) into:

$$\begin{aligned} S(\Phi(x)) = &-\frac{1}{2}\int d^4x\, \Phi'(x)[\Box + M^2]\Phi'(x) \\ &- \frac{1}{2}\kappa^2 \int d^4x \int d^4y J(x) D_F(x-y) J(y)\,, \end{aligned} \tag{1.44}$$

so that we can factorize the first term in the generating functional and integrate it out. We end up with a non-local action of the form:

$$S_{eff} = \int d^4x\, \mathcal{L}_\phi^{\text{free}} - \frac{\kappa^2}{2}\int d^4x \int d^4y J(x) D_F(x-y) J(y)\,. \tag{1.45}$$

In the integrand all the singularities are encoded in the Feynman propagator term, $D_F(x-y)$, so that $J(y)$ is regular when $y \to x$ and then we can expand it by Taylor:

$$J(y) = \sum_{n=0} \frac{1}{n!}(y-x)^{\mu_1}...(y-x)^{\mu_n}\partial^z_{\mu_1}...\partial^z_{\mu_n} J(z)|_x\,. \tag{1.46}$$

Defining $f(k^2) \equiv \frac{1}{k^2-M^2}$, the effective interaction action becomes:

$$\begin{aligned} S^I_{eff} &= -(-1)^n \frac{\kappa^2}{2} \int d^4x\, J(x) \int d^4y \\ &\cdot \int \frac{d^4k}{(2\pi)^4} \sum_{n=0} \frac{i^n}{n!} \partial^z_{\mu_1} ... \partial^z_{\mu_n} J(z)|_{z=x} f(k^2) \partial^{\mu_1}_k .... \partial^{\mu_n}_k e^{ik(x-y)} \\ &= -\frac{\kappa^2}{2} \int d^4x\, J(x) \int d^4k\, \delta^4(k) \sum_{n=0}^{\infty} \frac{i^n}{n!}\, \partial^k_{\mu_1} ... \partial^k_{\mu_n}\, f(k^2)\, \partial^{\mu_1}_z ... \partial^{\mu_n}_z J(z)|_{z=x} \\ &= -\sum_{n=0}^{\infty} \frac{\kappa^2}{2} \frac{i^n}{n!} \int d^4x\, J(x)\, \partial^{\mu_1}_k ... \partial^{\mu_n}_k f(k^2)|_{k=0}\, \partial^y_{\mu_1} ... \partial^y_{\mu_n} J(y)|_{y=x}\,. \end{aligned} \tag{1.47}$$

Every $2n-th$ term in the sum will receive contribution from the $2n-th$ term in the Taylor expansion of $f(k^2)$, $\sim n! \frac{g^{\mu_1\mu_2} ... g^{\mu_{n-1}\mu_n}}{M^n}$, so that the nonlocal interaction has become a local one which can be obtained from an interaction Lagrangian in powers of $\frac{E^2}{M^2}$:

$$\mathcal{L} = \sum \frac{c_i}{\Lambda^{D_i}} \mathcal{O}_i\,. \tag{1.48}$$

This method can be extended to integrate out heavy fermions and spin 1 bosons from the Lagrangian [16]. In hadronic tau decays one integrates out heavy quarks and the $W$ from the Standard Model Lagrangian (indeed we did it in a less formal version at the level of amplitudes in Section 1.2).

### 1.3.2 Effective Field Theories as a tool to resum large logarithms

Effective Field Theories (EFT) can be built in the form of Eq. (1.48). Even in the absence of knowledge about the dynamics of heavier degrees of freedom. One simply has to write the most general Lagrangian with the light degrees of freedom at a given energy and then fit the unknown couplings $c_i$ to data, which encode information about the dynamics of heavy particles.

If, as in our toy example, the dynamics of heavy particles is known, one simply needs to perform the matching either with path integrals or by calculating simple processes and requiring they should give the same prediction. One may think that knowing the "full" theory with heavy particles, the only usefulness of using the EFT is simplicity, but, in fact, this is not true because of quantum corrections. For example, a naive counting tells us that the short distance radiative corrections part of $S^h_{ew}$ in Eq. (1.19) should be $S^h_{ew} \sim \frac{\alpha}{\pi} \sim 0.1\%$. If one computes it, one gets around a 2%. The reason is that quantum loops are giving extra logarithms $\sim \log \frac{M_W^2}{m_\tau^2}$, which enhance those contributions. In the case of QED, the convergence

is still very good, but for QCD corrections, where $\frac{\alpha_s(m_\tau^2)}{\pi} \sim 0.1$, this means a breakdown of perturbation theory.

In order to solve the problem, one makes use of the EFT and, if the heavy dynamics is known and the matching is performed, makes use of renormalization group equations to resum them. Let us sketch the procedure. If one computes quantum corrections to a given operator, it needs to be renormalized:

$$\langle \mathcal{O}_i \rangle_B = Z_i(\epsilon, \mu) \langle \mathcal{O}_i(\mu) \rangle_R \,. \tag{1.49}$$

Since the bare operator is scale independent:

$$(\gamma_{\mathcal{O}_i} + \mu \frac{d}{d\mu}) \langle \mathcal{O}_i(\mu) \rangle_R = 0 \,, \tag{1.50}$$

where, taking $\alpha$ as example of coupling which generates quantum corrections, and assuming for the sake of simplicity that there is no mixing:[2]

$$\frac{\mu}{Z_i} \frac{dZ}{d\mu} \equiv \gamma_{\mathcal{O}_i} = \gamma_{\mathcal{O}_i}^{(1)} \frac{\alpha}{\pi} + \gamma_{\mathcal{O}_i}^{(2)} \left( \frac{\alpha}{\pi} \right)^2 + \dots \,. \tag{1.51}$$

Using now that the Lagrangian, invariant under renormalization scale, can be rewritten in terms of renormalized fields:

$$\mathcal{L} = \sum c_{iR} \, \mathcal{O}_{iR} \,, \tag{1.52}$$

one has the RGE for the Wilson coefficients:

$$\left( \mu \frac{d}{d\mu} - \gamma_{\mathcal{O}_i} \right) c_{iR} = 0 \,. \tag{1.53}$$

Then, the procedure to get the Wilson coefficients for the EFT is the following:

- Compute the anomalous dimension (from $Z_i(\epsilon, \mu)$) at order $(n)$, $\gamma_{\mathcal{O}_i}^{(n)}$.
- Compute quantum corrections at order $(n-1)$ in both theories.
- Performing the matching at a scale $\mu$ one gets the Wilson coefficients up to corrections $\alpha_\mu^n \log^n \frac{M^2}{\mu^2}$. The logical procedure is then to choose $\mu \sim M$.
- If now one computes a process with the EFT involving energies and masses of order $\sim p$, one gets unaccounted corrections of the order $\alpha^n \log^n \frac{\mu^2}{p^2}$. One

[2] The generalization to that case is relatively straightforward. One has to work with matrices instead of scalars. It can be found for example in [16].

| | | | | |
|---|---|---|---|---|
| $1$ | $\alpha \ln$ | $\alpha^2 \ln^2$ | $\alpha^3 \ln^3$ | ... $\alpha^n \ln^n$ |
| | $\alpha$ | $\alpha^2 \ln$ | $\alpha^3 \ln^2$ | ... $\alpha^n \ln^n$ |
| | | $\alpha^2$ | $\alpha^3 \ln$ | ... $\alpha^n \ln^n$ |
| | | | $\alpha^3$ | ... |
| | | | ... | $\alpha^n$ |

Table 1.1: Sketch of the different orders in perturbation theory with the naive counting (vertical dashed lines) and the one including EFT plus RGE methods (horizontal lines).

avoids them using the RGE of Eq. (1.53) to run the Wilson coefficients from $\mu \sim M$ to $\mu \sim p$, resumming the logarithms for which higher-order $\gamma_{O_i}^{(n+m)}$ are not responsible. The first unaccounted order will be then $\mathcal{O}(\alpha^n) + \mathcal{O}(\alpha^{n+1} \log) + ...\mathcal{O}(\alpha^m \log^{m-n}) + ....$

In Table 1.1 we sketch how the counting gets modified.

### 1.3.3 Operator Product Expansion in the vacuum

Let us recall the two point correlation function of quark currents given by Eq. (1.32):

$$\Pi(q) = i \int d^4x \, e^{iqx} \, \langle 0| \, T[J(x) J^\dagger(0)] \, |0\rangle \, , \tag{1.54}$$

with $J^\mu = \bar{d}(\bar{s})\Gamma u$, where $\Gamma$ is any Lorentz structure and we are omitting Lorentz indices for the sake of simplicity. In the presence of interactions, as long as perturbation theory is well-behaved, the product of quark currents is given in terms of the free ones by the usual Dyson series [17]:

$$T(J(x)J^\dagger(0)) = \sum \frac{i^n}{n!} \int dz_1 ... dz_n T(J^0(x) J^{0\,\dagger}(0) \mathcal{L}_{int,QCD}(z_1) ... \mathcal{L}_{int,QCD}(z_n)) \, . \tag{1.55}$$

The point is that, applying now the Wick theorem in every term of the last equation, one separates the singular part of them in $c$-numbers, given by the contractions of two-point operators, and normal product of operators with regular behavior when $x \to y$, so that one can Taylor expand them to get an OPE as in

Eq. (1.35) [18]:

$$T(J(x)J^{\dagger}(0)) = c_1 x^{-6} : 1 : + x^{-2} c_{\bar{q}q}(\mu) : m\bar{q}q(\mu) : + x^{-2} c_{GG}(\mu) : GG(\mu) : , \tag{1.56}$$

where :: denotes the normal product. Again the dimensionless, at least up to quantum corrections, Wilson coefficients can only depend on $x$ through logarithmic terms. In perturbation theory, when we introduce Eq. (1.56) into Eq. (1.54), the contribution of the nontrivial operators when contracted with the vacuum is zero, so it worthless calculating those Wilson coefficients. However, long-distance effects become important at low energies. The asymptotically free states are different and the vacuum as a state free from quarks and gluons stops making sense. Instead one assumes that at energies large enough, perturbative methods are enough to compute the Wilson coefficients in the same way one does when other final hadronic states are involved in the initial or final state, and that the remaining vacuum matrix elements acquire nonzero values, which can be studied with non-perturbative methods (or by fitting data), as one does with the usual long-distance hadronic matrix elements [19].

When inserting Eq. (1.56) into Eq. (1.54) and decomposing the final result in scalar Lorentz structures, $\Pi^{(i)}(Q^2 = -q^2)$, one ends up with the OPE of the correlators [19]:

$$\Pi^i(Q^2 = -q^2) = \sum_{i,D} c_i(\mu, Q^2) \frac{\mathcal{O}_{i,D}(\mu)}{Q^D} , \tag{1.57}$$

which, because of the logarithms appearing in the Wilson coefficients due to the quantum corrections, is not well defined for Minkowskian momentum ($q^2 > 0$). Notice how the OPE is only a well-behaved expansion for energies $Q^2$ large enough. The power of the OPE of the correlators will become obvious in the next chapters when we will relate it to tau data through different dispersion relations.

## 1.4 Chiral Perturbation Theory as an EFT

### 1.4.1 Parameterizing the degrees of freedom

One can rewrite the massless QCD Lagrangian for three flavors as:

$$\mathcal{L} = \bar{q}_L \not{D} q_L + \bar{q}_R \not{D} q_R + ... , \tag{1.58}$$

where $q = (u, d, s)^T$, sum over colors is implicit and we have neglected electroweak interactions in the covariant derivative. In the flavor space, the Lagrangian is manifestly invariant under $SU(3)_L \times SU(3)_R$ transformations. Set-

ting $q = (u_L,\, d_L,\, s_L,\, u_R,\, d_R,\, s_R)^T$ as a basis of the configurations, the matrix element of a transformation can be written as [20, 21]:

$$g = \begin{pmatrix} L & 0 \\ 0 & R \end{pmatrix}, \tag{1.59}$$

where $L(R)(x) = e^{i\lambda_i\theta_i}$ and $\lambda_i$ are the $SU(3)$ generators. Dynamical generation of a nonzero vacuum expectation value for the quark condensate breaks that $SU(3)_L \times SU(3)_R$ symmetry into $SU(3)_V$, since $\langle 0|\bar{q}q|0\rangle = \langle 0|\bar{q}_R q_L + \bar{q}_L q_R|0\rangle \neq 0$ leaves only invariant those group transformations in which $L = R$.

Because of the Goldstone Theorem, for every generator of the unbroken symmetry, there is an associated Goldstone boson. At energies small enough, they will be the only degrees of freedom of the theory.

In order to parametrize them we use the CCWZ formalism [22]. If we impose that a local field configuration is an excitation of the vacuum $\phi_V$, so that $\varphi(x) = \Xi(x)\phi_V$, being $\Xi(x) \in SU(3)_L \times SU(3)_R$, we can rewrite it as:

$$\Xi(x) = \begin{pmatrix} 1 & 0 \\ 0 & U(x) \end{pmatrix} \begin{pmatrix} V(x) & 0 \\ 0 & V(x) \end{pmatrix}, \tag{1.60}$$

where the the second matrix is a $SU(3)_V$ transformation. Since $\phi_V$ is invariant under any local $SU(3)_V$ (i.e. $L = R$) transformation, we can choose any arbitrary $V(x)$ without changing the configuration. In particular we choose $V(x) = \mathbb{I}$, so that all the possible configurations are parametrized by the local transformation of the right generators,

$$U(x) = e^{i\frac{\lambda_j \phi_j(x)}{F}}, \tag{1.61}$$

where $\lambda_j$ is a Gell-Mann matrix and $F$ is a dimensional quantity introduced to compensate the dimensions of $\phi_i$.

If now we make a global group transformation $g$ as defined in Eq. (1.59):

$$\varphi(x) \to g\varphi(x) \Longrightarrow \Xi(x) \to g\,\Xi(x)\,, \tag{1.62}$$

in general:

$$g\,\Xi(x) = \begin{pmatrix} 1 & 0 \\ 0 & RUL^\dagger \end{pmatrix} \begin{pmatrix} L & 0 \\ 0 & L \end{pmatrix} \neq \begin{pmatrix} 1 & 0 \\ 0 & U_1 \end{pmatrix}, \tag{1.63}$$

but the point is that we have the freedom of choosing that after the transformation the matrix $\Xi(x)$ has become instead:

$$\Xi(x) \to \Xi'(x) = g\Xi(x) \begin{pmatrix} V(x) & 0 \\ 0 & V(x) \end{pmatrix}, \tag{1.64}$$

with an arbitrary $V(x)$, because, as we stated before, vacuum and then the configuration $(g\varphi(x))$ is invariant under any local $SU(3)_V$ transformation. Choosing $V(x) = L^\dagger$, the transformed $\Xi'(x)$ is again parametrized by the local transformation associated to the right generators, becoming a valid parametrization for the degrees of freedom of the theory:

$$U(x) = e^{i\frac{\lambda_i \phi_i(x)}{F}} \quad U(x) \to RU(x)L^\dagger\,. \tag{1.65}$$

The dimensional constant $F$ was introduced so that the fields $\phi(x)$ can be identified as spin 0 bosons.

### 1.4.2 Building the lowest order Lagrangian

Following the prescription given in the previous section, we want to build the most general Lagrangian that respects the symmetries for $U(x)$, which parametrizes the available degrees of freedom at low energies. Imposing that the Lagrangian should be invariant under $SU(3)_L \times SU(3)_R$ transformations and knowing that under those transformations $U(x) \to RU(x)L^\dagger$, the invariant objects are flavor traces of objects with so many $U(x)$ as $U^\dagger(x)$ terms. On the other hand, because $U(x)$ is a unitary matrix we need to insert derivatives in order to have nontrivial terms. For every derivative we insert, we are adding an extra dimension to the operator. The first term in the EFT will be then the first nontrivial operator with minimal number of derivatives that respects both the group and Lorentz symmetries:

$$\mathcal{L} = \frac{F^4}{4} Tr(\partial_\mu U(x) \partial^\mu U(x))\,. \tag{1.66}$$

The prefactor becomes fixed by requiring that, when expanding $U(x)$, the kinetic term for the Goldstone bosons have the proper normalization. Higher-order corrections are of the order given by loop corrections, i.e.:

$$\text{Loop} \sim \left(\frac{p}{4\pi F}\right)^2 \times \text{Tree}\,, \tag{1.67}$$

where $p$ represent the energies entering into the process. Then the counting will be valid as far as $p \ll 4\pi F$. Divergences in those loops will be canceled by renormalizing the LECs of higher-order Lagrangians, which, as we saw in the previous section, encode the short-distance information of the process, in principle obtainable with lattice QCD and possible to estimate with analytic approaches such as R$\chi$T, which makes use of some extra assumptions. The alternative consists in fixing them using data, with the cost of losing some predictive power. Their natural order will be then the same one as the loop corrections.

### 1.4.3 Extending the Lagrangian with the use of external fields

The massless QCD Lagrangian does not represent all interactions involving quarks. We can generalize it to [23, 24]:

$$\mathcal{L} = \mathcal{L}^0_{QCD} + \bar{q}_L \gamma^\mu l_\mu q_L + \bar{q}_R \gamma^\mu r_\mu q_R - \bar{q}(s - i\gamma_5 p)q \ , \tag{1.68}$$

where $l_\mu, r_\mu, s, p$ are the external fields. $\mathcal{L}$ is invariant under local transformation of the symmetry if:

$$l_\mu \to L\, l_\mu\, L^\dagger + iL\, \partial_\mu L^\dagger \,, \tag{1.69}$$

$$r_\mu \to R\, l_\mu\, R^\dagger + iR\, \partial_\mu R^\dagger \,, \tag{1.70}$$

$$s + ip \to R\,(s + ip)\, L^\dagger \,. \tag{1.71}$$

Now, if we want to incorporate these external fields to the low energy Lagrangian, we have a very strong constraint. The functional form of the low-energy Lagrangian in terms of the external sources must be the same whether if they break or not chiral symmetry. If the short-distance Lagrangian is invariant under local transformations, which happens to be true if and only if those local transformations are imposed, the low-energy one must be invariant too. Then, only combinations of the $U$ with the external fields transforming as Eqs. (1.69) (1.70) and (1.71) invariant under local symmetry transformations are allowed.

Now we can build the most general low-energy Lagrangian. At first order in $p^2$ and in the external sources we have then [25]:

$$\mathcal{L} = \frac{F^2}{4} \langle D_\mu U D^\mu U + \chi U^\dagger + U \chi^\dagger \rangle \,, \tag{1.72}$$

where $\chi \equiv 2B_0(s + ip)$, being $B_0$ a LEC and $D_\mu = \partial_\mu U - i r_\mu U + i U l_\mu$.

Now, we explicitly break the symmetry by imposing that the external fields must reproduce the well-known short-distance SM Lagrangian:

$$s = \mathrm{diag}(m_u, m_d, m_s)\,, \tag{1.73}$$
$$r_\mu = eQA_\mu + \dots\,, \tag{1.74}$$
$$l_\mu = eQA_\mu + \dots\,. \tag{1.75}$$

Expanding and reparametrizing the Goldstone fields so that the mass Lagrangian corresponds with the usual one related to the spin 0 bosons (except for the small $\pi_0 - \eta_8$ mixing term), we have:

$$U(x) = e^{i\sqrt{2}\Phi(x)/F}\,, \tag{1.76}$$

with:

$$\Phi(x) = \begin{pmatrix} \frac{\pi_0}{\sqrt{2}} + \frac{\eta_8}{\sqrt{6}} & \pi^+ & K^+ \\ \pi^- & -\frac{\pi_0}{\sqrt{2}} + \frac{\eta_8}{\sqrt{6}} & K^0 \\ K^- & \bar{K}^0 & -\frac{2\eta_8}{\sqrt{6}} \end{pmatrix}, \tag{1.77}$$

so that squared meson masses become simple linear combinations of the quark masses times $B_0$. When setting momenta on-shell, one has $p^2 = M^2$. Then, the quark matrix $\chi$ should be counted as $\mathcal{O}(p^2)$. Taking this into account, Eq. (1.72) represents the most general $\chi$PT Lagrangian at order $\mathcal{O}(p^2)$ including quark mass corrections.

When computing amplitudes at $\mathcal{O}(p^4)$, one must calculate loop diagrams from the $\mathcal{O}(p^2)$ Lagrangian as well as the tree level amplitudes coming from the $\mathcal{O}(p^4)$ one. The most general Lagrangian incorporates 12 Low-Energy Constants (LECs):

$$\begin{aligned} \mathcal{L}_4 \quad &= L_1 \langle D_\mu U^\dagger D^\mu U\rangle^2 \,+\, L_2 \langle D_\mu U^\dagger D_\nu U\rangle \langle D^\mu U^\dagger D^\nu U\rangle \\ &+ L_3 \langle D_\mu U^\dagger D^\mu U D_\nu U^\dagger D^\nu U\rangle \,+\, L_4 \langle D_\mu U^\dagger D^\mu U\rangle \langle U^\dagger\chi + \chi^\dagger U\rangle \\ &+ L_5 \langle D_\mu U^\dagger D^\mu U \left(U^\dagger\chi + \chi^\dagger U\right)\rangle \,+\, L_6 \langle U^\dagger\chi + \chi^\dagger U\rangle^2 \\ &+ L_7 \langle U^\dagger\chi - \chi^\dagger U\rangle^2 \,+\, L_8 \langle \chi^\dagger U\chi^\dagger U + U^\dagger\chi U^\dagger\chi\rangle \\ &- iL_9 \langle F_R^{\mu\nu} D_\mu U D_\nu U^\dagger + F_L^{\mu\nu} D_\mu U^\dagger D_\nu U\rangle \,+\, L_{10} \langle U^\dagger F_R^{\mu\nu} U F_{L\mu\nu}\rangle \\ &+ H_1 \langle F_{R\mu\nu} F_R^{\mu\nu} + F_{L\mu\nu} F_L^{\mu\nu}\rangle \,+\, H_2 \langle \chi^\dagger\chi\rangle\,. \end{aligned} \tag{1.78}$$

where

$$F_L^{\mu\nu} = \partial^\mu \ell^\nu - \partial^\nu \ell^\mu - i[\ell^\mu, \ell^\nu]\,, \qquad F_R^{\mu\nu} = \partial^\mu r^\nu - \partial^\nu r^\mu - i[r^\mu, r^\nu]. \tag{1.79}$$

Notice that $H_1$ and $H_2$ are unphysical, since they do not contain the Goldstone boson fields. The counting tells us that the contribution from LECs should be of the same order than from loops, so that $L_i(\mu) \sim \frac{1}{4(4\pi)^2}$. The Lagrangian at $\mathcal{O}(p^6)$ was computed in Ref. [26] and contains 94 LECs.

The external fields can also be used to extract direct relations between Green Functions involving quarks and involving mesons. Since the generating functional can not depend on the field parametrization:

$$\begin{aligned} \exp\{iZ\} &= \int \mathcal{D}q\,\mathcal{D}\bar{q}\,\mathcal{D}G_\mu\,\exp\left\{i\int d^4x\,\mathcal{L}_{\rm QCD}\right\} \\ &= \int \mathcal{D}U\,\exp\left\{i\int d^4x\,\mathcal{L}_{\rm eff}\right\}, \end{aligned} \tag{1.80}$$

relations between Green functions in both theories, such as Noether currents, can be extracted by taking derivatives of the generating functional with respect to the external fields. For example, by taking derivatives with respect to the external scalar and pseudoscalar sources we learn that the constant $B_0$ is related to the quark condensate:

$$\langle 0|\bar{q}^j q^i|0\rangle = -f^2 B_0\,\delta^{ij}\ , \tag{1.81}$$

which means that the larger the parameter which controls the spontaneous chiral symmetry breaking, the larger the effect of the explicit one at low energies.

A more detailed review of $\chi$PT can be found in Ref. [24].

# Chapter 2

# QCD parameters from the V-A spectral functions

## 2.1 Introduction

As we saw in Section 1.2.3, experimental information on the two-point correlation function can be obtained using $\tau$ decay data. In this work, we focus on the non-strange $V - A$ one. Related to the fact that it would be zero if chiral symmetry remained unbroken at low energies, several cancellations are involved. In massless perturbative QCD (p-QCD), it is zero at all orders. Corrections due to the explicit chiral symmetry breaking, known to have worse behaved series [27] than the purely perturbative one, are suppressed by the very tiny quark masses. Therefore, the study of this $V-A$ spectral function becomes a unique opportunity to study non-perturbative QCD without perturbative contaminations [28–43].

A comprehensive phenomenological study of the non-strange $V - A$ spectral function using the 2005 release of ALEPH $\tau$ data [44] was done in Refs. [38–40]. One of the main motivations of this chapter, based on Ref. [45], consists in updating that study making use of the updated ALEPH data set [46].

### 2.1.1 Experimental spectral function

The experimental spectral functions are obtained from the invariant mass distributions $\frac{dN_\tau^{V/A}}{N_\tau ds}$. Using Eq. (1.31):

$$\rho_V^{(1)}(s) = \frac{dN_\tau^V}{N_\tau}\frac{m_\tau^2}{ds}\frac{\left(1-\frac{s}{m_\tau^2}\right)^{-2}\left(1+\frac{2s}{m_\tau^2}\right)^{-1}}{12\pi^2|V_{ud}|^2 B_e S_{ew}} \qquad s > 4m_\pi^2\,, \tag{2.1}$$

$$\rho_A^{(1)}(s) = \frac{dN_\tau^A}{N_\tau}\frac{m_\tau^2}{ds}\frac{\left(1-\frac{s}{m_\tau^2}\right)^{-2}\left(1+\frac{2s}{m_\tau^2}\right)^{-1}}{12\pi^2|V_{ud}|^2 B_e S_{ew}} \qquad s > 6m_\pi^2\,, \tag{2.2}$$

where we have used that $\rho_V^{(0)}(s) = 0$ and $\rho_A^{(0)}(s) = 2f_\pi^2\delta(s-m_\pi^2)$ in an excellent approximation. The first correction to those expressions comes from $\pi(1300)$. Since $f_{\pi(1300)}$ is very small [47–50], its numerical role is completely negligible.

Compared to the 2005 ALEPH data set, the new public version of the ALEPH $\tau$ data incorporates an improved unfolding of the measured mass spectra from detector effects and corrects some problems [51] in the correlations between unfolded mass bins. The improved unfolding brings an increased statistical uncertainty near the edges of phase space. It has also reduced the number of bins in the spectral distribution, as a larger bin size has been adopted.

### 2.1.2 The OPE of the V-A correlators

Because vacuum preserves parity, the two-point correlation function of the $VV-AA$ $ud$ quark currents is identical to the one with the left-handed and right-handed quark currents:

$$\begin{aligned}\Pi_{ud,LR}^{\mu\nu}(q) &\equiv i\int d^4x\, e^{iqx}\ \langle 0|\, T\left(L_{ud}^\mu(x)R_{ud}^{\nu\dagger}(0)\right)|0\rangle \\ &= (-g^{\mu\nu}q^2 + q^\mu q^\nu)\,\Pi_{ud,LR}^{(1)}(q^2) + q^\mu q^\nu\,\Pi_{ud,LR}^{(0)}(q^2)\,,\end{aligned} \tag{2.3}$$

where $L_{ud}^\mu(x) \equiv \bar{d}(x)\gamma^\mu(1-\gamma_5)u(x)$ and $R_{ud}^\mu(x) \equiv \bar{d}(x)\gamma^\mu(1+\gamma_5)u(x)$. The OPE of $\Pi(s) \equiv \Pi_{ud,LR}^{(0+1)}(s) \equiv \Pi_{ud,LR}^{(0)}(s) + \Pi_{ud,LR}^{(1)}(s)$ predicts a strong cancellation for this correlator compared to the $\Pi_{ud,VV+AA}^{(1+0)}(s)$ one. At NLO, Eq. (1.57) can be written as:

$$\Pi^{(1+0)}(Q^2=-q^2) = \sum_i c_i(\mu,Q^2)\frac{\mathcal{O}_{i,D}(\mu)}{Q^D} = \sum_D \frac{a_{D/2}(\mu) + b_{D/2}(\mu)\ln\frac{\mu^2}{Q^2}}{Q^D}\,, \tag{2.4}$$

where in general $b_{D/2}$ is $\alpha_s$ suppressed with respect to $a_{D/2}$. Because of chiral symmetry, the correlator is exactly zero in massless p-QCD . If we introduce

quark mass corrections of order $\frac{m_q^{2n}}{Q^{2n}}$ into the condensate of dimension $D = 2n$, this means that the $D = 0$ contribution vanishes. Indeed quark mass corrections are completely negligible at the energies we are dealing with ($\frac{m_d^2}{Q^2} \sim 10^{-5}$). Again, because of chiral symmetry, the contribution coming from the gluon condensate $\langle \frac{\alpha_s}{\pi} GG \rangle$ also vanishes and the only $D = 4$ contribution comes from the quark condensate. The leading contribution should be then [52]:

$$Q^4 \left[\Pi_{ud,V-A}(Q^2)\right]^{D=4} = \frac{8}{3} \frac{\alpha_s(Q)}{\pi} \langle (m_u + m_d) qq \rangle \,, \tag{2.5}$$

but is again suppressed by $\frac{\alpha_s}{\pi} \frac{m_q}{\Lambda}$. Therefore, if we approximate the dimension-D contribution by its leading order term $a_{D/2}$:

$$\Pi(Q^2 = -q^2) = \sum_D \frac{a_{D/2}(\mu)}{Q^D} \equiv \sum_D \frac{\mathcal{O}_D}{Q^D} \,, \tag{2.6}$$

then $\mathcal{O}_4 \approx 2 \cdot 10^{-5}\,\mathrm{GeV}^4$, small enough to be negligible compared to experimental uncertainties.

The $D = 6$ contribution is given at NLO by:

$$\begin{aligned}
[Q^6 \Pi(Q^2)]^{D=6} = \alpha_s(\mu) \Big\{ & (2\pi + A_8 \alpha_s(\mu)) \langle \bar{u} \lambda_i \gamma_\mu (1-\gamma_5) d \, \bar{d} \lambda_i \gamma^\mu (1+\gamma_5) u \rangle_\mu \\
& + \alpha_s A_1 \langle \bar{u} \gamma_\mu (1-\gamma_5) d \, \bar{d} \gamma^\mu (1+\gamma_5) u \rangle_\mu \Big\} \\
+ \ln \frac{Q^2}{\mu^2} \alpha_s^2 \Big\{ & B_8 \langle \bar{u} \lambda_i \gamma_\mu (1-\gamma_5) d \, \bar{d} \lambda_i \gamma^\mu (1+\gamma_5) u \rangle_\mu \\
& + B_1 \langle \bar{u} \gamma_\mu (1-\gamma_5) d \, \bar{d} \gamma^\mu (1+\gamma_5) u \rangle_\mu \Big\} \,,
\end{aligned} \tag{2.7}$$

where $\lambda_i$ are Gell-Mann matrices in the color space and the $B_i$ are obtained by expanding the LO anomalous dimension of the condensates and $A_i$ involve a full NLO calculation and depend on the renormalization prescription (HV or NDR). They can be found in Ref. [53]. Notice how, at leading order, only the color octet contributes.

### 2.1.3 Relating the OPE to experimental data with sum rules

The OPE is defined in the Euclidean axis, $q^2 < 0$. In order to compare with experimental data, one can try to perform the analytic continuation to the Minkowskian axis $q^2 > 0$. But it happens that, due to the logarithms of quantum corrections, the OPE expansion is not well-defined for $q^2 > 0$.

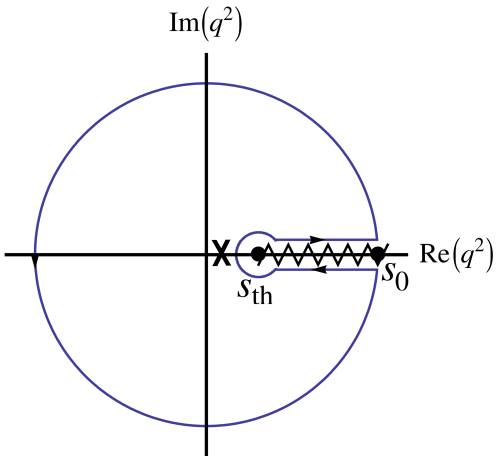


Figure 2.1: Analytic structure of $\Pi(s)$.

Instead, one uses that the physical correlators are analytic functions in all the complex plane, except for a cut in the positive real axis. Apart from the pion pole, this cut starts at $s_{th} = 4m_\pi^2$. When integrating along the circuit of Fig. 2.1 that correlator times an arbitrary weight function $\omega(s)$ analytic at least in the same complex region as the correlator except maybe for $s = 0$, one finds:

$$\int_{s_{\rm th}}^{s_0} \frac{ds}{s_0}\, \omega(s)\, \frac{1}{\pi}\, {\rm Im}\, \Pi(s) + \frac{1}{2\pi i} \oint_{|s|=s_0} \frac{ds}{s_0}\, \omega(s)\, \Pi(s)$$
$$= \; 2\, \frac{f_\pi^2}{s_0}\, \omega(m_\pi^2) + \frac{1}{s_0}\, {\rm Res}[\omega(s)\Pi(s), s=0]\,, \qquad (2.8)$$

where we have omitted the (1+0) super-index. In the first term one can introduce the experimental spectral function and, for large enough values of $s_0$, the OPE of $\Pi(s)$ becomes an excellent approximation for the integral along the circumference, except maybe for the region near the positive real axis [52, 54].

### 2.1.4 Quark-Hadron duality

Introducing the OPE into the previous equation one gets a very powerful relation between the physical low-energy correlator, described by meson interactions,

and the high energy one, calculated with the OPE in terms of quarks and gluons:

$$\int_{s_{\rm th}}^{s_0} \frac{ds}{s_0}\,\omega(s)\,\frac{1}{\pi}\,{\rm Im}\,\Pi(s) + \frac{1}{2\pi i}\oint_{|s|=s_0}\frac{ds}{s_0}\,\omega(s)\,\Pi^{\rm OPE}(s) + \delta_{\rm DV}[\omega(s),s_0]$$
$$= \; 2\,\frac{f_\pi^2}{s_0}\,\omega(m_\pi^2) + \frac{1}{s_0}\,{\rm Res}[\omega(s)\Pi(s), s=0]\,, \qquad (2.9)$$

where,

$$\delta_{\rm DV}[\omega(s),s_0] \;\equiv\; \frac{1}{2\pi i}\oint_{|s|=s_0}\frac{ds}{s_0}\,\omega(s)\,\Big[\Pi(s)-\Pi^{\rm OPE}(s)\Big]$$
$$= \int_{s_0}^{\infty}\frac{ds}{s_0}\,\omega(s)\,(\rho-\rho^{OPE})(s)\,, \qquad (2.10)$$

where in the second line we have performed the integral along the circuit of Fig. 2.2 and used that the OPE should be exact at infinite energy. In the same sense that the origin of the power corrections of the Operator Product Expansion is associated to corrections due to the tail of the asymptotic perturbative series, which is believed to behave as $e^{-C/\alpha_s(m_\tau^2)} \sim \frac{\Lambda^n}{Q^n}$ [55], quark-hadron Duality Violations (DVs) would originate from the tail of the asymptotically divergent OPE series. Differences between the physical correlators and their OPE aproximants, which at leading order approximate their analytical structure as series of poles in the origin, are believed to give terms exponentially suppressed that can be safely neglected in the Euclidean axis. However, when analytically continued to the Minkowskian one, they may become oscillatory and then not negligible.*

The $\delta_{\rm DV}[\omega(s),s_0]$ term is then dominated by the region near the Minkowskian axis. Using $\omega(s)$ such that it reduces the contribution of that region, for example taking:

$$\omega(s_0) = ... = \omega^{(n)}(s_0) = 0\,, \qquad (2.11)$$

where the superscript $(n)$ refers to the $n$-th derivative of the weight, suppresses DVs significantly. These kind of functions are known as $n+1$ pinched weight functions. Since the effect of power corrections is very suppressed, we will work in this chapter at leading order in the $\alpha_s$ expansion. Recalling Eq. (2.6) this means:

$$\Pi^{OPE}(Q^2=-q^2) = \sum_D \frac{\mathcal{O}_D}{Q^D}, \qquad \rho^{OPE}(s) = 0\,. \qquad (2.12)$$

*It is worth to mention that if the hadronic multiplicity is large enough, the convergence of the OPE prediction to the physical spectrum is observed to occur very fast even in the Minkowskian axis.

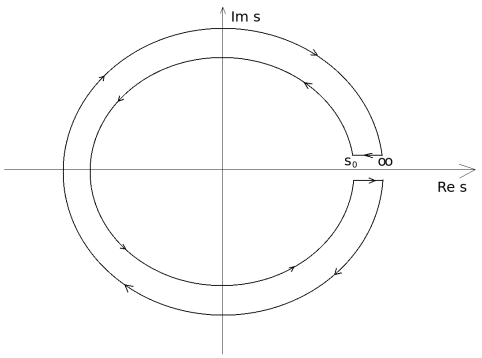


Figure 2.2: Integrating region for $\Pi_{DV}(s)$ to get Eq. (2.10).

In this approximation $\rho_{DV}(s) \equiv \rho(s) - \rho^{OPE}(s) = \rho(s)$. Using the Cauchy formula for $\omega(s) = \left(\frac{s}{s_0}\right)^n$:

$$\frac{1}{2\pi i}\oint_{|s|=s_0} ds\,\left(\frac{s}{s_0}\right)^n \Pi^{\rm OPE}(s) = (-1)^n \frac{\mathcal{O}_{2(n+1)}}{s_0^{n+1}}\,, \tag{2.13}$$

Eq. (2.9) becomes [9]:

$$\int_{s_{\rm th}}^{s_0} \frac{ds}{s_0}\,\left(\frac{s}{s_0}\right)^n \frac{1}{\pi}\,{\rm Im}\,\Pi(s) + (-1)^n \frac{\mathcal{O}_{2(n+1)}}{s_0^{n+1}} + \int_{s_0}^{\infty} \frac{ds}{s_0}\,\left(\frac{s}{s_0}\right)^n \rho_{DV}(s)$$
$$= \; 2\,\frac{f_\pi^2}{s_0}\,\left(\frac{m_\pi^2}{s_0}\right)^n + \frac{1}{s_0^{n+1}}\,{\rm Res}[s^n\Pi(s), s=0]\,, \tag{2.14}$$

DVs are expected to decrease fast when the hadronic multiplicity is increased. On the one hand, this means that they are smaller for the more inclusive channels. This can be seen if we compare the local DVs of the vector and axial channels (Fig. 2.3).* They are strongly suppressed in the sum, making the quark-hadron duality more powerful in the more inclusive V + A channel. On the other hand, they go fast to zero at higher energies, typically drawing exponentially suppressed oscillations [56–58]. In this chapter, we use the following parametrization to estimate uncertainties due to the high energy tail [39, 40, 56, 58–60]:

$$\rho_{DV}(s > s_z) \;=\; \kappa\, e^{-\gamma s}\,\sin\{\beta(s - s_z)\}\,, \tag{2.15}$$

*The sensibility of the local spectral function to $\alpha_s$ input is negligible compared to experimental uncertainties. Any reasonable $\alpha_s$ leads to the plot of Fig. 2.3.

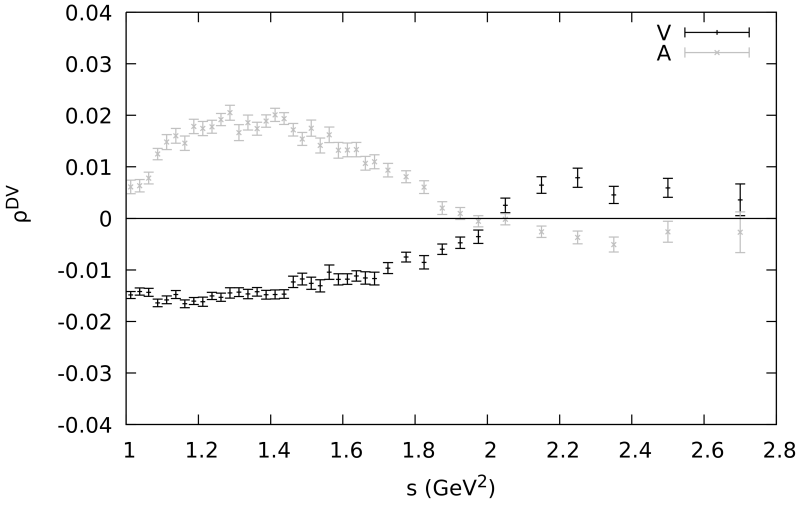


Figure 2.3: Experimental $\rho_{DV}$ for the V and A channel. Notice the strong cancellation in the sum. Theoretical uncertainties due to the needed OPE prediction are suppressed with respect to experimental uncertainties

The four free parameters $\kappa$, $\gamma$, $\beta$ and $s_z$ will be constrained by imposing well-known short-distance sum rules as well as a decent agreement with data at high energies. We are aware that the exact shape, dependent on the subtleties of every exclusive channel of the hadronic spectrum, is still far from the theoretical control.

A given parametrization for DVs is giving information on the high-energy shape of the $V - A$ spectral function and then, constraining the asymptotic behaviour of its OPE. In order to see that, one simply has to take Eq. (2.14) with $n \gg 1$. Only two terms survive in that limit, giving:

$$(-1)^n \frac{\mathcal{O}_{2(n+1)}}{s_0^{n+1}} + \int_{s_0}^{\infty} \frac{ds}{s_0} \left(\frac{s}{s_0}\right)^n \rho_{DV}(s) = 0 \tag{2.16}$$

For example, taking $\mathcal{O}_{2n} = a(-1)^n \Lambda^{2n} \Gamma(n)$, which incorporates the naive power counting as well as the expected $\Gamma$-like asymptotic divergence, the equality is recovered by taking $\rho_{DV}(s) = ae^{-\frac{s}{\Lambda^2}}$, which gives a naive intuition about why DVs should be exponentially suppressed. The parametrization of Eq. (2.15) is recovered by promoting $a$ and $\Lambda^2$ to complex numbers, taking the real part and renaming the constants. The $n$-dependence of the moments will be similar, but

modulated by a simple $n$-oscillating function. Note that the model dependence of an estimate of a condensate is stronger when we go to higher dimensions.

### 2.1.5 Different weights different physical parameters

Depending on the moment $\omega(s) = \left(\frac{s}{s_0}\right)^n$ we choose to study, we recover information about the spectral function in different energy regimes. Taking $n = 0, 1$ in Eq. (2.14) and using that the condensate contribution $\frac{\mathcal{O}_2}{s_0}$ and $\frac{\mathcal{O}_4}{s_0^2}$ can be safely neglected:

$$\int_{s_{\rm th}}^{s_0} \frac{ds}{s_0}\, \frac{1}{\pi}\, {\rm Im}\,\Pi(s) \;=\; 2\frac{f_\pi^2}{s_0} \,-\, \delta_{\rm DV}[1, s_0]\,, \tag{2.17}$$

$$\int_{s_{\rm th}}^{s_0} \frac{ds}{s_0}\, \frac{s}{s_0}\, \frac{1}{\pi}\, {\rm Im}\,\Pi(s) \;=\; 2\frac{f_\pi^2}{s_0}\frac{m_\pi^2}{s_0} \,-\, \delta_{\rm DV}[\frac{s}{s_0}, s_0]\,, \tag{2.18}$$

that are finite version of the Weinberg Sum Rules [61]. Sending $s_0$ to infinity, there are no DVs anymore. If we then multiply both equations respectively by $s_0$ and $s_0^2$, Eq. (2.17) receives a very tiny contribution from the $\mathcal{O}_2$ condensate and quantum corrections to it, *i.e.*, higher order terms in the $\alpha_s$ expansion of the two-dimensional contribution, make Eq. (2.18) divergent. However, in the chiral limit ($m_u = m_d = 0$) there are no dimensional operators below $D = 6$ [62], so that:

$$\int_{s_{\rm th}}^{\infty} ds\, \frac{1}{\pi}\, {\rm Im}\,\Pi|_{m_q=0}(s) \;=\; 2f_\pi|^2_{m_q=0}\,, \tag{2.19}$$

$$\int_{s_{\rm th}}^{\infty} ds\, s\, \frac{1}{\pi}\, {\rm Im}\,\Pi|_{m_q=0}(s) \;=\; 0\,, \tag{2.20}$$

which are the original WSRs. We will work with the finite (physical) version of them, *i.e.*, Eqs. (2.17) and (2.18).

For higher values of the power $n$, Eq. (2.9) gives relations involving the different OPE coefficients:

$$\begin{aligned}\int_{s_{\rm th}}^{s_0} \frac{ds}{s_0}\, \left(\frac{s}{s_0}\right)^n\, \frac{1}{\pi}\, {\rm Im}\,\Pi(s) \;&=\; (-1)^n\, \frac{\mathcal{O}_{2(n+1)}}{s_0^{n+1}} \\ &+ 2\frac{f_\pi^2 m_\pi^{2n}}{s_0^{n+1}} \,-\, \delta_{\rm DV}[\left(\frac{s}{s_0}\right)^n, s_0] \qquad (n \geq 2)\,.\end{aligned} \tag{2.21}$$

For negative values of $n = -m < 0$, the leading OPE does not give any contribution to the integration along the circumference $s = s_0$, but there is a non-zero residue at the origin proportional to the $(m-1)$th derivative of $\Pi(s)$ at $s = 0$. At low values of $s$ the correlator can be rigorously calculated within chiral perturbation theory ($\chi$PT) [23, 25, 63–65]. At present $\Pi(s)$ is known to $\mathcal{O}(p^6)$ [66], in terms of the so-called chiral low-energy couplings (LECs) that we can determine through the relations:

$$\begin{aligned}\int_{s_{\rm th}}^{s_0} \frac{ds}{s_0} \left(\frac{s}{s_0}\right)^{-1} \frac{1}{\pi} \,{\rm Im}\,\Pi(s) &= 2\,\frac{f_\pi^2}{m_\pi^2} + \Pi(0) - \delta_{\rm DV}[\left(\frac{s}{s_0}\right)^{-1}, s_0] \\ &\equiv -8\,L_{10}^{\rm eff} - \delta_{\rm DV}[\left(\frac{s}{s_0}\right)^{-1}, s_0]\,, \end{aligned} \tag{2.22}$$

$$\begin{aligned}\int_{s_{\rm th}}^{s_0} \frac{ds}{s_0} \left(\frac{s}{s_0}\right)^{-2} \frac{1}{\pi} \,{\rm Im}\,\Pi(s) &= 2\,\frac{f_\pi^2 s_0}{m_\pi^4} + \Pi'(0) s_0 - \delta_{\rm DV}[\left(\frac{s}{s_0}\right)^{-2}, s_0] \\ &\equiv 16\,C_{87}^{\rm eff} s_0 - \delta_{\rm DV}[\left(\frac{s}{s_0}\right)^{-2}, s_0]\,. \end{aligned} \tag{2.23}$$

The explicit expression of the correlator $\overline{\Pi}(s)$ at $\mathcal{O}(p^6)$ in $\chi$PT is given in App. A. The relation between the effective parameters $L_{10}^{\rm eff}$ and $C_{87}^{\rm eff}$ and their $\chi$PT counterparts, the LECs $L_{10}$ and $C_{87}$, will be discussed in Section 2.5.

## 2.2 A first estimation of the effective couplings

Using the updated ALEPH spectral function [46], we can determine $L_{10}^{\rm eff}$ and $C_{87}^{\rm eff}$ with Eqs. (2.22) and (2.23). As a first estimate, we neglect the DV terms and show in Fig. 2.4 the resulting effective couplings, for different values of $s_0$. As expected and as it was already observed in Ref. [38], the results exhibit a strong dependence on $s_0$ at low energies, where duality-violation corrections are not negligible. At larger momentum transfers the curves start to stabilize, indicating that the violations of duality become smaller. However, especially for $L_{10}^{\rm eff}$, the curves are not yet horizontal lines at $s_0$ near $m_\tau^2$, which implies that duality-violation effects are still present.

Instead of weights of the form $s^n$, we can try to reduce DV effects using pinched weight functions [32, 54, 67], which vanish at $s = s_0$ (or in the vicinity) where the OPE breaks down. Following Ref. [38], we employ the WSRs in Eqs. (2.17) and (2.18) and take $\omega_{-1,0}(s) = \left(\frac{s}{s_0}\right)^{-1}(1 - s/s_0)$ and $\omega_{-1}(s) =$

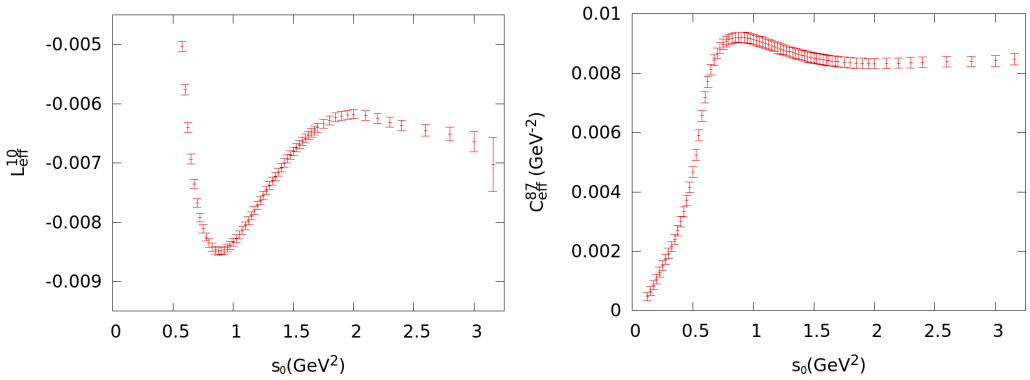


Figure 2.4: $L_{10}^{\rm eff}$ and $C_{87}^{\rm eff}$ from Eqs. (2.22) and (2.23), neglecting DVs, for different values of $s_0$.

$\left(\frac{s}{s_0}\right)^{-1}(1-s/s_0)^2$ for estimating $L_{10}^{\rm eff}$, and $\omega_{-2,0}(s) = \left(\frac{s}{s_0}\right)^{-2}(1-s^2/s_0^2)$ and $\omega_{-2}(s) = \left(\frac{s}{s_0}\right)^{-2}(1-s/s_0)^2(1+2s/s_0)$ for estimating $C_{87}^{\rm eff}$. Again, neglecting the DV terms, we plot the values of the effective couplings for different $s_0$ in Fig. 2.5. We observe that using these pinched weights the results converge and become stable below $s = m_\tau^2$. This suggests that DV effects are negligible at $s_0 \sim m_\tau^2$, when these pinched weight functions are used. Assuming that, we obtain:

$$L_{10}^{\rm eff} = -(6.49 \pm 0.05)\cdot 10^{-3}\,, \tag{2.24}$$

$$C_{87}^{\rm eff} = (8.40 \pm 0.18)\cdot 10^{-3}\ {\rm GeV}^{-2}\,. \tag{2.25}$$

## 2.3 Dealing with violations of quark-hadron duality

The stability under changes of $s_0$ of the $L_{10}^{\rm eff}$ and $C_{87}^{\rm eff}$ determinations is a necessary condition for vanishing duality violations. Another necessary condition we can test are the WSRs. We plot the lhs of Eqs. (2.17) and (2.18) minus the first term of the respective rhs in Fig. 2.6, together with the associated pinched

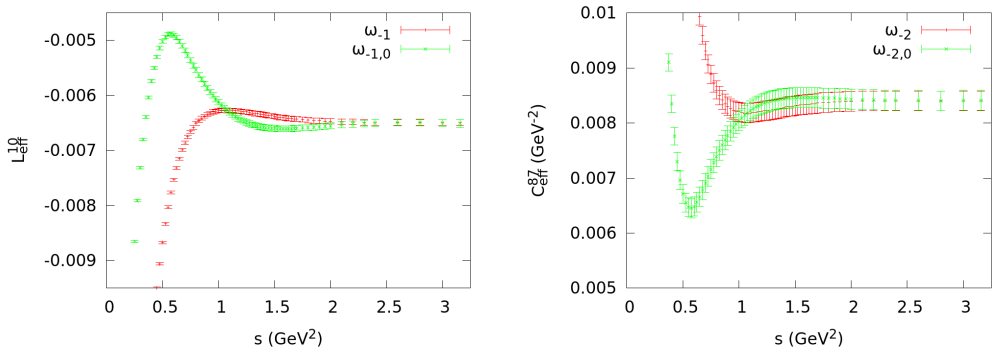


Figure 2.5: $L_{10}^{\rm eff}$ and $C_{87}^{\rm eff}$ at different values of $s_0$, using pinched weight functions and neglecting DVs.

WSR, *i.e.*, Eq. (2.17) - Eq. (2.18). Explicitly:

$$\mathrm{WSR1}(s_0) \equiv \int_{s_{\rm th}}^{s_0} \frac{ds}{s_0}\,\frac{1}{\pi}\,\mathrm{Im}\,\Pi(s) - 2\frac{f_\pi^2}{s_0}\,, \tag{2.26}$$

$$\mathrm{WSR2}(s_0) \equiv \int_{s_{\rm th}}^{s_0} \frac{ds}{s_0}\,\frac{1}{\pi}\,\mathrm{Im}\,\Pi(s) - 2\frac{f_\pi^2}{s_0}\frac{m_\pi^2}{s_0}\,, \tag{2.27}$$

$$\mathrm{WSR}_{\rm pinched}(s_0) \equiv \mathrm{WSR1}(s_0) - \mathrm{WSR2}(s_0)\,. \tag{2.28}$$

They predict cancellations with respect to the separate $V$ and $A$ channels, so we plot them together with the respective $V+A$. The very strong cancellations are observed from low energies and no duality violations are observed for the last bins compared to the experimental uncertainties, specially for the pinched WSRs, as expected. This is a remarkable result, since DVs are larger in the $V-A$ channel (see for example Fig. 2.3).

Even when it looks extremely unlikely, the plateau could be accidental and disappear at slightly higher values of $s_0$ where experimental data are not available, and the WSRs could be precisely satisfied just by chance. We want to gain more confidence on our numerical results and perform a reliable estimation of the uncertainties associated with DVs using Eq. (2.10). The problem is that the spectral function is experimentally unknown above $s = m_\tau^2$.

Fortunately, there are strong theoretical constraints on $\rho(s)$ that originate in the special chiral-symmetry-breaking properties of $\Pi(s)$, implying its very fast fall-off at large momenta. In addition to the two WSRs, the spectral function

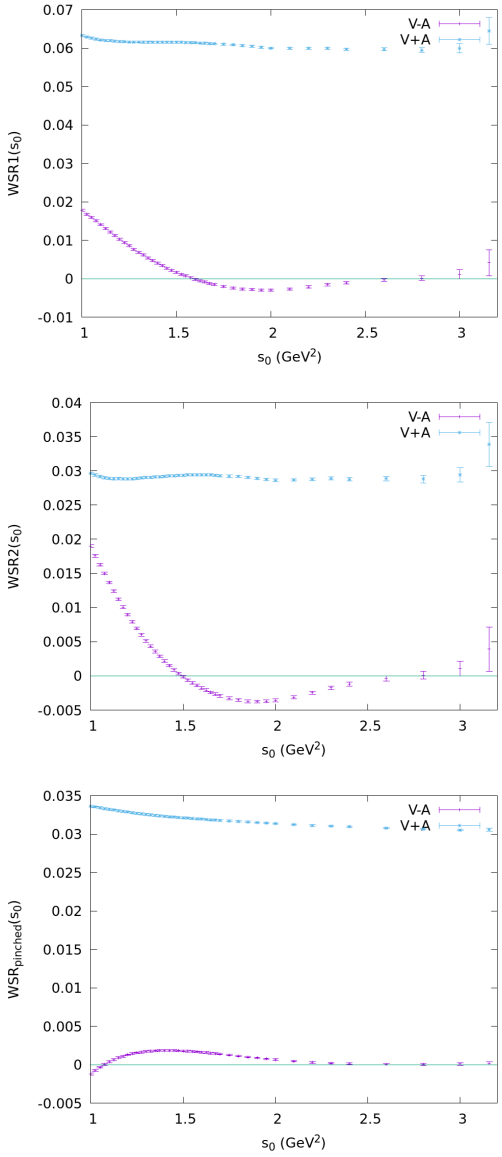


Figure 2.6: Tests of WSRs. Respectively, the first WSR, the second one and the combination of them which reduce its effects. We show the comparison with the $V + A$ channel.

should satisfy the so-called Pion Sum Rule ($\pi$SR), which determines the electromagnetic pion mass splitting in the chiral limit [68]:

$$\int_{s_{\rm th}}^{\infty} ds\; s\; \log\left(\frac{s}{\Lambda^2}\right)\; \frac{1}{\pi}\,{\rm Im}\,\Pi(s)\Big|_{m_q=0} \;=\; \left(m^2_{\pi^0}-m^2_{\pi^+}\right)_{\rm em}\; \frac{8\pi}{3\alpha}\; f^2_\pi\Big|_{m_q=0}\,. \quad (2.29)$$

Owing to the second WSR, the $\pi$SR does not depend on the arbitrary scale $\Lambda$. The rhs of this equation is well-known in Chiral Perturbation Theory ($\chi$PT) and, within the needed accuracy, we can identify in the lhs the spectral function in the chiral limit with the physical $\rho(s)$ because $m_q$ corrections are tiny.

### 2.3.1 Parametrization of the spectral function

All the theoretical and phenomenological knowledge we have about $\Pi(s)$ can be used to get an estimate of the DV uncertainties. In order to do that, we recall the ansatz for the spectral function at large values of $s$ of Eq. (2.15):

$$\rho(s>s_z) \;=\; \kappa\, e^{-\gamma s}\,\sin\{\beta(s-s_z)\}\,. \quad (2.30)$$

We will split the spectral integrations in two parts, using the experimental data in the lower energy range and the ansatz (2.30) at higher energies. From the ALEPH data we know that the $V-A$ spectral function has a zero around $s_z\sim 2$ GeV$^2$, which is represented in Eq. (2.30) through the $s_z$ parameter. We will take this zero as the separation point between the use of the data and the use of the model.

Our parametrization is compatible with the ALEPH spectral function above $s_z$. Fitting the parameters given in (2.30) to the ALEPH data in the interval $s\in(1.7\ {\rm GeV}^2, m_\tau^2)$, we obtain a very good fit with $\chi^2_{\rm min}/{\rm d.o.f.}=8.52/9$. In fact, the fit with the updated ALEPH data looks more reliable compared to the previous one, where a value of $\chi^2_{\rm min}/{\rm d.o.f.}\ll 1$ was obtained [39].

We want to stress that the exact $s$-dependence of the spectral function in the high-energy region cannot be derived from first principles. The ansatz (2.30) is just a convenient parametrization, consistent with present knowledge, that we are going to use to estimate theoretical uncertainties associated with violations of quark-hadron duality. Imposing that $\rho(s)$ should satisfy all known theoretical and experimental constraints, the free parameters in the ansatz will allow us to estimate how much freedom remains for the spectral function shape and, therefore, to obtain an additional estimate of the associated uncertainty.

There is an inherent systematic error in any work that estimates DV effects, namely the dependence on the chosen parametrization. The comparison with

other works that parametrize the data in a different way represents an important step in this regard.[†]

### 2.3.2 Selection of acceptable spectral functions

Following the procedure described in [39], we generate $3 \cdot 10^6$ tuples of the parameters $(\kappa, \gamma, \beta, s_z)$, randomly distributed in a rectangular region large enough to contain all the possible acceptable tuples. Among all generated tuples, we select those satisfying the following four physical conditions:

– The tuples must be consistent with the ALEPH data above $s = 1.7$ GeV$^2$, *i.e.*, they must be contained within the 90% C.L. region in the fit to the experimental ALEPH spectral function described before:

$$\chi^2 \; < \; \chi^2_{\rm min} \, + \, 7.78 \; = \; 16.30 \, . \tag{2.31}$$

Although we will only use the ansatz above $s_z \sim 2$ GeV$^2$, we impose the compatibility with the data from 1.7 GeV$^2$ to ensure the continuity of the spectral function in the matching region between the data and the model.

– The tuples must satisfy within the experimental uncertainties up to $s_z$ the first and second WSRs with:

$$\int_0^{s_z} ds \; \rho(s)^{\rm ALEPH} \, + \int_{s_z}^{\infty} ds \; \rho(s;\kappa,\gamma,\beta,s_z) = 17.0 \cdot 10^{-3} \, {\rm GeV}^2 \, , \tag{2.32}$$

$$\int_0^{s_z} ds \, s \, \rho(s)^{\rm ALEPH} + \int_{s_z}^{\infty} ds \; s \; \rho(s;\kappa,\gamma,\beta,s_z) = 0.24 \cdot 10^{-3} \, {\rm GeV}^4 \, , \tag{2.33}$$

where the right-hand-side errors are omitted as they are negligible compared to the left-hand-side ones. In the second WSR there are contributions of

[†] In Refs. [41, 43] the exact $s$-dependence of the resonance-based model (2.30) is assumed to be true for the $V$ and $A$ distributions separately, above $s \sim 1.55\,{\rm GeV}^2$, with channel-dependent parameters. Unfortunately, one must then perform a complex fit involving 9 parameters, including a model-dependent determination of the strong coupling, and use the parametrization near the $a_1$ resonance where it is not expected to work properly. In this way, uncertainties related to an $\alpha_s$ determination from the $V$ and $A$ spectral distributions are introduced in the analysis of the correlator $\Pi(s)$, which does not contain any perturbative contribution. As we will see in the next chapter, the resulting fit is very unstable with a dramatic dependence of the fitted parameters on the adopted assumptions. Moreover, the LECs and vacuum condensates are directly extracted from the fitted $V$ and $A$ spectral functions without imposing any further requirement, as WSRs and $\pi$SR are only checked to be satisfied within errors a posteriori, in contrast with our approach (see next subsection).

the form $\mathcal{O}(m_q^2 \alpha_s s_z)$, but they are negligible for the values of $s_z$ that we are considering.

– The tuples must satisfy within the experimental uncertainties the $\pi$SR:

$$\int_0^{s_z} ds\ s\ \log\left(\frac{s}{1\text{GeV}^2}\right) \rho(s)^{\text{ALEPH}} + \int_{s_z}^{\infty} ds\ s\ \log\left(\frac{s}{1\text{GeV}^2}\right) \rho(s;\kappa,\gamma,\beta,s_z) = -(10.9 \pm 1.3) \cdot 10^{-3}\,\text{GeV}^4\,. \tag{2.34}$$

The quoted error in the $\pi$SR takes into account that quark masses do not vanish in nature and we are using real data instead of chiral-limit one. We estimate this uncertainty taking for the pion decay constant the range $f_0 = (87 \pm 5)$ MeV [39], which includes the physical value and its estimated value in the chiral limit [69]. We also include a small uncertainty coming from the residual scale dependence of the logarithm, which is proportional to the second WSR.

We accept only those tuples that fulfill the four conditions. This requirement constrains the regions in the parameter space of the ansatz (2.30) that are compatible with both QCD and the data. From the initial set of $3 \cdot 10^6$ randomly generated tuples we obtain 3716 satisfying our set of minimal conditions. They represent the possible shapes of the spectral function beyond $s_z$, as shown in Fig. 2.7. In Fig. 2.8, we plot the statistical distribution of the parameters $(\kappa, \gamma, \beta, s_z)$ for the accepted tuples.

## 2.4 Determination of physical parameters, including DV uncertainties

For every selected tuple we have an acceptable spectral function[‡] that can be used to estimate the different physical parameters through the corresponding spectral integrals. Using Eqs. (2.22), (2.23) and (2.21) (for $n = 2, 3$) with $s_0 = s_z$, we determine $L_{10}^{\text{eff}}$, $C_{87}^{\text{eff}}$, $\mathcal{O}_6$ and $\mathcal{O}_8$ for each of the 3716 accepted tuples. The statistical distributions of the calculated parameters are shown in Fig. 2.9 (light gray).

[‡]Given by the ALEPH data below $s_z$ and by the parametrization (2.30) above that value.

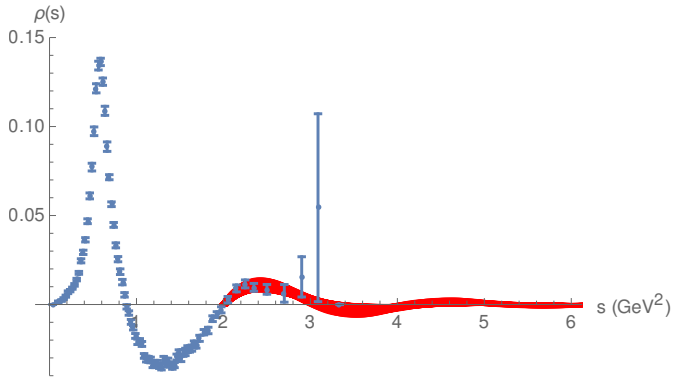


Figure 2.7: Updated ALEPH $V - A$ spectral function [46] (blue points) and all the "acceptable" spectral functions (red band above 2.0 GeV$^2$) that follow our parametrization and satisfy the physical conditions described in the main text.

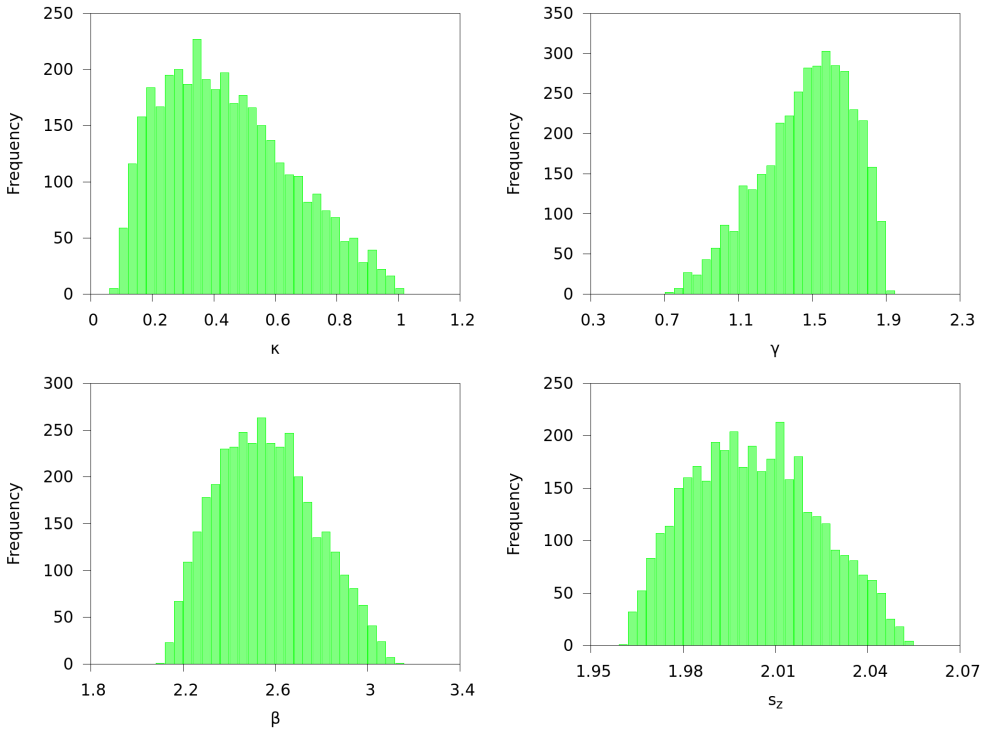


Figure 2.8: Distributions of the parameters ($\kappa$, $\gamma$, $\beta$, $s_z$) that satisfy the physical constraints. GeV units are used for dimensionful quantities.

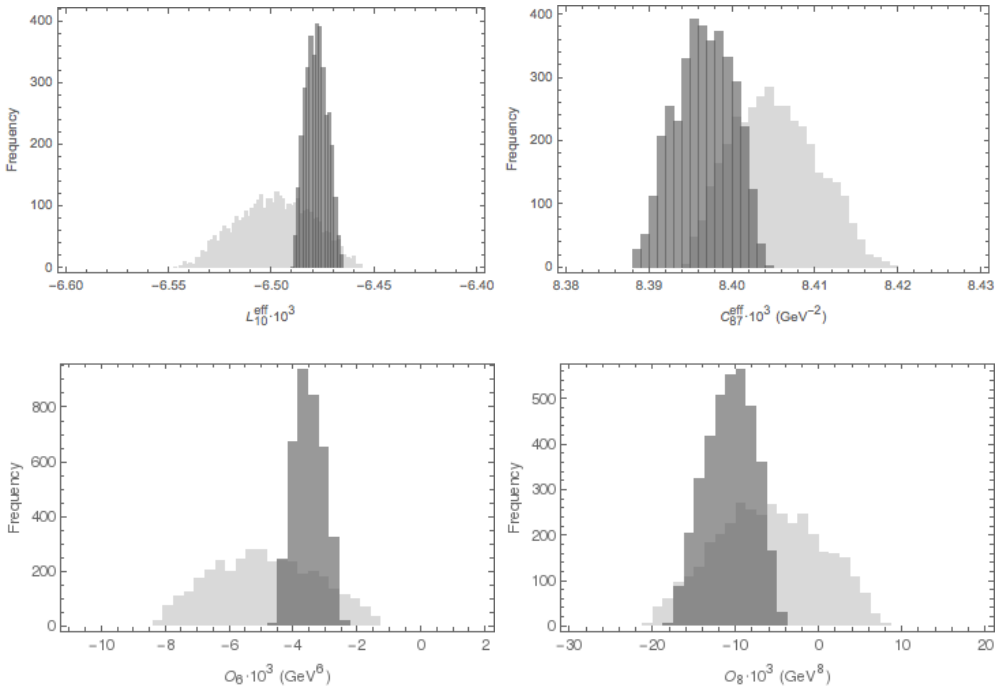


Figure 2.9: Statistical distribution of $L_{10}^{\text{eff}}$, $C_{87}^{\text{eff}}$, $\mathcal{O}_6$ and $\mathcal{O}_8$ for the tuples accepted, using $s^n$ weights (light gray) and pinched weight (dark gray) functions.

We can reduce both the experimental and the DV uncertainties using the following pinched weight functions [40]:

$$\int_{s_{\text{th}}}^{s_0} ds\, \frac{\rho(s)}{s^2}\left(1-\frac{s}{s_0}\right)^2\left(1+\frac{2s}{s_0}\right) = 16\, C_{87}^{\text{eff}} - 6\,\frac{f_\pi^2}{s_0^2} + 4\,\frac{f_\pi^2 m_\pi^2}{s_0^3} - \delta_{\text{DV}}[\omega_{-2}, s_0]\,, \tag{2.35}$$

$$\int_{s_{\text{th}}}^{s_0} ds\, \frac{\rho(s)}{s}\left(1-\frac{s}{s_0}\right)^2 = -8\, L_{10}^{\text{eff}} - 4\,\frac{f_\pi^2}{s_0} + 2\,\frac{f_\pi^2 m_\pi^2}{s_0^2} - \delta_{\text{DV}}[\omega_{-1}, s_0]\,, \tag{2.36}$$

$$\int_{s_{\text{th}}}^{s_0} ds\, \rho(s)\,(s-s_0)^2 = 2f_\pi^2 s_0^2 - 4f_\pi^2 m_\pi^2\, s_0 + 2f_\pi^2 m_\pi^4 + \mathcal{O}_6 - \delta_{\text{DV}}[\omega_2, s_0]\,, \tag{2.37}$$

$$\int_{s_{\text{th}}}^{s_0} ds\, \rho(s)\,(s-s_0)^2\,(s+2s_0) = -6f_\pi^2 m_\pi^2 s_0^2 + 4f_\pi^2 s_0^3 + 2f_\pi^2 m_\pi^6 - \mathcal{O}_8 - \delta_{\text{DV}}[\omega_3, s_0]\,. \tag{2.38}$$

Following the same method with these relations, we obtain new distributions of acceptable physical parameters, which are also shown in Fig. 2.9 (dark gray). From these new distributions we get:

$$L_{10}^{\rm eff} = (-6.477\,^{+\,0.004}_{-\,0.006} \pm 0.05)\cdot 10^{-3} = (-6.48 \pm 0.05)\cdot 10^{-3}\,, \quad (2.39)$$

$$\begin{aligned} C_{87}^{\rm eff} &= (8.399\,^{+\,0.002}_{-\,0.005} \pm 0.18)\cdot 10^{-3}\,{\rm GeV}^{-2} \\ &= (8.40 \pm 0.18)\cdot 10^{-3}\ {\rm GeV}^{-2}\,, \end{aligned} \quad (2.40)$$

$$\mathcal{O}_6 = (-3.6\,^{+\,0.5}_{-\,0.4} \pm 0.5)\cdot 10^{-3}\ {\rm GeV}^6 = (-3.6\,^{+\,1.0}_{-\,0.9})\cdot 10^{-3}\ {\rm GeV}^6\,, \quad (2.41)$$

$$\mathcal{O}_8 = (-1.0 \pm 0.3 \pm 0.2)\cdot 10^{-2}\ {\rm GeV}^8 = (-1.0 \pm 0.5)\cdot 10^{-2}\ {\rm GeV}^8\,. \quad (2.42)$$

The first errors correspond to DV uncertainties, computed from the dispersion of the histograms (corresponding to the 68% probability region) and the second errors are the experimental ones. The final uncertainties are computed from them assuming conservatively that they are 100% correlated.

We observe how in this approach pinched weight functions also reduce the DV effects, and that they are negligible for $L_{10}^{\rm eff}$ and $C_{87}^{\rm eff}$ at $s_0 \sim m_\tau^2$, compared with the experimental uncertainties. The results obtained for these two LECs are in perfect agreement with our first determinations in Eqs. (2.24) and (2.25), which did not include any estimate of DV. The corresponding spectral integrals contain weight functions with negative powers of $s$ that suppress the contribution from the upper end of the integration range, making DV negligible even without reducing them with pinched weight functions. This is no-longer true for the vacuum condensates $\mathcal{O}_6$ and $\mathcal{O}_8$, at least at energies where experimental uncertainties are not so small. The use of pinched weights is essential to suppress the contributions from the region around $s_0$ in the contour integration. This is clearly reflected in the strong reduction of uncertainties observed in the two lower panels of Fig. 2.9.

Actually, setting $DV = 0$ for the double-pinched weight functions in Eqs.(2.37) and (2.38), one obtains values for $\mathcal{O}_6$ and $\mathcal{O}_8$ that are perfectly compatible with our determinations in Eqs. (2.41) and (2.42), although with much larger experimental uncertainties. This is illustrated in Fig. 2.10, which shows how the extracted condensates stabilize at large $s_0$, around the right values but with very large error bars. The implementation of short-distance constraints (WSRs and $\pi$SR), through the procedure described in the previous section, has made possible to better pin down the spectral function in that region and obtain the more precise values in Eqs. (2.41) and (2.42).[§]

[§]In Chapter 4, some preliminary additional tests of DVs, such as the study of the dependence of the values on the point at which one assumes the parametrization becomes valid, and

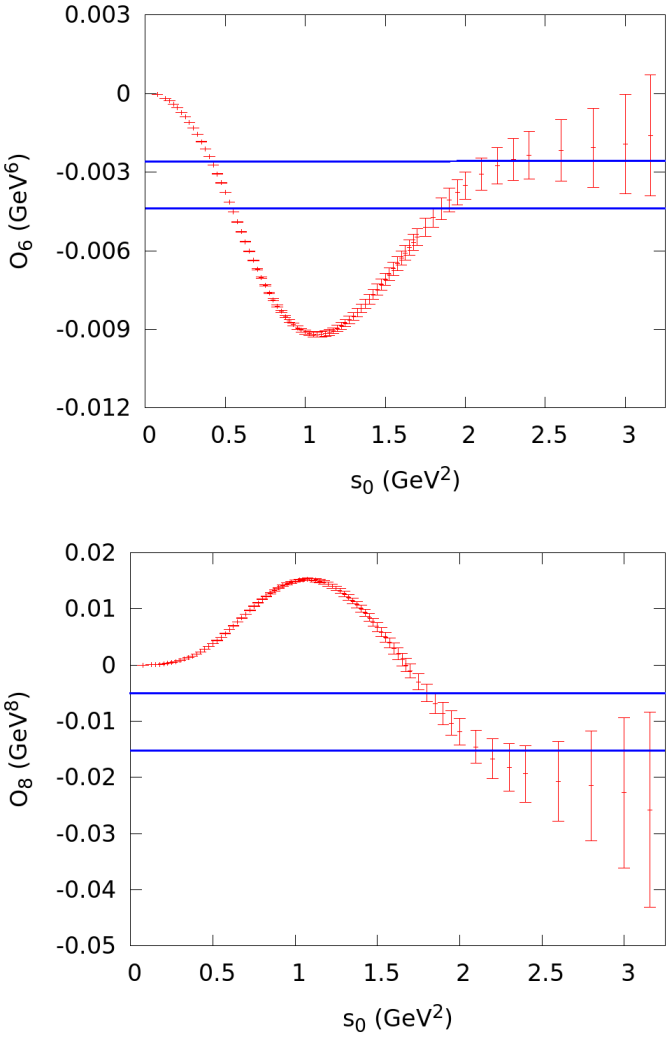


Figure 2.10: Values of the condensates $\mathcal{O}_6$ and $\mathcal{O}_8$ at different values of $s_0$ obtained from Eqs. (2.37) and (2.38) ignoring duality violations. By comparison, the values errorbars of the results obtained in Eqs. (2.41) and (2.42) are shown.

minor changes in the methods, aimed to reduce the correlation between DV and experimental uncertainties, are studied for the condensates.

| n | -2 | -1 | 0 | 1 | 2 |
|---|---|---|---|---|---|
| Experimental | 0.0083 | 0.00093 | 0.00064 | 0.00056 | 0.00051 |
| Duality | -0.00046 | -0.00047 | -0.00049 | -0.00050 | -0.0050 |

Table 2.1: Experimental uncertainties and DV contribution of the tuple with minimum $\chi^2$ for $\omega(s) = \left(\frac{s}{s_0}\right)^n$ and $s_0 = 2.8\,\text{GeV}^2$.

| $\omega(s)$ | $1-x$ | $C_{87}^{\text{eff}}$ | $L_{10}^{\text{eff}}$ | $\mathcal{O}_6$ | $R_{\tau\,V-A}$ |
|---|---|---|---|---|---|
| Experimental | 0.00013 | 0.0081 | 0.0004 | 0.000069 | 0.00012 |
| Duality | -0.00001 | -0.00001 | -0.000004 | -0.0000055 | -0.000019 |

Table 2.2: Experimental uncertainties and DV contribution at $s_0 = 2.8\,\text{GeV}^2$ of the tuple with minimum $\chi^2$ for $\omega(s) = (1-\frac{s}{s_0})^2$ and double pinched weight functions used to extract parameters.

Let us perform an additional test of the role of DVs that can be useful for the next chapter, where experimental uncertainties are lower than perturbative ones for the different moments, and also for motivating more precise experimental data, which could allow precise determinations at larger $s_0$. In Tables 2.1 and 2.2, we compare the experimental uncertainty and the DV contribution of the tuple of parameters associated with the minimum $\chi^2$ ($\chi^2_{min} = 7.78$) from $s_0 = 2.8\,\text{GeV}^2$ for several moments, the last point with an optimal experimental resolution. We find that the DV contribution is already smaller than experimental uncertainties for $\omega(s) = \left(\frac{s}{s_0}\right)^n$ when $n \leq 2$ and totally negligible when double pinching, in total agreement with the arguments based on $s_0-$stability.

Our results are in good agreement with those obtained previously in Ref. [40] with the 2005 ALEPH data set. Thus, the improvements incorporated in the 2014 release of the ALEPH data do not introduce sizable modifications of the physical outputs. Similar results have been obtained recently in Ref. [43], using also the 2014 ALEPH data set.

Ref. [43] emphasises the existence of a slight tension with the results obtained in Ref. [41] with the 1999 OPAL data set [70]. In view of this, we have repeated our numerical analyses with the OPAL spectral function [70]. As happened with the 2005 ALEPH data set, the fit of the ansatz (2.30) to the OPAL data in the interval $s \in (1.7\ \text{GeV}^2, m_\tau^2)$ has a $\chi^2_{\text{min}}/\text{d.o.f.} \ll 1$. Applying the same procedure

used for ALEPH, we have obtained the following results with the OPAL data:

$$L_{10}^{\rm eff} = (-6.42\,^{+0.10}_{-0.11})\cdot 10^{-3}\,, \tag{2.43}$$

$$C_{87}^{\rm eff} = (8.35\pm 0.29)\cdot 10^{-3}\ {\rm GeV}^{-2}\,, \tag{2.44}$$

$$\mathcal{O}_6 = (-5.7\,^{+1.5}_{-1.7})\cdot 10^{-3}\ {\rm GeV}^{6}\,, \tag{2.45}$$

$$\mathcal{O}_8 = (0.0\,^{+0.9}_{-0.7})\cdot 10^{-2}\ {\rm GeV}^{8}\,. \tag{2.46}$$

Owing to the larger uncertainties of the OPAL data, specially at higher values of $s$, the extracted parameters are less precise than those obtained with the ALEPH data. Nevertheless, comparing Eqs. (2.43)-(2.46) with (2.39)-(2.42), we observe a good agreement between both sets of results, the differences being only $0.5\,\sigma$, $0.1\,\sigma$, $1.1\,\sigma$ and $1.1\,\sigma$ for $L_{10}^{\rm eff}$, $C_{87}^{\rm eff}$, $\mathcal{O}_6$ and $\mathcal{O}_8$, respectively. We conclude that the much larger fluctuations obtained in Refs. [41, 43] between the results extracted from the two data sets are a consequence of the particular approach adopted in their DV analyses.[¶]

Finally, we can use double-pinched weight functions in order to estimate higher-dimensional condensates:

$$\int_{s_{\rm th}}^{s_0} ds\ \rho(s)\ (s-s_0)^2\,(s^2+2s_0s+3s_0^2)$$
$$= -8f_\pi^2m_\pi^2s_0^3+6f_\pi^2s_0^4+2f_\pi^2m_\pi^8+\mathcal{O}_{10}-\delta_{\rm DV}[\omega_4,s_0]\,, \tag{2.47}$$

$$\int_{s_{\rm th}}^{s_0} ds\ \rho(s)\ (s-s_0)^2\,(s^3+2s_0s^2+3s_0^2s+4s_0^3)$$
$$= -10f_\pi^2m_\pi^2s_0^4+8f_\pi^2s_0^5+2f_\pi^2m_\pi^{10}-\mathcal{O}_{12}-\delta_{\rm DV}[\omega_5,s_0]\,, \tag{2.48}$$

$$\int_{s_{\rm th}}^{s_0} ds\ \rho(s)\ (s-s_0)^2\,(s^4+2s_0s^3+3s_0^2s^2+4s_0^3s+5s_0^4)$$
$$= -12f_\pi^2m_\pi^2s_0^5+10f_\pi^2s_0^6+2f_\pi^2m_\pi^{12}+\mathcal{O}_{14}-\delta_{\rm DV}[\omega_6,s_0]\,, \tag{2.49}$$

$$\int_{s_{\rm th}}^{s_0} ds\ \rho(s)\ (s-s_0)^2\,(s^5+2s_0s^4+3s_0^2s^3+4s_0^3s^2+5s_0^4s+6s_0^5)$$
$$= -14f_\pi^2m_\pi^2s_0^6+12f_\pi^2s_0^7+2f_\pi^2m_\pi^{14}-\mathcal{O}_{16}-\delta_{\rm DV}[\omega_7,s_0]\,. \tag{2.50}$$

[¶]Since DV is not very relevant for the extraction of the LECs, Refs. [41, 43] obtain similar values for $L_{10}^{\rm eff}$ and $C_{87}^{\rm eff}$ with the two data sets. However, sizable differences show up in their determinations of $\mathcal{O}_6$ and $\mathcal{O}_8$ where DV is more important.

| $10^3 \cdot L_{10}^{\rm eff}$ | $10^3 \cdot C_{87}^{\rm eff}$ ($\mathrm{GeV}^{-2}$) | $10^3 \cdot \mathcal{O}_6$ ($\mathrm{GeV}^6$) | $10^2 \cdot \mathcal{O}_8$ ($\mathrm{GeV}^8$) | Reference | Comments |
|---|---|---|---|---|---|
| $-6.45 \pm 0.06$ | – | $-2.3 \pm 0.6$ | $-5.4 \pm 3.3$ | BPDS'06 [35] | ALEPH'05 + DV=0 |
| – | – | $-6.8\,^{+\,2.0}_{-\,0.8}$ | $3.2\,^{+\,2.8}_{-\,9.2}$ | ASS'08 [37] | ALEPH'05 + DV=0 |
| $-6.48 \pm 0.06$ | $8.18 \pm 0.14$ | – | – | GPP'08 [38] | ALEPH'05 + DV=0 |
| $-6.44 \pm 0.05$ | $8.17 \pm 0.12$ | $-4.4 \pm 0.8$ | $-0.7 \pm 0.5$ | GPP'10 [39, 40] | ALEPH'05 + $\mathrm{DV}_{V-A}$ |
| $-6.45 \pm 0.09$ | $8.47 \pm 0.29$ | $-6.6 \pm 1.1$ | $0.5 \pm 0.5$ | Boito'12 [41] | OPAL'99 + $\mathrm{DV}_{V/A}$ |
| $-6.50 \pm 0.10$ | – | $-5.0 \pm 0.7$ | $-0.9 \pm 0.5$ | DHSS'15 [42] | ALEPH'14 + DV=0 |
| $-6.45 \pm 0.05$ | $8.38 \pm 0.18$ | $-3.2 \pm 0.9$ | $-1.3 \pm 0.6$ | Boito'15 [43] | ALEPH'14 + $\mathrm{DV}_{V/A}$ |
| $-6.42\,^{+0.10}_{-0.11}$ | $8.35 \pm 0.29$ | $-5.7\,^{+1.5}_{-1.7}$ | $0.0\,^{+0.9}_{-0.7}$ | this work | OPAL'99 + $\mathrm{DV}_{V-A}$ |
| $-6.48 \pm 0.05$ | $8.40 \pm 0.18$ | $-3.6\,^{+\,1.0}_{-\,0.9}$ | $-1.0 \pm 0.5$ | this work | ALEPH'14 + $\mathrm{DV}_{V-A}$ |

Table 2.3: Compilation of recent determinations of the LECs and vacuum condensates.

Using these equations with the same method, we obtain from the ALEPH data:

$$\mathcal{O}_{10} = (5.6 \pm 1.2 \pm 0.8) \cdot 10^{-2}\ \mathrm{GeV}^{10} = (5.6 \pm 2.0) \cdot 10^{-2}\ \mathrm{GeV}^{10}\,, \quad (2.51)$$

$$\mathcal{O}_{12} = (-0.13\,^{+\,0.03}_{-\,0.05} \pm 0.02)\ \mathrm{GeV}^{12} = (-0.13\,^{+\,0.05}_{-\,0.07})\ \mathrm{GeV}^{12}\,, \quad (2.52)$$

$$\mathcal{O}_{14} = (0.24\,^{+\,0.11}_{-\,0.05} \pm 0.06)\ \mathrm{GeV}^{14} = (0.24\,^{+\,0.17}_{-\,0.11})\ \mathrm{GeV}^{14}\,, \quad (2.53)$$

$$\mathcal{O}_{16} = (-0.38\,^{+\,0.25}_{-\,0.10} \pm 0.13)\ \mathrm{GeV}^{14} = (-0.38\,^{+\,0.38}_{-\,0.23})\ \mathrm{GeV}^{16}\,. \quad (2.54)$$

However, the model dependence is stronger for these condensates and our confidence in the quoted uncertainties weaker.

### 2.4.1 Comparison with previous works

Our final results for $L_{10}^{\rm eff}$, $C_{87}^{\rm eff}$, $\mathcal{O}_6$ and $\mathcal{O}_8$ are compared in Table 2.3 with recent (post-2005) phenomenological determinations of these parameters, obtained with different data sets [44, 46, 70] and various DV parametrizations.[‖]

There is an excellent agreement among the different values quoted for the effective LECs $L_{10}^{\rm eff}$ and $C_{87}^{\rm eff}$, showing that these determinations are very solid and do not get affected by DV effects. In fact, as shown in Table 2.3, the precision has not changed in the last ten years. Nonetheless, the robustness of these determinations has increased significantly thanks to the thorough studies of DV effects

[‖] A complete list including theoretical estimates [71–73] and previous phenomenological determinations of these quantities (and of higher-dimensional condensates) [29–34,36,44,70,74–79] can be found in Refs. [9, 40].

with different approaches. The values obtained from different data sets are also in good agreement, although one can notice a difference of $1\,\sigma$ between the $C_{87}^{\rm eff}$ from the updated (2014) ALEPH data comparing with the old one (2005).

The different results for $\mathcal{O}_6$ and $\mathcal{O}_8$ are also in reasonable agreement, within the quoted uncertainties. A good control of DV effects is more important for these vacuum condensates. The use of pinched weights allows to sizably reduce their impact and obtain more reliable determinations. With the ALEPH'14 data one reaches a 30 % accuracy for $\mathcal{O}_6$, but the error remains still large (50 %) for $\mathcal{O}_8$. As commented before, we do not see any significant discrepancy between the results obtained from the OPAL and ALEPH data samples.

## 2.5 $\chi$PT couplings

The effective couplings $L_{10}^{\rm eff}$ and $C_{87}^{\rm eff}$ can be rewritten in terms of $\mathcal{O}(p^4)$ and $\mathcal{O}(p^6)$ couplings of the $\chi$PT Lagrangian [38, 66]:

$$\begin{aligned} L_{10}^{\rm eff} &\equiv -\frac{1}{8}\,\overline{\Pi}(0) \\ &= L_{10}^r(\mu) \,+\, \frac{1}{128\,\pi^2}\left[1-\log\left(\frac{\mu^2}{m_\pi^2}\right) \,+\, \frac{1}{3}\,\log\left(\frac{m_K^2}{m_\pi^2}\right)\right] \\ &- \frac{1}{8}\,(\mathcal{C}_0^r+\mathcal{C}_1^r)\,(\mu) - 2\,(2\mu_\pi+\mu_K)\,(L_9^r+2L_{10}^r)(\mu) \,+\, G_{2L}(\mu,s=0) \\ &+ \mathcal{O}(p^8)\,, \end{aligned} \tag{2.55}$$

$$\begin{aligned} C_{87}^{\rm eff} &\equiv \frac{1}{16}\,\overline{\Pi}\,'(0) \\ &= C_{87}^r(\mu) \,-\, \frac{1}{64\,\pi^2 f_\pi^2}\left[1-\log\left(\frac{\mu^2}{m_\pi^2}\right) \,+\, \frac{1}{3}\,\log\left(\frac{m_K^2}{m_\pi^2}\right)\right] L_9^r(\mu) \\ &+ \frac{1}{7680\,\pi^2}\left(\frac{1}{m_K^2}+\frac{2}{m_\pi^2}\right) - \frac{1}{2}\,G'_{2L}(\mu,s=0) \,+\, \mathcal{O}(p^8)\,, \end{aligned} \tag{2.56}$$

where $\overline{\Pi}$ is the pion subtracted correlator, the factors $\mu_i = m_i^2\log(m_i/\mu)/(16\pi^2 f_\pi^2)$ originate from one-loop corrections and $G_{2L}(\mu,s=0)$ and $G'_{2L}(\mu,s=0)$ are two-loop functions, whose numerical values are given in the App. A. We have also defined

$$\mathcal{C}_0^r = 32\,m_\pi^2\,(C_{12}-C_{61}+C_{80})\,, \tag{2.57}$$

$$\mathcal{C}_1^r = 32\,(m_\pi^2+2m_K^2)\,(C_{13}-C_{62}+C_{81})\,. \tag{2.58}$$

To first approximation the effective parameters correspond to the chiral couplings $L_{10}$ and $C_{87}$, which appear at $\mathcal{O}(p^4)$ and $\mathcal{O}(p^6)$, respectively, in the $\chi$PT expansion. The scale dependence of $L_{10}^r(\mu)$ is canceled by the one-loop logarithmic terms in the second line of Eq. (2.55), which are suppressed by one power of $1/N_C$ with respect to $L_{10}^r(\mu)$, where $N_C$ is the number of QCD colors. The remaining contributions in Eq. (2.55) contain the $\mathcal{O}(p^6)$ corrections, which unfortunately introduce other $\mathcal{O}(p^6)$ and $\mathcal{O}(p^4)$ chiral couplings (third line). The corrections to $C_{87}^r(\mu)$ in Eq. (2.56) only involve one additional LEC, $L_9^r(\mu)$, through a one-loop correction with the $\mathcal{O}(p^4)$ chiral Lagrangian.

It is convenient to give the following compact numerical form of these equations to ease their future use:

$$L_{10}^{\rm eff} = L_{10}^r - 0.00126 + \mathcal{O}(p^6) \,, \tag{2.59}$$

$$L_{10}^{\rm eff} = 1.53\, L_{10}^r + 0.263\, L_9^r - 0.00179 - \frac{1}{8}\,(\mathcal{C}_0^r + \mathcal{C}_1^r) + \mathcal{O}(p^8) \,, \tag{2.60}$$

$$C_{87}^{\rm eff} = C_{87}^r + 0.296\, L_9^r + 0.00155 + \mathcal{O}(p^8) \,, \tag{2.61}$$

where we have used $\mu = M_\rho$ as the reference value for the $\chi$PT renormalization scale. The uncertainties in these numbers are much smaller than those affecting the different LECs and can therefore be neglected.

Working with $\mathcal{O}(p^4)$ precision, the determination of $L_{10}^r(\mu)$ is straightforward and we find:

$$L_{10}^r(M_\rho) = -(5.22 \pm 0.05) \cdot 10^{-3} \qquad [\mathcal{O}(p^4) \text{ analysis}] \,. \tag{2.62}$$

As mentioned before, an $\mathcal{O}(p^6)$ determination of $L_{10}^r$ requires to know some next-to-next-to-leading-order (NNLO) LECs,** namely those in $\mathcal{C}_{0,1}^r$. This has motivated some interest in these quantities in the last few years. Here we briefly review the different approaches.

In the first $\mathcal{O}(p^6)$ determination of $L_{10}^r$ [38], $\mathcal{C}_0^r$ was extracted from a combination of phenomenological ($C_{61,12}^r$) [81–84] and theoretical ($C_{80}^r$, R$\chi$T) [66, 85]

**It also requires $L_9^r$, which we take from Ref. [80]: $L_9^r(M_\rho) = 5.93\ (43) \cdot 10^{-3}$. Let us notice that this is the value used also in all other $\mathcal{O}(p^6)$ extractions of $L_{10}^r$ from tau data.

| $L_{10}^r(M_\rho)$ $\times 10^3$ | $\mathcal{C}_0^r(M_\rho)$ $\times 10^3$ | $\mathcal{C}_1^r(M_\rho)$ $\times 10^3$ | Reference | Input |
|---|---|---|---|---|
| -4.06 (39) | +0.54 (42) | 0 (5) | GPP'08 [38] | $\Pi(0) + \mathcal{C}_0^{\text{pheno/R}\chi\text{T}} + 1/N_c$ |
| -3.10 (80) | -0.81 (82) | 14 (10) | Boito'12 [41] | $\Pi(0) + \Pi(s)_{\text{latt}}$ |
| -3.46 (32) | -0.34 (13) | 8.1 (3.5) | Boyle'14, GMP'14 [84,86] | $\Pi(0) + \Pi(s)_{\text{latt}} + \Delta\Pi(0)$ |
| -3.50 (17) | -0.35 (10) | 7.5 (1.5) | Boito'15 [43] | $\Pi(0) + \Pi(s)_{\text{latt}} + \Delta\Pi(0)$ |
| -4.08 (44) | +0.21 (34) | 0 (5) | this work | $\Pi(0) + \mathcal{C}_0^{\text{pheno/R}\chi\text{T}} + 1/N_c$ |
| -4.17 (35) | -0.43 (12) | -1 (6) | this work | $\Pi(0) + \Delta\Pi(0) + 1/N_c$ |

Table 2.4: Compilation of recent determinations of the LECs. The determinations of $L_{10}^{\text{eff}}$, *i.e.* $\Pi(0)$, are obtained as explained in Table 2.3. $1/N_c$ refers to Eq. (2.66), whereas $\Delta\Pi(0)$ refers to the sum rule given in Eq. (2.67). Additional details are given in the text.

inputs, namely[††]

$$C_{61}^r(M_\rho) = (1.7 \pm 0.6) \cdot 10^{-3}\ \text{GeV}^{-2} \quad [81,83,84]\,, \tag{2.63}$$

$$C_{12}^r(M_\rho) = (0.4 \pm 6.3) \cdot 10^{-5}\ \text{GeV}^{-2} \quad [82]\,, \tag{2.64}$$

$$C_{80}^r(M_\rho) = (2.1 \pm 0.5) \cdot 10^{-3}\ \text{GeV}^{-2} \quad [66,85]\,, \tag{2.65}$$

whereas $\mathcal{C}_1^r$, which was completely unknown at the time, was estimated using

$$|C_{62}^r - C_{13}^r - C_{81}^r| \;\leq\; \frac{1}{3}\,|C_{61}^r - C_{12}^r - C_{80}^r|\,, \tag{2.66}$$

*i.e.*, a simple educated guess based on the fact that those LECs are suppressed by a factor $1/N_C$. Using these numbers and Eq. (2.60), we obtain the results shown in Table 2.4 (5th row) and Fig. 2.11 (magenta point), which supersede those found in Ref. [38].

[††]This value of $C_{61}^r$ comes from a flavour-breaking finite-energy sum rule involving the correlator $\overline{\Pi}^{(0+1)}_{ud-us,VV}(0)$. The original result [81] has been updated recently [84], finding

$$32\,(m_K^2 - m_\pi^2)\,C_{61} + 1.06\,L_{10}^r \;=\; 0.00727\ (134)\ .$$

Since $L_{10}^r$ appears in this relation only at one loop, *i.e.* at $\mathcal{O}(p^6)$, we can use here an $\mathcal{O}(p^4)$ determination of $L_{10}^r$ to extract $C_{61}^r$. We can indeed see that the $L_{10}^r$ contribution to the $C_{61}^r$ error is subdominant. We use the conservative value $L_{10}^r = -0.0052\ (17)$ to extract $C_{61}^r$.

An alternative sum rule involving $L_{10}^r$ and $\mathcal{C}_0^r$ was recently derived in Ref. [84] from an analysis of the flavour-breaking left-right correlator $\overline{\Pi}^{(0+1)}_{ud-us,LR}(0)$, namely[‡‡]

$$\left[\overline{\Pi}^{(0+1)}_{ud,LR}(0) - \overline{\Pi}^{(0+1)}_{us,LR}(0)\right]_{\rm LEC} = -0.7218\, L_5^r + 1.423\, L_9^r + 2.125\, L_{10}^r - \frac{m_K^2 - m_\pi^2}{m_\pi^2}\, \mathcal{C}_0^r$$
$$= 0.0113\ (15)\,, \qquad (2.67)$$

again at $\mu = M_\rho$. Combining this constraint with the sum rule* in Eq. (2.60) and the naive inequality in Eq. (2.66), we obtain the results shown in Table 2.4 (6th row) and Fig. 2.11 (dark blue region). We see that $L_{10}^r$ is in excellent agreement with the value obtained using Eqs. (2.63-2.65) and has a smaller error. Concerning the NNLO LECs, almost the same value is obtained for $\mathcal{C}_1^r$, whereas a 1.8 $\sigma$ tension is present in the $\mathcal{C}_0^r$ case.

Another interesting development was performed in Ref. [86], where additional constraints on $L_{10}^r$, $\mathcal{C}_0^r$ and $\mathcal{C}_1^r$ were obtained from lattice simulations of the correlator $\overline{\Pi}(s)$ at unphysical meson masses. As shown in Table 2.4, the lattice data allow for a more accurate determination of the LECs, making unnecessary the use of the naive guess in Eq. (2.66). However, to derive the lattice constraints one needs to assume that the $\mathcal{O}(p^6)$ $\chi$PT expansion reproduces well the correlator at $s \sim -0.25\,\text{GeV}^2$, the energy region with smaller lattice uncertainties, which dominates these constraints. Unfortunately, it was shown in Ref. [41] that $\mathcal{O}(p^6)$ $\chi$PT does not approximate well enough $\overline{\Pi}(s)$ at these energies, taking into account the low uncertainties we are dealing with, and one needs to incorporate the so-far unknown $\mathcal{O}(p^8)$ chiral corrections.

In order to take advantage of the most precise lattice constraint, Ref. [43] makes the strong assumption that the missing $\mathcal{O}(p^8)$ chiral contributions are dominated by mass-independent terms, *i.e.*, $\overline{\Pi}(s) \approx \overline{\Pi}^{\chi\rm PT}_{\mathcal{O}(p^6)} + D\, s^2$, so that they cancel in the lattice-continuum difference $\Pi^{\chi\rm PT}_{\rm lattice} - \Pi^{\chi\rm PT}_{\rm physical}$. It is worth noting that this is not a good approximation at the previous chiral order, $\mathcal{O}(p^6)$, since more than 25% of the $\mathcal{O}(p^6)$ correction proportional to $s$ comes from known mass-dependent chiral terms. Therefore, the uncertainties associated with these lattice constraints seem at present underestimated.

[‡‡]We use the value obtained in Ref. [84] using 1999 OPAL data for the non-strange part, 0.0113 (15), instead of the more precise value of Ref. [43] from 2014 ALEPH data, 0.0111 (11), in order to avoid possible correlations with our determination of $L_{10}^{\rm eff}$.

*We use $L_5^r(M_\rho) = (1.19 \pm 0.25) \cdot 10^{-3}$ [87] and, once again, $L_9^r(M_\rho) = 5.93\ (43) \cdot 10^{-3}$ [80].

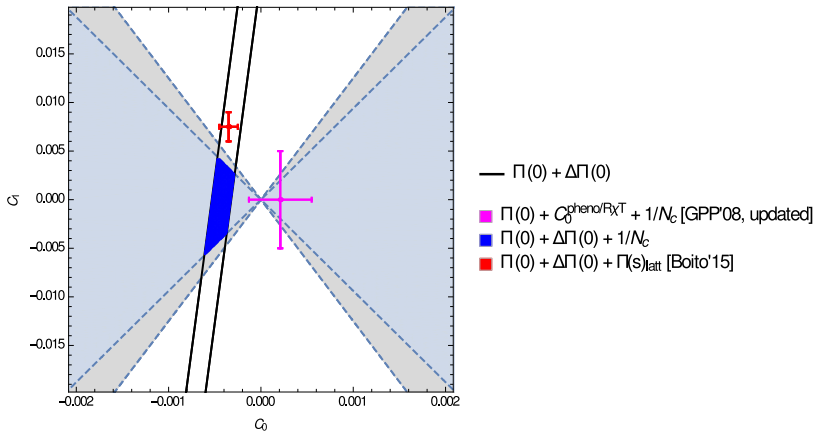


Figure 2.11: Latest determinations of the linear combinations of NNLO LECs $\mathcal{C}^r_{0,1}$, at $\mu = M_\rho$. We follow the same notation as in Table 2.4. The region allowed by the inequality of Eq. (2.66), inspired by large-$N_c$ arguments, is indicated in light blue, whereas the light gray area around it (dashed) simply represents a naive estimate of its error, namely 33%.

Additionally, correlations between the continuum and the lattice sum rules (*e.g.* due to $L^r_9$) are not publicly available. It is worth mentioning nonetheless that if we implement these lattice constraints[†] (instead of the inequality in Eq. (2.66)), neglecting such correlations, we reproduce the results of Ref. [43] except for the uncertainties associated to $L^r_5$ and $L^r_9$, for which the neglected correlations are likely to be relevant. Such an agreement is not surprising, as our determinations of the effective coupling $L^{\rm eff}_{10}$ were very close.

From Table 2.4 and Fig. 2.11 we see that the determinations obtained with the lattice constraints are (in most cases) significantly more precise than those using instead the inequality of Eq. (2.66). The agreement is reasonable (in the $0.5 - 1.7\,\sigma$ range depending on the quantity), taking into account that Eq. (2.66) is nothing but a naive educated guess, while the lattice improvement suffers from additional uncertainties not yet included in the quoted errors.

The determination of $C^r_{87}$ from $C^{\rm eff}_{87}$ at $\mathcal{O}(p^6)$ does not involve any unknown LEC. The relation (2.56) contains a one-loop correction of size $-(3.16 \pm 0.13) \cdot 10^{-3}$, which only depends on $L^r_9(M_\rho)$ and the pion and kaon masses, and small non-analytic two-loop contributions collected in the term $G'_{2L}(M_\rho, s = 0) =$

[†]We find that the constraint associated to the third lattice ensemble used in [43] fully dominates the fits.

$-0.28 \cdot 10^{-3}$ GeV$^{-2}$. In spite of its $1/N_C$ suppression, the one-loop correction is very sizable, decreasing the final value of the $\mathcal{O}(p^6)$ LEC:

$$C_{87}^r(M_\rho) \;=\; (5.10 \pm 0.22) \cdot 10^{-3}\ \text{GeV}^{-2}\,. \tag{2.68}$$

### 2.5.1 Previous determinations with other methods

Our phenomenological determinations of $L_{10}^r(M_\rho)$ and $C_{87}^r(M_\rho)$ from $\tau$ decay data are in good agreement with the large-$N_C$ estimates based on lowest-meson dominance [66, 88–92]:

$$\begin{aligned} L_{10} &= -\frac{F_V^2}{4M_V^2} + \frac{F_A^2}{4M_A^2} \;\approx\; -\frac{3f_\pi^2}{8M_V^2} \;\approx\; -5.4 \cdot 10^{-3}\,, \\ C_{87} &= \frac{F_V^2}{8M_V^4} - \frac{F_A^2}{8M_A^4} \;\approx\; \frac{7f_\pi^2}{32M_V^4} \;\approx\; 5.3 \cdot 10^{-3}\ \text{GeV}^{-2}\,. \end{aligned} \tag{2.69}$$

They also agree with the $C_{87}$ determinations based on Pade approximants [72,93], which are however unable to fix the renormalization-scale dependence that is of higher-order in $1/N_C$.

The resonance chiral theory (R$\chi$T) Lagrangian [89,90,94,95] was used to analyze the left-right correlator at NLO in the $1/N_C$ expansion in Ref. [73]. Matching the effective field theory description with the short-distance QCD behavior, both LECs are determined, keeping full control of their $\mu$ dependence. The predicted values [73]

$$\begin{aligned} L_{10}^r(M_\rho) &= -(4.4 \pm 0.9) \cdot 10^{-3}\,, \\ C_{87}^r(M_\rho) &= (3.6 \pm 1.3) \cdot 10^{-3}\ \text{GeV}^{-2}\,, \end{aligned} \tag{2.70}$$

are in good agreement with our determinations, although they are less precise.

Lattice determinations of the $\chi$PT LECs have improved considerably in recent times, although they are still limited to $\mathcal{O}(p^4)$ accuracy. The most recent simulations find:

$$L_{10}^r(M_\rho) \;=\; \begin{cases} -(5.7 \pm 1.1 \pm 0.7) \cdot 10^{-3} & [96]\,, \\ -(5.2 \pm 0.2\,^{+\,0.5}_{-\,0.3}) \cdot 10^{-3} & [97]\,. \end{cases} \tag{2.71}$$

These lattice results are in good agreement with our determinations, but their accuracy is still far from the phenomenological precision.

## 2.6 Conclusions

We have determined the LECs $L_{10}^{\rm eff}$ and $C_{87}^{\rm eff}$, using the recently updated ALEPH spectral functions [46], with the methods developed in Refs. [38–40]. Our final values, obtained using pinched weight functions with a statistical analysis that includes possible DV uncertainties, are:

$$L_{10}^{\rm eff} = (-6.48 \pm 0.05) \cdot 10^{-3} \,, \tag{2.72}$$

$$C_{87}^{\rm eff} = (8.40 \pm 0.18) \cdot 10^{-3} \ {\rm GeV}^{-2} \,. \tag{2.73}$$

These results are in excellent agreement with the values extracted with non-pinched weights and with those determined neglecting DV in Eqs. (2.24) and (2.25). Thus, DV does not play any significant role in the determination of LECs, where the weight functions strongly suppress the high energy region of the spectral integrations. Our results are in good agreement with the ones obtained previously with the 2005 release of the ALEPH $\tau$ data [40]:

$$L_{10}^{\rm eff} = (-6.44 \pm 0.05) \cdot 10^{-3} \,, \tag{2.74}$$

$$C_{87}^{\rm eff} = (8.17 \pm 0.12) \cdot 10^{-3} \ {\rm GeV}^{-2} \,. \tag{2.75}$$

The improvements introduced in the 2014 ALEPH data set did not bring major changes in these parameters. The values in Eqs. (2.72) and (2.73) also agree with the results obtained recently with the same experimental data but with a different approach in Ref. [43].

The statistical approach adopted in our analysis allows for a precise determination of the dimension-6 and 8 terms in the OPE of the left-right correlator $\Pi(s)$. We obtain:

$$\mathcal{O}_6 = (-3.6\, ^{+\,1.0}_{-\,0.9}) \cdot 10^{-3} \ {\rm GeV}^6 \,, \tag{2.76}$$

$$\mathcal{O}_8 = (-1.0 \pm 0.5) \cdot 10^{-2} \ {\rm GeV}^8 \,, \tag{2.77}$$

also compatible with the determinations performed in Refs. [40] (with non-updated ALEPH data) and [43] (with a different approach for estimating DV effects). Using the same method, some higher-dimensional terms in the OPE have also being estimated in Eqs. (2.51)-(2.54).

The numerical determination of the effective couplings $L_{10}^{\rm eff}$ and $C_{87}^{\rm eff}$ has allowed us to derive the corresponding LECs of the $\chi$PT Lagrangian. At $\mathcal{O}(p^6)$,

we find

$$L_{10}^r(M_\rho) = -(4.1 \pm 0.4) \cdot 10^{-3}\,, \tag{2.78}$$
$$C_{87}^r(M_\rho) = (5.10 \pm 0.22) \cdot 10^{-3}\,\mathrm{GeV}^{-2}\,. \tag{2.79}$$

The final value quoted for $L_{10}^r(M_\rho)$ takes into account our two different estimates in Table 2.4, keeping conservatively the individual errors in view of the present uncertainties induced by the NLO LECs.

# Chapter 3

# Determination of the QCD Coupling from ALEPH $\tau$ Decays

## 3.1 Introduction

In the previous chapter we made a comprehensive study of the phenomenology of the $\Pi^{(1+0)}_{V-A}(s)$ correlator. When studying the separate $\Pi^{(1+0)}_{V}(s)$ and $\Pi^{(1+0)}_{A}(s)$ ones, the formalism is basically the same. Eq. (2.8) can be rewritten as:

$$A^{\omega}_{V/A}(s_0) \equiv \int_{s_{th}}^{s_0} \frac{ds}{s_0}\omega(s)\,\mathrm{Im}\,\Pi_{V/A}(s) = \frac{i}{2}\oint_{|s|=s_0}\frac{ds}{s_0}\omega(s)\Pi_{V/A}(s)\,, \tag{3.1}$$

where $\omega(s)$ is required to be analytic at least in the same complex region as $\Pi(s)$ and $s_{th}$ is the hadronic threshold ($s_{th} = m_\pi^2$). We have absorbed absorbing the pion contribution into $\mathrm{Im}\,\Pi^{(0)}_{A}(s)$. Then again, for large enough values of $s_0$, the correlator in the integral along the circumference can be approximated by its OPE and the differences are called quark-hadron duality violations (DVs). The big difference with the $V-A$ case is that, as long as $s_0$ is large enough so the OPE makes sense, the purely perturbative contribution fully dominates the prediction for any $A^{\omega}_{V/A}$. This is specially true for the inclusive ratio:

$$R_\tau \;=\; \frac{\Gamma[\tau^- \to \nu_\tau \mathrm{hadrons}]}{\Gamma[\tau^- \to \nu_\tau e^- \overline{\nu}_e]}\,, \tag{3.2}$$

which in the SM, making use of Eq. (1.31), gives

$$R_\tau \;=\; 12\pi\,|V_{ud}|^2 S_{\rm ew}\left(A_{V+A}^{(\omega_\tau)} - 4\pi\frac{m_\pi^2}{m_\tau^2}\left(1-\frac{m_\pi^2}{m_\tau^2}\right)^2\frac{f_\pi^2}{m_\tau^2}\right)\,, \tag{3.3}$$

where:

$$\omega_\tau(s) = \left(1-\frac{s}{m_\tau^2}\right)^2\left(1+2\frac{s}{m_\tau^2}\right)\,. \tag{3.4}$$

Neglecting small logarithmic corrections coming from the $D \neq 0$ part of the OPE, which are suppressed by extra powers of $\alpha_s$, the first non-perturbative correction to $R_\tau$ comes from $\mathcal{O}_6$. Taking into account that the value of $\mathcal{O}_{6\,V+A}$ should be of the same order or even smaller than $\mathcal{O}_{6\,V-A}$, which we obtained before and that indeed, as we will see in Chapter 4, it can be obtained from the lattice by invoking relations in the chiral limit ($\mathcal{O}(p^0)$), one expects a very small power correction at the tau mass (1% of $R_\tau$, which roughly translates into a 5% to $\alpha_s(m_\tau)$).

There are strong reasons to state that DVs are completely negligible for $R_\tau$ compared to experimental or other theoretical uncertainties. First, the kinematic function $\omega_\tau(s)$ presents a double-pinch suppression thah considerably reduces DVs, as expected from pure theoretical grounds and checked with $V-A$ data in the previous chapter. Additionally, using $R_\tau$ we are in $s_0 = m_\tau^2$, a large enough value to have many hadronic thresholds opened, so that one is far from the resonance saturation regime and then one expects an optimal quark-hadron duality. This multiplicity is enhanced by the fact that $R_\tau$ is taking the fully inclusive non-strange $V+A$ spectral function. The expected DV suppression of $V+A$ with respect to $V-A$ can be checked where data are available (Figure 2.3).

Since this is an important point let us assess a numerical estimate of this suppression. As we previously studied,

$$\begin{aligned}\Delta A_{V/A}^{\omega,\rm DV}(s_0) \;&\equiv\; \frac{1}{2\pi i}\oint_{|s|=s_0}\frac{ds}{s_0}\,\omega(s)\,\Big[\Pi(s)-\Pi^{\rm OPE}(s)\Big]\\ &=\; \int_{s_0}^{\infty}\frac{ds}{s_0}\,\omega(s)\,(\rho-\rho^{OPE})(s)\,.\end{aligned} \tag{3.5}$$

Since they are expected (and observed in the region where we have data available) to go to zero very fast, typically exponentially, DVs are dominated by the region close to $s_0$ in Eq. (3.5). One natural magnitude to estimate the suppression of DVs in the $V+A$ channel with respect to the $V-A$ is then, provided the

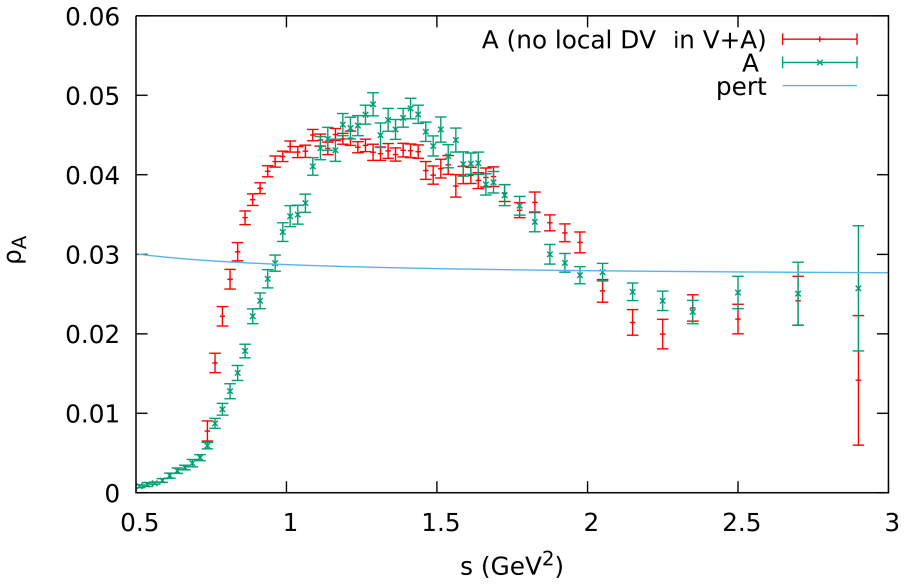


Figure 3.1: Experimental axial spectral function compared to the one obtained just using the vectorial one plus the rough assumption that V+A DVs are 0.

difference $2.8\,\mathrm{GeV}^2 - s_0$ is large enough:

$$\Delta_{rel} \equiv \frac{\int_{s_0}^{2.8\,\mathrm{GeV}^2} \frac{ds}{s_0} |\rho_{V+A} - \rho_{V+A}^{OPE}|(s)}{\int_{s_0}^{2.8\,\mathrm{GeV}^2} \frac{ds}{s_0} |\rho_{V-A} - \rho_{V-A}^{OPE}|(s)} \,. \tag{3.6}$$

Taking a large interval of $s_0$-values ($s_0 \in (1, 1.7)\,\mathrm{GeV}^2$), one finds that the ratio is always $\Delta_{rel} \approx 0.2$, in total agreement with the expected suppression. Nicely, one can predict the resonant $A$ spectrum in a decent approximation just using $V$ data and assuming that DVs in the more inclusive V+A channel are 0. This is illustrated in Figure 3.1. Notice how this precious model-independent suppression is lost in any DV study based on a semi-inclusive channel. Theoretically motivated models able to explain this suppression would be welcomed.

The suppression is rather clear and should be expected, because of the same theoretical reasons, at larger energies (although certainly not necessarily so large). Taking into account that different short-distance constraints were already satisfied in the $V - A$ channel within experimental uncertainties when $s_0 \sim m_\tau^2$ and that indeed experimental uncertainties are typically lower than perturbative ones, it

is very unlikely that the role of DV uncertainties becomes dominant if the high-energy tail is not very enhanced. Since $R_\tau$, as explained before, indeed efficiently suppresses it, its numerical role should be completely negligible.

A very naive, but certainly reliable, estimate of the non-perturbative correction to $R_\tau$ is taking $\mathcal{O}_{6V+A} = 0 \pm |\mathcal{O}_{6V-A}|$ to get:

$$\delta_{NP} = 4\pi^2 \left(-3\frac{\mathcal{O}_6}{m_\tau^6} - 2\frac{\mathcal{O}_8}{m_\tau^8}\right) - 16\pi^2 \frac{m_\pi^2}{m_\tau^2}\left(1 - \frac{m_\pi^2}{m_\tau^2}\right)^2 \frac{f_\pi^2}{m_\tau^2} = -0.002 \pm 0.014\,, \quad (3.7)$$

which it is in agreement with the different determinations that can be found in the literature. A determination of the 4-quark condensate $\langle \bar{u}\lambda_i\gamma_\mu d\, \bar{d}\lambda_i\gamma^\mu u\rangle_\mu$ would help to considerably reduce uncertainties in $\delta_{NP}$, since the other one appearing in the calculation, the $V-A$ version, can be obtained from the $V-A$ channel or from the lattice using the relations between vacuum condensates and $K \to \pi\pi$ matrix elements (see Chapter 4). Just to take a reference of the order of magnitude, it is worth to mention that in the Vacuum Saturation Approximation (VSA) one gets $\mathcal{O}_{6V-A} \sim -0.003\,\mathrm{GeV}^6$, in good agreement with the different phenomenological approaches, while for $\mathcal{O}_{6V+A} \sim -0.0007\,\mathrm{GeV}^6$.

The predicted value of $R_\tau$ is then completely dominated by the perturbative contribution, which is already known to $\mathcal{O}(\alpha_s^4)$ [98], and includes renormalization-group resummations of higher-order logarithm-induced corrections [54, 99]. Due to the low value of the $\tau$ mass scale, $\alpha_s(m_\tau^2)$ is sizable with a numerical value around 0.33 [7]. This makes $R_\tau$ more sensitive to the strong coupling than higher-energy observables, even if some of them can be predicted more accurately. Although $\alpha_s(m_\tau^2)$ has been only determined with a 4% accuracy, evolving it up in energy with the QCD renormalization-group equations, it implies a 1% precision on $\alpha_s(M_Z^2)$ [7, 100], which is a factor of two more accurate than the direct measurement of the strong coupling at the $Z$ peak [101–104]. The excellent agreement between these two determinations of $\alpha_s$, at very different mass scales, constitutes a very precise quantitative test of asymptotic freedom [105–107].

Since the strong coupling is not small at $\mu = m_\tau$, the predicted value of $R_\tau$ is quite sensitive to higher-order perturbative corrections. The induced perturbative uncertainties are, at present, the main limitation on the potentially achievable accuracy [7, 100, 108]. Nevertheless, at the current level of $\mathcal{O}(\alpha_s^4)$ precision, it is also necessary to analyze carefully the numerical role of the small non-perturbative contributions beyond the naive analysis. The most precise experimental analysis, performed with the ALEPH $\tau$ decay data [44], bounds non-perturbative effects to be safely below 1% [46, 109, 110], in agreement with theoretical expectations [52] and previous experimental studies [44, 70, 75, 111, 112] which confirmed the pre-

dicted suppression of this type of contributions. The ALEPH results have been criticized in recent years in a series of papers [113–115], advocating to pursue a slightly different type of analysis [60, 116], focused on observables which maximize the role of non-perturbative effects in order to better study them. However, these papers adopt an overly conservative attitude when judging previous work on the subject, while the uncertainties of their own analyses appear to be underestimated. Studying observables which are more sensitive to some types of non-perturbative contributions is interesting per-se and can help us to better understand QCD in the strong-coupling regime, but it is not necessarily the best strategy to perform a clean and accurate measurement of $\alpha_s$.

In this chapter, based on Ref. [117] we attempt a fresh numerical analysis of the ALEPH data, trying to assess the advantages and disadvantages of different possible approaches. Ideally, all sound theoretical methods should finally give similar results, complementing each other so that a combination of them would allow to maximize the amount and quality of the extracted information. However, current $\tau$ data suffer from strong correlations and large uncertainties, specially in the highest energy range, which severely limits the potential scope of a realistic statistical analysis and the maximum number of parameters to be fitted.

A description of the relation between the spectral function and the invariant mass distribution has been given in Chapter 1. The experimental invariant mass distribution is not really given in a continuum, but as series of correlated bins, narrow enough so that any integral with analytic weight functions can be approximated by rectangles with negligible uncertainties due to the discretization compared with the experimental uncertainties of the bins themselves. Taking that into account, the observables studied in this work (Eq. (3.1)) can be written as:

$$A_V^\omega(s_0) \;= F \sum_{s_i}^{s_0-\frac{\Delta s_0}{2}} \frac{\Delta N_V(s_i)}{N}\, \omega_i(s_i,s_0)\, H(s_0,s_i)\,, \tag{3.8}$$

$$\begin{aligned} A_A^\omega(s_0) \;&= F \sum_{s_i}^{s_0-\frac{\Delta s_0}{2}} \frac{\Delta N_A(s_i)}{N}\, \omega_i(s_i,s_0)\, H(s_0,s_i)\,, \\ &\quad + F\,\frac{m_\tau^2}{s_0}\left(1-\frac{m_\pi^2}{m_\tau^2}\right)^{-2} B_\pi\, \omega_i(m_\pi^2,s_0)\,, \end{aligned} \tag{3.9}$$

where $B_\pi$ is the branching ratio of the process $\tau \to \pi\nu_\tau$,

$$F \equiv \left[12\pi\, S_{\rm EW}\, |V_{ud}|^2 B_e\right]^{-1}, \tag{3.10}$$

collects all normalization factors,

$$H(s_0, s_i) = \frac{m_\tau^2}{s_0}\left(1 - \frac{s_i}{m_\tau^2}\right)^{-2}\left(1 + \frac{2s_i}{m_\tau^2}\right)^{-1} \tag{3.11}$$

and $\Delta s_0$ is the bin width of the bin centered at $s_0 - \frac{\Delta s_0}{2}$.

In Figure 3.2 we show the updated spectral functions measured by the ALEPH collaboration [46]. Together with the experimental data points, the figure shows the naive parton-model expectations (horizontal green lines) and the massless perturbative QCD predictions, using $\alpha_s(m_\tau^2) = 0.329$ (blue lines). This comparison shows beautifully, how the data approach the QCD predictions at the highest available energy bins, without any obvious need for non-perturbative corrections at $s = m_\tau^2$. Resonance structures are clearly visible at lower values of the hadronic invariant mass, specially the prominent $\rho(2\pi)$ and $a_1(3\pi)$ peaks, but as $s$ increases the opening of higher-multiplicity hadronic thresholds results in much smoother inclusive distributions, as expected from quark-hadron duality considerations [118]. The flattening of the spectral distribution is specially good in the most inclusive channel, $V + A$, where perturbative QCD seems to work even from $s \sim 1.2$ GeV$^2$, a surprisingly low value. The onset of the asymptotic perturbative QCD behavior appears obviously later in the semi-inclusive $V$ and $A$ distributions, which only starts to flatten at values of $s \sim 2\,\text{GeV}^2$.

Unfortunately, the experimental uncertainties on the last two (three in the axial distribution) experimental bins are very large, precisely in the highest energy domain where the short-distance QCD methods become more precise.

While most of the theoretical formalism needed for the extraction of the strong coupling has been presented, we still need to introduce some elements, such as the perturbative contribution, absent in the previous chapter, and some useful information about the known vacuum condensates. We present it in Section 3.2. The standard analysis of the data [52, 54, 119], adopted by the ALEPH Orsay group [46, 109, 110], is revised in Section 3.3, which performs a complete numerical study and comments on the quality and potential weaknesses of the final results. Sections 3.4 and 3.5 discuss some possible improvements and their limitations, and analyze the stability of the results, compared with the ones previously obtained in Section 3.3. In Section 3.6 we follow an alternative strategy, based on the Borel transform of the spectral distribution, in order to change the weights of

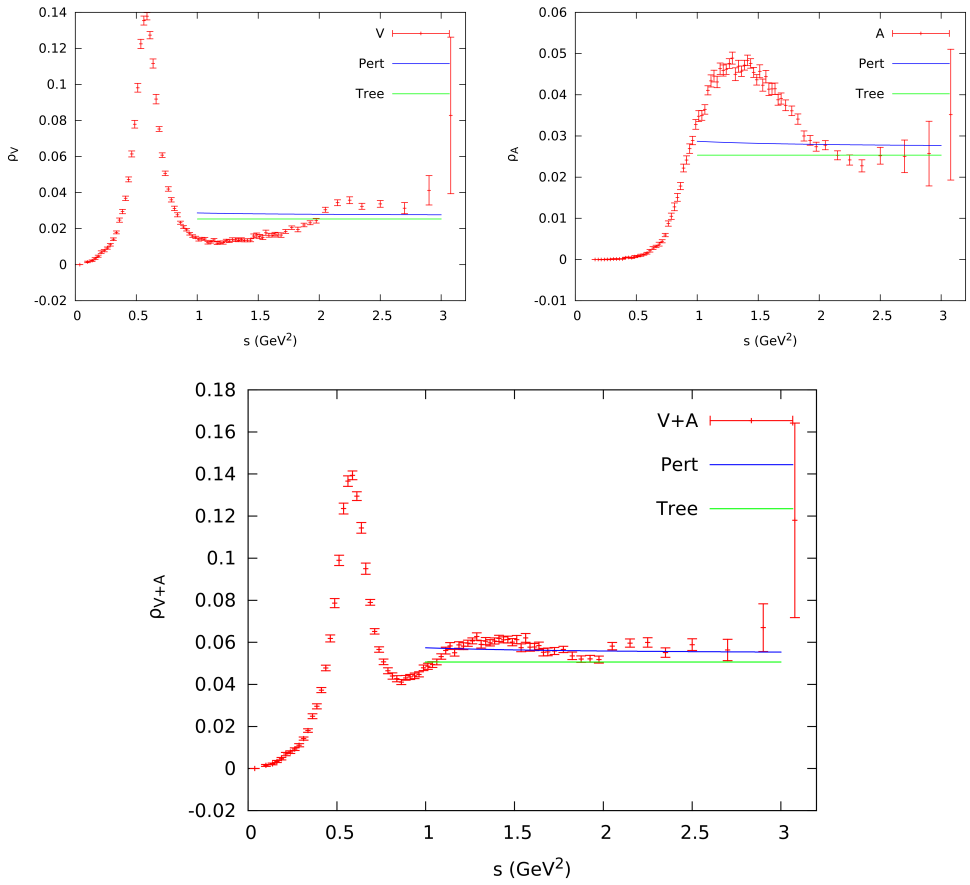


Figure 3.2: ALEPH spectral functions for the $V$, $A$ and $V + A$ channels [46].

different contributions/effects. While having its own weaknesses, this approach provides an additional handle to judge the reliability of the results extracted from current data.

The approach followed in Refs. [113–115] is critically studied in Section 3.7. Their results are based on an ad-hoc assumption on the functional form of the spectral function whose validity is unknown. As we will see, small modifications of this assumption, even keeping their ansatz and changing only the arbitrary energy point in which it is supposed to start to be valid, translate into sizable changes in the fitted value of $\alpha_s(m_\tau^2)$, which turns out to be strongly model dependent and

relies in some unjustified assumptions. We will see how, provided their statistical methods are right, the experimental information about the strong coupling is contained in a direct fit to the spectral function plus a point, corresponding to an integral. Once the fit is reasonably good, which can be achieved by fitting the four model parameters in an interval small enough, we will see how most of the tests made in those references add as many free parameters as independent data points in the fits, giving no information on the reliability of the model or of the $\alpha_s$ determination.

One still may argue, as done in Ref. [120], that one can build high-energy tails associated to values of the strong coupling incompatible with the values we obtained. We will show how the consequences of setting these a-priori strong coupling values are unreliable, since one has to introduce both very large dimensional corrections, with an artificial hierarchy which breaks the naive OPE counting from the first condensates, and huge DVs beyond the tau mass, only previously found in the $\rho$ resonance, contrary to the expected convergence to quark-hadron duality. We will see how the more one deviates from our $\alpha_s$, the more one needs a radical breaking on the counting.

The numerical determinations of $\alpha_s(m_\tau^2)$ obtained with all approaches turn out to be consistent, within their estimated errors. We compile all of them in Section 3.8, and conclude giving our final value for the determination of the strong coupling from $\tau$ decay.

## 3.2 OPE contribution to $A^{\omega}_{V/A}(s_0)$

In this section we show how to calculate the different OPE contributions to the integral along the circumference of Eq. (3.1), emphasizing the perturbative part.

### 3.2.1 Perturbative contribution

The main contribution to $A^{\omega}_{V/A}(s_0)$ comes from the perturbative part $A^{\omega,P}(s_0)$, which for massless quarks is identical for the vector and the axial-vector correlators, due to chiral symmetry. It can be extracted from the renormalization-scale

-invariant Adler function [121]:

$$D(s) \equiv -s\,\frac{d\,\Pi^P(s)}{ds} = \frac{1}{4\pi^2}\sum_{n=0}\tilde{K}_n(\xi)\,a_s^n(-\xi^2 s)\,, \tag{3.12}$$

where $a_s(s) \equiv \alpha_s(s)/\pi$ satisfies the renormalization-group equation:

$$2\,\frac{s}{a_s}\,\frac{d\,a_s(s)}{ds} = \sum_{n=1}\beta_n\,a_s^n(s)\,. \tag{3.13}$$

The perturbative coefficients $K_n \equiv \tilde{K}_n(\xi = 1)$ are known up to $n \leq 4$. For $N_f = 3$ flavours, one has: $K_0 = K_1 = 1$, $K_2 = 1.63982$, $K_3^{\overline{\rm MS}} = 6.37101$ and $K_4^{\overline{\rm MS}} = 49.07570$ [98, 122–126]. The homogeneous renormalization-group equation satisfied by the Adler function determines the corresponding scale-dependent parameters $\tilde{K}_n(\xi)$ [54, 127]. Although the dependence on the renormalization scale cancels exactly in the infinite sum, the truncation to a finite perturbative order leads to a scale dependence from the missing higher-order terms that must be taken into account when estimating perturbative uncertainties.

Integrating by parts Eq. (3.1), we can rewrite $A^{\omega,P}(s_0)$ in terms of the Adler function:

$$A^{\omega,P}(s_0) = \frac{i}{2s_0}\oint_{|s|=s_0}\frac{ds}{s}\,\left[W(s) - W(s_0)\right]\,D(s)\,, \tag{3.14}$$

with $W(s) \equiv \int_0^s ds'\,\omega(s')$. Introducing Eq. (3.12) in Eq. (3.14) and parameterizing the circumference as $s = -s_0\,e^{i\varphi}$, one gets:

$$A^{\omega,P}(s_0) = -\frac{1}{8\pi^2 s_0}\sum_{n=0}\tilde{K}_n(\xi)\int_{-\pi}^{\pi}d\varphi\,\left[W(-s_0 e^{i\varphi}) - W(s_0)\right]a_s^n(\xi^2 s_0 e^{i\varphi}). \tag{3.15}$$

The contour integral on the right-hand side only depends on $a_s(\xi^2 s_0)$. The integration can be performed, either truncating the integrand to a fixed perturbative order in $\alpha_s(\xi^2 s_0)$ (fixed-order perturbation theory, FOPT) [52], or solving exactly the differential $\beta$-function equation in the $\beta_{n>n_{\rm max}} = 0$ approximation (contour-improved perturbation theory, CIPT) [54, 99]. This second procedure should be preferred, as it sums big corrections arising for large values of $|\varphi|$, due to the long running of $a_s^n(\xi^2 s_0\,e^{i\varphi})$ along the contour integration [54]. Taking $n_{\rm max} = 1, 2, 3, 4$, one easily checks that CIPT leads to a fast perturbative convergence for the integrals and the numerical results are stable under changes of the

renormalization scale [54, 128]. On the other side, the slow convergence of the FOPT series leads to a much larger renormalization-scale dependence.

Since perturbation theory is known to be at best an asymptotic series, it has been argued that, in the asymptotic large-$n$ regime, the expected renormalonic behavior of the $K_n$ coefficients could induce cancellations with the running corrections, which would be missed by CIPT. This happens actually in the large-$\beta_1$ limit, which however does not approximate well the known $K_n$ coefficients (it predicts an alternating series) [129–131]. Models of higher-order corrections with this behavior have been advocated [132, 133], but the results are model dependent [134, 135]. The implications of a renormalonic behavior have been also studied using an optimal conformal mapping in the Borel plane and properly implementing the CIPT procedure within the Borel transform. Assuming that the known fourth-order Adler series is already dominated by the lowest ultraviolet ($u = -1$) and infrared ($u = 2, 3$) renormalons, the conformal mapping generates a full series of higher-order coefficients which result, after Borel summation, in a perturbative correction which is numerically close to the naive FOPT result [136–140].

For a fixed value of $\alpha_s(m_\tau^2)$, FOPT predicts a slightly larger perturbative contribution to $R_\tau$ than CIPT. Therefore, it leads to a smaller fitted value of $\alpha_s(m_\tau^2)$. In the absence of a better understanding of higher-order perturbative corrections, we will perform all our analyses with both procedures. Within a given perturbative approach, either CIPT or FOPT, we will estimate the perturbative uncertainty varying the renormalization scale in the interval $\xi^2 \in (0.5\,,\,2)$. Additionally, we will truncate the perturbative series at $n = 5$, taking $K_5 = 275 \pm 400$ [108] as an educated guess of the maximal range of variation of the unknown fifth-order contribution. These two sources of theoretical uncertainty will be combined quadratically.

In order to give a combined determination for the strong coupling, we will finally average the CIPT and FOPT results. Since the previously estimated perturbative uncertainties do not fully account for the difference between these two prescriptions, we will conservatively assess the final error adding in quadrature half the difference between the CIPT and FOPT values to the smallest of the CIPT and FOPT errors. We want to emphasize that the perturbative errors are at present the largest source of uncertainty in the determination of the strong coupling from $\tau$ decays.

### 3.2.2 Non-perturbative contribution

Since OPE corrections are going to be small, we can again safely neglect the logarithmic dependence on $s$ of the Wilson coefficients (Eq. (2.6)), so that $\mathcal{O}_{D,\,V/A}$ is an effective $s$-independent vacuum condensate of dimension $D$. To simplify notation, together with the genuine non-perturbative contributions which have $D \geq 4$, the inverse-power corrections of pure perturbative origin, induced by the finite quark masses, are traditionally included in the sum. It gives tiny contributions to $R_\tau$ smaller than $10^{-4}$ [27, 52, 127].

The lowest-dimensional vacuum condensate contributions are [52], safely neglecting light quark mass corrections,

$$\mathcal{O}_{4,V/A} \;=\; \frac{1}{12}\left[1-\frac{11}{18}\,a_s\right]\,\langle a_s GG\rangle \;+\; \left[1+\frac{\pm 36-23}{27}\,a_s\right]\,\langle (m_u+m_d)\,\bar{q}q\rangle\,. \quad (3.16)$$

The size of the quark condensate is determined by chiral symmetry to be [23, 65, 141]

$$\langle (m_u+m_d)\,\bar{q}q\rangle \;=\; -m_\pi^2 f_\pi^2 \;\approx\; -1.6\cdot 10^{-4}\,\mathrm{GeV}^4 \;\approx\; -1.6\cdot 10^{-5}\,m_\tau^4\,, \quad (3.17)$$

and, therefore, is not going to be very relevant in our numerical analyses. The gluon condensate has been analyzed in many works [142], since its first phenomenological estimate in Ref. [19], but unfortunately its numerical size is still quite uncertain, and indeed there is no strong evidence of a non-zero gluon condensate [143]. As a conservative estimate, one can quote the range [52]

$$\langle a_s GG\rangle \;\approx\; (0.02\pm 0.01)\;\mathrm{GeV}^4 \;\approx\; (1.7\pm 0.8)\cdot 10^{-4}\;\times\;(12\,m_\tau^4)\,, \quad (3.18)$$

where in the last expression we have included the factor 1/12 in Eq. (3.16) to better appreciate its possible numerical impact in the $\tau$ hadronic width. As we are going to see next, $R_\tau$ is insensitive to the $D = 4$ OPE contribution [144] and, given the small numerical size of (3.18), the invariant-mass distribution in $\tau$ decays does not help much in pinning down the gluon condensate.

Inserting Eq. (2.6) in Eq. (3.1), one finally gets the non-perturbative contribution to $A^{\omega}_{V/A}$:

$$A^{\omega,NP}_{V/A}(s_0) \;=\; \frac{i}{2}\,\sum_D\,\mathcal{O}_{D,\,V/A}\,\oint_{|s|=s_0}\frac{ds}{s_0}\,\frac{\omega(s)}{(-s)^{D/2}} \;=\; \pi\,\sum_D\,a_{-1,\,D}\,\frac{\mathcal{O}_{D,\,V/A}}{s_0^{D/2}}\,, \quad (3.19)$$

where $a_{-1,\,D}$ is the $-1$ coefficient of the Laurent expansion of $\omega(s=-s_0x)/x^{D/2}$:

$$\omega(-s_0x) \;=\; \sum_n a_{n,\,D}\; x^{n+D/2}\,. \tag{3.20}$$

## 3.3 ALEPH determination of $\alpha_s(m_\tau^2)$

The determination of Ref. [46] takes $s_0 = m_\tau^2$, the maximum energy for which we have data from $\tau$ decays, where the OPE is supposed to be a better approximation. The weight functions chosen in this analysis have the functional form:

$$\omega_{kl}(s) \;=\; \left(1-\frac{s}{m_\tau^2}\right)^{2+k}\left(\frac{s}{m_\tau^2}\right)^{l}\left(1+\frac{2s}{m_\tau^2}\right)\,, \tag{3.21}$$

with $(k,l) = \{(0,0),(1,0),(1,1),(1,2),(1,3)\}$. All these weights have at least a double zero at $s = s_0 = m_\tau^2$, to numerically suppress the contributions to the contour integral from the region near the positive real axis, so that duality-violation effects are minimized. The corresponding moments are normalized with the moment $(k,l) = (0,0)$, in order to reduce experimental correlations and to incorporate in the $V+A$ fit the more precise determination of $R_{\tau,V+A}$ with a universality-improved leptonic branching ratio, subtracting the small contribution of final states with non-zero strangeness.

From Eq. (3.19), we see that the moments $A^{\rm ALEPH}_{kl,V/A} \equiv A^{\omega_{kl}}_{V/A}(m_\tau^2)$ depend on the following free parameters:

$$\begin{aligned}
A^{\rm ALEPH}_{00,V/A} &= A^{\rm ALEPH}_{00,V/A}(a_s, \mathcal{O}_{6\,V/A}, \mathcal{O}_{8\,V/A})\,,\\
A^{\rm ALEPH}_{10,V/A} &= A^{\rm ALEPH}_{10,V/A}(a_s, \langle a_sGG\rangle, \mathcal{O}_{6\,V/A}, \mathcal{O}_{8\,V/A}, \mathcal{O}_{10\,V/A})\,,\\
A^{\rm ALEPH}_{11,V/A} &= A^{\rm ALEPH}_{11,V/A}(a_s, \langle a_sGG\rangle, \mathcal{O}_{6\,V/A}, \mathcal{O}_{8\,V/A}, \mathcal{O}_{10\,V/A}, \mathcal{O}_{12\,V/A})\,,\\
A^{\rm ALEPH}_{12,V/A} &= A^{\rm ALEPH}_{12,V/A}(a_s, \mathcal{O}_{6\,V/A}, \mathcal{O}_{8\,V/A}, \mathcal{O}_{10\,V/A}, \mathcal{O}_{12\,V/A}, \mathcal{O}_{14\,V/A})\,,\\
A^{\rm ALEPH}_{13,V/A} &= A^{\rm ALEPH}_{13,V/A}(a_s, \mathcal{O}_{8\,V/A}, \mathcal{O}_{10\,V/A}, \mathcal{O}_{12\,V/A}, \mathcal{O}_{14\,V/A}, \mathcal{O}_{16\,V/A})\,.
\end{aligned} \tag{3.22}$$

Since every new moment adds at least one additional unknown parameter to the previous ones, it seems that no new information is introduced by adding them. This would not be the case if, as it is assumed in Ref. [46], the contribution of the condensates of dimension $D > 8$, $A^{\rm ALEPH}_{kl,V/A}\big|_D \sim \pi\,\mathcal{O}_{D,V/A}/m_\tau^D$, is negligible. Assuming that, the fit becomes possible and we obtain the results shown in Table 3.1, in good agreement with the ones obtained in Ref. [46].

| Channel | $\alpha_s(m_\tau^2)$ | $< a_s GG >$ ($10^{-3}$ GeV$^4$) | $\mathcal{O}_6$ ($10^{-3}$ GeV$^6$) | $\mathcal{O}_8$ ($10^{-3}$ GeV$^8$) |
|---|---|---|---|---|
| V (FOPT) | $0.328\,^{+0.013}_{-0.007}$ | $8\,^{+7}_{-14}$ | $-3.2\,^{+0.8}_{-0.5}$ | $5.0\,^{+0.4}_{-0.7}$ |
| V (CIPT) | $0.352\,^{+0.013}_{-0.011}$ | $-8\,^{+7}_{-7}$ | $-3.5\,^{+0.3}_{-0.3}$ | $4.9\,^{+0.4}_{-0.5}$ |
| A (FOPT) | $0.304\,^{+0.010}_{-0.007}$ | $-15\,^{+5}_{-8}$ | $4.4\,^{+0.5}_{-0.4}$ | $-5.8\,^{+0.3}_{-0.4}$ |
| A (CIPT) | $0.320\,^{+0.011}_{-0.010}$ | $-25\,^{+5}_{-5}$ | $4.3\,^{+0.2}_{-0.2}$ | $-5.8\,^{+0.3}_{-0.3}$ |
| V+A (FOPT) | $0.319\,^{+0.010}_{-0.006}$ | $-3\,^{+6}_{-11}$ | $1.3\,^{+1.4}_{-0.8}$ | $-0.8\,^{+0.4}_{-0.7}$ |
| V+A (CIPT) | $0.339\,^{+0.011}_{-0.009}$ | $-16\,^{+5}_{-5}$ | $0.9\,^{+0.3}_{-0.4}$ | $-1.0\,^{+0.5}_{-0.7}$ |

Table 3.1: Fitted parameters from the $V$, $A$ and $V + A$ spectral functions, using the $\omega_{kl}(s)$ weight functions in Eq. (3.21) with $(k, l) = \{(0,0), (1,0), (1,1), (1,2), (1,3)\}$. The results are given for two different treatments of the perturbative contributions, FOPT and CIPT. The quoted uncertainties include experimental and theoretical errors.

Using the five moments in Eq. (3.22), we have fitted four parameters: $\alpha_s(m_\tau^2)$, the gluon condensate, $\mathcal{O}_6$ and $\mathcal{O}_8$. Table 3.1 gives the fitted results, separately for the $V$, $A$ and $V + A$ channels. Moreover, all analyses have been done twice, using the two different treatments of the perturbative QCD series, FOPT and CIPT. As expected, the values of $\alpha_s(m_\tau^2)$ obtained with FOPT are systematically lower than the CIPT results. All fits result in very precise values of the strong coupling, while rather large errors are obtained for the three vacuum condensates. This just reflects the high sensitivity of the moments to $\alpha_s$, and the minor numerical impact of the non-perturbative power corrections at $s_0 = m_\tau^2$.

As it was already observed in the pioneering experimental determinations of $\alpha_s(m_\tau^2)$ [75], there is some tension among the parameters fitted from different channels, which may indicate underestimated uncertainties, either in the experimental data or from non-perturbative effects not yet included in the analysis, such as higher-dimensional condensate contributions or unaccounted duality violations. On pure theoretical grounds [52], one expects the separate $V$ and $A$ correlators to be more sensitive to higher-dimensional OPE corrections than $V + A$. On the other hand, the analysis of the $V - A$ two-point function made in the previous chapter suggests that violations of duality are indeed very efficiently suppressed in pinched moments.

The uncertainties quoted in Table 3.1 have been estimated as follows. First we do a direct fit to the data, ignoring theoretical uncertainties, but taking into

account all experimental errors and correlations. The statistical quality of these fits, as measured by their $\chi^2$/d.o.f., is better when the CIPT approach is used. The vector channel gives quite satisfactory fits ($\chi^2$/d.o.f. = 0.4 and 0.8 for FOPT and CIPT), while the axial one has a bad $\chi^2$/d.o.f. $\sim 4$ for both CIPT and FOPT, being worse in the last case. For $V + A$ one gets $\chi^2$/d.o.f. = 2.4 (FOPT) and 1.7 (CIPT). While these $\chi^2$ values do not have a real confidence-level meaning (theoretical errors are not yet included), they do give some indication about the relative quality of the different fits and their expected sensitivity to missing contributions. We then repeat all fits varying the renormalization scale and the fifth-order Adler coefficient within their allowed ranges, $\xi^2 \in (0.5, 2)$ and $K_5 = 275 \pm 400$, and use the variation of the results to estimate the theoretical uncertainties. Theoretical and experimental uncertainties are finally combined in quadrature, giving the final errors indicated in the table. One could instead use the results of the first fit to estimate the theoretical covariance matrices and then perform a full $\chi^2$ minimization, including theoretical and experimental errors together. We have checked that both methods give consistent results, but the first one allows us to better assess the non-linear dependence with $\xi^2$.

Since we have five moments in this fit, we have freedom for fitting also the $D = 10$ condensate instead of simply neglecting it. Incorporating $\mathcal{O}_{10}$ in the global fit, we obtain the results shown in Table 3.2. Obviously, we can no-longer estimate the fit quality since there are now as many fitted parameters as moments, but we can still evaluate the statistical errors through the $\chi^2$ function. One observes that introducing a new degree of freedom results in a sizable increase of the uncertainties of the fitted condensates. This is not a surprise, given the large correlations present in the data which strongly limit the amount of true information that can be extracted. Adding more free parameters, one is just artificially increasing their possible range of variation by allowing correlated cancellations among them. However, this also puts a word of caution on the reliability of the different extracted parameters. Neglecting $\mathcal{O}_{10}$, has an important effect on the fitted value of $\mathcal{O}_8$ which is forced to reabsorb the missing higher-dimensional contributions.

The strong coupling value turns out to be very stable in all fits. The largest variation on the fitted $\alpha_s$ value occurs in the $A$ channel, the one with the worse $\chi^2$, where the strong coupling increases sizably when allowing for a non-zero $\mathcal{O}_{10}$ contribution. The most reliable results are the ones from the more inclusive $V + A$ channel, which has a smaller $\mathcal{O}_6$ correction because there is a cancellation

| Channel | $\alpha_s(m_\tau^2)$ | $< a_s GG >$ ($10^{-3}$ GeV$^4$) | $\mathcal{O}_6$ ($10^{-3}$ GeV$^6$) | $\mathcal{O}_8$ ($10^{-3}$ GeV$^8$) | $\mathcal{O}_{10}$ ($10^{-3}$ GeV$^{10}$) |
|---|---|---|---|---|---|
| V (FOPT) | $0.320\,^{+0.016}_{-0.014}$ | $10\,^{+9}_{-17}$ | $-4\,^{+3}_{-2}$ | $6\,^{+2}_{-2}$ | $-2\,^{+5}_{-5}$ |
| V (CIPT) | $0.337\,^{+0.020}_{-0.019}$ | $-1\,^{+10}_{-10}$ | $-5\,^{+2}_{-2}$ | $6\,^{+2}_{-2}$ | $-4\,^{+4}_{-4}$ |
| A (FOPT) | $0.347\,^{+0.022}_{-0.021}$ | $-31\,^{+16}_{-33}$ | $11\,^{+5}_{-4}$ | $-12\,^{+4}_{-4}$ | $15\,^{+9}_{-9}$ |
| A (CIPT) | $0.373\,^{+0.029}_{-0.029}$ | $-50\,^{+18}_{-16}$ | $10\,^{+3}_{-3}$ | $-11\,^{+3}_{-3}$ | $14\,^{+7}_{-7}$ |
| V+A (FOPT) | $0.333\,^{+0.013}_{-0.012}$ | $-8\,^{+10}_{-24}$ | $7\,^{+7}_{-4}$ | $-5\,^{+4}_{-6}$ | $12\,^{+12}_{-9}$ |
| V+A (CIPT) | $0.355\,^{+0.016}_{-0.015}$ | $-23\,^{+10}_{-8}$ | $5\,^{+3}_{-3}$ | $-5 \pm 3$ | $10\,^{+8}_{-8}$ |

Table 3.2: Fitted parameters from the $V$, $A$ and $V + A$ spectral functions, using the $\omega_{kl}(s)$ weight functions in Eq. (3.21) with $(k,l) = \{(0,0),(1,0),(1,1),(1,2),(1,3)\}$, but including $\mathcal{O}_{10}$ in the fit. The quoted uncertainties include experimental and theoretical errors.

between the $V$ and $A$ contributions [52].* If we take as reference the $V+A$ value of Table 3.1 and we add quadratically the difference with the $V + A$ value of Table 3.2, as a conservative estimate of uncertainties for having neglected the higher-dimensional condensates, we obtain:

$$\begin{aligned} \alpha_s(m_\tau^2)^{\rm CIPT} &= 0.339\,^{+\,0.019}_{-\,0.017} \\ \alpha_s(m_\tau^2)^{\rm FOPT} &= 0.319\,^{+\,0.017}_{-\,0.015} \end{aligned} \qquad \longrightarrow \qquad \alpha_s(m_\tau^2) = 0.329\,^{+\,0.020}_{-\,0.018}\,. \tag{3.23}$$

In order to quote a final value, we have averaged the CIPT and FOPT results, keeping conservatively the minimum uncertainty and adding quadratically half their difference as an additional systematic error.

The sensitivity to the $D = 4$ OPE correction is very low and, comparing the two tables, one observes a strong correlation with the higher-dimensional corrections. The fitted central values suggest an unphysical negative value for the gluon condensate [19] but the uncertainties are too large to be significant. Applying the same procedure as before, we obtain the averaged value:

$$\langle \tfrac{\alpha_s}{\pi}\, GG \rangle = \left(-9\,^{+\,10}_{-\,11}\right) \cdot 10^{-3}\ {\rm GeV}^4\,, \tag{3.24}$$

which is consistent with zero and, taking into account the large errors, still compatible with the usually quoted range in Eq. (3.18). Repeating the same for $\delta_{NP}$

*In the $V+A$ channel the tables give the fitted values of the sum $\mathcal{O}_{D,V}+\mathcal{O}_{D,A}$. The relevant correction is however the average $\frac{1}{2}\,(\mathcal{O}_{D,V}+\mathcal{O}_{D,A})$.

| Channel | $\alpha_s(m_\tau^2)$ | $< a_s GG >$ ($10^{-3}$ GeV$^4$) | $\mathcal{O}_6$ ($10^{-3}$ GeV$^6$) | $\mathcal{O}_8$ ($10^{-3}$ GeV$^8$) |
|---|---|---|---|---|
| V (FOPT) | $0.331\,^{+0.012}_{-0.006}$ | $-5\,^{+7}_{-14}$ | $-2.4\,^{+0.9}_{-0.5}$ | $2.4\,^{+0.3}_{-0.5}$ |
| V (CIPT) | $0.356\,^{+0.012}_{-0.009}$ | $-22\,^{+7}_{-8}$ | $-2.8\,^{+0.2}_{-0.1}$ | $2.1\,^{+0.3}_{-1.1}$ |
| A (FOPT) | $0.305\,^{+0.009}_{-0.005}$ | $-5\,^{+4}_{-8}$ | $3.9\,^{+0.5}_{-0.3}$ | $-3.2\,^{+0.2}_{-0.3}$ |
| A (CIPT) | $0.320\,^{+0.010}_{-0.007}$ | $-15\,^{+4}_{-4}$ | $3.8\,^{+0.1}_{-0.1}$ | $-3.3\,^{+0.1}_{-0.2}$ |
| V+A (FOPT) | $0.319\,^{+0.010}_{-0.005}$ | $-3\,^{+5}_{-11}$ | $1.5\,^{+1.3}_{-0.7}$ | $-0.8\,^{+0.4}_{-0.8}$ |
| V+A (CIPT) | $0.338\,^{+0.010}_{-0.008}$ | $-16\,^{+5}_{-5}$ | $1.1\,^{+0.2}_{-0.2}$ | $-1.0\,^{+0.4}_{-1.0}$ |

Table 3.3: Fitted parameters from the $V$, $A$ and $V+A$ spectral functions, using the same weights as in Table 3.1 but taking away the factor $(1+2s/m_\tau^2)$. The quoted uncertainties include experimental and theoretical errors.

one finds:

$$\delta_{NP}^{FOPT} = -0.006 \pm 0.016\,, \tag{3.25}$$

$$\delta_{NP}^{CIPT} = -0.005 \pm 0.011\,. \tag{3.26}$$

In order to test the stability of these results, we have repeated all fits taking away from the weight functions the factor $(1+2s/m_\tau^2)$ in Eq. (3.21). This eliminates the highest-dimensional condensate contribution to each moment, at the price of making $A_{00,V/A}$ sensitive to the gluon condensate. Although one also loses the additional experimental information from the $\tau$ lifetime, the new weights are less sensitive to the higher energy range of the experimental distribution which, as shown in Figure 3.2, is poorly-defined. The fitted results for $\alpha_s$ and the vacuum condensates, obtained in this way, are shown in Tables 3.3 (taking $\mathcal{O}_{10}=0$) and 3.4 (including $\mathcal{O}_{10}$ in the fit). They are in complete agreement with the results of the previous fits, given in Tables 3.1 and 3.2. However, all $\chi^2$/d.o.f. turn out now to be smaller than one.

The central values of the fitted parameters are very stable, specially the strong coupling, and the sensitivity of $\alpha_s$, $\mathcal{O}_4$ and $\mathcal{O}_6$ to vacuum condensates with $D>10$ is indeed negligible. From the results in Tables 3.3 and 3.4, applying the same procedure as before, we get the averages:

$$\left.\begin{array}{l} \alpha_s(m_\tau^2)^{\rm CIPT} \;=\; 0.338\,^{+\,0.014}_{-\,0.012} \\ \alpha_s(m_\tau^2)^{\rm FOPT} \;=\; 0.319\,^{+\,0.013}_{-\,0.010} \end{array}\right. \quad\longrightarrow\quad \alpha_s(m_\tau^2) \;=\; 0.329\,^{+\,0.016}_{-\,0.014}\,, \tag{3.27}$$

| Channel | $\alpha_s(m_\tau^2)$ | $< a_s GG >$ ($10^{-3}$ GeV$^4$) | $\mathcal{O}_6$ ($10^{-3}$ GeV$^6$) | $\mathcal{O}_8$ ($10^{-3}$ GeV$^8$) | $\mathcal{O}_{10}$ ($10^{-3}$ GeV$^{10}$) |
|---|---|---|---|---|---|
| V (FOPT) | $0.318\,^{+0.043}_{-0.042}$ | $10\,^{+46}_{-48}$ | $-5\,^{+7}_{-7}$ | $6\,^{+11}_{-11}$ | $-4\,^{+12}_{-12}$ |
| V (CIPT) | $0.336\,^{+0.056}_{-0.055}$ | $-1\,^{+54}_{-54}$ | $-5\,^{+7}_{-7}$ | $6\,^{+11}_{-11}$ | $-4\,^{+12}_{-11}$ |
| A (FOPT) | $0.336\,^{+0.052}_{-0.051}$ | $-39\,^{+62}_{-67}$ | $9\,^{+10}_{-10}$ | $-12\,^{+15}_{-15}$ | $9\,^{+16}_{-16}$ |
| A (CIPT) | $0.360\,^{+0.064}_{-0.064}$ | $-54\,^{+68}_{-68}$ | $8\,^{+7}_{-7}$ | $-11\,^{+13}_{-13}$ | $8\,^{+13}_{-13}$ |
| V+A (FOPT) | $0.327\,^{+0.030}_{-0.029}$ | $-13\,^{+35}_{-39}$ | $4\,^{+11}_{-11}$ | $-6\,^{+17}_{-17}$ | $5\,^{+18}_{-18}$ |
| V+A (CIPT) | $0.348\,^{+0.040}_{-0.039}$ | $-26\,^{+41}_{-41}$ | $3\,^{+9}_{-9}$ | $-5\,^{+16}_{-16}$ | $4\,^{+17}_{-17}$ |

Table 3.4: Fitted parameters from the $V$, $A$ and $V + A$ spectral functions, using the same weights as in Table 3.3 and including $\mathcal{O}_{10}$ in the fit. The quoted uncertainties include experimental and theoretical errors.

$$\langle \tfrac{\alpha_s}{\pi}\, GG \rangle \;=\; (-10 \pm 13) \cdot 10^{-3}\ \text{GeV}^4\,, \tag{3.28}$$

and:

$$\delta_{NP}^{FOPT} = -0.007 \pm 0.016\,, \tag{3.29}$$

$$\delta_{NP}^{CIPT} = -0.005 \pm 0.005\,. \tag{3.30}$$

These numbers are in excellent agreement with the previous determination in Eqs. (3.23) and (3.24), performed with the ALEPH moments, and the values obtained for $\alpha_s(m_\tau^2)$ are even more accurate.

## 3.4 Optimal moments

The moments $\omega_{kl}(s)$ used in the previous analyses were suggested in Ref. [119] as a way to minimize the large statistical and systematic uncertainties of the initial LEP data. All of them incorporate the kinematical factor $\omega_{00}(s)$, present in Eq. (3.3), allowing for a direct use of the measured invariant-mass distribution. This makes unnecessary to reconstruct the spectral functions, dividing the raw data by $\omega_{00}(s)$, which enhances the systematically- and statistically-limited tail of the $s$ distribution. On the negative side, these moments involve higher-dimensional condensates and the experimental precision deteriorates with increasing values of $k$ and/or $l$. Nowadays, since we have well-determined and

quite precise spectral functions,[†] based on the full LEP data sample, it is possible to investigate whether there are better moments, more suitable for a precise QCD analysis.

In order to reduce DVs, we could consider the simplest $n$-pinched weight functions

$$\omega^{(n,0)}(x) \;=\; (1-x)^n \;=\; \sum_{k=0}^{n} (-1)^k \left( \begin{array}{c} n \\ k \end{array} \right) x^k \,, \tag{3.31}$$

with $x = s/s_0$. However, the moments generated by these weights get non-perturbative corrections from all condensates with dimension $D \leq 2(n+1)$. We would like to become sensitive to the lowest-dimensional condensates without too much contamination from higher-order terms in the OPE. It is possible to build a family of weight functions which project on one single condensate contribution, while still having a zero at $x = 1$:

$$\omega^{(1,n)}(x) \;=\; 1 - x^{n+1} \;=\; (1-x) \;\sum_{k=0}^{n} x^k \,. \tag{3.32}$$

The corresponding moments are only sensitive to $\mathcal{O}_{2(n+2)}$. As an intermediate case, the following weight functions have a double pinch and generate moments with only two condensate contributions, $\mathcal{O}_{2(n+2)}$ and $\mathcal{O}_{2(n+3)}$:

$$\omega^{(2,n)}(x) \;=\; (1-x)^2 \;\sum_{k=0}^{n} (k+1)\, x^k \;=\; 1 - (n+2)\, x^{n+1} + (n+1)\, x^{n+2} \,. \tag{3.33}$$

Notice that $\omega^{(2,1)}(x) = \omega_{00}(x)$, the lowest moment used in the ALEPH-like analysis.

Since every moment

$$A_{V/A}^{(n,m)}(s_0) \;\equiv\; A_{V/A}^{\omega^{(n,m)}}(s_0) \;=\; \int_{s_{\rm th}}^{s_0} \frac{ds}{s_0}\, \omega^{(n,m)}(s)\; {\rm Im}\, \Pi_{V/A}(s) \tag{3.34}$$

with $n = 1$ or $n = 2$ introduces a new condensate correction with respect $A_{V/A}^{(n,m-1)}(s_0)$, it is not possible to perform a fully complete fit of $\alpha_s$ and some power corrections only using a few single-pinched or doubly-pinched moments. Nevertheless, one can still make some approximations and a few consistency tests, which we attempt next.

[†]Note, however, that the large uncertainties observed in the higher-energy bins of the spectral functions in Figure 3.2 originate in the kinematical factor $\omega_{00}(s)$ which suppresses the end-point of the $\tau$ decay distribution.

| Moment | $\alpha_s(m_\tau^2)$ | | Moment | $\alpha_s(m_\tau^2)$ | |
|---|---|---|---|---|---|
| $(n,m)$ | FOPT | CIPT | $(n,m)$ | FOPT | CIPT |
| (1,0) | $0.315\,^{+0.012}_{-0.007}$ | $0.327\,^{+0.012}_{-0.009}$ | (2,0) | $0.311\,^{+0.015}_{-0.011}$ | $0.314\,^{+0.013}_{-0.009}$ |
| (1,1) | $0.319\,^{+0.010}_{-0.006}$ | $0.340\,^{+0.011}_{-0.009}$ | (2,1) | $0.311\,^{+0.011}_{-0.006}$ | $0.333\,^{+0.009}_{-0.007}$ |
| (1,2) | $0.322\,^{+0.010}_{-0.008}$ | $0.343\,^{+0.012}_{-0.010}$ | (2,2) | $0.316\,^{+0.010}_{-0.005}$ | $0.336\,^{+0.011}_{-0.009}$ |
| (1,3) | $0.324\,^{+0.011}_{-0.010}$ | $0.345\,^{+0.013}_{-0.011}$ | (2,3) | $0.318\,^{+0.010}_{-0.006}$ | $0.339\,^{+0.011}_{-0.008}$ |
| (1,4) | $0.326\,^{+0.011}_{-0.011}$ | $0.347\,^{+0.013}_{-0.012}$ | (2,4) | $0.319\,^{+0.009}_{-0.007}$ | $0.340\,^{+0.011}_{-0.009}$ |
| (1,5) | $0.327\,^{+0.015}_{-0.013}$ | $0.348\,^{+0.014}_{-0.012}$ | (2,5) | $0.320\,^{+0.010}_{-0.008}$ | $0.341\,^{+0.011}_{-0.009}$ |

Table 3.5: Values of the strong coupling extracted from a single $A^{(n,m)}(s_0)$ moment of the $V+A$ distribution, at $s_0 = 2.8$ GeV$^2$, neglecting all non-perturbative corrections.

### 3.4.1 OPE corrections neglected

Neglecting all OPE corrections, one can directly extract $\alpha_s(m_\tau^2)$ from a single $A^{(n,m)}(s_0)$ moment. Comparing the values extracted with different choices of $(n,m)$, one can then assess the size of the neglected contributions. For instance, $A^{(0,0)}(s_0)$ does not get any OPE correction, but it is not protected against duality-violation effects. On the other extreme, $A^{(2,3)}(s_0)$ is well protected by a double pinch and gets inverse power corrections with $D = 10$ and 12.

Since we are going to test also some non-pinched weights, we take $s_0 = 2.8$ GeV$^2$ as reference point, so that we avoid the problems associated with the last two experimental bins. The results of this exercise are shown in Table 3.5, for all $A^{(n,m)}(s_0)$ moments of the $V+A$ distribution with $n = 1, 2$ and $0 \leq m \leq 5$. In all cases, the fitted values are well within the error ranges of our determinations in Eq. (3.23). Notice the good stability displayed by the results from the moments $(2, m \geq 2)$, suggesting that condensates with $D > 6$ play indeed a very minor role. A similar behavior is observed in the moments $(1, m)$ which, however, result in slightly larger values of the strong coupling for all values of the parameter $m$.

A clean test of the magnitude of DV effects is provided by the $A^{(0,0)}(s_0)$ moment, where OPE corrections are absent. One finds in this case $\alpha_s(m_\tau^2)^{\rm CIPT} = 0.352\,^{+0.023}_{-0.022}$ and $\alpha_s(m_\tau^2)^{\rm FOPT} = 0.333\,^{+0.024}_{-0.018}$, in agreement with Eq. (3.23) despite being a non-protected moment.

### 3.4.2 Combined fit to $A^{(n,0)}(s_0)$ moments

Using all $A^{(n,0)}(s_0)$ moments with $n \leq N$, one can determine $\alpha_s(m_\tau^2)$ and $\mathcal{O}_{D\leq 2N}$, neglecting the $\mathcal{O}_{2(N+1)}$ contribution to the last moment. The strong coupling is mostly affected by the non-protected $(0,0)$ moment, although the effects of DVs may be reduced by the rest of weight functions, which do have pinching protection. We show in Table 3.6 the results from global fits to the $(n,0)$ moments with $0 \leq n \leq 3$, taking $\mathcal{O}_8 = 0$. Again, the agreement with Eq. (3.23) is remarkable.

| Channel | $\alpha_s(m_\tau^2)$ | $< a_s GG >$ ($10^{-3}$ GeV$^4$) | $\mathcal{O}_6$ ($10^{-3}$ GeV$^6$) |
|---|---|---|---|
| V (FOPT) | $0.310\,^{+0.010}_{-0.005}$ | $11\,^{+7}_{-12}$ | $-3.8\,^{+0.9}_{-0.6}$ |
| V (CIPT) | $0.328\,^{+0.011}_{-0.007}$ | $2\,^{+7}_{-7}$ | $-4.1\,^{+0.4}_{-0.5}$ |
| A (FOPT) | $0.328\,^{+0.011}_{-0.007}$ | $-28\,^{+9}_{-20}$ | $5.8\,^{+1.3}_{-0.7}$ |
| A (CIPT) | $0.352\,^{+0.012}_{-0.008}$ | $-41\,^{+8}_{-7}$ | $5.3\,^{+0.4}_{-0.5}$ |
| V+A (FOPT) | $0.319\,^{+0.010}_{-0.007}$ | $-7\,^{+7}_{-16}$ | $2.0\,^{+2.0}_{-1.1}$ |
| V+A (CIPT) | $0.340\,^{+0.011}_{-0.009}$ | $-18\,^{+6}_{-5}$ | $1.2\,^{+0.5}_{-0.8}$ |

Table 3.6: Global fit to the $A^{(n,0)}(s_0)$ moments with $0 \leq n \leq 3$, taking $\mathcal{O}_8 = 0$.

### 3.4.3 Combined fit to $A^{(2,m)}(m_\tau^2)$ moments

From the moments $A^{(2,m)}(m_\tau^2)$ with $1 \leq m \leq N$, one can determine $\alpha_s(m_\tau^2)$ and $\mathcal{O}_{D\leq 2(N+1)}$, neglecting the $\mathcal{O}_{2(N+2)}$ and $\mathcal{O}_{2(N+3)}$ contributions to the last two moments. In this case, the whole set of selected moments is well protected from DV effects by a double pinch. The results obtained with $N = 5$ are shown in Tables 3.7 and 3.8. The first one is a global fit, assuming $\mathcal{O}_{12} = \mathcal{O}_{14} = \mathcal{O}_{16} = 0$, while Table 3.8 only assumes $\mathcal{O}_{14} = \mathcal{O}_{16} = 0$ and has then as many fitted parameters as moments.

Since the previous tests suggested that the neglected higher-dimensional condensates do not play any significant role on the fitted value of the strong coupling, the results of these fits should be very reliable, specially in the $V + A$ case. Of course, adding one more parameter to the fit allows for a wider range of variation, increasing the fitted errors, which explains the differences between the two tables. The small sensitivity to the vacuum condensates is reflected in their large statistical uncertainties, specially in Table 3.8. Their fitted values agree with

| Channel | $\alpha_s(m_\tau^2)$ | $\mathcal{O}_6$ ($10^{-3}$ GeV$^6$) | $\mathcal{O}_8$ ($10^{-3}$ GeV$^8$) | $\mathcal{O}_{10}$ ($10^{-3}$ GeV$^{10}$) |
|---|---|---|---|---|
| V (FOPT) | $0.315\,^{+0.011}_{-0.007}$ | $-5.2\,^{+0.8}_{-0.5}$ | $6.7\,^{+0.5}_{-0.7}$ | $-4.5\,^{+0.4}_{-0.3}$ |
| V (CIPT) | $0.334\,^{+0.012}_{-0.009}$ | $-5.3\,^{+0.3}_{-0.4}$ | $6.7\,^{+0.4}_{-0.4}$ | $-4.6\,^{+0.2}_{-0.3}$ |
| A (FOPT) | $0.318\,^{+0.011}_{-0.007}$ | $6.5\,^{+0.9}_{-0.5}$ | $-7.6\,^{+0.5}_{-0.4}$ | $4.9\,^{+0.4}_{-0.3}$ |
| A (CIPT) | $0.338\,^{+0.013}_{-0.012}$ | $6.3\,^{+0.3}_{-0.4}$ | $-7.7\,^{+0.4}_{-0.3}$ | $4.8\,^{+0.2}_{-0.4}$ |
| V+A (FOPT) | $0.317\,^{+0.010}_{-0.005}$ | $1.3\,^{+1.7}_{-1.0}$ | $-0.9\,^{+0.9}_{-1.4}$ | $0.3\,^{+0.8}_{-0.5}$ |
| V+A (CIPT) | $0.336\,^{+0.011}_{-0.009}$ | $0.9\,^{+0.4}_{-0.7}$ | $-0.9\,^{+0.5}_{-0.5}$ | $0.1\,^{+0.3}_{-0.7}$ |

Table 3.7: Global fit to the $A^{(2,m)}(s_0)$ moments with $1 \leq m \leq 5$, taking $\mathcal{O}_{12} = \mathcal{O}_{14} = \mathcal{O}_{16} = 0$.

| Channel | $\alpha_s(m_\tau^2)$ | $\mathcal{O}_6$ ($10^{-3}$ GeV$^6$) | $\mathcal{O}_8$ ($10^{-3}$ GeV$^8$) | $\mathcal{O}_{10}$ ($10^{-3}$ GeV$^{10}$) | $\mathcal{O}_{12}$ ($10^{-3}$ GeV$^{12}$) |
|---|---|---|---|---|---|
| V (FOPT) | $0.318\,^{+0.013}_{-0.012}$ | $-5\,^{+3}_{-2}$ | $6\,^{+3}_{-4}$ | $-3\,^{+5}_{-5}$ | $-2\,^{+5}_{-5}$ |
| V (CIPT) | $0.336\,^{+0.017}_{-0.016}$ | $-5\,^{+2}_{-2}$ | $6\,^{+3}_{-3}$ | $-4\,^{+4}_{-4}$ | $-1\,^{+4}_{-4}$ |
| A (FOPT) | $0.339\,^{+0.018}_{-0.017}$ | $11\,^{+4}_{-3}$ | $-15\,^{+5}_{-5}$ | $16\,^{+9}_{-8}$ | $-11\,^{+8}_{-8}$ |
| A (CIPT) | $0.364\,^{+0.024}_{-0.022}$ | $10\,^{+2}_{-2}$ | $-14\,^{+5}_{-5}$ | $14\,^{+7}_{-7}$ | $-9\,^{+7}_{-7}$ |
| V+A (FOPT) | $0.329\,^{+0.012}_{-0.011}$ | $6\,^{+6}_{-4}$ | $-9\,^{+7}_{-9}$ | $13\,^{+12}_{-10}$ | $-12\,^{+9}_{-11}$ |
| V+A (CIPT) | $0.349\,^{+0.016}_{-0.014}$ | $4\,^{+3}_{-3}$ | $-8\,^{+6}_{-6}$ | $10\,^{+8}_{-8}$ | $-10\,^{+8}_{-8}$ |

Table 3.8: Global fit to the $A^{(2,m)}(s_0)$ moments with $1 \leq m \leq 5$, taking $\mathcal{O}_{14} = \mathcal{O}_{16} = 0$.

the results quoted in Tables 3.1 and 3.2. On the other side, the determinations of the strong coupling are quite precise and in excellent agreement with the fits performed in Section 3.3. Notice the very good stability displayed in Table 3.7, where similar central values for $\alpha_s(m_\tau^2)$ are obtained from the $V$, $A$ and $V + A$ channels.

Taking again as reference the results from the $V + A$ fits in Table 3.7, and adding quadratically the differences between the two tables, as a conservative estimate of the uncertainties from neglected higher-dimensional condensates, we obtain

$$\begin{array}{l} \alpha_s(m_\tau^2)^{\rm CIPT} \;=\; 0.336\,^{+\,0.018}_{-\,0.016} \\ \alpha_s(m_\tau^2)^{\rm FOPT} \;=\; 0.317\,^{+\,0.015}_{-\,0.013} \end{array} \qquad \longrightarrow \qquad \alpha_s(m_\tau^2) \;=\; 0.326\,^{+\,0.018}_{-\,0.016}\,, \quad (3.35)$$

and

$$\delta_{NP}^{FOPT} = -0.006 \pm 0.012 \tag{3.36}$$

$$\delta_{NP}^{CIPT} = -0.005 \pm 0.008 \tag{3.37}$$

Once more, we get results in perfect agreement with the values of the strong coupling obtained in Eqs. (3.23) and (3.27). Given the different sensitivity to higher-dimensional condensates of the moments used in each approach, and the many tests we have performed showing the negligible numerical impact of higher-order power corrections, our determination of $\alpha_s(m_\tau^2)$ appears to be very solid and much more stable than what one could expect from the quoted uncertainties, indicating that our error estimates are indeed conservative.

## 3.5 Including information from the $s_0$ dependence

Given the large relative uncertainties on the small power-suppressed corrections, one would like to find additional inputs to constrain the range of fitted parameters. One possibility is to look at different values of $s_0$. In Figures 3.3 and 3.4 we plot as a function of $s_0$ the experimental moments $A^{(n,0)}(s_0)$, associated with the simplest $n$-pinched weight functions in Eq. (3.31), for the $V$, $A$ and $\frac{1}{2}(V+A)$ channels, together with the perturbative part of $A^{(n,0)}(s_0)$ predicted with the value of $\alpha_s(m_\tau^2)$ given in Eq. (3.23).

Perturbation theory appears to reproduce well the data at large values of $s_0 \sim m_\tau^2$, without any clear need for sizable power corrections, except perhaps in $A_V^{(3,0)}(s_0)$. Notice the excellent agreement obtained for the $V+A$ channel of $A^{(0,0)}(s_0)$, the only moment whose non-perturbative OPE contribution is known to be negligible. The agreement with perturbation theory extends to quite low values of $s_0$, even if this is the moment most exposed to DVs, suggesting that DV uncertainties are indeed within the quoted errors of $\alpha_s(m_\tau^2)$. The moment $A^{(1,0)}(s_0)$, which can only get corrections from $\mathcal{O}_4$, shows above $s_0 \sim 2$ GeV$^2$ a surprisingly good agreement with its pure perturbative prediction in all channels ($V$, $A$ and $V+A$). In spite of being only protected by a single pinch factor, the data points for this moment closely follow the central values predicted by CIPT. In that energy range both, DVs and $D=4$ power corrections, appear to be too small to become numerically visible within the much larger perturbative uncertainties covering the shaded areas of the figure. The higher moments $A^{(2,0)}(s_0)$ and $A^{(3,0)}(s_0)$ are slightly more sensitive to non-perturbative corrections. The

different curves seem to prefer a power correction with different signs for the $V$ and $A$ distributions, which cancels to a good extent in $V + A$. This fits nicely with the expected $\mathcal{O}_{6,V/A}$ contribution. However, in the moment $A^{(2,0)}(s_0)$, the merging of the $V$, $A$ and $V + A$ curves above $s_0 \sim 2.2$ GeV$^2$ suggests a very tiny numerical effect from this source in the high-energy range. Only the moment $A^{(3,0)}(s_0)$ appears to have still some sensitivity to power corrections at $s_0 \sim m_\tau^2$.

In order to better assess the dominant perturbative errors, we present in Figure 3.5, as a function of $s_0$, the perturbative predictions for the doubly-pinched moments $A^{(2,0)}(s_0)$, $A^{(2,1)}(s_0)$ and $A^{(2,2)}(s_0)$, at different loop approximations within FOPT (left) and CIPT (right), with the same value of $\alpha_s(m_\tau^2)$ given above. Note that the $\alpha_s^5$ contribution is just an educated guess estimate, taking for the fifth-order Adler coefficient the value $K_5 = 275$. For the known perturbative orders, CIPT seems to present a better convergence. Additionally, we observe a slightly better perturbative behavior for the two moments which are independent of the $\mathcal{O}_4$ condensate, in agreement with the models considered in Ref. [133]. However, new coefficients of the Adler function would be needed to extract any reliable conclusions. Moreover, a moment with a better perturbative behavior is not necessarily the best one to determine the strong coupling, since the sensitivity of the moments to $\alpha_s(m_\tau^2)$ plays a crucial role too.

Naively, the pinched moments seem suitable for performing phenomenological fits. However, as it was already observed long time ago in Ref. [119], a fit of the $s_0$ dependence turns out to be nearly equivalent to a direct fit of the spectral function $\rho(s_0) = \frac{1}{\pi}\,\mathrm{Im}\,\Pi(s_0)$, a quantity which cannot be described rigorously with the OPE. This is immediately seen, studying the derivative with respect to the moment end-point $s_0$. For the simpler $n$-pinched moments $A^{(n,0)}(s_0)$, one finds

$$s_0\,\frac{d}{ds_0}\,A^{(n,0)}(s_0) \;=\; \delta_{n,0}\,\pi\,\rho(s_0) + n\,A^{(n-1,0)}(s_0) - (n+1)\,A^{(n,0)}(s_0)\,. \qquad (3.38)$$

Thus, if we make a fit of consecutive $s_0$ points, we are removing pinchs; *i.e.*, the only new experimental information we get adding $A^{(n,0)}(s_0 + \Delta s_0)$ to a fit with $A^{(n,0)}(s_0)$ is the same integral with one pinch less. After adding $n$ bins, we are just testing $\rho(s_0)$. A fit with $m$ $s_0$ points of the moment $A^{(n,0)}(s_0)$ is going to be equivalent to a fit with:

$$\left\{A^{(n,0)}(s_0)\,,\,A^{(n-1,0)}(s_0)\,,\,\cdots\,,\,A^{(0,0)}(s_0)\,,\,\rho(s_0)\,,\,\rho(s_0+\Delta s_0)\,,\,...,\rho(s_0+(m-n-2)\Delta s_0)\right\}\,. \qquad (3.39)$$

Thus, we are directly using information about the local structure of the spectral function.

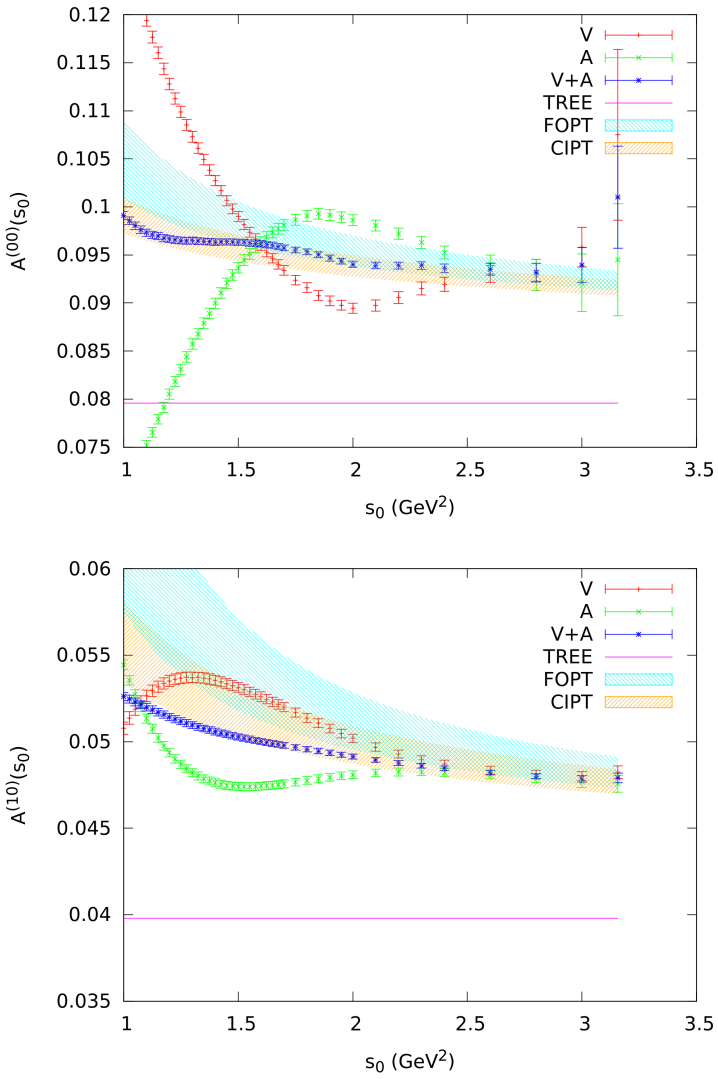


Figure 3.3: Dependence on $s_0$ of the experimental moments $A^{(0,0)}(s_0)$ and $A^{(1,0)}(s_0)$, associated to the pinched weight functions of Eq. (3.31), together with their purely perturbative predictions calculated using the strong coupling obtained in the r.h.s. of Eq. (3.23). Data points are shown for the $V$ (red), $A$ (green) and $\frac{1}{2}(V+A)$ (blue) channels.

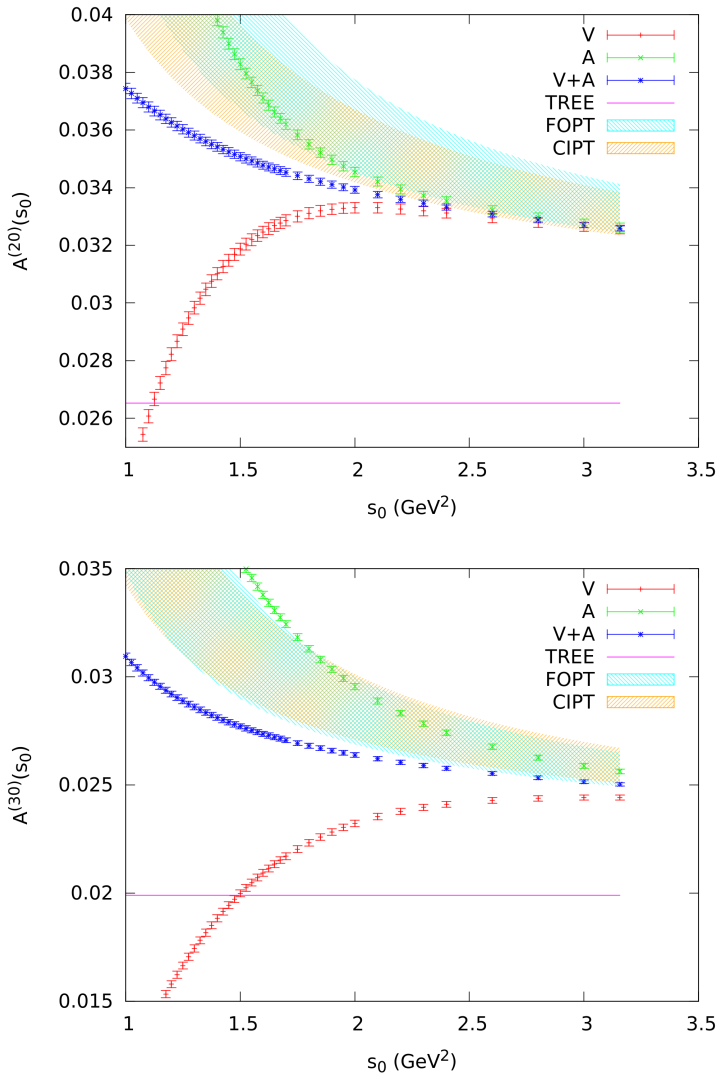


Figure 3.4: Dependence on $s_0$ of the experimental moments $A^{(2,0)}(s_0)$ and $A^{(3,0)}(s_0)$, associated to the pinched weight functions of Eq. (3.31), together with their purely perturbative predictions calculated using the strong coupling obtained in the r.h.s. of Eq. (3.23). Data points are shown for the $V$ (red), $A$ (green) and $\frac{1}{2}(V+A)$ (blue) channels.

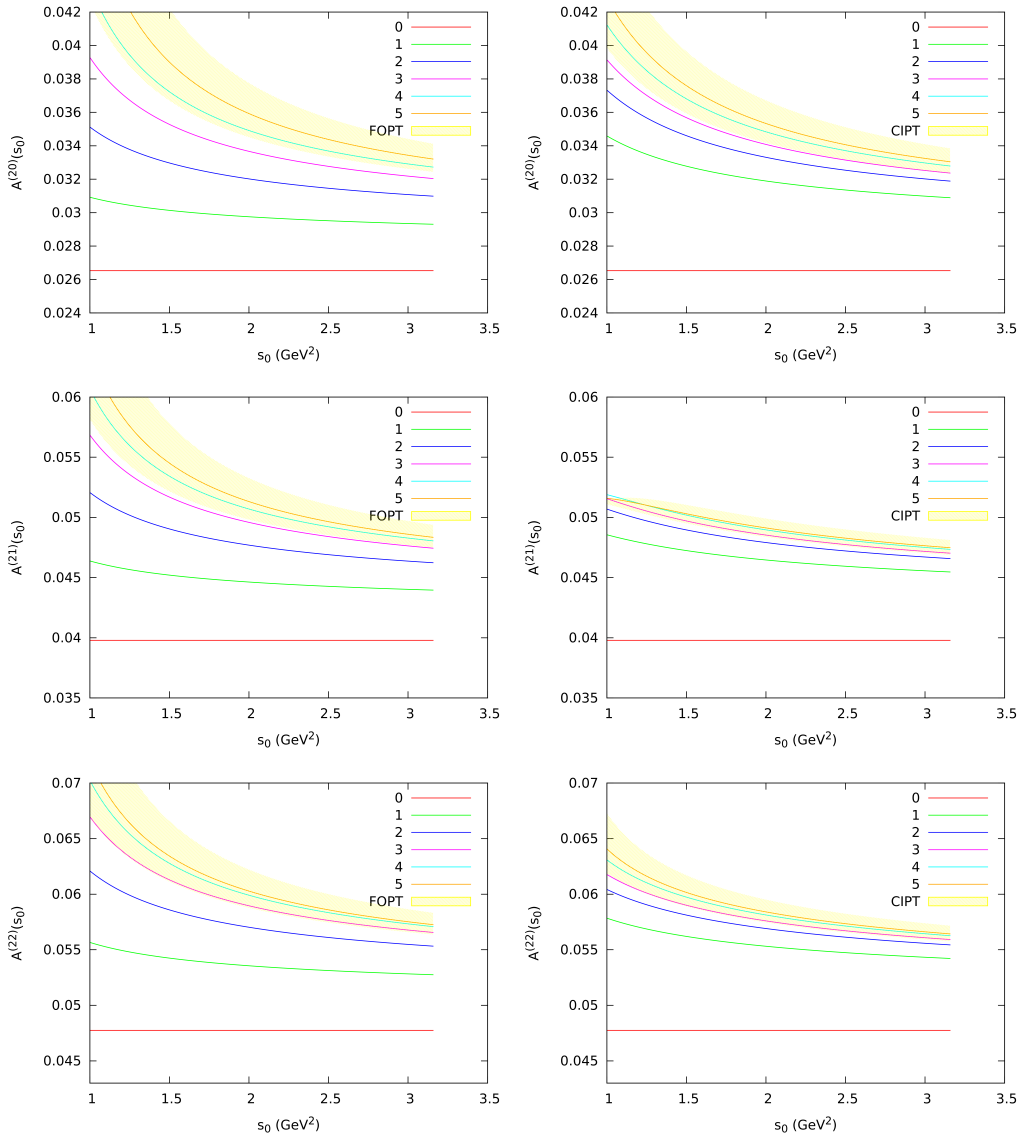


Figure 3.5: Dependence on $s_0$ of the perturbative contributions to the moments $A^{(2,0)}(s_0)$, $A^{(2,1)}(s_0)$ and $A^{(2,2)}(s_0)$, constructed with the doubly-pinched weight functions in Eq. (3.33), calculated in FOPT (left panels) and CIPT (right panels) at several loop approximations. The filled areas correspond to $\alpha_s(m_\tau^2) = 0.329\,^{+0.020}_{-0.018}$.

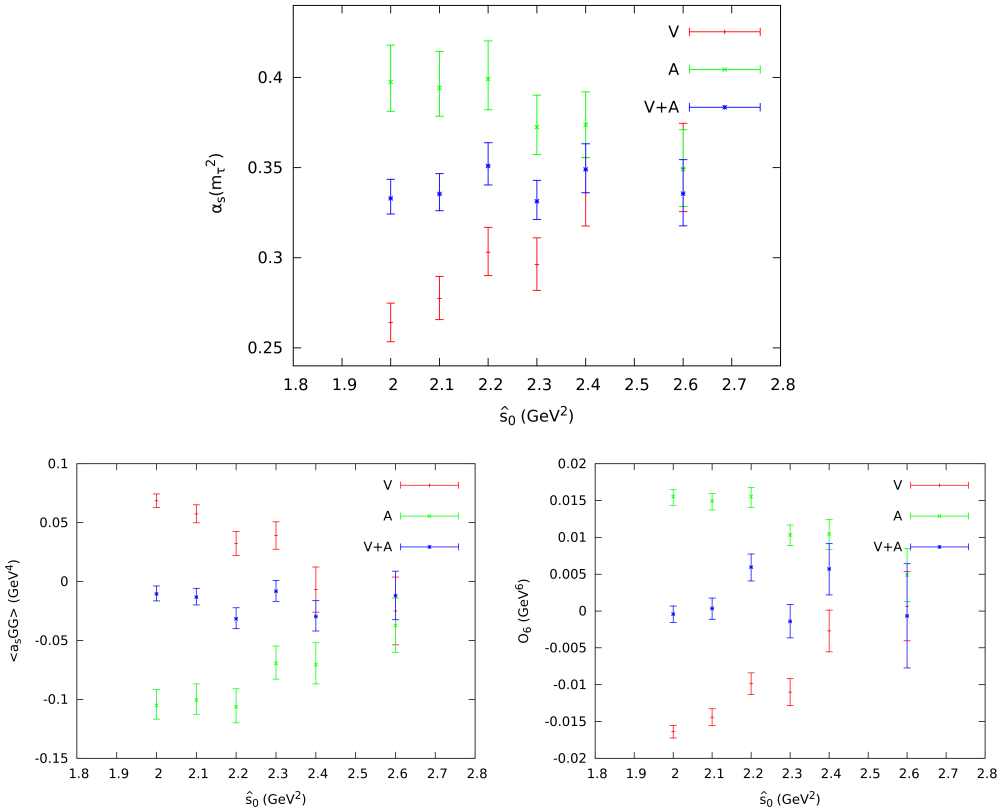


Figure 3.6: Parameters fitted in CIPT with the moment $A^{(2,0)}(s_0)$, as a function of the starting $s_0$ value of the fit, $\hat{s}_0$.

Not surprisingly, the functional dependence of the moments with $s_0$ manifests the violations of quark-hadron duality which are obviously present in the physical hadronic spectrum. Once this is properly understood, an analysis of the $s_0$ dependence can nevertheless provide enlightening information on the relevance of DVs in different energy regimes. With this caveat in mind, we study next the doubly-pinched moments $A^{(2,0)}(s_0)$, $A^{(2,1)}(s_0)$ and $A^{(2,2)}(s_0)$, making different fits with the 9 available bins above $s_0 = 2\,\text{GeV}^2$. In order to avoid too large data correlations, we will restrict every fit to just one moment $A^{(2,m)}(s_0)$, with three free parameters: $\alpha_s(m_\tau^2)$, $\mathcal{O}_{2(m+2)}$ and $\mathcal{O}_{2(m+3)}$.

In Figure 3.6 we plot the values of the three parameters fitted in CIPT with the moment $A^{(2,0)}(s_0)$ (very similar conclusions are obtained with FOPT and for

| Moment | Method | $\alpha_s(m_\tau^2)$ | Lower-$D$ Condensate ($10^{-3}$ GeV$^D$) | Higher-$D$ Condensate ($10^{-3}$ GeV$^D$) |
|---|---|---|---|---|
| $A^{(2,0)}(s_0)$ | FOPT | $0.331\,^{+0.013}_{-0.018}$ | $-9\,^{+12}_{-4}$ | $-4\,^{+3}_{-7}$ |
| $A^{(2,0)}(s_0)$ | CIPT | $0.333\,^{+0.011}_{-0.009}$ | $-11\,^{+7}_{-6}$ | $0 \pm 1$ |
| $A^{(2,1)}(s_0)$ | FOPT | $0.322\,^{+0.010}_{-0.006}$ | $3\,^{+1}_{-2}$ | $0 \pm 2$ |
| $A^{(2,1)}(s_0)$ | CIPT | $0.334\,^{+0.011}_{-0.009}$ | $0 \pm 1$ | $2 \pm 2$ |
| $A^{(2,2)}(s_0)$ | FOPT | $0.319\,^{+0.009}_{-0.006}$ | $-2\,^{+3}_{-2}$ | $-1\,^{+4}_{-5}$ |
| $A^{(2,2)}(s_0)$ | CIPT | $0.334\,^{+0.011}_{-0.009}$ | $2 \pm 2$ | $-5 \pm 4$ |

Table 3.9: Fitted results in the $V+A$ channel, using the weight functions of Eq. (3.33) and ignoring DV effects. The value given for the $D=4$ condensate refers to $\langle \frac{\alpha_s}{\pi} GG \rangle$. The quoted uncertainties include experimental and perturbative errors.

the other moments) as a function of the starting $s_0$ value of the fit, $\hat{s}_0$, for the $V$, $A$ and $V+A$ channels. The points with error bars shown at a given value of $\hat{s}_0$ represent the results of the fit using only the values of the moments at $s_0 \geq \hat{s}_0$, *i.e.*, at the bins above $\hat{s}_0$. Since we need to fit three parameters, four points at least are needed. Thus, the highest value $\hat{s}_0 = 2.6$ GeV$^2$ gives the results of a fit to the last four $s_0$ bins, while for the lowest value $\hat{s}_0 = 2.0$ GeV$^2$ the nine bins are included in the fit.

As expected, the figure shows a strong dependence on $\hat{s}_0$ in the $V$ and $A$ channels, as well as completely incompatible values for $\alpha_s(m_\tau^2)$ and $\langle \frac{\alpha_s}{\pi} GG \rangle$ in the lower $\hat{s}_0$ range, where it has been assumed that the OPE is able to reproduce the shape of the spectral function. However, when we go to higher values of $\hat{s}_0$, the $V$ and $A$ fitted parameters start to converge towards the much more stable $V+A$ results. The stability of the $V+A$ fit in the whole range of $\hat{s}_0$ values analyzed is quite surprising. DV effects are present (we are sensitive to the spectral function itself) and clearly manifest in the $V$ and $A$ plotted points, but their size seems to be quite suppressed in the more inclusive $V+A$ distribution. This qualitative behavior is easily understood looking at the experimental spectral functions in Fig. 3.2 and observing the flattening of the highest energy points in the $V+A$ curve, with a clear compensation of the vector and axial-vector departures from local duality.

Ignoring completely any possible effects from violations of duality, a direct fit of the $V+A$ moments for the 9 available points above $s_0 = 2\,\text{GeV}^2$ gives the results shown in Table 3.9. Each horizontal line corresponds to the fit of a single moment $A^{(2,k)}(s_0)$ $(k = 0, 1, 2)$, either with FOPT or CIPT. The fitted

values are in good agreement with the ones obtained before in Tables 3.1 and 3.2, for the same channel. The sensitivity to the power corrections turns out to be very bad, being all fitted results compatible with zero. On the other side, one obtains very stable values for the strong coupling with moderate errors. The CIPT result is stable with the three moments giving practically the same value $\alpha_s(m_\tau^2)^{\rm CIPT} = 0.335 \pm 0.010$, while a weighted average of the three FOPT results (keeping the smallest error) translates into $\alpha_s(m_\tau^2)^{\rm FOPT} = 0.323 \pm 0.008$. However, all these fits have a very low quality ($\chi^2_{\rm min}$/d.o.f.), indicating the presence of the neglected DV effects. Adding then quadratically half of the difference between the maximum and minimum values of $\alpha_s(m_\tau^2)$ given in Figure 3.6 for this channel, as a conservative estimate of DV uncertainties, one obtains:

$$\begin{array}{l} \alpha_s(m_\tau^2)^{\rm CIPT} \;=\; 0.335 \pm 0.014 \\ \alpha_s(m_\tau^2)^{\rm FOPT} \;=\; 0.323 \pm 0.012 \end{array} \qquad \longrightarrow \qquad \alpha_s(m_\tau^2) \;=\; 0.329 \pm 0.013\,. \tag{3.40}$$

Doing the same for the $A^{(2,1)}(s_0)$ moment to get $\delta_{NP}$, one finds:

$$\delta_{NP}^{FOPT} = -0.008 \pm 0.011\,, \tag{3.41}$$

$$\delta_{NP}^{CIPT} = -0.004 \pm 0.008\,. \tag{3.42}$$

## 3.6 An alternative approach

So far, we have been exploring different strategies adopted in previous works, analyzing their advantages and weaknesses. The standard approach followed in Section 3.3 appears to be on solid ground, once systematic uncertainties are properly estimated. Higher-order condensates and violations of duality are neglected, but the numerical impact of these effects can be shown to be small enough when appropriate pinched weight functions are used. In particular, the more inclusive $V + A$ channel provides a very reliable determination of the strong coupling, given in Eq. (3.23). The stability of this result has been carefully studied in Sections 3.3 and 3.4, using different weights. In all cases, the fits provided consistent determinations of $\alpha_s(m_\tau^2)$, in excellent agreement with (3.23).

The possibility to extract additional information on the higher-dimensional vacuum condensates from the $s_0$ dependence of the moments was investigated in Section 3.5. It was shown there that varying $s_0$ turns out to be equivalent to a fit of the measured hadronic distribution on the physical region (the positive real axis), where the OPE cannot be applied. Nevertheless, the fits performed with the $V + A$ spectral function exhibit a quite surprising stability, suggesting

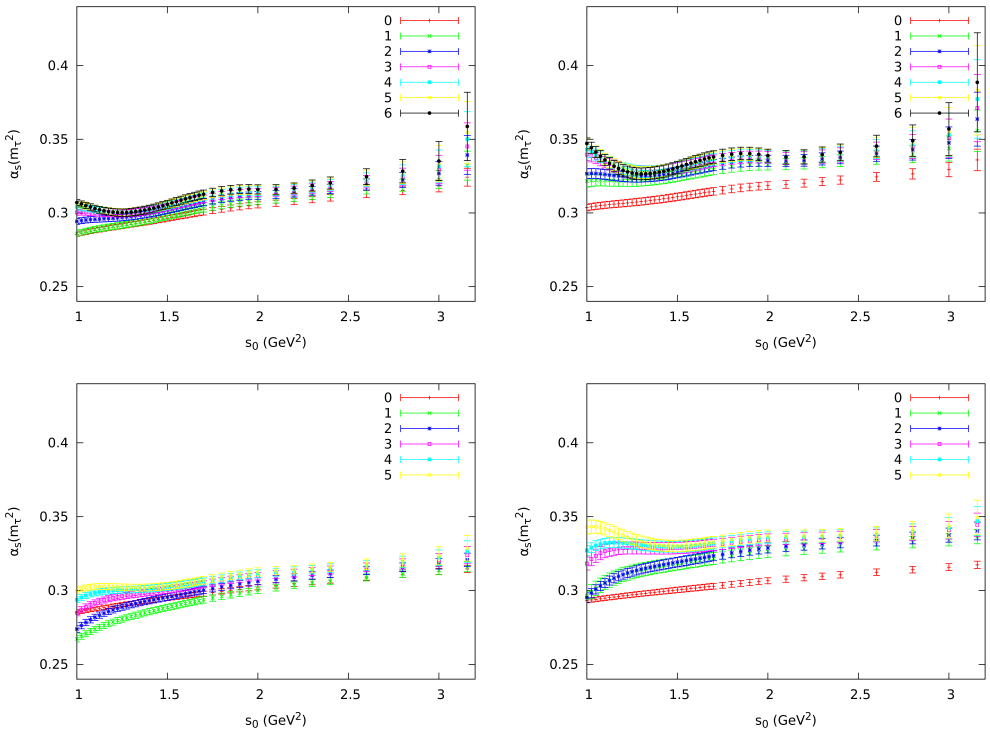


Figure 3.7: $V+A$ determinations of $\alpha_s(m_\tau^2)$ from different moments, as function of $s_0$, fitted ignoring all non-perturbative corrections. The top panels show the results extracted from $A^{(1,n)}(s_0)$ with $\{n = 0, ..., 6\}$, while the bottom panels correspond to $A^{(2,n)}(s_0)$ with $\{n = 0, ..., 5\}$. FOPT fits are on the left and CIPT on the right. Only experimental uncertainties have been included.

that higher-order condensates and DV uncertainties are not large in this channel. Taking the fluctuations with $s_0$ into account to conservatively estimate the theoretical uncertainties, we finally obtained a determination of $\alpha_s(m_\tau^2)$ from the $s_0$ dependence, given in Eq. (3.40). The surprising agreement with (3.23) suggests a much better behavior of perturbative QCD at low invariant masses than naively expected. This had been already noticed long time ago in the pioneering analyses of the $s_0$ dependence performed in Refs. [44, 75, 111, 145, 146].

To better appreciate this fact, we plot in Figure 3.7, as a function of $s_0$, the results of fits to different $A^{\omega}_{V+A}(s_0)$ moments, ignoring all non-perturbative effects. The different curves correspond to the weight functions $\omega^{(1,n)}(x)$ (top

panels) and $\omega^{(2,n)}(x)$ (bottom panels), defined in Eqs. (3.32) and (3.33), for $\{n = 0, ..., 6\}$ and $\{n = 0, ..., 5\}$, respectively. These pure perturbative determinations are shown with the two alternative prescriptions for the $\alpha_s$ expansion, FOPT (left) and CIPT (right). The non-perturbative corrections to these 13 different moments are completely different, carrying a broad variety of inverse powers of $s_0$:

$$A_{V+A}^{(1,n),\rm NP}(s_0) \;=\; (-1)^n\,\pi\,\frac{\mathcal{O}_{2n+4,V+A}}{s_0^{n+2}}\,, \tag{3.43}$$

$$A_{V+A}^{(2,n),\rm NP}(s_0) \;=\; (-1)^n\,\pi\,\left\{(n+2)\,\frac{\mathcal{O}_{2n+4,V+A}}{s_0^{n+2}} + (n+1)\,\frac{\mathcal{O}_{2n+6,V+A}}{s_0^{n+3}}\right\} \tag{3.44}$$

Therefore, one would expect a splitting among the different moments for a given value of $s_0$ that should increase at lower energies. This is however not seen in the figure, which exhibits a quite surprising clustering of the different curves with a very similar dependence on $s_0$. The OPE contributions do not seem to be the dominant feature behind the slight $s_0$ dependence observed. The small difference in normalization observed for the $A^{(k,0)}(s_0)$ CIPT case ($k = 0, 1$) seems more related to perturbative uncertainties. Notice that only the experimental errors have been shown in the plots.

From this perturbative exercise one could perhaps conclude that we have been too conservative when worrying about possible uncertainties from higher-dimensional condensate corrections, because their effects are not manifest in the $V + A$ analyses, with the current experimental accuracy.

The situation seems to be different for the separate vector and axial-vector channels, with more resonance structure in their spectral functions which only flatten at higher values of $s$, specially in the $A$ case. The fitted results are less stable and we have already seen in Figure 3.3 a more clear indication of a sizeable power correction with $D = 6$, in agreement with theoretical expectations. Nevertheless, in the higher energy bins the power corrections seem to decrease very fast, and the fitted results from both channels tend to converge towards the more stable $V + A$ values.

DVs appear to be more important in the semi-inclusive $V$ and $A$ channels, except for the higher energy bins. We can try to reduce these effects by adding an exponencial term to the weight functions. The same kind of weights were used long time ago in Refs. [19] to extract the so-called SVZ sum rules. We will pay the prize of enhancing the unknown high-energy condensate contributions. Since

they are smaller for the $A^{(1,n)}$ weights, we will take

$$\omega_a^{(1,n)}(x) \;=\; \left(1 - x^{n+1}\right)\, \mathrm{e}^{-ax}\,, \tag{3.45}$$

which gives an OPE correction

$$A_{V/A}^{\omega_a^{(1,n)},\mathrm{NP}}(s_0) \;=\; \pi \,\sum_D \,\frac{\mathcal{O}_{D,V/A}}{s_0^{D/2}}\,\frac{a^{\frac{D}{2}-1}}{(\frac{D}{2}-1)!}\,\left\{1 \,+\, \theta(D-4-2n)\,\frac{(-1)^n}{a^{n+1}}\,\frac{(\frac{D}{2}-1)!}{(\frac{D}{2}-n-2)!}\right\}, \tag{3.46}$$

with $\theta(z) = 1$ for $z \geq 0$ and zero otherwise. When $a = 0$ we recover (3.43). Notice that the OPE corrections become independent of $n$ when $a \gg 1$, since all moments are equal in that limit.

Owing to the exponential weight factor, all vacuum condensates contribute to the moments. Therefore, if the non-perturbative uncertainties are dominated by power corrections, one should expect from Eq. (3.46) that a determination of the strong coupling neglecting those terms would become immediately more unstable under variations of $s_0$ than in the $a = 0$ case, and that the splitting among moments at a given value of $s_0$ would increase, before they converge in the limit $a \to \infty$.

In Figure 3.8 we show, as function of $s_0$, the determinations of $\alpha_s(m_\tau^2)$ extracted from 7 different $A_{V/A}^{\omega_a^{(1,n)}}(s_0)$ moments ($n = 0, \ldots, 6$), neglecting all non-perturbative corrections. We show the results obtained with CIPT and three different choices of $a = 0, 1, 2$. Again, only experimental uncertainties have been included in the plots.

It is evident from the panels that with a non-zero Borel parameter $a$ one gets more stable results, and the different moments converge very soon when $a$ is increased. This indicates that, for these weight functions and for the plotted ranges of $s_0$ and $a$, non-perturbative uncertainties are probably more affected by DV effects than by power corrections. Of course, if one takes $a$ too large, higher-dimensional condensate corrections will become dominant, and the extracted values of $\alpha_s(m_\tau^2)$ will depend strongly on $s_0$. We observe in Figure 3.8 that this is actually starting to happen in the $V$ channel, at $a \sim 2$.

In Figure 3.9, we plot the determinations of $\alpha_s(m_\tau^2)$ at a fixed[‡] value of $s_0 = 2.8\ \mathrm{GeV}^2$, as a function of the Borel parameter $a$. We observe how in the region where the strong coupling is stable, *i.e.*, $\frac{d\alpha_s}{da} \sim 0$, there is a similar stability range under variations of $s_0$, for every moment. This reinforces the idea that there exist

[‡]We take this value as a reference point because it is the largest invariant-mass bin with enough experimental resolution.

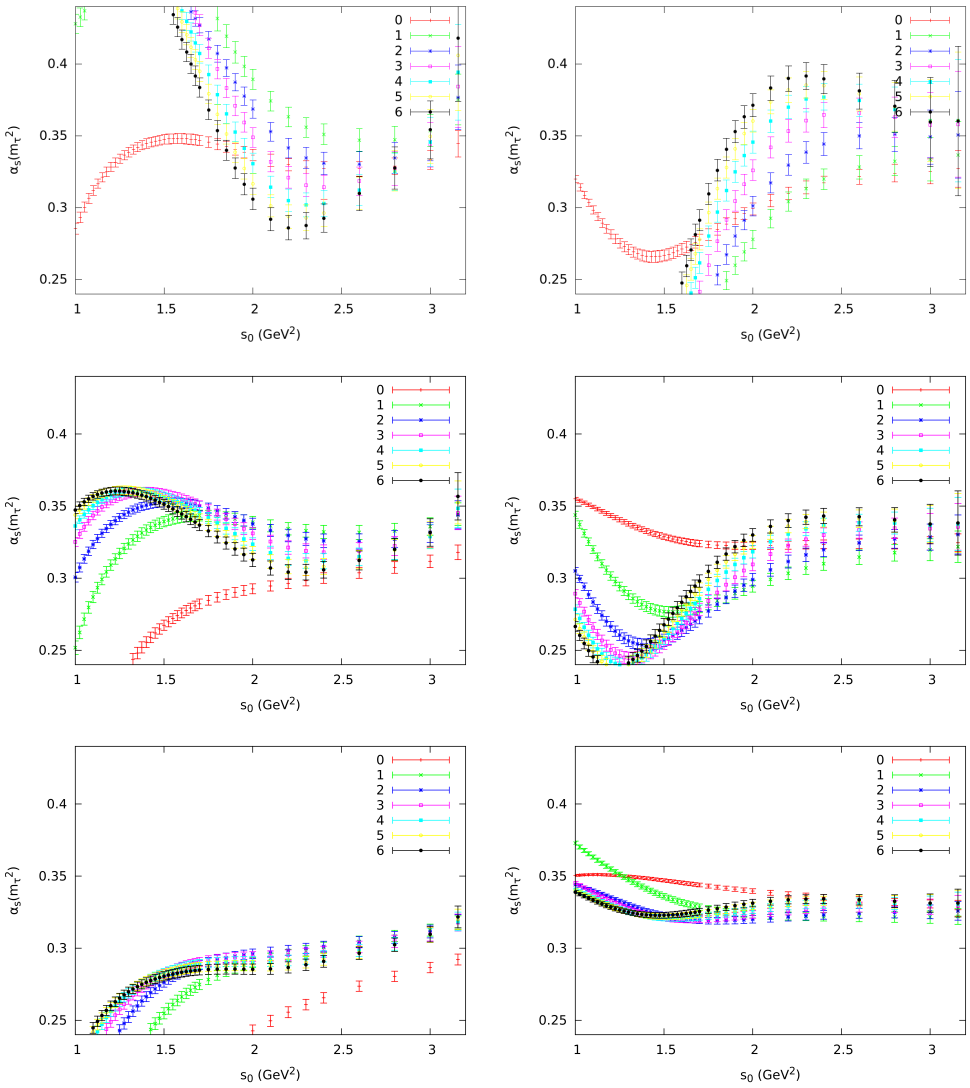


Figure 3.8: CIPT determinations of $\alpha_s(m_\tau^2)$ from the moments $A^{\omega_a^{(1,n)}}_{V/A}(s_0)$, as function of $s_0$, ignoring all non-perturbative corrections and evaluated at $a = 0$ (top), 1 (middle) and 2 (bottom). The left (right) panels correspond to the vector (axial-vector) distribution. Only experimental uncertainties have been included.

a range of values of $a$, large enough to minimize DV effects and not so large to

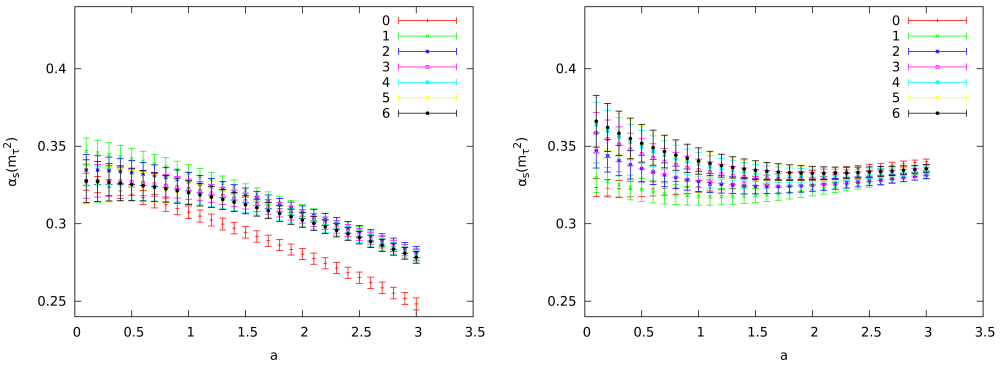


Figure 3.9: CIPT seterminations of $\alpha_s(m_\tau^2)$ from the moments $A_{V/A}^{\omega_a^{(1,n)}}(s_0)$, at $s_0 = 2.8$ GeV$^2$ and ignoring all non-perturbative corrections, for different values of the Borel parameter $a$ (V on the left and A on the right). Only experimental uncertainties are included.

get dominant condensate corrections, so that it is the best region for determining $\alpha_s(m_\tau^2)$.

In order to extract a reliable value for the strong coupling, using what we know, we start by taking as reference the point $s_0 = 2.8$ GeV$^2$. For every moment and channel ($V$ or $A$), we only accept values of $\alpha_s$ in the stability region of the Borel transform,[§] *i.e.*, those whose central values are within the experimental errors of the derivative-zero point $\frac{d\alpha_s}{da} = 0$. For every value of $a$ in that region, we have an $\alpha_s(m_\tau^2)$ value. Its error is calculated adding quadratically to the experimental error the perturbative uncertainty, estimated varying $K_5$ and the scale $\xi$ with the same criteria as above, and the non-perturbative one, calculated conservatively as the maximum value minus the minimum one in the region $s_0 \in [2, 2.8]$ GeV$^2$. We choose as the optimal value for every moment the one that gives the minimum total error. Finally, we take as central value of the 7 moments the one closest to the average and its error summed quadratically to half the difference between the maximum and minimum $\alpha_s(m_\tau^2)$ value (as a second non-perturbative uncertainty, more related with the neglected vacuum condensates)

[§]We have checked that results are not really different if we remove this condition. This happens because the Borel-stable region is very similar to the $s_0$-stable one, for all moments at every experimental channel, as one would expect if all non-perturbative effects are indeed small in that Borel region.

to get a conservative estimate of the total uncertainty. We obtain in this way:

$$\begin{aligned}
\alpha_s(m_\tau^2)^{V,\mathrm{CIPT}} &= 0.326\,^{+0.021}_{-0.019}\,, \\
\alpha_s(m_\tau^2)^{A,\mathrm{CIPT}} &= 0.325\,^{+0.018}_{-0.014}\,, \\
\alpha_s(m_\tau^2)^{V,\mathrm{FOPT}} &= 0.314\,^{+0.015}_{-0.011}\,, \\
\alpha_s(m_\tau^2)^{A,\mathrm{FOPT}} &= 0.320\,^{+0.019}_{-0.016}\,. \qquad (3.47)
\end{aligned}$$

Thus, we find a very good consistency between the determinations performed in the vector and axial-vector channels. Taking the average of both experimental channels and keeping the minimum error, we get finally

$$\begin{aligned}
\alpha_s(m_\tau^2)^{\mathrm{CIPT}} &= 0.325\,^{+0.018}_{-0.014} \\
\alpha_s(m_\tau^2)^{\mathrm{FOPT}} &= 0.317\,^{+0.015}_{-0.011}
\end{aligned}
\qquad \longrightarrow \qquad
\alpha_s(m_\tau^2) = 0.321\,^{+0.016}_{-0.012}\,. \qquad (3.48)$$

One can play a similar game with the $V+A$ channel. The resulting $\alpha_s(m_\tau^2)$ determinations are plotted in Figures 3.10 and 3.11, as function of $s_0$ and $a$, respectively. Since for $V+A$ one observes a slightly different behavior in FOPT and CIPT, the results of both perturbative approaches are shown in the figures. Increasing the Borel parameter $a$ does not bring in this case any clear improvement in the stability under $s_0$ (Figure 3.10), because the DV effects are smaller for $V+A$. When we reduce the tiny DV effects, the condensate corrections could become dominant. The different qualitative behavior observed in Figure 3.11 for FOPT and CIPT reflects the difficulties in extracting conclusions with this method about the tiny non-perturbative corrections in the $V+A$ channel, within the much larger perturbative uncertainties.

Applying the same method as in the separate vector and axial-vector channels, in FOPT we can derive from these plots a combined determination of the strong coupling in a completely straightforward way. A little bit more care has to be taken in CIPT because of the absence of a derivative-zero point ($\frac{d\alpha_s(m_\tau^2)}{da} = 0$) in Figure 3.11. We can try two different possibilities: either accept only the small stability region in the separate V and A channels, or apply the method without imposing that constraint. We find the same result with both procedures. Our final results from the $V+A$ channel are:

$$\begin{aligned}
\alpha_s(m_\tau^2)^{\mathrm{CIPT}} &= 0.328\,^{+0.014}_{-0.013} \\
\alpha_s(m_\tau^2)^{\mathrm{FOPT}} &= 0.318\,^{+0.015}_{-0.012}
\end{aligned}
\qquad \longrightarrow \qquad
\alpha_s(m_\tau^2) = 0.323\,^{+0.015}_{-0.013}\,, \qquad (3.49)$$

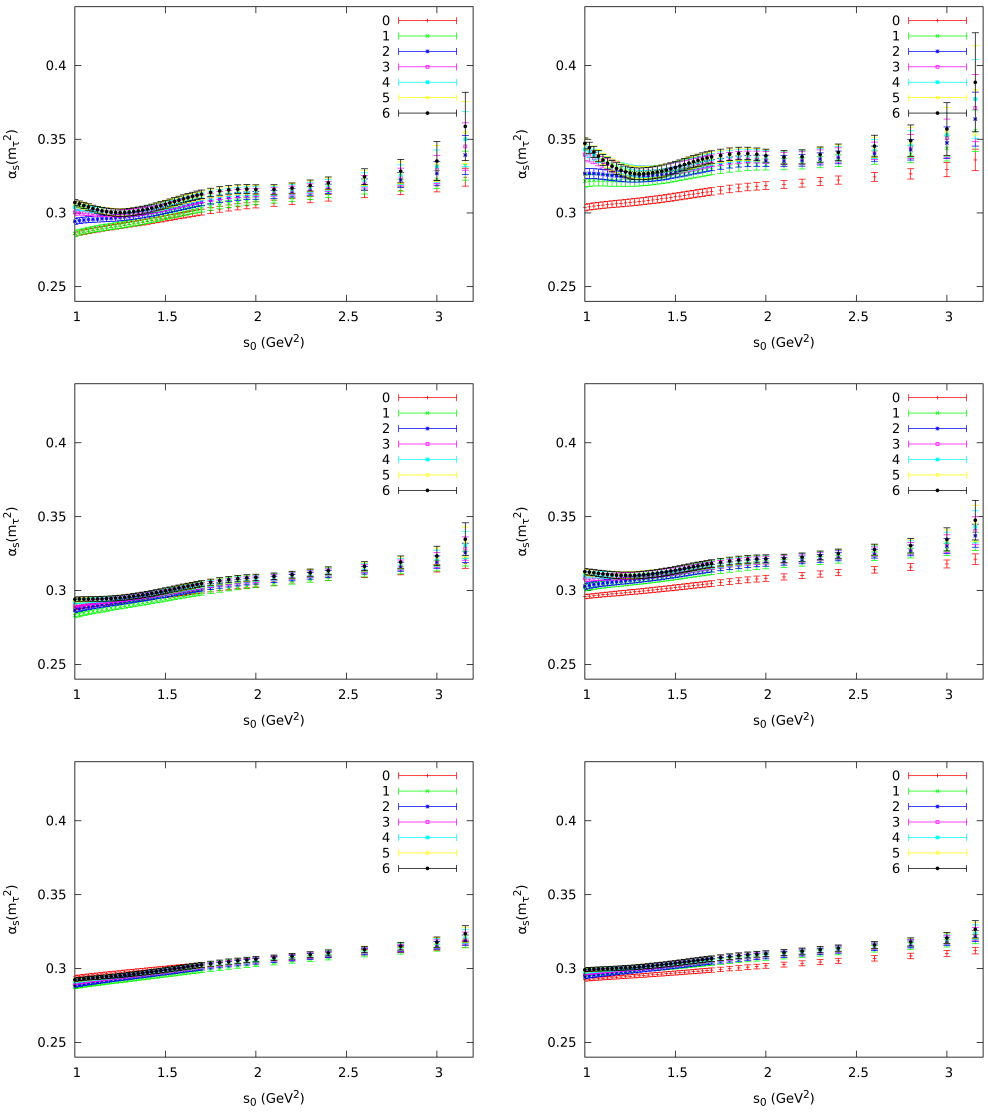


Figure 3.10: Determinations of $\alpha_s(m_\tau^2)$ from the moments $A^{\omega_a^{(1,n)}}_{V+A}(s_0)$, as function of $s_0$, ignoring all non-perturbative corrections and evaluated at $a = 0$ (top), 1 (middle) and 2 (bottom). The left (right) panels correspond to FOPT (CIPT). Only experimental uncertainties have been included.

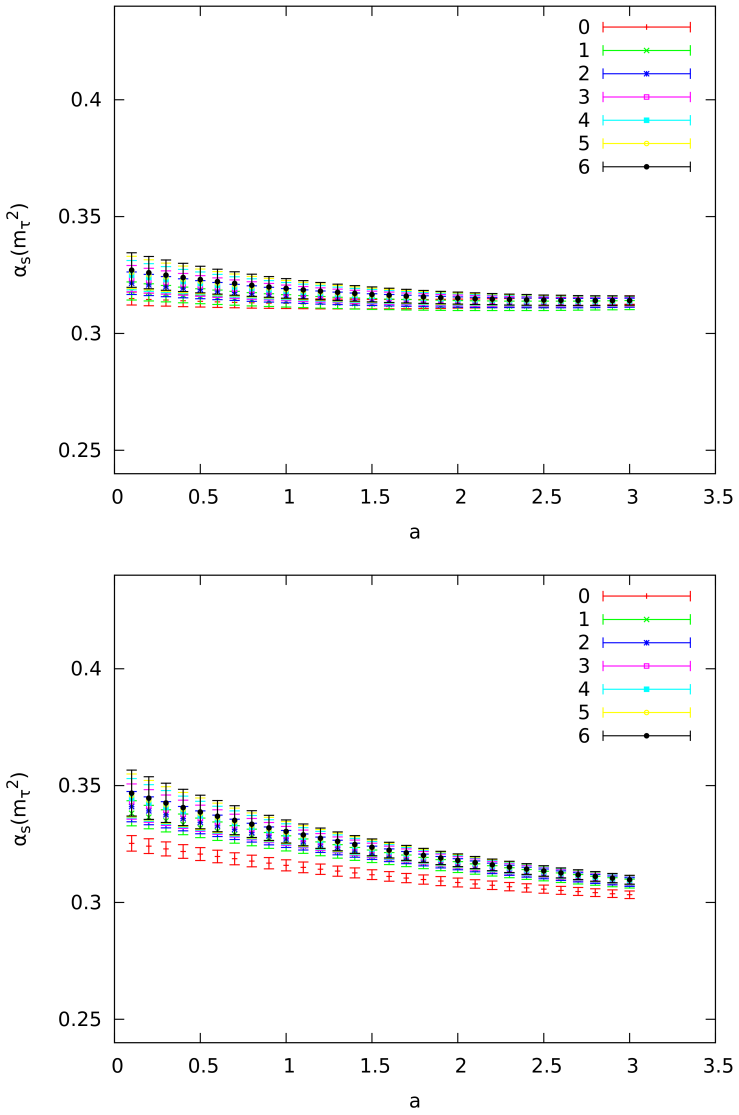


Figure 3.11: Determinations of $\alpha_s(m_\tau^2)$ from the moments $A^{\omega_a^{(1,n)}}_{V+A}(s_0)$, at $s_0 = 2.8$ GeV$^2$ and ignoring all non-perturbative corrections, for different values of $a$ (FOPT at top and CIPT at bottom). Only experimental uncertainties are included.

in good agreement with (3.48).

## 3.7 Modeling duality violations

In order to study violations of duality, Refs. [113–115] parametrize the differences between the physical spectral functions and their OPE approximations with the following ansatz:

$$\Delta\rho^{\rm DV}_{V/A}(s) \;=\; e^{-(\delta_{V/A}+\gamma_{V/A}s)}\;\sin\left(\alpha_{V/A}+\beta_{V/A}s\right), \qquad\qquad s>\hat{s}_0\,. \tag{3.50}$$

Although it is theoretically well motivated, this functional form cannot be derived from first principles, which unavoidably introduces some model dependence in their analyses. This combination of an oscillatory function with an exponential damping is assumed to describe the fall-off of DVs at very high energies. However, nobody really knows from which $\hat{s}_0$ value it might start to be a valid approximation.

Having a model for the spectral function, to be fitted to data, one can then estimate the DV correction to Eq. (3.1) through the identity [39, 45, 55, 59]

$$\Delta A^{\omega,{\rm DV}}_{V/A}(s_0) \;\equiv\; \tfrac{i}{2}\oint_{|s|=s_0}\tfrac{ds}{s_0}\,\omega(s)\,\left\{\Pi_{V/A}\,(s)-\Pi^{\rm OPE}_{V/A}(s)\right\} \;=\; -\pi\int_{s_0}^{\infty}\tfrac{ds}{s_0}\,\omega(s)\,\Delta\rho^{\rm DV}_{V/A}(s)\quad. \tag{3.51}$$

The strategy adopted in Refs. [113–115] consists in making a global fit to the $s_0$ dependence of the moments $A^{\omega}_{V/A}(s_0)$, in order to fit $\alpha_s(m_\tau^2)$, the vacuum condensates and the eight spectral function parameters in Eq. (3.50), assuming the ansatz is valid above $\hat{s}_0\sim 1.55\,{\rm GeV}^2$. They make a large amount of different fits and tests in agreement with many observables and with the same values for the model parameters, which may lead to the conclusion that the model is giving a very precise prediction of DVs. In this large section, we will start by showing how most of those tests are consequence of the following:

1. Using an ad-hoc model for the spectral function with 4 parameters fitted to data, so that necessarily there is agreement with it in some region, as for any chosen parametrization.

2. Adding data points which gives no information about the relevant parameters for the $\alpha_s$ extraction, *i.e.*, any other $\alpha_s$ would also be in agreement with those data points.

3. Adding to the original fit a number of independent data points equal to the number of new theoretical parameters one introduces into the fit, so that

the new parameters will adapt to the values of the new data points without new information on $\alpha_s$.

4. Testing agreement between data and theory of observables which are simple functions of points already fitted, so that provided the original fit is in agreement (which obviously it is, see point 1), necessarily those observables are.

We will briefly analyze the consequences of these points and we will see how small modifications in the ansatz or in the arbitrary threshold $\hat{s}_0$ lead to a completely different prediction for the strong coupling, so that one can even tune the model parameters to extract any $\alpha_s$ with the same agreement with data.

Then, one natural worrisome, reflected in Ref. [120] might arise: if using that approach one can build DV models for getting any $\alpha_s$, does it mean that from tau data is impossible to extract any reliable $\alpha_s$? Is then our previous study wrong? We will see, using as example the central fit of Ref. [115], how the consequences of setting a value of $\alpha_s(m_\tau^2)$ which differs from our determination needs to introduce two things:

1. A huge and unreliable DV above the $\tau$ mass.

2. Huge condensates, making the OPE divergent series at the $\tau$ mass, breaking the expected naive counting from the first condensates.

Since this scenario is unjustified (in the sense that one can choose parameters so that it does not happen), we finally argue that this breaking of the counting is comparable with fine tuning high-order perturbative coefficients, so that one can land outside from the interval quoted in theoretical uncertainties.

### 3.7.1 Deconstructing a model-dependent analysis

Let us recall Eq. (3.1) with the modified OPE

$$A^{\omega}_{V/A}(s_0) \equiv \int_{s_{th}}^{s_0} \frac{ds}{s_0}\omega(s)\,\mathrm{Im}\,\Pi_{V/A}(s) = \frac{i}{2}\oint_{|s|=s_0}\frac{ds}{s_0}\omega(s)\Pi^{\mathrm{OPE}}_{V/A}(s) + \Delta A^{\omega,\mathrm{DV}}_{V/A}(s_0)\,. \tag{3.52}$$

If, following the prescription of Ref. [115], one fits data from a channel with the five model parameters $\alpha_s, \delta_V, \gamma_V, \alpha_V, \beta_V$ from the $s_0-$dependence of the $\omega(s) = 1$ moment, $\{A_V(s_0), s_0 \in [\hat{s}_0, m_\tau]\}$, obviously there are some $\hat{s}_0$ for which there is agreement with data. Without any further theoretical or experimental reason, just because in the $V$ channel there is a local maximum in the p-value so that

$p \approx 5\%$, they assume the model becomes exactly true from $\hat{s}_0 = 1.55\,\mathrm{GeV}^2$. This leads to:

$$\alpha_s^{FOPT}(m_\tau^2) = 0.298 \pm 0.011\,, \tag{3.53}$$

$$\alpha_s^{CIPT}(m_\tau^2) = 0.312 \pm 0.014\,. \tag{3.54}$$

Using the information on the spectral function, we have the experimental $A_V(s_0)$ in the interval $s_0 \in [\hat{s}_0, m_\tau]$. From the definition of $A_V(s_0)$, it is obvious that this is the same as fitting $A_V(\hat{s}_0)$ plus the experimental spectral function $\rho_V(s)$ in the interval $(\hat{s}_0, m_\tau]$. One can reconstruct one set of data points from the other by using the trivial identity:

$$s_0 A_V(s_0) = \pi \int_{\hat{s}_0}^{s_0} ds \rho(s) + s_0 A_V(\hat{s}_0)\,. \tag{3.55}$$

Then, once the original fit, necessarily in good agreement with data in some interval $s_0 \in [\hat{s}_0, m_\tau]$, presents such agreement for $A_V(s_0)$, then there is no way that the spectral function is in disagreement with data in that interval. A test checking that is then worthless and by no means is a test of the model, as one may infer from Ref. [115].

The first extension to this fit can be using information from the $A$ spectral function. If, as done in that work, one chooses again $\hat{s}_0 = 1.55\,\mathrm{GeV}^2$, the interval $s_0 \in [\hat{s}_0, m_\tau]$ happens to be small enough to be compatible with the model, which is not a surprise if one takes into account that one is inserting other 4 free parameters and experimental uncertainties are larger in this channel. However, because of these larger uncertainties, no useful information for $\alpha_s$ can be extracted from including the $A$ channel. Basically one gets that any reasonable value of the strong coupling $\alpha_s(m_\tau) \sim 0.3 \pm 0.1$ is compatible with data when introducing those new free parameters. One might question himself: is there in the $A$ channel a value of $\hat{s}_0$ small enough so that one can predict (a model-dependent) $\alpha_s(m_\tau)$ with similar precision to the previous (model-dependent) $\alpha_s(m_\tau)$ and with a similar p-value? Interestingly, there is. This starts happening at $\hat{s}_0 = 1.475\,\mathrm{GeV}^2$ and a local maximum in the p-value ($p = 16\%$) is found in $\hat{s}_0 = 1.3\,\mathrm{GeV}^2$, where one finds $\alpha_s^{\mathrm{FOPT}}(m_\tau^2) = 0.332 \pm 0.011$. If data had happened to be less precise in the $V$ channel, maybe this would have been the final $\alpha_s$ value of this approach.

Then, Ref. [115] makes extra fits by adding other weight functions to the previous one,

$$\{A^1(s_0), A^{1-x^2}(s_0), A^{1-3x^2-2x^3}(s_0)\,;\, s_0 > \hat{s}_0\}\,, \tag{3.56}$$

where $x = \frac{s}{s_0}$. Making a linear transformation of the data points that, taking into account correlations, leaves the $\chi^2$ invariant, one finds that fitting those points is mathematically equivalent to fit:

$$\{A^1(s_0), A^{x^2}(s_0), A^{x^3}(s_0)\,;\, s_0 > \hat{s}_0\}\,. \tag{3.57}$$

But then, using that:

$$A^{x^2}(s_0) = \frac{1}{s_0^3}\pi \int_{\hat{s}_0}^{s_0} s^2\rho(s) + A^{x^2}(\hat{s}_0)\,, \tag{3.58}$$

$$A^{x^3}(s_0) = \frac{1}{s_0^4}\pi \int_{\hat{s}_0}^{s_0} s^4\rho(s) + A^{x^3}(\hat{s}_0)\,, \tag{3.59}$$

and that, as we showed before, the spectral function is already fitted[¶] when fitting $A^1(s_0)$, only two independent data points have been added to the fit, $A^{x^2}(\hat{s}_0)$ and $A^{x^3}(\hat{s}_0)$. Since additionally they depend respectively on $\mathcal{O}_6$ and $\mathcal{O}_8$, which are added as free parameters to be fitted, at the end one is adding to the original fit as many independent data points as unknown theoretical parameters, so that the quality of the fit is going to be necessarily the same and, when marginalizing over $\mathcal{O}_6$ and $\mathcal{O}_8$, the $\chi^2$ distribution is going to be identical. Adding this fit to the previous one is then a tautology in the sense that the same result must arise.

Ref. [115] acknowledges that the correlation matrix is singular (which it is consequence of unnecessarily adding the same data points several times) and instead of trivially fixing the problem (by removing such data points), they obtain the central value of the theoretical parameters by putting to zero the huge correlation among different moments, which distortions the central value of the fit. Then they use a method presented in the appendix of Ref. [113], based on some assumptions, to estimate uncertainties. If it is correct, the result must reduce to the fit we just explained when removing the double-counted experimental data points. But then again the fit is the same as the original one and the same result for the parameters must arise.

[¶]Explicitly from Eq. (3.55):

$$\rho(s_0) = \frac{1}{\pi}([A_V^1(s_0) - A_V^1(\hat{s}_0)] + A_V^{'1}(s_0)s_0)\,. \tag{3.60}$$

As far as the binning is prepared to be able to integrate by summing over them, as it is in this occasion and what it should be preferred so that no model-dependent extra assumptions in the shape of the spectral function have to be taken, the derivative of $A_V^1(s_0)$ is nothing else but the difference $\frac{A_V^1(s_0)-A_V^1(s_0-\Delta s_0)}{\Delta s_0}$.

Then the first WSR is shown as additional test, but again it was impossible not to satisfy it once one acknowledges that any $\alpha_s$ is compatible with the $A$ channel in this model-dependent approach. As we studied in the previous chapter, the WSR involves the $\omega(s) = 1$ weight function. One has:

$$A_V(s_0) = A^P(s_0; \alpha_s^V) + \Delta A_V^{DV}(s_0)\,, \tag{3.61}$$

$$A_A(s_0) = A^P(s_0; \alpha_s^A) + \Delta A_A^{DV}(s_0)\,, \tag{3.62}$$

where $A^P$ is the perturbative prediction. When one imposes the strong coupling to be the same in the $A$ channel than in the $V$, the first term of the rhs of the previous equations cancels when taking the difference, leaving necessarily:

$$A_{V-A}(s_0) = \Delta A_{V-A}^{DV}(s_0)\,, \tag{3.63}$$

which is the first WSR. In other words, the only way the first WSR may not be satisfied in this approach is by obtaining incompatible values for $\alpha_s$ in the separate $V$ and $A$ channels. Since this is impossible because the $A$ channel is compatible with any $\alpha_s$, this test is satisfied by construction.

The rest of tests consist in plotting moments (or linear combinations of them) $A^{x^n}(s_0)$ that make use of extra fitted parameters. One has:

$$A^{x^n}(s_0) = A^{x^n}(\hat{s}_0; \mathcal{O}_{n+1}) + \frac{\pi}{s_0}\int_{\hat{s}_0}^{s_0} ds\, x^n\, \rho(s)\,. \tag{3.64}$$

Again once one imposes agreement between $A^{x^n}(\hat{s}_0; \mathcal{O}_{n+1})$ and data introducing the free parameter $\mathcal{O}_{n+1}$, the agreement to all data points is guaranteed if one has previously fitted the spectral function in an interval with the 4 model parameters of $\rho_V$ plus the 4 model parameters of $\rho_A$. Again, these tests are satisfied by any possible model in some interval.

### 3.7.2 Performing nontrivial tests of the model

Up to now, the only tool we have to judge the ad-hoc model is the fact that in some interval, taking appropriate values of 4 free parameters, is in agreement with data. Unfortunately, it is very far from a definite tool to judge it, since one can imagine a very large amount of models in agreement with data in some interval. In order to test the reliability of the strong coupling one obtains with it, one still can perform some tests:

| n | $\alpha_s(m_\tau^2)$ | $\delta$ | $\gamma$ | $\alpha$ | $\beta$ | p-value (% ) |
|---|---|---|---|---|---|---|
| 0 | $0.298 \pm 0.010$ | $3.6 \pm 0.5$ | $0.6 \pm 0.3$ | $-2.3 \pm 0.9$ | $4.3 \pm 0.5$ | 5.3 |
| 1 | $0.300 \pm 0.012$ | $3.3 \pm 0.5$ | $1.1 \pm 0.3$ | $-2.2 \pm 1.0$ | $4.2 \pm 0.5$ | 5.7 |
| 2 | $0.302 \pm 0.011$ | $2.9 \pm 0.5$ | $1.6 \pm 0.3$ | $-2.2 \pm 0.9$ | $4.2 \pm 0.5$ | 6.0 |
| 4 | $0.306 \pm 0.013$ | $2.3 \pm 0.5$ | $2.6 \pm 0.3$ | $-1.9 \pm 0.9$ | $4.1 \pm 0.5$ | 6.6 |
| 8 | $0.314 \pm 0.015$ | $1.0 \pm 0.5$ | $4.6 \pm 0.3$ | $-1.5 \pm 1.1$ | $3.9 \pm 0.6$ | 7.7 |

Table 3.10: Fitted values of $\alpha_s(m_\tau^2)$, in FOPT, and the spectral function parameters, modifying the ansatz (3.50) with a power $s^n$ (GeV units).

1. Is the strong coupling $\alpha_s$ dependent on the parametrization or, at least, is the parametrization given by the model the only one reproducing data from the selected threshold?

2. If we change the arbitrary threshold $\hat{s}_0$, is the determination of the strong coupling stable?

3. Is the convergence to the model soft, so that one may predict reasonably well the spectral function below the selected threshold $\hat{s}_0$?

Let us start addressing the point 1 by buying just for the moment that $\hat{s}_0 = 1.55\,\mathrm{GeV}^2$. One may think that the previous model is exceptional because is able to fit data in the interval $(\hat{s}_0, m_\tau)$ with "only" four parameters. Indeed one can easily find better models, for example multiplying the functional form (3.50) with a polynomial. We have repeated the exercise multiplying the ansatz with a simple power $s^n$, to avoid increasing the number of parameters. When varying the power $n$, one finds "better models" (higher p-values) of the spectral function than the default "$n = 0$" and, dramatically, they provide significantly higher values of the strong coupling. In Table 3.10 we illustrate a few examples of this simple exercise, varying $n$ between 0 and 8. One immediately appreciates the strong correlation between $\alpha_s(m_\tau^2)$ and the power $n$. The statistical quality of the fit improves with growing values of $n$, while the exponential parameters $\delta_V$ and $\gamma_V$ adapt themselves to compensate the growing of the ansatz spectral function at high values of $s$ with the net result of a smaller DV correction. As the fit quality improves, the central value of the fitted $\alpha_s(m_\tau^2)$ approaches the result of the ALEPH-like fit in Eq. (3.23). The $\alpha_s(m_\tau^2)$ value is then clearly model dependent.

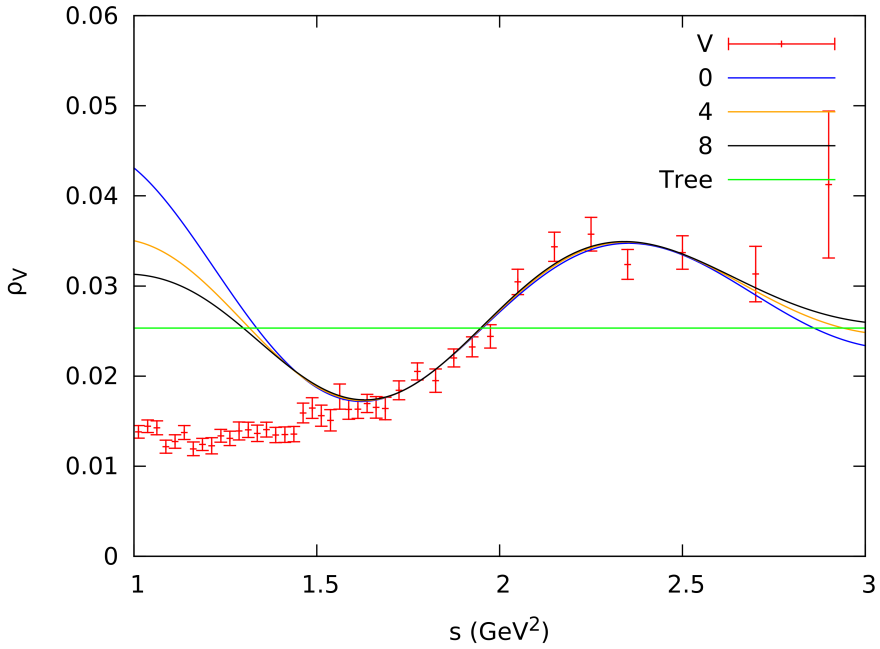


Figure 3.12: Vector spectral function $\rho_V(s)$, fitted with the ansatz (3.50) multiplied by a power $s^n$, for different values of $n = 0, 4, 8$, compared with the data points.

Figure 3.12 compares the measured vector spectral function with the fitted ansatz for $n = 0$, 4 and 8. Although all models reproduce well the spectral function in the fitted region, they deviate very fast from the data below 1.55 GeV$^2$, exhibiting a clear failure of the assumed ansatz. As the power $n$ increases, the fit quality slightly improves and the ansatz slowly approaches the data at values of the invariant mass below the fitted range.

Probably the clearest weakness of the model becomes manifest when the point 2 is addressed. Even if the parametrization given by Eq. (3.50) happened to exactly reproduce the convergence to the QCD spectral function, we have no clue about from which $\hat{s}_0$ value this should be true. This problem might be familiar to the reader, since it is analogous to the problem of convergence to quark-hadron duality: for a given observable, from which energy the OPE prediction is able to reproduce data with a given precision? However, there are two important differences.

The first one is that we know things about how the convergence of the OPE to data should be and we have channels in which this can be explicitly studied where we have data available and with known short-distance constraints (see the previous chapter): it is better in the most inclusive channels, it is very fast, typically exponentially and DVs are very suppressed when inserting pinched weight functions (which leads to the very strong quantitative arguments presented before to state that DVs are negligible for certain $A^{\omega}_{V+A}(s_0)$). This basically means that predictions based on sum rules neglecting DVs, *i.e.*, neglecting $\int_{s_0}^{\infty} \frac{ds}{s_0}\omega(s)\rho_{DV}(s)$ are going to be dominated by the region very close to $s_0$, so that fluctuations in those determinations when varying $s_0$ in a conservative range of energies (as done in the determination of the previous section) gives the order of DV uncertainties, independently on the exact shape of the unknown tail of the spectral function. However, we have no clue on how the convergence to the model is supposed to work. Maybe this approach should implement a model of violations of duality violations.

The second one is that we know that the OPE must converge to data on QCD grounds. Not only we cannot say from which energy data is supposed to converge to the parametrization. We cannot even say if it approximately does it from any point, because it is not QCD.

Even with all that in mind, one can still change $\hat{s}_0$ and hope that there is not a dramatic dependence on it in some interval, so that if we are lucky the hypothetically "physical" $\hat{s}_0$ might be at some point of that interval. But not even that is true. We have performed a fit to the $s_0$ dependence of $A_V^{(0,0)}(s_0)$, above some minimum value $\hat{s}_0$. The results of this exercise are presented in Figure 3.13, using FOPT to handle the perturbative series (the same conclusions, with correspondingly larger values of $\alpha_s(m_\tau^2)$, are obtained in the CIPT case). The left panel shows, as a function of $\hat{s}_0$, the value of $\alpha_s(m_\tau^2)$ extracted from a fit to all $s_0$ bins with $s_0 > \hat{s}_0$, while the right panel gives the associated p-values of the different fits. One immediately notices the very poor statistical quality of these fits, with very low p-values in all cases. If the model were reliable, it should work better at higher hadronic invariant masses. However, the p-value becomes worse when we go to higher values of $\hat{s}_0$ and significant deviations from the model are observed. Even worse, the fitted values of $\alpha_s(m_\tau^2)$ do not present the stability one should expect. Fluctuations of the order of $1\,\sigma$ are observed, just removing 1 of the $\sim 20$ points included in the fit.

Let us finally address the third point. Legitimately, assuming carelessly exact quark-hadron duality at the tau mass for any moment has been criticized for a very simple reason. If at lower energies $s < m_\tau^2$ there is not an exact duality

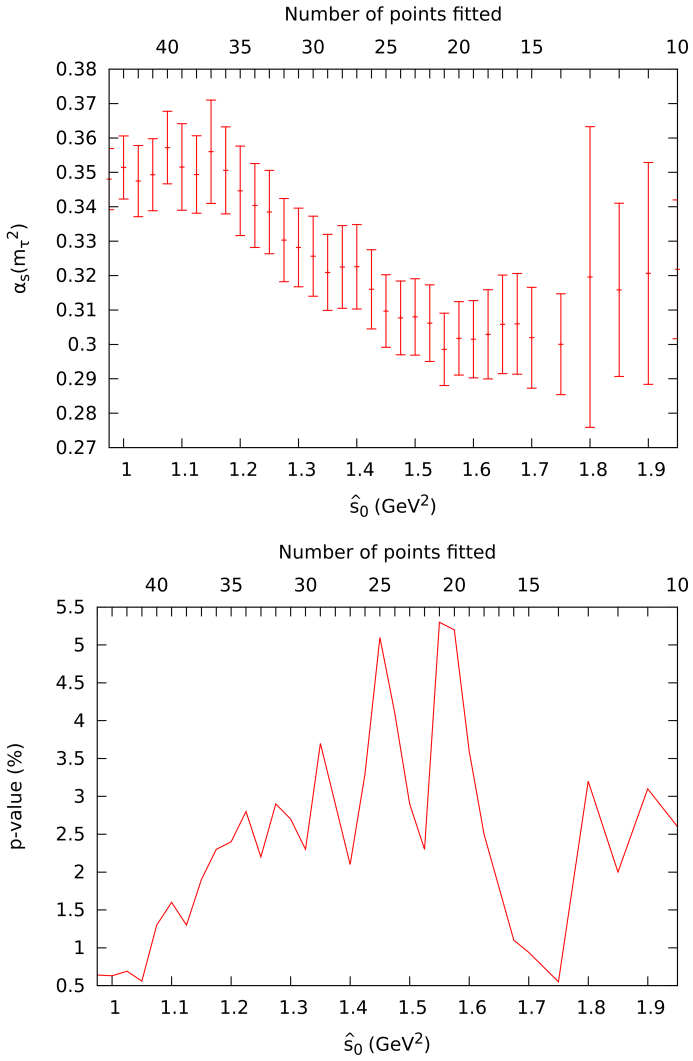


Figure 3.13: FOPT determination of $\alpha_s(m_\tau^2)$ from the $s_0$ dependence of $A_V^{(0,0)}(s_0)$, fitting all $s_0$ bins with $s_0 > \hat{s}_0$, as function of $\hat{s}_0$, using the approach of Ref. [115].

quark-hadron, why is going to be so at $m_\tau^2$? Certainly, convergence of the spectral function to its OPE description must be relatively fast, but it is completely unnatural to think that is going to be exact from $m_\tau^2$, because it did not happen

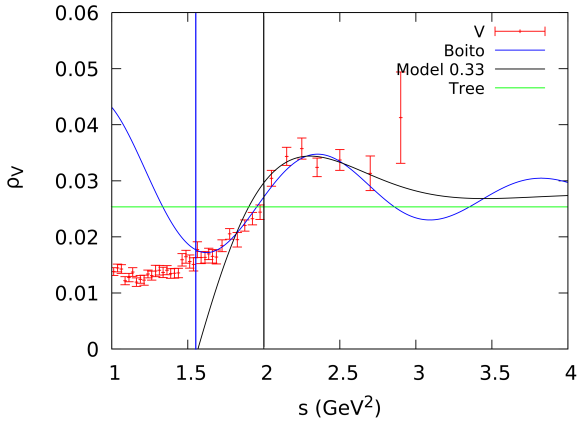


Figure 3.14: Comparison between the tuple prediction of Ref. [115], the tuple associated to $\alpha_s^{\rm FOPT}(m_\tau^2) = 0.330$ and data. Notice how below the explicitly fitted interval, the deviation is dramatic for both tuples.

before and because $m_\tau$ is in principle just an arbitrary energy. The claim that DVs should be small in the $V + A$ channel for most of the weight functions is based, besides of the theoretical point that the hadronic multiplicity is large at that energy, on the fact that the spectral function is very well approximated by its OPE approximant from very low energies. The minimal requirement we should ask to a model is the same: below the fitted energy region (where we have used free parameters to ensure agreement to data), is the convergence to the model soft? In order to answer this question, we plot the model prediction together with the spectral function. Below the fitted data region one can see how the model dramatically deviate from data, so that one necessarily has to unreliably assume that the model is not only exactly but also abruptly valid from $\hat{s}_0 = 1.55\,\text{GeV}$ without any reason. One can play with that and assume that instead is abruptly valid, for example, from $\hat{s}_0 = 2\,\text{GeV}$. Then, taking the tuple $(\alpha_s^{\rm FOPT}, \delta_V, \gamma_V, \alpha_V, \beta_V) = (0.330, 0.51, 1.88, 0.84, 2.78)$ one gets agreement with data in $[2\,\text{GeV}^2, m_\tau]$ with a p-value of an 8%, to be compared with the extremely poor p-value of a 0.6% of the central tuple of the $\hat{s}_0 = 1.55\,\text{GeV}$ fit of Ref. [115] in the same interval or (maybe fairer) with the 5% in $[1.55\,\text{GeV}^2, m_\tau]$. If one ignores the bad convergence of the tuple below the fitted region (Fig. 3.14), why should the value $\alpha_s^{\rm FOPT} = 0.298$ should be chosen instead of $\alpha_s^{\rm FOPT} = 0.330$? By changing $\hat{s}_0$ one can build tuples with any possible $\alpha_s$.

Unfortunately, the conclusion of this section is that the determination of $\alpha_s$ of Ref. [115] is strongly model-dependent and that it fails when some minimal tests about its reliability are performed. If one ignores those tests as a tool to evaluate the reliability of the model, indeed any strong coupling can be imposed a priori in total agreement with data even unreliably assuming that there is some energy from which the parametrization gives an exact description of nature. It is enough to choose the appropriate tuple $(\hat{s}_0, \delta_V, \gamma_V, \beta_V, \alpha_V)$.

### 3.7.3 Consequences of building DV models with a priori values of $\alpha_s(m_\tau^2)$ deviated from the physical one

In previous sections we have studied different approaches to deal with non perturbative uncertainties. We have seen how, when fitting different sets of moments whose DVs are expected to be completely negligible, introducing only those operators with lower dimensions as free parameters is enough to make the quality fit optimal, as expected by any OPE expansion ($\frac{\Lambda^{2n}}{m_\tau^{2n}}$) well-behaved at the tau mass for the first few terms. By adding condensates to the fit and testing stability we have added systematic uncertainties. We have obtained for all those fits, dependent on different neglected dimensional condensates, the same results. We have also seen how, within uncertainties, the same strong coupling is the only one it succeeds in precisely predicting many different moments at $s_0 \approx m_\tau^2$ for all the different channels in the expected scenario in which DVs (both because of the increasing hadronic multiplicity near $s_0 \sim m_\tau^2$ and because of the results of the study of $V-A$ sum rules) and dimensional condensates are not dominating uncertainties. We have also seen how the purely perturbative prediction with our obtained value of $\alpha_s$ is able to reproduce in a very large interval the $s_0$ dependence of $A^1_{V+A}(s_0)$, the only moment insensitive to condensates, even when it is specially sensitive to DVs. Independently on the exact shape of the spectral function, this means that assuming that DVs are going to zero relatively fast, so that the $\rho$-like resonance regime has been overpassed (which is clearly observed in a wide interval below the $\tau$ mass), it is basically impossible that they are larger than the obtained uncertainties, since they cannot be larger than the fluctuations observed in the region where data are available. The determination of the Section 3.5 is, in fact, nothing else but a way to study this, since at the end a fit to the energy dependence to a given moment is equivalent to fit the energy dependence on that moment $A^1(s_0)$ with only $\alpha_s$. By changing $\hat{s}_0$, the preferred value of the strong coupling changes in the same order than the fluctuations of Fig. 3.3. In an interval generous enough it should give the order of DV uncertainties. Again the same value for the strong coupling is obtained by this approach.

The only way of escaping from our quoted uncertainties of the strong coupling is by imposing by hand that systematic uncertainties are larger. The less unreliable way of doing this would be by arguing that higher-order perturbative coefficients are only apparently converging to a value before asymptotically diverge, but that such a value is not the physical one. Sadly, there is no way to prove the opposite and one has to rely on the apparently good convergence, good behavior under the change of scale and good agreement for different moments at nearly the tau mass and to quote conservative estimates of uncertainties.

The way suggested by Ref. [120] consists in imposing a priori an arbitrary $\alpha_s$,[‖] and imposing that the differences between the value we obtained and the a priori one must be caused by non perturbative effects. The first problem one has to fix is the large difference between the perturbative prediction obtained with that $\alpha_s$ and data for $A^1(s_0)$ at all energies in the channel with lower DVs ($V + A$). The only non-perturbative way of explaining this difference is by imposing a large high-energy tail of the difference between the spectral function and its OPE approximant. The more deviated is the a priori $\alpha_s$ from the one obtained in this work, the more unreliable the high-energy tail must be. For example, for the value of $\alpha_s$ given in Ref. [120], they use the high-energy tail showed in Fig. 3.15. An artificial and unreliable DV tail, only comparable with the one found in the $\rho$ resonance, where the energy is so low that the OPE even does not make sense, is put by hand as compensating effect, so that the moment $A^1$ converges to the a priori $\alpha_s$ in a Heaviside-like way (bottom panel of Fig. 3.15), comparable to the way data is assumed to converge to the model tuple at $\hat{s}_0$. Notice how, if only semi-inclusive $V$ or $A$ data existed, which suffer from larger DVs, imposing the same a priori $\alpha_s$ would have had less unreliable predictions, since it is more reasonable to assume that DVs can affect a strong coupling determination based on those separate channels for $A^1(s_0)$, as we have actually discussed in previous sections and what leads us to use only $\alpha_s$ from the $V + A$ channel for the final determination.

However, imposing artificial shapes for the spectral function is necessary, but not enough to justify any strong coupling, because one can build weight functions, such as the one used by ALEPH or the different sets we already used, which efficiently suppress them. In that case, if one does not want to impose extra $\rho$-like resonances at $s_0 \sim 2m_\tau^2$, one needs to compensate the poor perturbative predictions one gets with the unphysical $\alpha_s$ for the different moments by compensating with fine-tuned huge condensates values. The larger the deviation

[‖] In the sense that, as we showed in the previous section, any $\alpha_s$ can be imposed a priori with that approach.

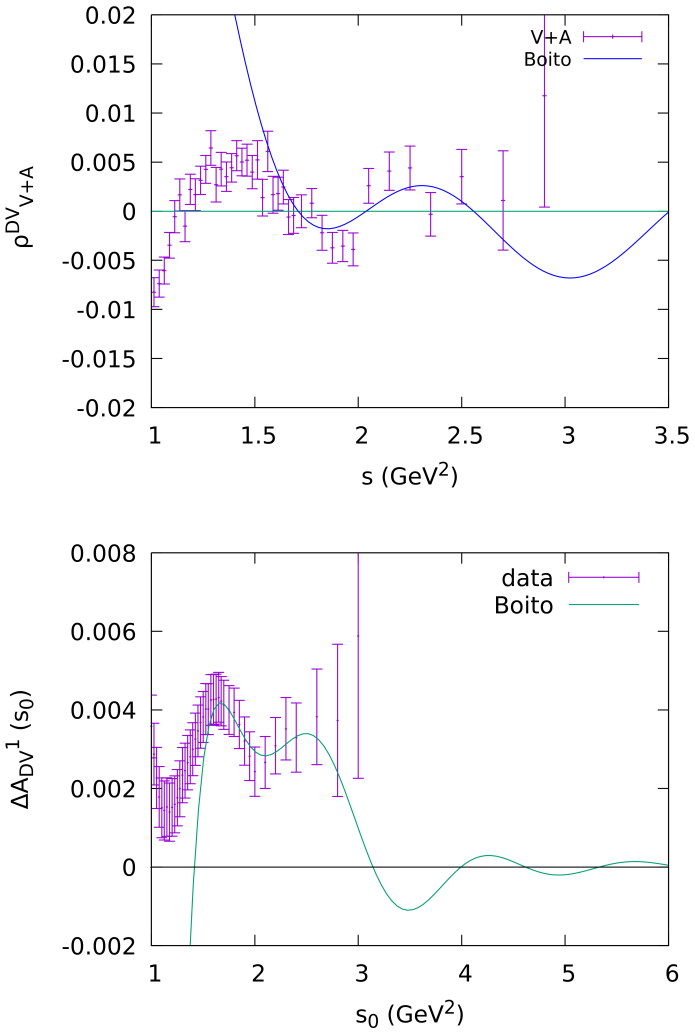


Figure 3.15: Comparison between the tuple of Ref. [115] and data for the spectral function and for $\Delta A^{1,\mathrm{DV}}_{V/A}(s_0)$.

from $\alpha_s$ is, the larger the condensates and the more unreliable values one needs to compensate for those effects.

The scaling of the condensates, which is supposed to resum the asymptotically divergent high-energy perturbative QCD tail, is naively expected to go in the tau

mass as $\frac{\mathcal{O}_D}{m_\tau^D} \sim \left(\frac{\Lambda^2}{m_\tau^2}\right)^{D/2}$, where $\Lambda$ is the QCD scale, $\Lambda \sim \Lambda_{\bar{M}S}^{n_f=3} \sim 0.34\,\text{GeV}$ [147]. The OPE, however, is expected to be also asymptotically divergent, typically with a behavior similar to the $\Gamma$ function, so that one conservatively might expect instead $\frac{\mathcal{O}_D}{m_\tau^D} \sim \left(\frac{\Lambda^2}{m_\tau^2}\right)^{D/2} \Gamma[\frac{D}{2}]$. The few known condensates ($\langle qq\rangle$, $\frac{\alpha_s}{\pi}\langle GG\rangle$ and $\mathcal{O}_{6,V-A}$) are in agreement with that counting. If the counting is correct, our $\alpha_s$ determination, which has additionally tried to uncover possible deviations from it with many different tests without any success, is certainly independent on the high-energy shape of the spectral function (as far as no astonishing deviations are observed at very high energies, which indeed would put into doubt some of the QCD grounds).

For example, even the $\alpha_s^{FOPT} = 0.298$ model tuple is already suppressing DVs at $s_0 \sim m_\tau^2$ for the moment $A^{1-x^2}(s_0)$ in the $V+A$ channel, so that the only non-perturbative way of explaining the discrepancy between data and the perturbative prediction $\alpha_s^{FOPT} = 0.298$ is by assigning it to $\mathcal{O}_{6\,V+A}$. The result is that $\mathcal{O}_{6\,V+A} = 0.0155\,\text{GeV}^6$, which would mean a complete breaking in the OPE counting:

$$\frac{\mathcal{O}_{6\,V+A}}{\mathcal{O}_{4\,V+A}} \sim 4.7\,\text{GeV}^2, \tag{3.65}$$

$$\frac{\mathcal{O}_{6\,V+A}}{\mathcal{O}_{6\,V-A}} \sim 5\,, \tag{3.66}$$

$$B_{6\,V+A} \equiv \frac{\mathcal{O}_{6\,V+A}}{\mathcal{O}_{6\,V+A}^{VSA}} \approx -26 \qquad (B_{6\,V-A} \approx 1)\,. \tag{3.67}$$

Then, the prediction on $R_\tau$, with completely negligible DVs, is doubly distorted both for the value of $\alpha_s$ and $\mathcal{O}_6$ and the only way of compensating it is with an also huge $\mathcal{O}_8 = 0.046\,\text{GeV}^8$, so that $\frac{\mathcal{O}_8}{3\Lambda_{MS}^2\mathcal{O}_6} \sim 9$ , which would mean that the OPE diverges from the first term near the tau mass. While it is impossible to axiomatically rule out this tuple, the fact that it has nothing special and that its consequences would mean a breaking of the OPE counting, it is certainly conservative leaving it at $\sim 2\sigma$ from our final value. Modeling DVs, at least how it has been performed until now, does not seem to be the best approach to reduce the possible weaknesses in the $\alpha_s$ determinations performed in Ref. [46].

## 3.8 Summary

We have presented a thorough numerical reanalysis of the $\alpha_s$ determination from $\tau$ decay data, using the most recent release of the experimental ALEPH data [46]. Our main goal has been to achieve a quantitative assessment of the role of non-perturbative effects, either from inverse-power corrections or violations of duality. While these corrections are known to be small [7, 52, 100, 108], the current level of $\mathcal{O}(\alpha_s^4)$ perturbative precision requires a careful study of this type of contributions.

In order to be sensitive to non-perturbative effects, one needs to go beyond the very clean $R_\tau$ ratio [52] and investigate moments of the hadronic invariant-mass distribution in $\tau$ decays [119]. Several strategies have been advocated in previous works, with different advantages and disadvantages. We have investigated all of them, trying to uncover their potential hidden weaknesses and test the stability of the obtained results under slight variations of the assumed inputs. Moreover, we have put forward various novel approaches which allow to study complementary aspects of the problem.

Perturbative uncertainties from unknown higher-order corrections dominate the final error of the $\alpha_s(m_\tau^2)$ determination, being at present the main limitation on the achievable accuracy [7]. In particular, two different prescriptions to handle the renormalization-group-improved perturbative series, CIPT and FOPT, lead to systematic differences on the extracted value of the strong coupling, with $\alpha_s(m_\tau^2)$ slightly smaller in the FOPT case. While CIPT resums very efficiently the known sources of large logarithms [54, 99], the more naive FOPT procedure has been advocated to approach better the Borel-summed result if the series is already asymptotic at $\mathcal{O}(\alpha_s^4)$ [132,136]. In the absence of a better understanding of the perturbative behavior at higher orders, we have performed all our analyses with the two prescriptions.

In Table 3.11 we summarize our determinations of $\alpha_s(m_\tau^2)$, obtained with different methods from the $V + A$ spectral distribution. The numbers in the table are representative of the various strategies that we have investigated, and all of them have been corroborated with additional tests and stability studies of the final numerical results. Overall, our results exhibit a very consistent pattern, being the agreement among them much better than what one should expect from the quoted uncertainties.

Our first determination in Eq. (3.23), using the same moments as in the standard ALEPH analysis, is in very good agreement with the results of Ref. [46]. We have increased the uncertainties to account for the potential sensitivity to higher-order inverse-power corrections. However, taking away the $(1 + 2s/m_\tau^2)$

| Method & Eq. (#) | $\alpha_s(m_\tau^2)$ | | |
|---|---|---|---|
| | CIPT | FOPT | Average |
| ALEPH moments (3.23) | $0.339\,^{+0.019}_{-0.017}$ | $0.319\,^{+0.017}_{-0.015}$ | $0.329\,^{+0.020}_{-0.018}$ |
| Modified ALEPH moments (3.27) | $0.338\,^{+0.014}_{-0.012}$ | $0.319\,^{+0.013}_{-0.010}$ | $0.329\,^{+0.016}_{-0.014}$ |
| $A^{(2,m)}$ moments (3.35) | $0.336\,^{+0.018}_{-0.016}$ | $0.317\,^{+0.015}_{-0.013}$ | $0.326\,^{+0.018}_{-0.016}$ |
| $s_0$ dependence (3.40) | $0.335 \pm 0.014$ | $0.323 \pm 0.012$ | $0.329 \pm 0.013$ |
| Borel transform (3.49) | $0.328\,^{+0.014}_{-0.013}$ | $0.318\,^{+0.015}_{-0.012}$ | $0.323\,^{+0.015}_{-0.013}$ |

Table 3.11: Summary of the most reliable determinations of $\alpha_s(m_\tau^2)$, performed in the $V + A$ channel.

factor from the ALEPH weights (3.21), we found basically the same results with smaller errors, as shown in (3.27). This suggests that our error enlargement was too pessimistic. In any case, it provides a very strong consistency check. Taking away the $(1+2s/m_\tau^2)$ factor, one eliminates the highest-dimensional contribution to each moment.

In Section 3.4 we have analyzed alternative families of weights to better understand the potential role of different types of non-perturbative corrections. The study of optimal moments, which are only sensitive to particular condensate dimensions, brings more light on the numerical size of these effects. From a combined fit of five different $A^{(2,m)}$ moments ($1 \leq m \leq 5$), we have obtained the results in Eq. (3.35), in perfect agreement with the previous determinations. Similar values are obtained from the global fit of $A^{(n,0)}$ moments ($0 \leq n \leq 3$) in Table 3.6.

Neglecting all non-perturbative effects, one can determine the strong coupling with a single moment. The comparison among results extracted from different moments provides then a direct assessment on the missing contributions. While the moment $A^{(2,m)}$ is sensitive to $\mathcal{O}_{2(m+2)}$ and $\mathcal{O}_{2(m+3)}$, $A^{(1,m)}$ only gets corrections from $\mathcal{O}_{2(m+2)}$. In Table 3.5 we show the values of $\alpha_s(m_\tau^2)$ extracted from 12 different moments with completely different sensitivity to the neglected inverse power corrections. The good agreement among them suggest that vacuum condensate corrections are very small in the $V + A$ case. Moreover, for all moments the fitted value of the strong coupling agrees with the more solid determinations in Table 3.11 which do take non-perturbative effects properly into account.

A different handle to uncover signals of non-perturbative dynamics is provided by the $s_0$ dependence of the moments. This has been carefully studied in Section 3.5. Comparing the $s_0$ dependence of a few experimental $A^{(n,0)}(s_0)$

moments ($0 \leq n \leq 3$) with their values predicted with perturbative QCD, one finds the results shown in Figure 3.3, where $\alpha_s(m_\tau^2)$ has been fixed to the value in Eq. (3.23). In spite of the fact that all non-perturbative contributions have been neglected, the theoretical curves reproduce well the data at large values of $s_0 \sim m_\tau^2$. In the $V + A$ distribution the agreement extends to surprisingly low values of $s_0$, specially for $n = 0$ and 1. In particular, the data appear to closely follow the CIPT predictions for $A^{(0,0)}(s_0)$ and $A^{(1,0)}(s_0)$, the moments most exposed to violations of duality. These effects (and $\mathcal{O}_4$ in the $n = 1$ case) appear to be too small to become visible within the much larger perturbative uncertainties. The higher moments seem to indicate a more sizable $D = 6$ contribution, with opposite signs for the $V$ and $A$ distributions, which cancels to a large extent in $V + A$ as expected theoretically. The different $V$, $A$ and $V + A$ curves merge in the higher $s_0$ range, suggesting a tiny numerical effect at $s_0 \sim m_\tau^2$.

In Figure 3.7 we show, as a function of $s_0$, independent determinations of $\alpha_s(m_\tau^2)$ extracted from 13 different moments of the $V + A$ distribution, ignoring all non-perturbative effects. The clear clustering of the different curves is another strong indication that inverse power corrections are small for $V + A$.

One can try to fit the strong coupling, together with the appropriate power corrections, from the $s_0$ dependence of a given moment. However, this is not really justified because it turns out to be equivalent to a direct fit of the spectral function, and the OPE does not work in the physical real axis at those energies. The functional dependence of the moments with $s_0$ should necessarily manifest the violations of quark-hadron duality which are present in the hadronic spectrum. This is seen in Figure 3.6 which shows the fitted parameters from the moment $A^{(2,0)}(s_0)$, as a function of $\hat{s}_0$, the starting $s_0$ value of the fit. There is a clear dependence on $\hat{s}_0$ for the $V$ and $A$ distributions, in the lower $\hat{s}_0$ range, which however converges to the more stable $V + A$ results at higher values of $\hat{s}_0$. The stability of the extracted $V + A$ values is surprising, but it can be understood looking to the experimental spectral function in Figure 3.2 and observing the flattening of the $V + A$ curve with increasing values of the hadronic invariant mass, which manifests an evident compensation of the vector and axial-vector departures from local duality.

Ignoring DV effects, but including in the uncertainties the variations with $\hat{s}_0$, one gets from the $V + A$ data in Figure 3.2 the values of $\alpha_s(m_\tau^2)$ given in Eq. (3.40). The agreement with the other determinations looks very good, which provides a good consistency test of the negligible role of DV effects in the results quoted in Eqs. (3.23), (3.27) and (3.35).

An alternative approach, based on Borel weights, has been explored in Section 3.6. It has been shown there that the exponential suppression of the weights allows to find stability regions in both $s_0$ and the Borel parameter $a$, where it is possible to extract clean determinations of the strong coupling from the separate vector and axial-vector distributions, in very good agreement with the $V + A$ results shown in Table 3.11. Applying the same method in the combined $V + A$ channel one gets the results in Eq. (3.49).

In Section 3.7 we have followed the strategy advocated in Refs. [113–115], modeling DVs through a functional ansatz with several parameters which are directly fitted to the physical spectral functions. While we are able to reproduce the numerical results of Ref. [115], they turn out to be quite unstable and have a bad statistical quality, so that systematic uncertainties appear to be underestimated in that work. Making small changes in the assumed functional form of the ansatz one finds very significant fluctuations in the fitted value of $\alpha_s(m_\tau^2)$, which is highly correlated with the model parameters. One easily finds models of the spectral function giving the central values for the strong coupling shown in Table 3.11, and with much better statistical quality ($\chi^2$, p-value) than the model assumed in Ref. [115]. Therefore, this determination is model dependent.

Our final conclusion is that the results quoted in Table 3.11 are very solid (except perhaps the one from the $s_0$ dependence). The overall agreement among determinations extracted under very different assumptions clearly shows their reliability and even indicates that our uncertainties are probably too conservative. In order to quote combined values, we can make a naive average, but taking into account that the uncertainties are fully correlated. We find:

$$\begin{aligned} \alpha_s(m_\tau^2)^{\rm CIPT} &= 0.335 \pm 0.013\,, \\ \alpha_s(m_\tau^2)^{\rm FOPT} &= 0.320 \pm 0.012\,. \end{aligned} \tag{3.68}$$

The same results are obtained irrespective or whether one includes or not in the average the determination from the $s_0$ dependence of the moments in Eq. (3.40), exhibiting a very good numerical stability. Averaging the CIPT and FOPT "averages" in Table 3.11, we quote as our final determination of the strong coupling

$$\alpha_s(m_\tau^2) = 0.328 \pm 0.013\,. \tag{3.69}$$

These results agree with the value of the strong coupling extracted from $R_\tau$ in Ref. [7].

After evolution up to the scale $M_Z$, the strong coupling decreases to

$$\alpha_s^{(n_f=5)}(M_Z^2) \;=\; 0.1197 \pm 0.0015\,, \tag{3.70}$$

in excellent agreement with the direct measurement at the $Z$ peak from the $Z$ hadronic width, $\alpha_s(M_Z^2) \;=\; 0.1197 \pm 0.0028$ [102]. The comparison of these two determinations provides a beautiful test of the predicted QCD running; *i.e.* a very significant experimental verification of asymptotic freedom:

$$\alpha_s^{(n_f=5)}(M_Z^2)\Big|_\tau - \alpha_s^{(n_f=5)}(M_Z^2)\Big|_Z \;=\; 0.0000 \pm 0.0015_\tau \pm 0.0028_Z\,. \tag{3.71}$$

The agreement is also very good with the recent and very precise determination from the lattice [148]:

$$\alpha_s^{(n_f=5)}(M_Z^2)\Big|_{\rm latt} = 0.1185 \pm 0.0008\,. \tag{3.72}$$

It is also worth it to remark that some approaches, such as Deep Inelastic Scattering [149] and specially Soft-Collinear Effective Theory (SCET), prefer lower values for $\alpha_s$. For example, Ref. [150] finds:

$$\alpha_s^{(n_f=5)}(M_Z^2)\Big|_{\rm SCET} = 0.1123 \pm 0.0015\,. \tag{3.73}$$

Improvements on the determination of $\alpha_s(m_\tau^2)$ from $\tau$ decay data would require high-precision measurements of the spectral functions, specially in the higher kinematically-allowed energy bins. Both higher statistics and a good control of experimental systematics are needed, which could be possible at the forthcoming Belle-II experiment. On the theoretical side, one needs an improved understanding of higher-order perturbative corrections.

# Chapter 4

# Relations between $K \to \pi\pi$ matrix elements and vacuum condensates

## 4.1 Introduction

In Chapter 2 we performed a phenomenological study of $\Pi^{(1+0)}_{VV-AA}(s)$ using the ALEPH spectral functions. Exploiting dispersive relations and short-distance constraints, we were able to obtain LECs of $\chi$PT and some effective condensates. In Ref. [151] it was shown that two vacuum matrix elements can be related to the following two $K \to \pi\pi$ ones at $\mathcal{O}(p^0)$:

$$\begin{aligned}\langle \mathcal{Q}_7 \rangle_\mu &\equiv \langle (\pi\pi)_{I=2} | \mathcal{Q}_7 | K^0 \rangle_\mu \\ &= \langle (\pi\pi)_{I=2} | \bar{s}_a \Gamma^\mu_L d_a (\bar{u}_b \Gamma^R_\mu u_b - \frac{1}{2} \bar{d}_b \Gamma^R_\mu d_b - \frac{1}{2} \bar{s}_b \Gamma^R_\mu s_b) | K^0 \rangle_\mu \,, \qquad (4.1) \\ \langle \mathcal{Q}_8 \rangle_\mu &\equiv \langle (\pi\pi)_{I=2} | \mathcal{Q}_8 | K^0 \rangle_\mu \\ &= \langle (\pi\pi)_{I=2} | \bar{s}_a \Gamma^\mu_L d_b (\bar{u}_b \Gamma^R_\mu u_a - \frac{1}{2} \bar{d}_b \Gamma^R_\mu d_a - \frac{1}{2} \bar{s}_b \Gamma^R_\mu s_a) | K^0 \rangle_\mu \,, \qquad (4.2)\end{aligned}$$

with $\Gamma_\mu^{R(L)} \equiv \gamma_\mu(1 \pm \gamma_5)$ and $a$ and $b$ color indices. Invoking the soft-meson theorem, one has:

$$\lim_{k,p,q\to 0} \langle (\pi\pi)_{I=2}|\mathcal{Q}_7|K^0\rangle = -\frac{2}{F^3}\langle \mathcal{O}_1\rangle_\mu \,, \tag{4.3}$$

$$\lim_{k,p,q\to 0} \langle (\pi\pi)_{I=2}|\mathcal{Q}_8|K^0\rangle = -\frac{2}{F^3}\left(\frac{1}{2}\langle \mathcal{O}_8\rangle_\mu + \frac{1}{N_c}\langle \mathcal{O}_1\rangle_\mu\right) , \tag{4.4}$$

where $k$, $p$ and $q$ are the momenta of the particles and

$$\mathcal{O}_1 \equiv \frac{1}{2}\bar{d}\,\Gamma_\mu^L u\; \bar{u}\Gamma_R^\mu d \,, \tag{4.5}$$

$$\mathcal{O}_8 \equiv \frac{1}{2}\bar{d}\,\Gamma_\mu^L \lambda_i u\; \bar{u}\Gamma_R^\mu \lambda_i d \,, \tag{4.6}$$

where $\lambda_i$ are $SU(3)$ Gell-Mann color matrices.

As it was shown in [53, 74, 151], making use that one can rewrite Eq. (2.7) in terms of $\langle \mathcal{O}_1\rangle_\mu$ and $\langle \mathcal{O}_8\rangle_\mu$ as:

$$\begin{aligned}[Q^6\Pi_{V-A}(Q^2)]^{D=6} &= 2\alpha_s(\mu)\Big\{(2\pi + A_8\alpha_s(\mu))\langle \mathcal{O}_8\rangle_\mu + \alpha_s A_1\langle \mathcal{O}_1\rangle_\mu\Big\} \\ &\quad + 2\alpha_s^2 \ln\frac{Q^2}{\mu^2}\Big\{B_8(\mu^2)\langle \mathcal{O}_8\rangle_\mu + B_1\langle \mathcal{O}_1\rangle_\mu\Big\} \,, \end{aligned} \tag{4.7}$$

those relations can be used to extract $\langle (\pi\pi)_{I=2}|\mathcal{Q}_7|K\rangle$ and $\langle (\pi\pi)_{I=2}|\mathcal{Q}_8|K\rangle$ in the chiral limit ($\mathcal{O}(p^0)$) from the $V-A$ spectral function $\left(\rho_{V-A}(s) \equiv \frac{\mathrm{Im}\,\Pi_{V-A}(s)}{\pi}\right)$ coming from $\tau$-decay data. At that time, only preliminary ALEPH spectral functions were known. Since then, the final ALEPH spectral functions [44], later updated with some improvements [46,109], were published. As we did in Chapter 2, in this work we use the updated experimental non-strange V − A spectral function of Ref. [46]. These updates and further development of techniques to assess DV uncertainties [39,40,43,45,55,56,59,67,152] motivate a fresh numerical analysis. We present some preliminary results in this chapter of an ongoing collaboration in this direction [153].

Since, to the best of our knowledge, no explicit proof of the relations of matrix elements given in Eqs. (4.3) and (4.4) can be found in the literature, we present a simplified derivation of it in App. B. In Chapter 2 (Eq. (2.9)), generic polynomial sum rules were derived at LO in $\alpha_s$. Since one of the 4-quark vacuum condensates above only enters in $\tau$ data at NLO, we derive in Section 4.2 the generic polynomial sum rules at NLO, where one needs to take into account

the logarithmic corrections in the OPE. We also show why we avoid using other sum rules only defined in the chiral limit.

In Section 4.3, we find that, when trying to obtain vacuum matrix elements, the current precision of $\tau$ data enforces us to use sum rules at LO in $\alpha_s$, so that we only have access to one of the two vacuum condensates. Fortunately, the contribution of the other vacuum condensates to $\langle \mathcal{Q}_8 \rangle_\mu$ will be argued to be small. We perform a careful phenomenological re-analysis of the $D = 6$ effective condensate, with some additional tests and small changes with respect to Chapter 2 aimed to improved its determination. We obtain self-consistent values from different approaches, which translates into a derivation of $\langle \mathcal{Q}_8 \rangle_\mu$.

Alternatively, in the same sense that our knowledge of the $D = 2$ and $D = 4$ contributions to $\Pi_{V-A}^{OPE}$ allow us to considerably reduce both experimental and DV uncertainties in the extraction of different physical parameters, we can use the determination of $\langle \mathcal{Q}_7 \rangle_\mu$ and $\langle \mathcal{Q}_8 \rangle_\mu$ from the lattice to obtain the $D = 6$ contribution at NLO in $\alpha_s$, which translates into a further reduction of them. We apply it for the determination of $f_\pi$ and $\langle \mathcal{O}_8 \rangle_\mu$ in Section 4.4.

## 4.2 Polynomial Sum Rules

Taking Eq. (2.9) with an arbitrary weight function of the form $\omega\,(s \equiv s_0 x) = \sum_{n=0}^{\infty} c_n x^n$:

$$\int_{s_{th}}^{s_0} \frac{ds}{s_0}\, \omega(s)\, \mathrm{Im}\, \Pi(s) - \frac{i}{2} \oint_{|s|=s_0} \frac{ds}{s_0} \left(\frac{s}{s_0}\right)^n \Pi(s) = 2\pi \frac{f_\pi^2}{s_0} \omega(m_\pi^2)\,. \tag{4.8}$$

Recalling the NLO version of the OPE, *i.e.*, Eq. (2.4):

$$\begin{aligned} \Pi^{(1+0)}(Q^2 = -q^2) &= \sum_{p=D/2} \frac{a_p(\mu) + b_p(\mu) \ln \frac{Q^2}{\mu^2}}{Q^{2p}} \\ &= \sum_p \frac{1}{(s_0)^p} \frac{a_p^M(\mu, s_0) + b_p(\mu) \ln \frac{Q^2}{s_0}}{\left(\frac{Q^2}{s_0}\right)^p}\,, \end{aligned} \tag{4.9}$$

where $b_p$ is $\alpha_s$-suppressed with respect to $a_p$ and:*

$$a_p^M(\mu, s_0) = a_p(\mu) + b_p(\mu) \ln \left(\frac{s_0}{\mu^2}\right)\,. \tag{4.10}$$

*Notice that at leading order $a_p$ reduces to $\mathcal{O}_{2p}$ as defined in Chapter 2.

Introducing it into Eq. (4.8):

$$\int_{s_{th}}^{s_0}\frac{ds}{s_0}\omega(s)\,\mathrm{Im}\,\Pi(s)=2\pi\frac{f_\pi^2}{s_0}\omega(m_\pi^2)-\pi\sum_{n=0}^{\infty}\sum_{p=1}^{\infty}\frac{1}{(-s_0)^p}c_n d_p^{(n)} - \int_{s_0}^{\infty}\frac{ds}{s_0}\omega(s)\,\mathrm{Im}\,\Delta_{DV}(s)\,, \tag{4.11}$$

with $\omega(s)=\sum_n c_n x^n$,

$$d_p^{(n)}=\begin{cases} a_p^M & \text{if} \quad p=n+1 \\ \frac{b_p}{n-p+1} & \text{if} \quad p\neq n+1 \end{cases}\,, \tag{4.12}$$

and $\Delta_{DV}\equiv\Pi(s)-\Pi^{\mathrm{OPE}}(s)$. Explicitly, for the first moments one obtains:

$$\int_{s_{th}}^{s_0}\frac{ds}{s_0}\,\mathrm{Im}\,\Pi(s)=2\pi\frac{f_\pi^2}{s_0}+\pi\left(-\frac{b_3}{2s_0^3}+\frac{b_4}{3s_0^4}-\frac{b_5}{4s_0^5}+...\right) - \int_{s_0}^{\infty}\frac{ds}{s_0}\,\mathrm{Im}\,\Delta_{DV}(s)\,, \tag{4.13}$$

$$\int_{s_{th}}^{s_0}\frac{ds}{s_0}\frac{s}{s_0}\,\mathrm{Im}\,\Pi(s)=2\pi\frac{f_\pi^2 m_\pi^2}{s_0^2}+\pi\left(-\frac{b_3}{s_0^3}+\frac{b_4}{2s_0^4}-\frac{b_5}{3s_0^5}+...\right) - \int_{s_0}^{\infty}\frac{ds}{s_0}\frac{s}{s_0}\,\mathrm{Im}\,\Delta_{DV}(s)\,, \tag{4.14}$$

$$\int_{s_{th}}^{s_0}\frac{ds}{s_0}\left(\frac{s}{s_0}\right)^2\mathrm{Im}\,\Pi(s)=2\pi\frac{f_\pi^2 m_\pi^4}{s_0^3}+\pi\left(\frac{a_3^M}{s_0^3}+\frac{b_4}{s_0^4}-\frac{b_5}{2s_0^5}+...\right) - \int_{s_0}^{\infty}\frac{ds}{s_0}\left(\frac{s}{s_0}\right)^2\mathrm{Im}\,\Delta_{DV}(s)\,, \tag{4.15}$$

$$\int_{s_{th}}^{s_0}\frac{ds}{s_0}\left(\frac{s}{s_0}\right)^3\mathrm{Im}\,\Pi(s)=2\pi\frac{f_\pi^2 m_\pi^6}{s_0^3}-\pi\left(\frac{a_4^M}{s_0^4}+\frac{b_3}{s_0^3}-\frac{b_5}{s_0^5}+...\right) - \int_{s_0}^{\infty}\frac{ds}{s_0}\left(\frac{s}{s_0}\right)^3\mathrm{Im}\,\Delta_{DV}(s)\,. \tag{4.16}$$

There are other sum rules, such as the pion sum rule [68], which are defined in the chiral limit and usually involve integration up to infinity. In order to get precise enough information for this study, one needs to approximate $\mathrm{Im}\,\Pi(s)\approx$

$\mathrm{Im}\,\Pi_{m_q=0}$.[†] The effect of $m_q$ in the physical spectrum must be certainly small given the small values of $m_u$ and $m_d$. However, V − A sum rules involve strong cancellations themselves and then those effects may become non-negligible.

As an example to illustrate this, let us compare the physical and the chiral version of $\omega^{(2,0)}(s) \equiv \left(1-\frac{s}{s_0}\right)^2$ at LO, which is one of the key weight functions in this work:

$$\int_{s_{th}}^{s_0} \frac{ds}{s_0}\left(1-\frac{s}{s_0}\right)^2 \mathrm{Im}\,\Pi(s) = 2\pi\frac{f_\pi^2}{s_0} - 4\pi\frac{f_\pi^2 m_\pi^2}{s_0^2} + 2\pi\frac{f_\pi^2 m_\pi^4}{s_0^3} + \pi\frac{a_3}{s_0^3} + \delta_{DV}^{\omega^{(2,0)}}(s_0)\,, \tag{4.17}$$

$$\int_{s_{th}}^{s_0} \frac{ds}{s_0}\left(1-\frac{s}{s_0}\right)^2 \mathrm{Im}\,\Pi_{m_q=0}(s) = 2\pi\frac{F^2}{s_0} + \pi\frac{a_3^0}{s_0^3} + \delta_{DV}^{\omega^{(2,0)},0}(s_0)\,. \tag{4.18}$$

where the 0 tag denotes the values of the constant in the chiral limit. In order to have sensibility for obtaining $a_3$ at $s_0 \sim 2\,\mathrm{GeV}^2$, one needs a precision of $\pi\frac{|a_3|}{s_0^3} \sim 0.0015$. In fact, the experimental resolution is good enough. However, the difference between both equation is dominated by:[‡]

$$\int_{s_{th}}^{s_0} \frac{ds}{s_0}\left(1-\frac{s}{s_0}\right)^2 \left(\mathrm{Im}\,\Pi(s) - \mathrm{Im}\,\Pi_{m_q=0}(s)\right) \approx 2\pi\frac{f_\pi^2 - F^2}{s_0}\,. \tag{4.19}$$

Taking $f_\pi \sim 92\,\mathrm{MeV}$ and $F \sim 87\,\mathrm{MeV}$ one obtains for $s_0 = 2\,\mathrm{GeV}^2$, that the uncertainty due to taking $\mathrm{Im}\,\Pi(s) \approx \mathrm{Im}\,\Pi_{m_q=0}(s)$ is $2\pi\frac{f_\pi^2-F^2}{s_0} \sim 0.0028$, much larger than any other source of uncertainty and a 200% of the value of $a_3$.

Since this may also happen if we include in the determination sum rules only valid in the chiral limit, we opt for not using them.

[†] A comprehensive study trying to assess these differences for some exclusive channels can be found in Ref. [154]. However, this method is far from giving chiral spectral functions with the precision we need.

[‡] The possibility of a systematic cancellation between $\delta_{DV}^{\omega^{(2,0)}}(s_0) - \delta_{DV}^{\omega^{(2,0)},0}(s_0)$ and $f_\pi - F$ can be discarded when one observes that this problem is dramatically enhanced with an increasing $s_0$, while DVs go to zero fast.

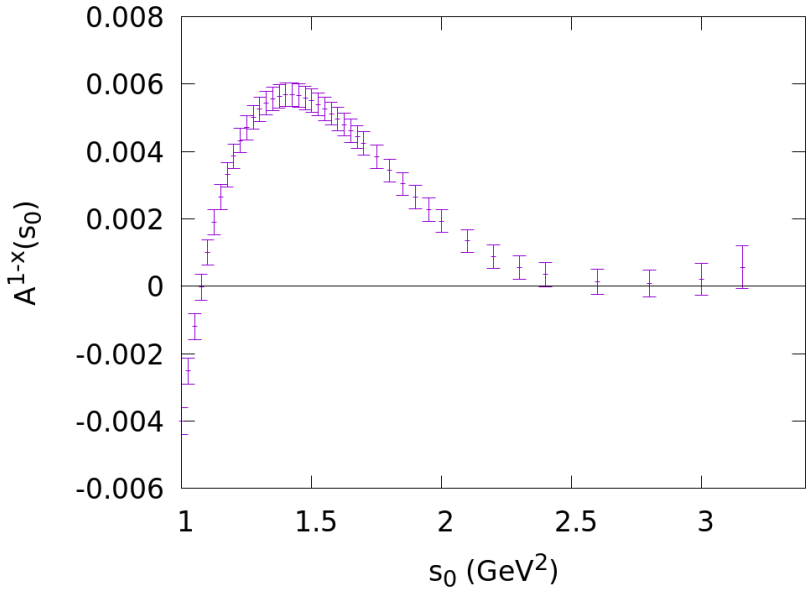


Figure 4.1: lhs of equation (4.20) as a function of $s_0$.

## 4.3 Determination of $\langle(\pi\pi)_{I=2}|Q_8|K^0\rangle$

### 4.3.1 Connecting $a_3(s_0)$ with $\langle(\pi\pi)_{I=2}|Q_8|K^0\rangle_{s_0}$

The limitations of the current sensitivity of $\tau$ data to $D = 6$ contributions enforce us to work at LO in $\alpha_s$. In order to illustrate this, we plot in Figure 4.1 the lhs of Eq. (4.11) for $\omega(s) = \left(1 - \frac{s}{s_0}\right)$. Even if we only consider $\alpha_s$ corrections for the $D = 6$ contribution, , *i.e.*, $b_{n>3} = 0$, one obtains:

$$A^{1-x}(s_0) \equiv \int_{s_{th}}^{s_0} \frac{ds}{s_0}\left(1 - \frac{s}{s_0}\right) \mathrm{Im}\,\Pi(s)$$
$$= \pi \frac{b_3}{2s_0^3} - \int_{s_0}^{\infty} \frac{ds}{s_0}\left(1 - \frac{s}{s_0}\right) \mathrm{Im}\,\Delta_{DV}(s) + 2\pi \frac{f_\pi^2}{s_0^2}\left(1 - \frac{m_\pi^2}{s_0}\right) . \quad (4.20)$$

Clearly this weight function is optimal to get $b_3$: it does not contain any other $a_i$ and it sets $\omega(s_0) = 0$, so it reduces DV uncertainties and experimental ones from the high-energy region. However, at $s_0 = m_\tau^2$, where DVs may be suppressed enough, uncertainties are too large to get any information about $b_3$. Instead, working at LO we can use that equation as a constraint to improve our

sensitivity to $a_3$. Eq. (4.10) determines the scale of our determination: $\mu \sim s_0$. Otherwise, large logarithmic corrections of that equation would break the LO counting $a_3^M(\mu) = a_3(\mu)(1 + \mathcal{O}(\alpha_s))$. At leading order we have from Eq. (2.7):

$$a_3^M(\mu) = a_3(\mu) = 4\pi\langle\alpha_s\mathcal{O}_8\rangle_\mu\,. \tag{4.21}$$

Taking into account the large value of the NLO corrections coming from $A_8$ in Eq. (4.21), we assign a 25% of uncertainty to the final $\langle\mathcal{Q}_8\rangle_\mu$. We also assume that, within the large uncertainties we have,* the vacuum condensate is equal to its chiral version, so that we can use the relations of Eqs. (4.1) and (4.2). In order to extract $\langle\mathcal{Q}_8\rangle_\mu$, we still would need $\langle\mathcal{O}_1\rangle_\mu$. However we have strong reasons to neglect its contribution to $\langle\mathcal{Q}_8\rangle_\mu$. In the large-$N_c$ limit $\frac{\langle\mathcal{Q}_7\rangle_\mu}{\langle\mathcal{Q}_8\rangle_\mu} = 0$ at order $\mathcal{O}(p^0)$. In the Vacuum Saturation Approximation (VSA), one has $\frac{\langle\mathcal{Q}_7\rangle_\mu}{\langle\mathcal{Q}_8\rangle_\mu} = \frac{1}{N_c}$ [53]. This suppression is supported by the different phenomenological and lattice analysis (for example see [53, 155, 156]), which points out to a suppression of $\langle\mathcal{Q}_7\rangle_\mu$ with respect to $\langle\mathcal{Q}_8\rangle_\mu$ beyond the naive $\frac{1}{3}$. Combining $\frac{Q_7}{Q_8} \leq \frac{1}{N_c}$ with Eqs. (4.3) and (4.4) one obtains:

$$|\langle\mathcal{Q}_8\rangle_\mu^{\langle\mathcal{O}_1\rangle_\mu}| \leq \frac{|\langle\mathcal{Q}_8\rangle_\mu^{\langle\mathcal{O}_8\rangle_\mu}|}{N_c^2}\,\frac{1}{1-\frac{1}{N_c^2}}\,, \tag{4.22}$$

where $\langle\mathcal{Q}_8\rangle_\mu^{\langle\mathcal{O}_1\rangle_\mu}$ and $\langle\mathcal{Q}_8\rangle_\mu^{\langle\mathcal{O}_8\rangle_\mu}$ are respectively the contributions of $\langle\mathcal{O}_1\rangle_\mu$ and $\langle\mathcal{O}_8\rangle_\mu$ to $\langle\mathcal{Q}_8\rangle_\mu$ in Eq. (4.4). We use this inequality to make a preliminary estimate of systematic uncertainty associated to neglecting $\langle\mathcal{O}_1\rangle_\mu$. At LO in $\alpha_s$, and neglecting it, the value of $\langle\mathcal{Q}_8\rangle_\mu$ in the chiral limit is given by:

$$\lim_{p,q,k=0}\langle(\pi\pi)_{I=2}|\mathcal{Q}_8|K^0\rangle_\mu = -\frac{a_3(\mu)}{4\pi\alpha_s(\mu)F^3}\,. \tag{4.23}$$

Since our determination with $\tau$ decays is made at different scales $\mu = \sqrt{s_0} \sim m_\tau$, there are not large logarithms involved and we can take $a_3$ as a constant (NLO uncertainties in $\alpha_s$ are already taken into account).

The determination of $a_3$ becomes equivalent to the one of $\mathcal{O}_6$ of Chapter 2. In the following subsection we revisit it, introducing some extra tests and trying to implement some improvements. In order to compare with determinations made with other methods at other scales, both for $a_3(\mu)$ and $\langle\mathcal{Q}_8\rangle_\mu$, one has to take into account that ours is made at $\mu = m_\tau$ and then to use the full running to compare with other scales.

*As we already did in Chapter 2 we take conservatively $F = 0.087 \pm 0.005\,\text{GeV}$.

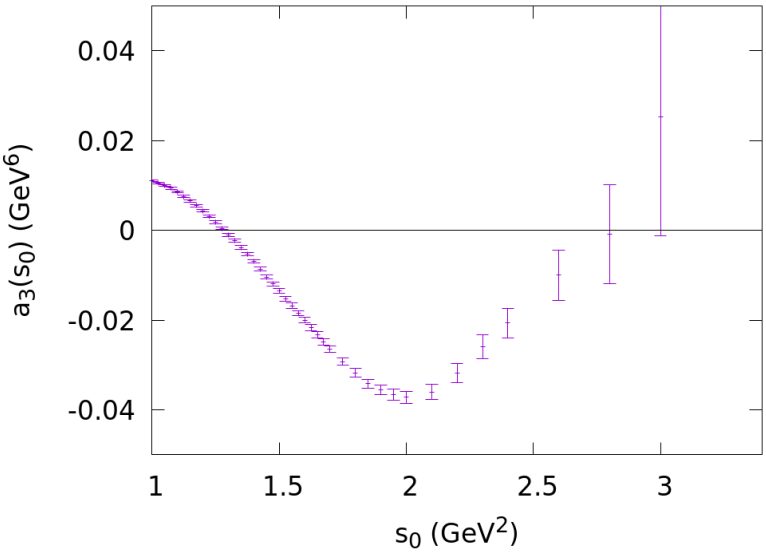


Figure 4.2: Reescaled version of the moment associated to $\omega(s = s_0 x) = x^2$, so that at $s_0$ large enough converges to $a_3(s_0)$.

### 4.3.2 Determination of $a_3$ using pinched-weight functions

Naively, one could try to estimate $a_3$ by directly using the LO version ($b_i = 0$) of Eq. (4.15) hoping that at energies large enough DVs are negligible. This should reflect in a plateau at high energies when making the trivial reescaling of that equation, so that it converges to $a_3$ for large enough values of $s_0$. However, when we plot it in Figure 4.2 we observe that both experimental uncertainties and DVs are huge. This is because the factor $x^2$ ($x \equiv \frac{s}{s_0}$) of the weight function is enhancing both the contribution of the high-energy part of the spectral function, where the worst experimental data is available, and its higher energy tail, which gives large DV uncertainties (see Eq. (4.11)).

Fortunately we can use the pinching technique (as we actually did in Chapter 2) to reduce both uncertainties. One takes $\omega(s)$ such that $\omega(s_0) = ... = \omega^{(n-1)}(s_0) = 0$, so that for example $\omega(s_0 x) = 1 - x$ is a pinch weight function and $\omega(s_0 x) = (1 - x)^2$ a double-pinched one. Using those weights we obtain the values of $a_3(s_0)$ of Fig. (4.3), to be compared with Fig. (4.2). Experimental uncertainties are clearly reduced and a plateau has arisen. One still may argue, by taking an artificial shape for the high-energy tail of the spectral function, that

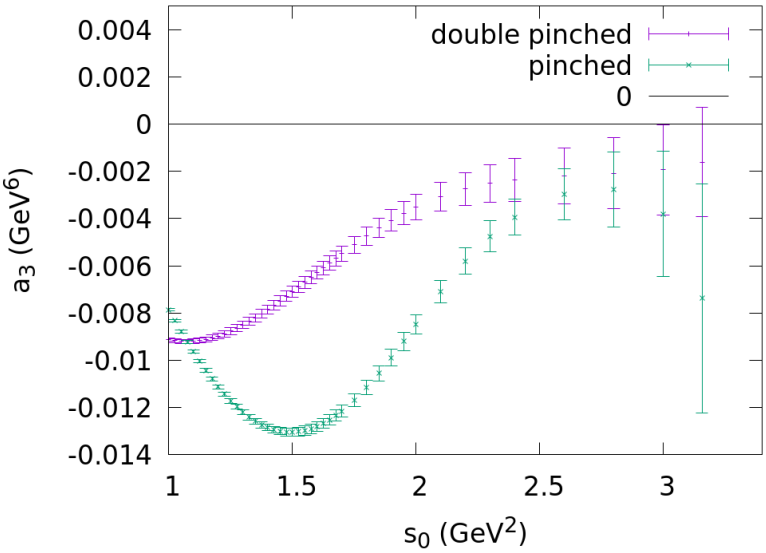


Figure 4.3: Pinched weight functions as a function of $s_0$ reescaled so that at $s_0$ large enough converge to $a_3(s_0)$.

this plateau might be temporary. However, since there is an increasing hadronic multiplicity at $s_0 \sim m_\tau^2$, DVs should go to zero very fast when increasing energies and this scenario becomes very unlikely. Together with the fact that at large energies both pinched weight functions give the same value of $a_3$, it is a reasonable assumption to state that DVs are relatively small for large $s_0$ when doubly pinching.

Taking that into account, we take as central value the last one within the experimental error bars of the following ones, *i.e.*, $s_0 = 2.2$ GeV$^2$ and as estimate of DVs its difference with the last one with an acceptable experimental resolution, *i.e.*, $s_0 = 2.8$ GeV$^2$. We obtain:

$$a_3 = (-2.8 \pm 0.5_{\text{exp}} \pm 0.7_{\text{DV}}) \cdot 10^{-3}\,\text{GeV}^3 = (-2.8 \pm 0.9) \cdot 10^{-3}\,\text{GeV}^3\,. \quad (4.24)$$

### 4.3.3 Determination of $a_3$ modeling DVs

An alternative approach to estimate DVs consists in trying to guess how it is the spectral function[†] above the region where data is available. In order to do that, a parametrization is unavoidable and, then, some model-dependence arises. We try to relax that model-dependence by allowing data not to obey extrictly the model but imposing they must obey WSRs (Eqs. (4.13) and (4.14) with $b_i = 0$). The ansatz we use is [39, 40, 56–58, 60].

$$\rho(s) = \frac{1}{\pi}\kappa e^{-\gamma s}\sin\left(\beta(s - s_z)\right) \quad s > \hat{s}_0\,. \tag{4.25}$$

Following the procedure of Chapter 2, we generate random tuples of parameters $(\kappa, \gamma, \beta, s_z)$, so that every one of them represent a possible spectral function above a threshold $\hat{s}_0$. If we perform a fit with ALEPH data, we find that there are no significant deviations (p-value above a 5%) from this specific model below $\hat{s}_0 = 1.25\,\mathrm{GeV}^2$. However, the model is only motivated as an approximation at higher energies, where the hadronic multiplicity is also higher. Again, as in Chapter 2, we accept tuples only in the 90% C.L. ($\chi^2 < \chi^2_{\mathrm{min}} + 7.78$). Doing that, we try to relax the model dependence by allowing small deviations of data from it.

In Chapter 2 we imposed here for the tuples the short-distance constraints, *i.e.*, the WSRs. However, experimental uncertainties due to those constraints in the tuples happen to be correlated in a nontrivial way with the experimental uncertainty in the final parameters (they are different moments of the spectral function). In order to avoid that, we perform, for every accepted spectral function, a combined fit of Eqs. (4.13), (4.14), (4.15) to extract $a_3$. Then we only accept those spectral functions that are compatible with the WSRs, selecting only the ones whose p-value in the combined fit are larger than a 5%. Then, for every accepted spectral function, we have an $a_3$ value. The DV uncertainty is estimated as the width of the remaining distribution. We plot the distribution for $\hat{s}_0 = 1.7\ \mathrm{GeV}^2$ in Fig. 4.4.

As we argued in the previous chapter, one minimal requirement that should be imposed is independence on the chosen $\hat{s}_0$ for a large enough range, since its choice is somehow arbitrary. We have repeated our procedure for different thresholds with the results of Table 4.1. The agreement is acceptable. We choose $\hat{s}_0 = 1.7\ \mathrm{GeV}^2$ as our optimal threshold, large enough to have some hadronic multiplicity and small enough to be able to constrain the space of parameters.

[†] At LO in $\alpha_s$, $\rho(s) = \rho_{DV}(s)$.

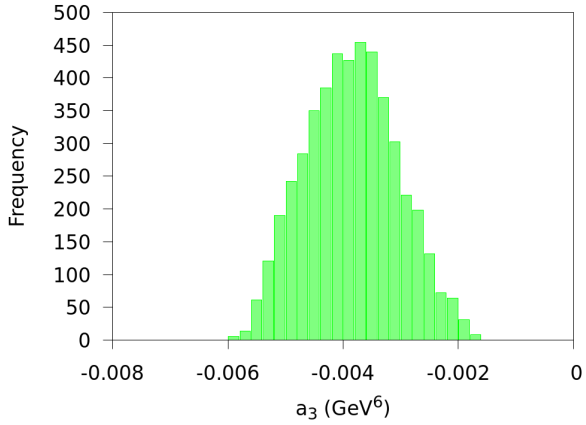


Figure 4.4: Distribution for $a_3$ obtained with the tuples procedure.

| $\hat{s}_0(\text{GeV}^2)$ | 1.25 | 1.4 | 1.55 | 1.7 | 1.9 |
|---|---|---|---|---|---|
| $a_3(10^{-3}\text{GeV}^6)$ | $-5.3\,^{+0.7}_{-0.5}$ | $-5.1\,^{+0.7}_{-0.5}$ | $-5.3\,^{+0.5}_{-0.3}$ | $-3.7\,^{+1.3}_{-0.9}$ | $-3.8\,^{+1.8}_{-1.0}$ |

Table 4.1: Value of $a_3$ obtained with our tuple procedure for different $\hat{s}_0$.

We obtain:

$$a_3 = (-3.7\,^{+1.3}_{-0.9\ \text{DVs}} \pm 0.1_{\text{exp}}) \cdot 10^{-3}\,\text{GeV}^2\,. \tag{4.26}$$

However, notice that, even in the case that the ansatz were exactly true from some threshold $\hat{s}_0$, one could find that the "physical" $\hat{s}_0$ is larger and then that the "physical" spectral function could be not well approximated by the parameters we obtained. Actually, assuming small DVs with double pinch could be giving more accurate results than assuming the model with the parameters we have obtained. This motivates averaging both of them. Fortunately, in this case both methods are in good agreement. Our final value, taking conservatively the quadratic sum of the lowest uncertainty and half of the difference between central values, is:

$$a_3 = (-3.1 \pm 1.0) \cdot 10^{-3}\ \text{GeV}^6\,. \tag{4.27}$$

This is also in total agreement with the previous determination made in Chapter 2 and the determination of Ref. [43] with a different procedure.

### 4.3.4 Final value for $\langle(\pi\pi)_{I=2}|\mathcal{Q}_8|K^0\rangle$ and comparison with large-$N_c$ limit

Inserting the value of Eq. (4.27) into Eq. (4.23):

$$\begin{aligned}\langle(\pi\pi)_{I=2}|\mathcal{Q}_8|K^0\rangle_{2\,\mathrm{GeV}} &= (1.14 \pm 0.37_{a_3} \pm 0.29_{\mathrm{pert}} \pm 0.14_{\langle\mathcal{O}_1\rangle_\mu})\ \mathrm{GeV}^3 \\ &= (1.14 \pm 0.49)\ \mathrm{GeV}^3\,, \end{aligned} \tag{4.28}$$

where the running from $m_\tau^2$ to $s_0 = 2\,\mathrm{GeV}$ ($\langle Q\rangle_{2\mathrm{GeV}^2} \approx 1.05\langle Q\rangle_{m_\tau}$) has been safely neglected.[‡]

We can compare with the value one obtains in the large-$N_c$ limit. Applying Fierz transformations one obtains:

$$\mathcal{Q}_8 = -12\sum_i e_i\,\bar{q}P_L d\;\bar{s}P_R q = -12\sum_i e_i L_{2i}R_{i3}\,, \tag{4.29}$$

where $P_{L(R)} = \frac{1\mp\gamma_5}{2}$ and $L_{ij}(R_{ij}) \equiv \bar{q}_j P_{L(R)} q_i$. Using that in the large-$N_c$ limit the product of two color-singlet quark currents factorizes at the hadron level into two current matrix elements and that at first order in $\chi$PT, $L_{ij}(R_{ij}) = -\frac{F^2}{2}B_0 U(U^\dagger)$, the relevant contribution is:

$$\mathcal{Q}_8^{N_c} = -i3\sqrt{2}B_0^2 F K^0\pi^+\pi^-\,, \tag{4.30}$$

therefore:

$$A_{i\to f}(\langle\pi^+\pi^-|S-I|K^0\rangle) = 3\sqrt{2}B_0^2 F\,(2\pi^4)\,\delta^4(p_f - p_i)\,. \tag{4.31}$$

Using that the matrix element is defined such that $A_{i\to f} = -i(2\pi^4)\,\delta^4(p_f - p_i)M_{i\to f}$:

$$\langle\pi^+\pi^-|\mathcal{Q}_8|K^0\rangle^{N_c} = 3i\sqrt{2}B_0^2 F\,, \tag{4.32}$$

$$\langle\pi^0\pi^0|\mathcal{Q}_8|K^0\rangle^{N_c} = 0\,. \tag{4.33}$$

Therefore, using Eq. (B.12) one obtains the leading contribution in the large-$N_c$ limit:

$$\langle(\pi\pi)_{I=2}|\mathcal{Q}_8|K^0\rangle^{N_c}_{2\,\mathrm{GeV}} = 2FB_0^2 = 2\frac{M_{K_0}^4 F}{(m_d+m_s)^2} = 1.1\ \mathrm{GeV}^3\,, \tag{4.34}$$

[‡]Since from $m_\tau$ to 2 GeV there are no large logarithms involve, they are fully accounted by perturbative uncertainties and indeed resuming them is not justified.

in total agreement with Eq. (4.28).

## 4.4 Obtaining $a_3$ from the lattice to get further constraints

Instead of using data to extract $K \to \pi\pi$ matrix elements, one may choose to use existing lattice determinations of $K \to (\pi\pi)_{I=2}$ matrix elements to get the $D = 6$ contribution of $\Pi^{OPE}(s)$. From [156], one has in the Naive Dimensional Regularization (NDR) $\bar{MS}$ for 4 active flavors in the large-$N_c$ limit:

$$\langle Q_7 \rangle_{3\,\mathrm{GeV}} = 0.36 \pm 0.03\,, \tag{4.35}$$

$$\langle Q_8 \rangle_{3\,\mathrm{GeV}} = 1.6 \pm 0.1\,. \tag{4.36}$$

In order to get the $\mathcal{Q}_i$ at $s_0$ we use the $10 \times 10$ QCD and QED running matrix for the Wilson coefficients at NLO. Running to $\mu = m_c$, performing the matching to $N_f = 3$ and running to $\mu = \sqrt{s_0}$, one has, except for the small mixing with other operators, $\langle \mathcal{Q}_7 \rangle_\mu$ and $\langle \mathcal{Q}_8 \rangle_\mu$ at $s_0$. One obtains for $s_0 = m_\tau^2$:

$$\begin{pmatrix} \langle \mathcal{Q}_7 \rangle_{m_\tau} \\ \langle \mathcal{Q}_8 \rangle_{m_\tau} \end{pmatrix} = \begin{pmatrix} 1.03 & -0.077 \\ 0.000 & 0.798 \end{pmatrix} \begin{pmatrix} \langle \mathcal{Q}_7 \rangle_{3\,\mathrm{GeV}} \\ \langle \mathcal{Q}_8 \rangle_{3\,\mathrm{GeV}} \end{pmatrix}, \tag{4.37}$$

which translates into:[§]

$$\begin{aligned} a_3(m_\tau^2) &= -(4.2 \pm 1.0_{m_q=0} \pm 0.8_F \pm 0.3_{latt}) \cdot 10^{-3}\,\mathrm{GeV}^6 \\ &= -(4.2 \pm 1.3) \cdot 10^{-3}\,\mathrm{GeV}^6\,, \end{aligned} \tag{4.38}$$

$$b_3(m_\tau^2) = -(1.2 \pm 0.3) \cdot 10^{-4}\,\mathrm{GeV}^6\,, \tag{4.39}$$

where we have included an extra 25% uncertainty in order to take into account corrections to the chiral limit ($\mathcal{O}(p^2)$). Notice the good agreement with Eq. (4.27). As we observed above, double pinching reduces both experimental and DV uncertainties. Given that $a_3$ is suppressed by six power of energy, the determination from the lattice is enough to make its uncertainties smaller than the experimental ones. Eq. (4.17) becomes then a powerful constraint that can be used to test the different aspects of QCD involved. For example, one can use that equation to get $f_\pi$. In Figure 4.5 we plot the rescaled version of Eq. (4.17), so that $\sqrt{2} f_\pi(s_0)$ converges to $\sqrt{2} f_\pi$ when DVs are negligible.

[§]Notice how the knowledge of both $\langle \mathcal{Q}_7 \rangle_\mu$ and $\langle \mathcal{Q}_8 \rangle_\mu$ allow to get $\langle \mathcal{O}_1 \rangle_\mu$ and $\langle \mathcal{O}_8 \rangle_\mu$. Then the full $D = 6$ contribution of the OPE at NLO in $\alpha_s$.

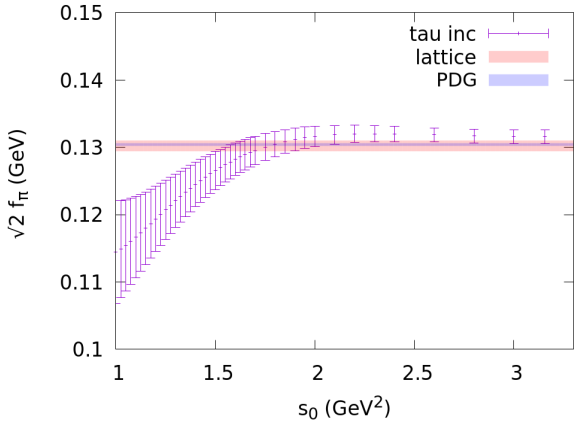


Figure 4.5: Equation (4.17) rescaled so that at $s_0$ large enough converge to $f_\pi$. By comparison we show the PDG value and the one obtained from lattice [69].

The stable plateau is a clear sign of vanishing DVs at $m_\tau$, as we expected for this moment. Indeed, if one estimates DV uncertainties as the contribution of the tuple associated to the minimum $\chi^2$ of the model (performing the fit from $s_{th} = 1.7\,\text{GeV}^2$) one obtains that it is one order of magnitude below experimental uncertainties at $s_0 \sim m_\tau^2$.[¶] Taking that into account, we obtain:

$$\begin{aligned}\sqrt{2}f_\pi &= (131.58 \pm 0.90_{\text{exp}} \pm 0.42_{\text{chiral}} \pm 0.30_F \pm 0.11_{\text{latt}})\text{MeV} \\ &= (131.6 \pm 1.0)\,\text{MeV}\,. \end{aligned} \tag{4.40}$$

Since the short-distance constraint on $a_3$ involves the weight function $\omega(x) = x^2$, it is giving information on the high-energy region of the spectral function. Because of it, the other determination that may get benefited from this additional constraint is the $D = 8$ condensate $a_4$ (equivalent to $\langle \mathcal{O}_8 \rangle_\mu$ from Chapter 2). Now we can use the triple pinch $\omega(x) = (1-x)^3$ to try to further reduce DV uncertainties. We display it in Figure 4.6, to be compared with the bottom panel of Figure 2.10. Uncertainties are still large but a softer $s_0$ dependence, compatible with a plateau, is observed. If we assume that DVs are negligible for this channel at $s_0 = 2\ \text{GeV}^2$, we get:

$$a_4 = -(0.5 \pm 0.6) \cdot 10^{-2}\ \text{GeV}^8\,, \tag{4.41}$$

[¶]Similar results arise when changing the threshold or taking the minimum from other models, such as the one from Ref. [43].

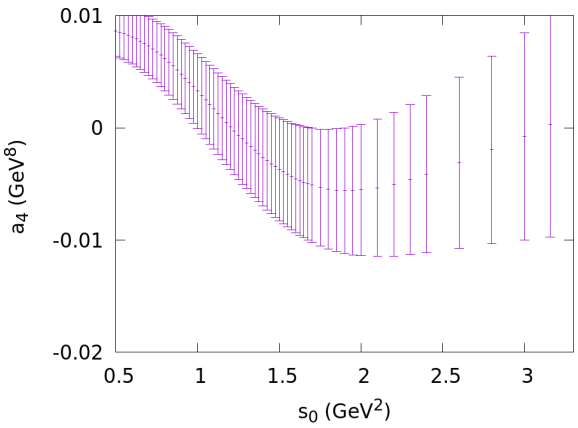


Figure 4.6: Pinched weight functions as a function of $s_0$ reescaled so that at $s_0$ large enough converge to $a_3$.

where the uncertainty is dominated by the value of $a_3$. Alternatively we can play with our conservative tuple procedure[‖] using $a_3(s_0)$ from the lattice and impossing Eq. (4.15) to get for $s_{th} = 1.7\,\text{GeV}^2$ the distribution of Fig. 4.7, we obtain:

$$a_4 = -(0.9^{+0.7}_{-0.4}) \cdot 10^{-2}\,\text{GeV}^8\,. \tag{4.42}$$

Averaging and taking the lower uncertainty summed quadratically to the difference of central values one has:

$$a_4 = -(0.7 \pm 0.6) \cdot 10^{-2}\,\text{GeV}^8\,. \tag{4.43}$$

## 4.5 Conclusions

In this work we have made a phenomenological analysis of the relations between the $D = 6$ operators appearing in the OPE of the $\Pi_{V-A}(s)$ correlator and $K \to (\pi\pi)_{I=2}$ matrix elements. We directly connect the $\langle \mathcal{Q}_8 \rangle_\mu$ contribution with the effective $D = 6$ condensate $a_3$. Using tau data we get $a_3$ with a careful study

[‖] Corrections to the finite version of the WSRs due to $b_3$ (Eqs. (4.13) and (4.14)) are taken into account. The difference $\rho_{DV}(s) - \rho(s)$ also receives a contribution from $b_3$, but it is numerically negligible.

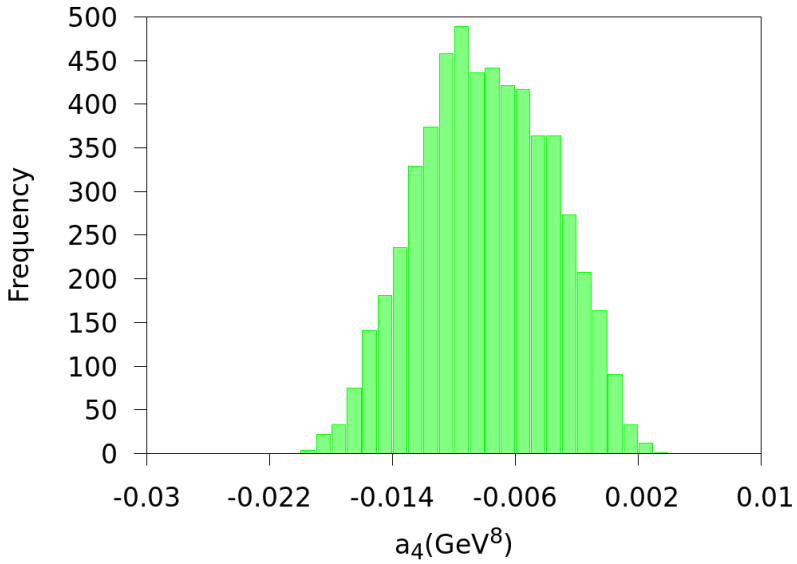


Figure 4.7: Distribution for $a_4$ obtained with the tuples procedure.

of DVs, which preliminarily gives in the chiral limit:

$$\begin{aligned}\langle(\pi\pi)_{I=2}|\mathcal{Q}_8|K^0\rangle_{2\text{GeV}} &= (1.14 \pm 0.41_{a_3} \pm 0.29_{\text{pert}} \pm 0.14_{\langle\mathcal{O}_1\rangle_\mu})\ \text{GeV}^3 \\ &= (1.14 \pm 0.49)\ \text{GeV}^3\,, \end{aligned} \tag{4.44}$$

in good agreement with other works that use similar methods and also with other lattice determinations.

On the other hand, taking $\langle\mathcal{Q}_7\rangle_\mu$ and $\langle\mathcal{Q}_8\rangle_\mu$ from the lattice, one can invoke the same relations to get the full leading $D = 6$ contribution of the V-A correlator at NLO in the chiral limit. Using the very good knowledge on the short distance behaviour of that correlator, one can define dispersion relations to make very precise physics predictions involving QCD data dominated by the complex $\sim 1$ GeV region. For example we have obtained $f_\pi$ with a precision of a 0.8%:

$$\sqrt{2} f_\pi = (131.6 \pm 1.0)\,\text{MeV}\,. \tag{4.45}$$

Finally, we also obtain a value of:

$$a_4 = -(0.7 \pm 0.6) \cdot 10^{-2}\,\text{GeV}^8\,, \tag{4.46}$$

for the $D = 8$ condensate, in good agreement with our previous determination, but more robust.

# Chapter 5

# Hadronic tau decays as new physics probes

## 5.1 Introduction

In previous chapters we have explored some of the most powerful QCD methods in hadronic tau decays to obtain precise and competitive predictions for different physical parameters. A natural question then arises. Assuming there is new physics at high energies, is it possible that hadronic tau decays might be affected by it?

If the answer were not, we could take our results as determinations of physical parameters free from contaminations from potential BSM physics, so that eventually they can be used as inputs to study other observables sensitive to them.

If it is so, we can take the physical parameters we need for the SM prediction of tau observables from other sources not affected by new physics effects, such as the lattice, and then compare to experiment. Since we know that there is good agreement between SM predictions and data in the tau sector, this comparison would translate into constraints.

At first sight one could be tempted not to look for new physics in the electroweak sector at hadronic tau decays. Since naively one is working at $E \sim \text{GeV}$ scales, one may think that new physics entering at a scale $\sim \Lambda$ is suppressed by a factor $\sim \frac{1\,\text{GeV}^2}{\Lambda^2}$, so that it is completely worthless to look for new physics at $E \sim 1\,\text{GeV}$. This argument is indeed correct when studying for example the process $e^- e^+ \to q\bar{q}$ at invariant mass $q^2 \sim 1\,\text{GeV}^2$, where, with the current precision, one is completely unable to see even the correction coming from the $Z$ boson

propagator, so obviously one is also unable to uncover new physics either weakly coupled at similar scales or at higher energy scales. However, the weak nature of the $\tau$ decays makes them suppressed by two powers of the vev $v$, so that a prediction with a relative uncertainty $r$ is typically sensitive to scales $\Lambda \sim (r^{-\frac{1}{2}} v)$. As we will see, in a general enough framework such as the Standard Model as Effective Field Theory (SM-EFT), hadronic tau decays are able to set competitive bounds in some Wilson Coefficients, which means that indeed they become a practically unexplored new physics probe.

This Chapter is about an ongoing work. The final results will be presented in forthcoming publications [157]. In this regard, the results given in this chapter should be understood as preliminary. In Section 5.2 we present the most general extension of the Fermi Lagrangian for the process $\tau \to n\nu_\tau$, where $n$ is a hadronic state, that one can build with some minimal assumptions. We also show how the couplings we obtained can be related with the (slightly less general) SM-EFT ones [158, 159].

In Section 5.3 we make a study of the different exclusive non-strange channels. The main limitation of these channels is basically the same one as for making precise physics within the SM framework. The theoretical description of QCD form factors, which encode the non-perturbative hadron dynamics of strong interactions, is far from being controlled theoretically. However, some powerful constraints can be obtained for some channels. We study the single hadron decay, the only one traditionally used as a new physics probe. For the non-strange decay, its hadron dynamics is encoded in a single unknown constant, $f_\pi$, which can be obtained from the lattice. Then, we briefly analyze the study of Ref. [160], which was able to obtain a powerful constraint to new physics from the $\eta\pi$ channel, and finally we analyze the two-pion channel. Even when there is a not very well known form factor involved, one is able to relate it to the one appearing in the process $e^+e^- \to \pi\pi$ invoking isospin relations. Owing to the impressive experimental precision of this channel, this link provides a very powerful tool to constrain new physics.

In Section 5.4, we study the potential of inclusive tau decays. Relations between QCD spectral functions and invariant mass distributions get modified by new physics effects in a way that depends on the new physics couplings [9,161]. Using the inclusive methods previously studied, one can get several constraints in this sector.

Combining information coming from all the relations, we are able to constrain all the couplings. We give the results of that combination in Section 5.5, where we also perform the matching with the SM-EFT. Hadronic tau decays allow us

to get unique low-energy bounds, complementing the information coming from other Electroweak Precision Observables (EWPO) [162]. Additionally, one can compare these bounds with the ones that can obtain from LHC data, which is very sensitive to four-fermion operators.

In section 5.6, we take a look at the strange part. Because of the poorest theoretical knowledge of the exclusive channels and the worse experimental resolution, we are not able to find bounds for all the couplings, but we find two new physics constraints.

## 5.2 Theoretical framework

The part of the Effective Fermi Lagrangian responsible for the process $\tau \to \nu_\tau n$, arising when integrating out the heavy degrees of freedom of the SM (see Chapter 1) can be generalized to the most general six-dimensional one by only assuming that the low-energy degrees of freedom correspond to the known SM particles and that the most general Lorentz invariant Lagrangian is [158, 159]:*

$$\begin{aligned}\mathcal{L}_{\text{eff}} \;=\; & -\frac{G_F V_{ud}}{\sqrt{2}}\Bigg[\Big(1+\epsilon_L^{d\tau}\Big)\bar{\tau}\gamma_\mu(1-\gamma_5)\nu_\tau\cdot\bar{u}\gamma^\mu(1-\gamma_5)d \\ & +\epsilon_R^{d\tau}\;\bar{\tau}\gamma_\mu(1-\gamma_5)\nu_\tau\;\bar{u}\gamma^\mu(1+\gamma_5)d \\ & +\;\bar{\tau}(1-\gamma_5)\nu_\tau\cdot\bar{u}\Big[\epsilon_S^{d\tau}-\epsilon_P^{d\tau}\gamma_5\Big]d \\ & +\epsilon_T^{d\tau}\;\bar{\tau}\sigma_{\mu\nu}(1-\gamma_5)\nu_\tau\cdot\bar{u}\sigma^{\mu\nu}(1-\gamma_5)d\Bigg]+\text{h.c.} \qquad (5.1)\end{aligned}$$

Five new couplings $\epsilon_i^{d\tau}$ have arisen and in the following section we are constraining them assuming that they are small, so that for different observables we can define a Taylor expansion on those $\epsilon_i^{d\tau}$ and keep the linear terms. This is not a strong assumption, since alternative solutions to the dominance of the $V-A$ currents were ruled out many years ago. Doing that, one can generalize Eq. (1.19). If we define $H_{AB}(s)$ as the trivial generalization of Eq. (1.21) for the currents $V(A)^\mu = \bar{d}\gamma^\mu(\gamma^\mu\gamma_5)u$, $S=\bar{d}u$, $P=\bar{d}\gamma_5 u$ and $T^{\mu\nu}=\bar{d}\sigma^{\mu\nu}u$, with the Lorentz

*We focus here on the non-strange decays. The most general Lagrangian appearing for strange decays is functionally the same. One simply has to make the change $d \to s$.

decomposition defined as:

$$H^{\mu\nu}_{AA(VV)}(q) = [q^\mu q^\nu - g^{\mu\nu}q^2]H^{(1)}_{AA(VV)}(q^2) + q^\mu q^\nu H^{(0)}_{AA(VV)}(q^2)\,, \tag{5.2}$$

$$H^{\mu}_{VS(AP)}(q) = q^\mu H_{VS(AP)}(q^2)\,, \tag{5.3}$$

$$H^{\mu\nu\rho}_{VT}(q) = i[q^\rho g^{\mu\nu} - q^\nu g^{\mu\rho}]H_{VT}(q^2)\,, \tag{5.4}$$

one has

$$\begin{aligned} d\Gamma(s) = {} & \frac{G_F^2|V_{uD}|^2 S_{ew}^h m_\tau^5}{16\pi}\frac{ds}{m_\tau^2}\left(1-\frac{s}{m_\tau^2}\right)^2 \\ & \times\Bigg\{(1+2\epsilon_L^{d\tau}+2\epsilon_R^{d\tau})\left[\left(1+2\frac{s}{m_\tau^2}\right)H^{(1)}_{VV}(q^2)+H^{(0)}_{VV}(q^2)\right] \\ & + (1+2\epsilon_L^{d\tau}-2\epsilon_R^{d\tau})\left[\left(1+2\frac{s}{m_\tau^2}\right)H^{(1)}_{AA}(q^2)+H^{(0)}_{AA}(q^2)\right] \\ & + 2\epsilon_S^{d\tau}\frac{H_{VS}(q^2)}{S_{ew}^h m_\tau} - 2\epsilon_P^{d\tau}\frac{H_{AP}(q^2)}{S_{ew}^h m_\tau} \\ & + 12\epsilon_T^{d\tau}\frac{H_{VT}(q^2)}{S_{ew}^h m_\tau}\Bigg\}\,, \end{aligned} \tag{5.5}$$

where $\epsilon_i^{d\tau}$ refers to the real part.[†]

Due to the conservation of vector and axial currents, trivial relations between $H^{(0)}_{VV(AA)}(q^2)$ and $H_{VS(AP)}(q^2)$ can be obtained. In order to see that, let us take the derivative of

$$(2\pi)^4\delta^4(q-p_n)\langle n(p_n)|J_\mu(0)|0\rangle = \int d^4x\, e^{-iqx}\langle n(p_n)|J_\mu(x)|0\rangle\,, \tag{5.6}$$

where $J_\mu(x) = e^{i\hat{P}x}J(0)e^{-i\hat{P}x}$ is an vector or an axial current, so that

$$\begin{aligned} 0 &= \int d^4x\,(-iq_\mu e^{-iqx}\langle n(p_n)|J_\mu(x)|0\rangle + e^{-iqx}\langle n(p_n)|\partial^\mu J_\mu(x)|0\rangle) \\ &= (2\pi)^4\delta^4(q-p_n)\,(-iq_\mu\langle n(p_n)|J^\mu(0)|0\rangle + \langle n(p_n)|\partial^\mu J_\mu(0)|0\rangle)\,. \end{aligned} \tag{5.7}$$

[†]Small corrections, coming from the imaginary part of $\epsilon_T^{d\tau}$, might arise in some exclusive channels. However, we take into account that those contributions are zero or negligibly small for the ones we are studying. Owing to Eqs. (5.11) and (5.12) derived below, $H_{VS}$ and $H_{AP}$ are reals and there is no contribution from $\mathrm{Im}\,\epsilon_S^{d\tau}$ or $\mathrm{Im}\,\epsilon_P^{d\tau}$ at $\mathcal{O}(\epsilon)$.

Since the the octet vector and axial currents do not present any anomaly, their divergences can be calculated using the classical equation of motion:

$$\begin{aligned}\partial^\mu A_\mu &= i(m_u + m_d)P\,,\\ \partial^\mu V_\mu &= i(m_d - m_u)S\,.\end{aligned} \tag{5.8}$$

so that introducing them into Eq. (5.7) one obtains the well-known relations among hadronic matrix elements

$$\langle n(p_n)|P|0\rangle = \frac{1}{m_u + m_d} p_{n\,\mu}\langle n(p_n)|A^\mu|0\rangle\,, \tag{5.9}$$

$$\langle n(p_n)|S|0\rangle = \frac{1}{m_d - m_u} p_{n\,\mu}\langle n(p_n)|V^\mu|0\rangle\,, \tag{5.10}$$

Multiplying $H^{\mu\nu}_{VV(AA)}$ by $q_\mu q_\nu$ and applying those identities, one obtains

$$s^2 H^{(0)}_{AA} = s(m_d + m_u)H_{AP}\,, \tag{5.11}$$

$$s^2 H^{(0)}_{VV} = s(m_d - m_u)H_{VS}\,, \tag{5.12}$$

from which Eq. (5.5) becomes

$$\begin{aligned}d\Gamma(s) = {}& \frac{G_F^2 |V_{uD}|^2 S_{ew}^h m_\tau^5}{16\pi}\frac{ds}{m_\tau^2}\left(1 - \frac{s}{m_\tau^2}\right)^2\\ \cdot\Bigg\{&(1 + 2\epsilon_L + 2\epsilon_R)\left[\left(1 + 2\frac{s}{m_\tau^2}\right)H^{(1)}_{VV}(q^2) + \left(1 + 2\epsilon_S\frac{s}{(m_d - m_u)S_{ew}^h m_\tau}\right)H^{(0)}_{VV}(q^2)\right]\\ &+(1 + 2\epsilon_L - 2\epsilon_R)\left[\left(1 + 2\frac{s}{m_\tau^2}\right)H^{(1)}_{AA}(q^2) + \left(1 - 2\epsilon_P\frac{s}{(m_d + m_u)S_{ew}^h m_\tau}\right)H^{(0)}_{AA}(q^2)\right]\\ &+ 12\epsilon_T^{d\tau}\frac{H_{VT}(q^2)}{S_{ew}^h m_\tau}\Bigg\}\,.\end{aligned} \tag{5.13}$$

In order to compare with other observables still in a model-independent way, we can use our knowledge on the dynamics of particle physics beyond the Fermi Theory. The SM is known to give a precise prediction of the high-energy dynamics. Assuming that no new particles arise at energies $E \lesssim v$, so that the scale of new physics $\Lambda$ satisfies $\Lambda \gg v$, one can integrate them out at the SM scale leaving an Effective Lagrangian in terms of the SM particles dominated by the

lowest dimensions.[‡] In the same way that one can build the $\chi$PT Lagrangian just by building the most general Lagrangian with the Goldstone bosons allowed by the chiral symmetry up to a given dimension without any extra assumptions about the dynamics of strong interactions at higher energies, one can build the most general one with the SM particles and symmetries up to a given dimension, so that one is generalizing the SM in a model-independent way. This is the philosophy of the SM-EFT, which also assumes that the spontaneous symmetry breaking is linearly realized. The first dimension that gives a non-zero extension to the SM prediction for our process is the $D = 6$ one. Let us fix the notation by writing the Lagrangian as:

$$\mathcal{L}_6 = \sum_n \hat{w}_{(n)} \frac{\mathcal{Q}_n}{\Lambda^2} = \sum_n w_{(n)} \frac{\mathcal{Q}_n}{v^2} \,, \tag{5.14}$$

so that $w_{(n)} \equiv \frac{v^2}{\Lambda^2}\hat{w}_{(n)} \sim \frac{v^2}{\Lambda^2}$ are flavor matrices of couplings. We work in the Warsaw Basis [163]. There are two different ways in which those operators can give a contribution to the couplings of Eq. (5.1) when integrating out the rest of heavy particles of the SM:

- Modifying one of the vertex $W\tau\nu_\tau$ or $W\bar{q}q'$, so that when integrating out the $W$, the new $G_F$ is not $\frac{g^2}{2\sqrt{2}M_W^2}$ anymore. They must contain the two fermions and the $W$, which must enter through non-diagonal parts of the covariant derivative[§]. Inspecting the operators of the Warsaw basis, it is clear that only operators which close the remaining dimensions with two Higgs, which after the SSB become vevs, can give a contribution. They are

$$\mathcal{Q}_{\varphi l}^{(3)} = \varphi^\dagger i\overleftrightarrow{D}_\mu^I \varphi\, \bar{l}_p \gamma^\mu l_r \,, \tag{5.15}$$

$$\mathcal{Q}_{\varphi q}^{(3)} = \varphi^\dagger i\overleftrightarrow{D}_\mu^I \varphi\, \bar{q}_p \gamma^\mu q_r \,, \tag{5.16}$$

$$\mathcal{Q}_{\varphi ud} = i(\tilde{\varphi}^\dagger D_\mu \varphi)(\bar{u}_p \gamma^\mu d_r) \,, \tag{5.17}$$

  with $D_\mu^I$ defined in Ref. [163].

[‡]One can still think in BSM physics created by light particles (e.g. $M \sim 10\,\text{GeV}$) weakly coupled to standard ones. In this case, one could integrate them out to obtain the Lagrangian of Eq. (5.1), so that the generalized Fermi Theory is still true but not the SM-EFT. In this sense, the generalized Fermi Theory is more general.

[§]Operators with the antisymmetric tensor $W_{\mu\nu}$, which contains a partial derivative, do not generate any contribution of dimension six when integrating the $W$ out.

- Introducing operators that contain all the initial and final fields. They are simply the operators which contain the four-fermion fields of the process:

$$\mathcal{Q}_{lq}^{(3)} = \bar{l}_p \gamma_\mu \tau^I l_r \, \bar{q}_s \gamma^\mu \tau^I q_t \,, \tag{5.18}$$

$$\mathcal{Q}_{ledq} = \bar{l}_p^j e_r \, \bar{d}_s q_t^j \,, \tag{5.19}$$

$$\mathcal{Q}_{lequ}^{(1)} = \bar{l}_p^j \, e_r \epsilon_{jk} \, \bar{q}_s^k u_t \,, \tag{5.20}$$

$$\mathcal{Q}_{lequ}^{(3)} = \bar{l}_p^j \sigma_{\mu\nu} e_r \, \epsilon_{jk} \, \bar{q}_s^k \sigma^{\mu\nu} u_t \,. \tag{5.21}$$

After the SSB, we are enforced to diagonalize the quark mass matrices, for example by redefining $u_L \to V^\dagger u_L$, which breaks the $U(3)^5$ flavor symmetry introducing matrix elements with other quark families involved. Performing the matching with the Lagrangian of Eq. (5.1) one finally obtains [164]:

$$V_{11} \cdot \epsilon_L^{d\tau} = V_{11} \, [w_{\varphi l}^{(3)}]_{\tau\tau} + [w_{\varphi q}^{(3)} \, V]_{11} - [w_{lq}^{(3)} \, V]_{\tau\tau 11} \,, \tag{5.22}$$

$$V_{11} \cdot \epsilon_R^{d\tau} = \frac{1}{2} [w_{\varphi ud}]_{11} \,, \tag{5.23}$$

$$V_{11} \cdot \epsilon_{S/P}^{d\tau} = -\frac{1}{2} [w_{lequ}^\dagger \, V \pm w_{ledq}^\dagger]_{\tau\tau 11} \,, \tag{5.24}$$

$$V_{11} \cdot \epsilon_T^{d\tau} = -\frac{1}{2} [(w_{\ell equ}^{(3)})^\dagger \, V]_{\tau\tau 11} \,. \tag{5.25}$$

## 5.3 Exclusive decays

In this section we analyze the potential of the different decay channels when looking for new physics. The same difficulties commented in Section 1.2 when analyzing the problem of predictability concerning exclusive channels due to unknown form factors are present here, which limits the amount of channels that can be used to test potential New Physics. At the level of precision we work, only single and two hadrons decays are found to be competitive.¶

### 5.3.1 One-pion decay

The only single-hadron decay mediated by a non-strange current is the one-pion decay. Because of its pseudoscalar nature, it cannot decay through vector or

¶Invoking CVC and isospin symmetry, the only form factor involving the SM process $\tau \to \pi^- \pi^0 \eta \nu_\tau$ can be related to the one appearing to $e^+ e^-$, giving a predictive power of $5-10\%$ [165], which, in principle, is below the precision we obtain from other channels.

scalar current. Then using Eq. (5.13), the generalization of Eq. (1.24) is trivial:

$$\Gamma(\tau \to \pi\nu_\tau) = \frac{G_F^2|V_{ud}|^2 m_\tau^3 f_\pi^2}{8\pi}\left((1+2\epsilon_L^{d\tau}+2\epsilon_R^{d\tau}) - \frac{2m_\pi^2}{m_\tau(m_d+m_u)}\epsilon_P^{d\tau}\right) \cdot (1+\delta_{RC}^{(\pi)})\,, \tag{5.26}$$

where $\delta_{RC}^{(\pi)}$ refers to short and long distance radiative corrections. Now, in order to extract constraints for the new physics couplings we need precise inputs for $G_F^2|V_{ud}|^2$ and $f_\pi$ either unaffected by new physics couplings or affected by them in a known way. In the case of $G_F^2|V_{ud}|^2$ one can obtain the couplings from interactions involving the first family only [166], so that:

$$G_F^2|V_{ud}|^2 = \tilde{G}_F^2|\tilde{V}_{ud}|^2\left(1-2\epsilon_L^{de}-2\epsilon_R^{de}\right)\,, \tag{5.27}$$

where now $\tilde{G}_F^2|\tilde{V}_{ud}|^2$ can be obtained from first family experiments very precisely and $f_\pi$ can be extracted from the lattice without NP contaminations [69]:

$$\sqrt{2}f_\pi = 0.1302 \pm 0.0008\,. \tag{5.28}$$

Finally, the small radiative corrections can be obtained by trivially combining $\delta R_{\tau/\pi}$ from Ref. [167] with the radiative correction to the muonic pion decay of Ref. [168]. One obtains:

$$\delta_{RC}^{(\pi)} = 0.0192 \pm 0.0025\,. \tag{5.29}$$

Putting everything together, one finds:

$$\epsilon_L^{d\tau} - \epsilon_L^{de} - \epsilon_R^{d\tau} - \epsilon_R^{de} - \frac{m_\pi^2}{m_\tau(m_u+m_d)}\epsilon_P = -(1.5 \pm 6.7)\cdot 10^{-3}\,. \tag{5.30}$$

The uncertainty is dominated by $f_\pi$, so that future improvements coming from the lattice would improve this constraint.

### 5.3.2 Two-hadron decay

For the two-hadron decay, one has to compute $H_{VT}(s)$, which involves one additional matrix element:

$$\langle P^- P^0|\bar{d}\sigma^{\mu\nu}u|0\rangle = -i(p_-^\mu p_0^\nu - p_-^\nu p_0^\mu)F_T^{PP'}\,. \tag{5.31}$$

One has:

$$H_{VT}(s) = \frac{(F_T(s)F_V^*(s))C_{PP'}\lambda^{3/2}(s, m_P^{-2}m_P^2)}{48\pi^2 s^2}\,, \tag{5.32}$$

from which Eq. (1.30) generalizes to:[‖]

$$\begin{aligned}\frac{d\Gamma_{\tau\to H^- H'^0\nu_\tau}}{ds} = {}& \frac{G_F^2|V_{uD}^2|m_\tau^3}{768\pi^3 s^3} S_{ew}^h C_{HH'}^2 \left(1-\frac{s}{m_\tau}\right)^2 \lambda^{3/2}(s, m^2, m'^2) \\ & \cdot (1 + 2\epsilon_L^{d\tau} + 2\epsilon_R^{d\tau})\Bigg\{ \left(1 + 2\frac{s}{m_\tau^2}\right)|F_V^{HH'}(s)|^2 \\ & + \left(1 + 2\epsilon_S^{d\tau}\frac{s}{(m_d - m_u)m_\tau S_{ew}^h}\right)\frac{3\Delta_{HH'}^2}{\lambda(s, m^2, m'^2)}|F_S^{HH'}(s)|^2 \\ & + \frac{12\epsilon_T^{d\tau} s}{C_{HH'} m_\tau S_{ew}^h} F_T^*(s)\, F_V(s)\Bigg\}. \end{aligned} \tag{5.33}$$

Notice how the quark mass suppression of the spin-0 part due to the $\Delta_{HH'} = m_H^2 - m_{H'}^2 \sim B_0 m_q$ is not there in general for the nonstandard $\epsilon_S^{d\tau}$ current.

#### 5.3.2.1 $\tau \to \pi^- \eta \nu_\tau$

Sensitivity to New Physics in this channel has been studied in Ref. [160]. In the SM, the process is forbidden by $G$-parity, *i.e.*, it cannot be formed through strong interactions in the isospin limit ($F_S(0) \sim F_V(0) \sim \frac{\sqrt{3}}{4}\frac{m_d - m_u}{4m_s} \sim 10^{-2}$). This suppression is confirmed by the different experiments, which still have not observed this process and which have set upper limits very close to the ones expected by different SM studies. A quick inspection of Eq. (5.33) allows one to check that the order of magnitude of the SM vector and scalar contribution should be similar since, naively substituting $s \to M_R \sim$ GeV, $\frac{3\Delta_{\eta\pi}^2}{\lambda(s, m^2, m'^2)} \sim \frac{16 B_0^2 m_s^2}{3 M_R^4} \sim 0.3$.[**] The large enhancement of the $\epsilon_S^{d\tau}$ part, $2\frac{M_R^2}{(m_d - m_u)m_\tau} \sim 5 \cdot 10^2$ pushes the theoretical expectation far above the current experimental limits on the Branching Ratio, except if $\epsilon_S^{d\tau}$ is very small.[††] Using results from the analysis

[‖] We are neglecting the small phase shift of $F_T(s)$ with respect to $F_V(s)$. Including it one would obtain $\mathrm{Re}(\epsilon_T^{d\tau} F_T(s) F_V^*(s))$, where $\epsilon_T^{d\tau}$ would refer to the complex coupling, not to the real part of it.

[**] More careful studies (see for example Table 1 of Ref. [169]) suggest that indeed the scalar contribution to the BR is slightly larger.

[††] Notice how as far as the channel is not discovered and the dominance of the SM part is confirmed, in any careful analysis, as in the one made in Ref. [160], the $\epsilon_S^{d\tau\,2}$ part should be included, because it is going to be dominant.

in Ref. [160] and adding theory errors in a very conservative way [169], we find:

$$\epsilon_S^{d\tau} = -(6 \pm 15) \cdot 10^{-3} \,. \tag{5.34}$$

#### 5.3.2.2 $\tau \to \pi^- \pi^0 \nu_\tau$

The very small difference between the pion masses allows one to neglect the scalar contribution even with the enhancement of the nonstandard current. In order to have sensitivity to new physics, we need a very precise and reliable theoretical prediction for the vector form factor from first principles. Even when such a description is not available at the level of precision we need, we can make use of the isospin relation between the vector form factor and the one appearing in the process $e^+e^- \to \pi^+\pi^-$, unaffected by potential new physics at electroweak scales (see discussion above). Explicitly one finds:

$$\begin{aligned} \sigma(s) &= \frac{\alpha_0^2 \pi \lambda^{3/2}(s, m_{\pi^+}^2, m_{\pi^-}^2)}{3s^4} |F_V^{\pi^+\pi^-}(s)|^2 \\ &= \frac{\alpha_0^2 \pi \lambda^{3/2}(s, m_{\pi^0}^2, m_{\pi^-}^2)}{3s^4} |F_V(s)|^2 R_{IB}(s) \,. \end{aligned} \tag{5.35}$$

where $F_V^{\pi^+\pi^-}(s)$ is the vector form factor appearing in $e^+e^- \to \pi^+\pi^-$ process and $R_{IB}$ absorbs isospin breaking effects.*

The only extra form factor is the tensor one and, since it enters suppressed by new physics, too much precision is not needed for setting bounds on the associated coupling. We assume:

$$F_T(s) = F_T(0) F_V(s) \,, \tag{5.36}$$

which is exact in the elastic region [171], holds in the dominant $\rho$ resonance region. We find the same relation making use of R$\chi$T, generalized to include tensor sources [172, 173], we find at first order (see App. C). We work in that approximation taking the normalization from the lattice $F_T(0) \approx 2\sqrt{2}\, 0.663\, \text{GeV}^{-1}$ [174],

*Indeed $R_{IB}$ also absorbs other small effects arising in the $\tau - e^+e^-$ comparison such as FSR. See for example Ref. [170].

so that one has:†

$$\begin{aligned}\frac{d\Gamma_{\tau\to\pi^-\pi^0\nu_\tau}}{ds} &= \frac{G_F^2|V_{uD}^2|m_\tau^3}{384\pi^3 s^3} S_{ew}^h \left(1-\frac{s}{m_\tau^2}\right)^2 \lambda^{3/2}(s,m^2,m'^2) \\ &\quad \cdot |F_V^{\pi\pi}(s)|^2 \left(1+2\frac{s}{m_\tau}\right)\left\{(1+2\epsilon_L^{d\tau}+2\epsilon_R^{d\tau})+\frac{6\sqrt{2}sF_T(0)}{\left(1+2\frac{s}{m_\tau^2}\right)m_\tau}\epsilon_T^{d\tau}\right\} \\ &\equiv \frac{d\tilde{\Gamma}}{ds}\left\{(1+2\epsilon_L^{d(\tau-e)}+2\epsilon_R^{d(\tau-e)})+\frac{6\sqrt{2}sF_T(0)}{\left(1+2\frac{s}{m_\tau^2}\right)m_\tau}\epsilon_T^{d\tau}\right\}, \end{aligned} \tag{5.37}$$

where $\frac{d\tilde{\Gamma}}{ds}$ is now a function of $\tilde{G}_F\tilde{V}_{ud}$, defined in Eq. (5.27).

Now we can take advantage of the comparison made in Ref. [176] between the $e^+e^-$ and $\tau$ SM prediction of the contribution of $\pi\pi$ to $g-2$,

$$a_\mu^{had/LO} \equiv \frac{1}{4\pi^3}\int_{4m_\pi^2}^{m_\tau^2} dsK(s)\sigma(s)\,, \tag{5.38}$$

with $\sigma(s)$ defined in Eq. (5.35) and

$$K(s) = \int_0^1 dx \frac{x^2(1-x)}{x^2+\frac{s}{m_\mu^2}(1-x)}\,. \tag{5.39}$$

Introducing electron-positron data, Ref. [176] gets, in $10^{-10}$ units, $a_\mu^{had/LO}[\pi\pi,e^+e^-] = 507.1\pm2.6$, while introducing the form factor $F_V(s)$ of Eq. (5.37) with $\epsilon=0$ and no new physics effects in $G_F$ and $V_{ud}$ they obtain $a_\mu^{had/LO}[\pi\pi,\tau]_{SM} = 516.2\pm3.6$, while taking them into account one finds:

$$\begin{aligned} a_\mu^{had/LO}[\pi\pi,e^+e^-] = a_\mu^{had/LO}[\pi\pi,\tau]_{SM}\Bigg(1-2\epsilon_L^{d(\tau-e)}-2\epsilon_R^{d(\tau-e)} \\ -\epsilon_T^{d\tau}\frac{6\sqrt{2}F_T(0)m_\tau\int\frac{ds}{s}\frac{d\Gamma}{ds}K(s)\frac{s}{m_\tau^2}\left(1-\frac{s}{m_\tau^2}\right)^{-2}\left(1+2\frac{s}{m_\tau^2}\right)^{-2}}{\int\frac{ds}{s}\frac{d\Gamma}{ds}K(s)\left(1-\frac{s}{m_\tau^2}\right)^{-2}\left(1+2\frac{s}{m_\tau^2}\right)^{-1}}\Bigg), \end{aligned} \tag{5.40}$$

where we have safely neglected the small isospin corrections $R_{IB}(s)$ in the $\epsilon_T^{d\tau}$ integral. Using publicly available $\tau\to\pi\pi\nu_\tau$ data from ALEPH for that integral

†Useful angular and kinematic distributions including NP effects were recently derived in Ref. [175].

and the numbers given above we obtain:

$$\epsilon_L^{d\tau} - \epsilon_L^{de} + \epsilon_R^{d\tau} - \epsilon_R^{de} + 1.66\,\epsilon_T^{d\tau} = 0.0089(44)\,. \tag{5.41}$$

## 5.4 Inclusive decays

### 5.4.1 Relating the experimental invariant mass distributions to the QCD spectral functions in the SM-EFT framework

When summing over all possible decay channels, $H_{AB}(s)$ from Eq. (5.13) become spectral functions $\rho_{AB}(s)$ of two-point correlation functions, which can be computed at large energies at the quark-gluon level. Even when, exactly in the same way as in the SM, this OPE description does not work in the low-momenta Minkowskian region where data live, one can define dispersion relations to relate observables, now potentially affected by new physics contaminations, to precise QCD predictions.

The same separation between the $V$ and $A$ spectral functions as in the SM can still be made in this framework. Again, one can separate the hadronic states in $n_{V,A}$ such that

$$\langle n_V|J_A|0\rangle = 0\,, \tag{5.42}$$
$$\langle n_A|J_V|0\rangle = 0\,, \tag{5.43}$$

so that $\langle n| = \{\langle n_V|, \langle n_A|\}$. The sum over all possible $n_V(n_A)$ states in Eq. (5.13) cancels the matrix elements containing axial (vector) currents, $H_{AI}(H_{VI})$, and it is the same as the sum over all possible channels $n$ for the ones containing vectorial (axial) ones. Consequently, one can make the substitution $\sum H_{AI}(H_{VI}) \to \rho_{VI}(\rho_{AI})$ to obtain, from Eq. (5.13),

$$\begin{aligned}
\frac{dN_\tau^V}{N_\tau ds} \equiv \tau_\tau^{exp}\frac{d\Gamma_V}{ds} &= \frac{12\pi|V_{ud}|^2\,B_e'\left(1-\frac{s}{m_\tau^2}\right)^2}{m_\tau^2} \\
&\cdot\left[S_{ew}\left(1+\frac{2s}{m_\tau^2}\right)(1+2\epsilon_{L+R}^{d\tau})\,\mathrm{Im}\,\Pi_{VV}^{(1+0)}(s)\right. \\
&-\frac{2s}{m_\tau^2}S_{ew}\left(1+2\epsilon_{L+R}^{d\tau}+\epsilon_S^{d\tau}\frac{m_\tau}{S_{ew}^h(m_u-m_d)}\right)\mathrm{Im}\,\Pi_{VV}^{(0)}(s) \\
&\left.+\,12\epsilon_T^{d\tau}\frac{\mathrm{Im}\,\Pi_{VT}(s)}{m_\tau S_{ew}^h}\right]\,,
\end{aligned} \tag{5.44}$$

$$\frac{dN_\tau^A}{N_\tau ds} \equiv \tau_\tau^{exp} \frac{d\Gamma_A}{ds} = \frac{12\pi |V_{ud}|^2 \, B'_e \, S_{ew} \left(1 - \frac{s}{m_\tau^2}\right)^2}{m_\tau^2}$$
$$\cdot \left[ \left(1 + \frac{2s}{m_\tau^2}\right) (1 + 2\epsilon_{L-R}^{d\tau}) \, \mathrm{Im}\, \Pi_{AA}^{(1+0)}(s) \right.$$
$$\left. - \frac{2s}{m_\tau^2} \left(1 + 2\epsilon_{L-R}^{d\tau} + \epsilon_P^{d\tau} \frac{m_\tau}{S_{ew}^h (m_u + m_d)}\right) \mathrm{Im}\, \Pi_{AA}^{(0)}(s) \right], \tag{5.45}$$

where $\tau_\tau^{exp}$ is the experimental mean lifetime of the $\tau$, $B'_e$ must be understood not as the experimental branching ratio $\tau \to e\nu_\tau\nu_e$, but as:

$$B'_e = \frac{G_F^2 \tau_\tau^{exp}}{192\pi^3} m_\tau^5 \left(1 + \frac{3}{5}\frac{m_\tau^2}{M_W^2}\right) \left(1 + \frac{\alpha(m_\tau)}{2\pi}\left(\frac{25}{4} - \pi^2\right)\right). \tag{5.46}$$

Notice how using the same inputs for $G_F$ and $|V_{ud}|$ than in the exclusive study, the new physics contamination is the same:

$$B'_e |V_{ud}|^2 = \tilde{B}_e |\tilde{V}_{ud}|^2 (1 - 2\epsilon_L^{de} - 2\epsilon_R^{de}), \tag{5.47}$$

where $\tilde{B}_e$ is the expression obtained using $\tilde{G}_F$ in Eq. (5.46).

As we explained in Chapter 2, the contribution from the spin-0 part of the spectral functions to the continuum is negligible. Taking this into account, one obtains the experimental effective spectral functions $\mathrm{Im}\, \Pi_V^{N(1)}(s)$ in terms of the QCD ones:[‡]

$$\mathrm{Im}\, \Pi_V^{N(1)}(s) \equiv \frac{dN_{\tau,V}}{N_\tau ds} \frac{m_\tau^2}{12\pi |\tilde{V}_{ud}|^2 \tilde{B}_e S_{ew}} \left(1 - \frac{s}{m_\tau^2}\right)^{-2} \left(1 + \frac{2s}{m_\tau^2}\right)^{-1}$$
$$= (1 + 2\epsilon_{L+R}^{\tau-e}) \, \mathrm{Im}\, \Pi_{VV}^{(1)}(s) + 12\epsilon_T^{d\tau} \left(1 + \frac{2s}{m_\tau^2}\right)^{-1} \frac{\mathrm{Im}\, \Pi_{VT}}{m_\tau}(s), \tag{5.48}$$

$$\mathrm{Im}\, \Pi_A^{N(1)}(s) = \frac{dN_{\tau,A}}{N_\tau ds} \frac{m_\tau^2}{12\pi |\tilde{V}_{ud}|^2 \tilde{B}_e S_{ew}} \left(1 - \frac{s}{m_\tau^2}\right)^{-2} \left(1 + \frac{2s}{m_\tau^2}\right)^{-1}$$
$$= (1 + 2\epsilon_{L-R}^{\tau-e}) \, \mathrm{Im}\, \Pi_{AA}^{(1)}(s). \tag{5.49}$$

[‡]From now on, we will safely take $S_{ew}^h \approx 1$ for the $\epsilon$ prefactors.

where:

$$\epsilon^{\tau-e}_{L+R} \equiv \epsilon^{d\tau}_L + \epsilon^{d\tau}_R - \epsilon^{de}_L - \epsilon^{de}_R \,, \tag{5.50}$$
$$\epsilon^{\tau-e}_{L-R} \equiv \epsilon^{d\tau}_L - \epsilon^{d\tau}_R - \epsilon^{de}_L - \epsilon^{de}_R \,. \tag{5.51}$$

### 5.4.2 Obtaining Sum Rules

Let us recall the relation obtained exploiting the analyticity of the QCD $V$ and $A$ correlators of Eq. (3.52):

$$\int_{s_{th}}^{s_0} \frac{ds}{s_0} \left(\frac{s}{s_0}\right)^n \mathrm{Im}\,\Pi^{(1+0)}_{V\pm A} \pm 2\pi \frac{f_\pi^2}{s_0} \left(\frac{m_\pi^2}{s_0}\right)^n - \frac{i}{2} \oint_{|s|=s_0} \frac{ds}{s_0} \left(\frac{s}{s_0}\right)^n \Pi^{(1+0),\,\mathrm{OPE}}_{V\pm A} - \delta^{(n)}_{DV,\,V\pm A}(s_0) = 0 \,. \tag{5.52}$$

Inserting the experimental spectral functions, we obtain:

$$\int_{s_{th}}^{s_0} \frac{ds}{s_0} \left(\frac{s}{s_0}\right)^n \mathrm{Im}\,\Pi^{N(1+0)}_{V\pm A} \pm 2\pi \frac{f_\pi^2}{s_0} \left(\frac{m_\pi^2}{s_0}\right)^n - \frac{i}{2} \oint_{|s|=s_0} \frac{ds}{s_0} \left(\frac{s}{s_0}\right)^n \Pi^{(1+0),\,\mathrm{OPE}}_{V\pm A}$$
$$- \delta^{(n)}_{DV,\,V\pm A}(s_0) = 2(\epsilon^{\tau-e}_{L+R} \pm \epsilon^{\tau-e}_{L-R}) \int_0^{s_0} \frac{ds}{s_0} \left(\frac{s}{s_0}\right)^n \mathrm{Im}\,\Pi^{N(1+0)}_V(s)$$
$$\mp 4\pi \frac{f_\pi^2}{s_0} \left(\frac{m_\pi^2}{s_0}\right)^n \epsilon^{\tau-e}_{L-R} + 12\epsilon^{d\tau}_T \int_{s_{th}}^{s_0} \frac{ds}{s_0} \left(\frac{s}{s_0}\right)^n \left(1 + \frac{2s}{m_\tau^2}\right)^{-1} \frac{\mathrm{Im}\,\Pi_{VT}}{m_\tau}(s) \,, \tag{5.53}$$

where we have safely taken in the rhs,

$$\int_0^{s_0} \frac{ds}{s_0} \left(\frac{s}{s_0}\right)^n \mathrm{Im}\,\Pi^{(1+0)}_V(s) \approx \int_0^{s_0} \frac{ds}{s_0} \left(\frac{s}{s_0}\right)^n \mathrm{Im}\,\Pi^{(1+0)}_A(s) \,. \tag{5.54}$$

#### 5.4.2.1 Computation of the $\Pi_{VT}$ integral

We can make use of the analytic properties of the $\Pi_{VT}(s)$ correlator as well as its OPE to estimate its contribution. We can rewrite:

$$2i \int_0^{s_0} \frac{ds}{s_0} \left(\frac{s}{s_0}\right)^n \frac{\mathrm{Im}\,\Pi_{VT}(s)}{s + \frac{s_0}{2a}} + \oint_{|s|=s_0} \frac{ds}{s_0} \left(\frac{s}{s_0}\right)^n \frac{\Pi_{VT}(s)}{s + \frac{s_0}{2a}} = \frac{2\pi i}{(-2a)^n} \frac{\Pi_{VT}(-\frac{s_0}{2a})}{s_0} \,, \tag{5.55}$$

where $a \equiv \frac{s_0}{m_\tau^2} > \frac{1}{2}$.* The OPE of $\Pi_{VT}(s)$ should be a good approximation in both the second integral and the rhs of Eq. (5.55) as far as $a \lesssim 1$. In the Euclidean axis it is given, up to $\alpha_s$ and higher dimensional contributions, by [177]:

$$\Pi_{VT}^{OPE}(Q^2) \approx -\frac{2}{Q^2}\langle 0|\bar{q}q|0\rangle + \frac{N_c}{8\pi^2}\hat{m}\ln(Q^2)\ . \tag{5.56}$$

Using its analytic continuation in the integral one obtains

$$\oint \frac{ds}{s_0}\left(\frac{s}{s_0}\right)^n \frac{\Pi_{VT}^{OPE}(s)}{s+\frac{s_0}{2a}} = \frac{2\pi i}{(-2a)^n}\Pi_{VT}^{OPE}\left(-\frac{s_0}{2a}\right) + \oint_{NP}\frac{ds}{s_0}\left(\frac{s}{s_0}\right)^n \frac{\Pi_{VT}^{OPE}(s)}{s+\frac{s_0}{2a}}\ , \tag{5.57}$$

where $\oint_{NP}$ is the integral along the circumference taken out the residual parts due to the pole in $-\frac{s_0}{2a}$, which exactly cancels with the rhs of Eq. (5.55).† The isospin conserving part of the mass correction gives:

$$\begin{aligned}\oint_{NP}\frac{ds}{s_0}\left(\frac{s}{s_0}\right)^n &\frac{\Pi_{VT,\hat{m}}^{OPE}(s)}{s+\frac{s_0}{2a}}\frac{i\hat{m}N_c}{4\pi s_0(-2a)^n} \\ &= \left[\sum_{k=1}^{n}\binom{n}{k}\frac{(-1)^k}{k}[(1+2a)^k-1]+\ln(1+2a)\right]\ ,\end{aligned} \tag{5.58}$$

and the quark condensate contribution:

$$\oint_{NP}\frac{ds}{s_0}\left(\frac{s}{s_0}\right)^n \frac{\Pi_{VT,\langle\bar{q}q\rangle}^{OPE}(s)}{s+\frac{s_0}{2a}} = \frac{8\pi i}{m_\tau^2 s_0}\langle 0|\bar{q}q|0\rangle_{s_0}\delta_{n,0}\ , \tag{5.59}$$

where we have chosen $\mu^2 = s_0$. We finally have:

$$\begin{aligned}&\int_{s_{th}}^{s_0}\frac{ds}{s_0}\left(\frac{s}{s_0}\right)^n\left(1+\frac{2s}{m_\tau^2}\right)^{-1}\frac{\mathrm{Im}\,\Pi_{VT}}{m_\tau}(s) = \frac{im_\tau}{4}\oint_{|s|=s_0\,NP}\frac{ds}{s_0}\frac{\Pi_{VT}^{OPE}(s)}{s+\frac{s_0}{2a}} \\ &= -\frac{m_\tau\hat{m}N_c}{16\pi s_0(-2a)^n}\left[\sum_{k=1}^{n}\binom{n}{k}\frac{(-1)^k}{k}[(1+2a)^k-1]+\ln(1+2a)\right] \\ &- 2\pi\delta_{n,0}\frac{\langle 0|\bar{q}q|0\rangle_{s_0}}{s_0 m_\tau}\ .\end{aligned} \tag{5.60}$$

*Otherwise the pole would be outside from the integral region.

†Notice that, because of this cancellation, the same result arises if one takes $a < \frac{1}{2}$.

It can be easily checked that the quark mass correction is $\sim 10^{-4}$, so that it can be safely neglected. Before taking it into account one should worry even about the $\alpha_s$ corrections to $\langle 0|\bar{q}q|0\rangle$ [178] and corrections from higher dimensions.

#### 5.4.2.2 Computation of the $\Pi_{V\pm A}$ integral

For the purely perturbative part, we follow the same procedure as in Chapters 2 and 3. Details on the calculation have been extensively discussed in those chapters. The only difference is that instead of using data to obtain the strong coupling, we take $\alpha_s(M_Z^2) = 0.1182 \pm 0.0012$ from the lattice [179], which should be free from new physics effects.

For the non-perturbative part of the OPE, we work, with the exception of the improvement made in Section 5.4.4, at leading order in $\alpha_s$. Thus, $\mathcal{O}_D$ is independent on $Q^2$. Its contribution is:

$$A_{V\pm A}^{OPE\,(n)}(s_0) \;\equiv\; \frac{i}{2}\oint_{|s|=s_0}\frac{ds}{s_0}\left(\frac{s}{s_0}\right)^n\;\Pi_{V\pm A}^{\rm OPE}(s) = -\frac{\pi\mathcal{O}_{2(n+1)}}{(-s_0)^{n+1}}\,. \tag{5.61}$$

Since in principle they are unknown and we do not want to take any value potentially contaminated with new physics effects, we will take conservatively (see discussion of Chapters 2 and 3):

$$\mathcal{O}_{2n} \sim (0 \pm 0.4^{2n}\Gamma(n))\ \text{GeV}^{2n}\,. \tag{5.62}$$

#### 5.4.2.3 Putting everything together

Recalling Eq. (5.53), but inserting the results of the previous sections, one has:

$$\begin{aligned}\int_{s_{th}}^{s_0}\frac{ds}{s_0}\left(\frac{s}{s_0}\right)^n \text{Im}\,\Pi_{V\pm A}^{N(1+0)} \pm 2\pi\frac{f_\pi^2}{s_0}\left(\frac{m_\pi^2}{s_0}\right)^n - 2A_p^{(n)}(s_0) + \frac{\pi\mathcal{O}_{2(n+1)}}{(-s_0)^{n+1}} - \delta_{DV,\,V\pm A}^{(n)}(s_0)&\\ = 24\pi\,\delta_{n,0}\,\epsilon_T^{d\tau}\frac{|\langle 0|\bar{q}q|0\rangle_{s_0}|}{s_0 m_\tau} \mp 4\pi\frac{f_\pi^2}{s_0}\left(\frac{m_\pi^2}{s_0}\right)^n \epsilon_{L-R}^{\tau-e}&\\ + 2(\epsilon_{L+R}^{\tau-e} \pm \epsilon_{L-R}^{\tau-e})\int_{s_{th}}^{s_0}\frac{ds}{s_0}\left(\frac{s}{s_0}\right)^n \text{Im}\,\Pi_V^{N(1)}(s)\,,&\end{aligned} \tag{5.63}$$

where $A_p^{(n)}(s_0)$ refers to the purely perturbative contribution given in Eq. (3.15) with $\omega(s) = \left(\frac{s}{s_0}\right)^n$ for the $V+A$ channel and must be put to zero for the $V-A$ one.

We safely approximate the integrals in the rhs of the equation as $s_0-$independent. For example for $n = 0$ one obtains:

$$\int_{s_{th}}^{s_0} \frac{ds}{s_0} \,\mathrm{Im}\,\Pi_V^{N(1)}(s) \approx 0.095 \pm 0.004\,. \tag{5.64}$$

On the other hand the prefactor that comes with $\epsilon_T^{d\tau}$ gives [180]:

$$24\pi \frac{|\langle 0|\bar{q}q|0\rangle_{s_0}|}{m_\tau^3} = 0.220 \pm 0.051 \pm 0.022 = 0.22 \pm 0.05\,. \tag{5.65}$$

The first uncertainty is associated to $\langle 0|\bar{q}q|0\rangle_{s_0}$ and the second one to higher orders in $\alpha_s$.

Finally, taking into account that $2\pi \frac{f_\pi^2}{m_\tau^2} = 0.0169$, the pion mass correction of the rhs is negligible and the contribution of that term has the same $s_0$-dependence as the $\epsilon_T^{d\tau}$ term.

### 5.4.3 Numerical Analysis

In order to obtain constraints one need to estimate the lhs of Eq. (5.63) at some $s_0$, lhs($s_0$). We do it in this section for both, the $V + A$ and the $V - A$ channels, using data from the ALEPH collaboration [46]. In order to avoid new physics contaminations, we take $f_\pi$ from the lattice [69].

#### 5.4.3.1 V+A

In the $V + A$ channel we have chosen the integral of the spectral function, whose associated weight function is:

$$\omega(s) = 1\,, \tag{5.66}$$

and $R_\tau$, whose associated weight is:

$$\omega_\tau(s) = \left(1 - \frac{s}{m_\tau^2}\right)^2 \left(1 + 2\frac{s}{m_\tau^2}\right)\,. \tag{5.67}$$

The former is especially interesting because is free from uncertainties coming from dimensional condensates. Even if DVs are enhanced for this weight (as we discussed in previous chapters), the smaller DVs observed in the $V + A$ channel where data is available allows us to constraint them reliably.

On the other hand, $R_\tau$ is especially interesting because, as we discussed in Chapter 3, its DV effects are completely negligible and because the first dimensional correction is suppressed by six powers of the mass of the $\tau$.

We choose not to introduce data points based on additional weight functions because we do not find possible to disentangle among non-perturbative and new physics effects in more complex fits without extra assumptions. The same argument can be applied for the $V-A$ channel.

**Integral of the spectral function.-** We plot in Figure 5.1 the lhs of the Eq. (5.63) for $n=0$ ignoring all uncertainties but the experimental ones.

We take as reference point the last one with experimental uncertainty not too large, *i.e.*, $s_0 = 2.8\,\text{GeV}^2$. Estimating DVs is not trivial. Usually the OPE prediction is $s_0-$independent and one can estimate DV uncertainties looking at the size of its typically damped oscillatory behavior. Now, because of the $\epsilon_i^{d\tau}$ terms, we have to make a more aggressive statement and to say that there is not a cancellation between the $s_0$-dependence due to the $\epsilon$ terms and the one coming from DVs,* so that the last ones are at most of the size of these fluctuations.

Taking the difference between the maximum and the minimum in the $s_0 \in (1.5, 2.8)\,\text{GeV}^2$ interval as estimates of DVs one obtains for the lhs of Eq. (5.63) ($\omega(s)=1$):

$$\begin{aligned}\text{lhs}(2.8\,\text{GeV}^2) &= (2.90 \pm 1.96_{\text{exp}} \pm 1.82_{\text{DVs}} \pm 0.84_{\alpha_s} \pm 0.72_{\text{CIFOPT}} \pm 0.54_{\text{pert}}) \cdot 10^{-3} \\ &= (2.9 \pm 2.9) \cdot 10^{-3}\,, \end{aligned} \tag{5.68}$$

***$R_\tau$.-*** From the fit of the HFLAV collaboration [181]:†

$$B_{V+A} = 0.6185 \pm 0.0010\,, \tag{5.69}$$

$$B_\pi = 0.10810 \pm 0.00053\,, \tag{5.70}$$

where $B_{V+A}$ is the experimental branching ratio of $\tau$ to non-strange hadronic states plus $\nu_\tau$ and $B_\pi$ the one to $\pi\nu_\tau$. One can obtain the experimental value of

*This is partially justified by the fact that the $s_0-$dependence of the $\epsilon^{d\tau}$ terms is monotonous in contrast with the fluctuating behavior expected and observed due to DVs.

†Notice that the fit of that collaboration is made by summing over hadronic channels. Leptonic decays, which would potentially contaminate the results with new physics effects in a nontrivial way, are not used to reduce uncertainties in that fit.

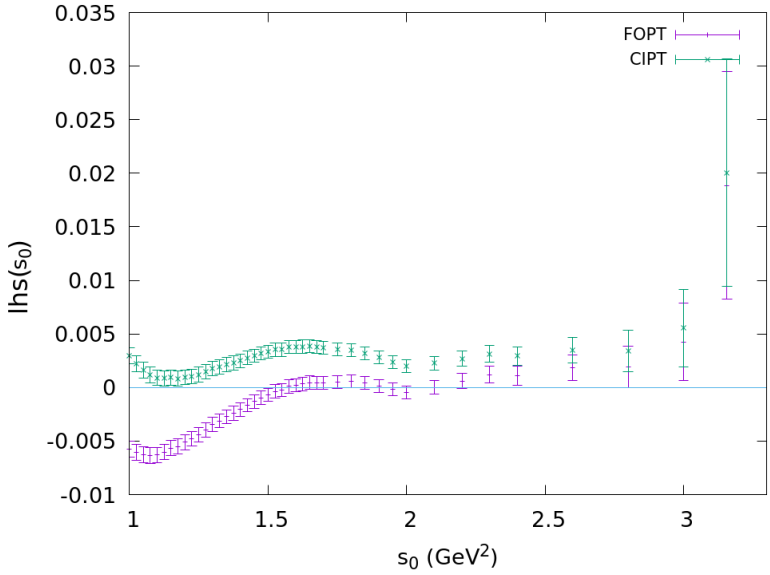


Figure 5.1: lhs of Eq. (5.63) for $n = 0$ and $V + A$ ignoring all uncertainties but the experimental ones.

the moment associated to the total decay ratio:

$$\int_{s_{th}}^{m_\tau^2} \frac{ds}{m_\tau^2} \left(1 - \frac{s}{s_0}\right)^2 \left(1 + \frac{2s}{m_\tau^2}\right) \mathrm{Im}\,\Pi_{V\pm A}^{N(1+0)} = 0.07861 \pm 0.00022\,. \tag{5.71}$$

As we discussed in Chapter 3, DVs are very suppressed in this channel. Neglecting them for the lhs of Eq. (5.63) with $\omega_\tau$ as defined in Eq. (5.67), one finds:

$$\begin{aligned} \mathrm{lhs}(m_\tau^2) &= (0.7 \pm 2.5_{\mathrm{OPE}} \pm 0.7_{\mathrm{CIFOPT}} \pm 0.6_{\alpha_s} \pm 0.4_{\mathrm{pert}} \pm 0.2_{\mathrm{exp}}) \cdot 10^{-3} \\ &= (0.7 \pm 2.6) \cdot 10^{-3}\,. \end{aligned} \tag{5.72}$$

#### 5.4.3.2 V-A

In the $V - A$ channel DVs are larger, so the best theoretical predictions, which directly translate into better new physics constraints, come from those observables that reduce them. Fortunately, we have a better knowledge of the first condensates of its OPE. Since the $D = 2$ and $D = 4$ condensates are known to be numerically negligible, one has full knowledge, except for tiny $\alpha_s$ corrections,

of the power correction of Eq. (5.63) for $n = 0$ and $n = 1$. When setting the $\epsilon_i^{d\tau} = 0$, one recovers the WSRs studied in Chapters 2 and 4. We take the combination of both WSRs that is known to efficiently reduce DV uncertainties by making use of a pinch weight function, as defined in the previous chapters:

$$\omega^{(1,0)}(s) \equiv \left(1 - \frac{s}{s_0}\right) , \tag{5.73}$$

and a combination of them with the moment $\omega(s) = s^2$ that sets a double pinch to further reduce them:

$$\omega^{(2,0)}(s) \equiv \left(1 - \frac{s}{s_0}\right)^2 , \tag{5.74}$$

but paying the price of introducing dependence on the $D = 6$ condensate.

**$\omega^{(1,0)}(s)$.-** Due to the reduced DVs associated to $\omega^{(1,0)}(s)$, one can hope that at $s \sim 2.8\,\text{GeV}^2$ DVs are negligible. We plot the $s_0$-dependence of the lhs of Eq. (5.63) associated to that weight function in Fig. 5.2.

The plateau could be a sign of DVs going to zero. However, the $s_0-$dependence of the $\epsilon$ prefactors make again this argument weaker. One could have DV effects that accidentally cancel with the ones coming from the $\epsilon$ prefactors. If somehow aggressively we assume DV are smaller than experimental uncertainties for this moment, one obtains for the lhs of Eq. (5.63) with $\omega^{(1,0)}(s)$:

$$\text{lhs}(2.8\,\text{GeV}^2) = (0.19 \pm 0.46) \cdot 10^{-3} . \tag{5.75}$$

Instead, we opt, much more conservatively, for adding as estimate of DV uncertainties the difference with the value of the lhs of Eq. (5.63) in $s_0 = 2\,\text{GeV}^2$, which translates into

$$\text{lhs}(2.8\,\text{GeV}^2) = (0.19 \pm 1.89_{\text{DVs}} \pm 0.46_{\text{exp}}) \cdot 10^{-3} = (0.2 \pm 1.9) \cdot 10^{-3} . \tag{5.76}$$

**$\omega^{(2,0)}(s)$.-** Given the very small DVs of this channel, the $\mathcal{O}_6$ uncertainty fully dominates. The SM version of this moment was already studied in previous chapters (see for example Eq. (4.17)). One obtains:

$$\text{lhs}(m_\tau^2) = -(0.1 \pm 0.8_{\mathcal{O}_6} \pm 0.3_{\text{exp}}) \cdot 10^{-3} = -(0.1 \pm 0.9) \cdot 10^{-3} . \tag{5.77}$$

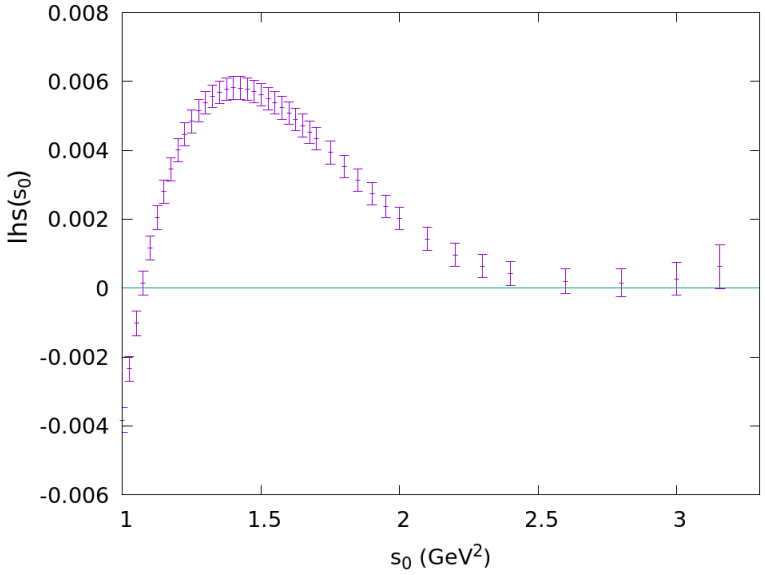


Figure 5.2: lhs of Eq. (5.63) for $\omega^{(1,0)}(s)$ and $V-A$ ignoring all uncertainties but the experimental ones.

#### 5.4.3.3 Constraints

Summarizing, we have 4 constraints whose uncertainties are very weakly correlated:

$$0.190(8)\,\epsilon_{L+R}^{\tau-e} + 0.152(8)\,\epsilon_{L-R}^{\tau-e} + 0.25(5)\,\epsilon_{T}^{d\tau} = (2.9 \pm 2.9)\cdot 10^{-3}\,, \tag{5.78}$$

$$0.096(4)\,\epsilon_{L+R}^{\tau-e} + 0.062(4)\,\epsilon_{L-R}^{\tau-e} + 0.22(5)\,\epsilon_{T}^{d\tau} = (0.7 \pm 2.6)\cdot 10^{-3}\,, \tag{5.79}$$

$$0.096(4)\,\epsilon_{L+R}^{\tau-e} - 0.058(4)\,\epsilon_{L-R}^{\tau-e} + 0.25(5)\,\epsilon_{T}^{d\tau} = (0.2 \pm 1.9)\cdot 10^{-3}\,, \tag{5.80}$$

$$0.066(4)\,\epsilon_{L+R}^{\tau-e} - 0.032(4)\,\epsilon_{L-R}^{\tau-e} + 0.22(5)\,\epsilon_{T}^{d\tau} = -(0.1 \pm 0.9)\cdot 10^{-3}\,. \tag{5.81}$$

### 5.4.4 Exploiting lattice determinations of $K \to \pi\pi$ to improve the last NP constraint

We can take advantage of the study made in the previous chapter when we used determinations of $\langle \mathcal{Q}_8 \rangle_\mu$ and $\langle \mathcal{Q}_7 \rangle_\mu$ coming from the lattice to obtain the $D = 6$ contribution of the OPE of the $V-A$ correlator at NLO in $\alpha_s$. Instead of using the weight $\omega^{(2,0)}(s)$ to obtain a very precise value of $f_\pi$, as we did in

Chapter 4, we can take it again from the lattice.[‡] In Figure 5.3 we plot the lhs of Eq. (5.63) as a function of $s_0$.

Again, there is not an ultimate reason to state that DVs are completely negligible. However, typical oscillatory behavior associated to them is not seen at large energies and different model fits within the SM to the spectral function predict they can be neglected. Indeed, one would need a very artificial shape to make them noticeable. Taking into account that the hadronic multiplicity at $s_0 \sim m_\tau^2$ is large, the convergence of the spectral function to the OPE prediction should be fast and this scenario becomes very unlikely.

So, finally one obtains:

$$\begin{aligned} 0.066(4)\,\epsilon_{L+R}^{\tau-e} - 0.032(4)\,\epsilon_{L-R}^{\tau-e} + 0.22(5)\,\epsilon_T^{d\tau} \\ &= (0.34 \pm 0.23_{\rm exp} \pm 0.20_{f_\pi^{\rm latt}} \pm 0.10_{m_q=0} \pm 0.08_{F_{m_q}=0} \pm 0.03_{Q_i^{\rm latt}}) \cdot 10^{-3} \\ &= (0.34 \pm 0.34) \cdot 10^{-3}\,, \end{aligned} \tag{5.82}$$

which supersedes Eq. (5.81).

## 5.5 Combined results

Combining the preliminary results coming from both the exclusive and inclusive constraints, one obtains at $\mu = 2\,\text{GeV}$:

$$\begin{pmatrix} \epsilon_L^\tau - \epsilon_L^e + \epsilon_R^\tau - \epsilon_R^e \\ \epsilon_R^\tau \\ \epsilon_S^\tau \\ \epsilon_P^\tau \\ \epsilon_T^\tau \end{pmatrix} = \begin{pmatrix} 1.0 \pm 1.5 \\ 0.2 \pm 1.6 \\ -0.6 \pm 1.5 \\ 0.6 \pm 1.4 \\ -0.06 \pm 0.75 \end{pmatrix} \times 10^{-2}\,, \tag{5.83}$$

with

$$\rho = \begin{pmatrix} 1 & 0.93 & 0 & -0.67 & -0.97 \\ & 1 & 0 & -0.86 & -0.96 \\ & & 1 & 0 & 0 \\ & & & 1 & 0.73 \\ & & & & 1 \end{pmatrix}. \tag{5.84}$$

Now one can run from $\mu = 2\,\text{GeV}$ to $M_Z$ [164] and then perform the matching with the SM-EFT using Eq. (5.25). In the $V_{CKM} = 1$ limit for the New Physics

[‡]Correlations are taken into account in the combined fit.

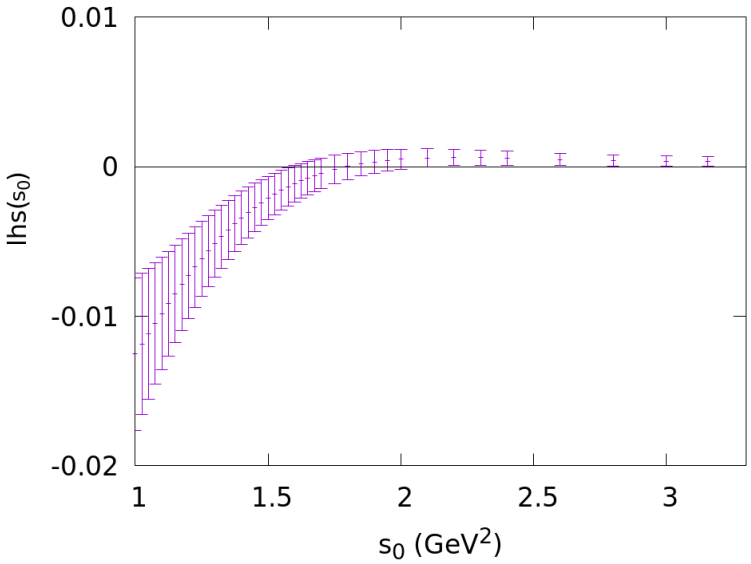


Figure 5.3: lhs of Eq. (5.63) for $\omega^{(2,0)}(s)$, as defined in Eq. (5.74), as a function of $s_0$ ignoring all uncertainties but the experimental ones.

terms, we have four SM-EFT operators which have not been constrained before. Combining these constraints with the existing ones from other Electroweak Precision Observables (EWPO) [162] one finds

$$\begin{aligned}&[w_{lq}^{(3)}, w_{lequ}, w_{ledq}, w_{lequ}^{(3)}]_{\tau\tau 11} \\ &\quad = (1.2 \pm 2.9, -0.3 \pm 1.1, 1.0 \pm 1.1, -0.6 \pm 1.4) \times 10^{-2}\,,\end{aligned} \tag{5.85}$$

after marginalizing, which are not only very strong but also unique low-energy bounds. Additionally, a competitive value, comparable with the one obtained with neutron beta decays [182], is obtained for $w_{\varphi ud}$. Including hadronic tau decays in the global fit of Ref. [162] one finds

$$w_{\varphi ud} = -(0.5 \pm 1.1) \times 10^{-2}. \tag{5.86}$$

On the other hand, one can compare with the sensitivity to those operators in LHC observables. In order to do that, one has to assume that there are no new degrees of freedom not only at scales around the vev, but also at the scales

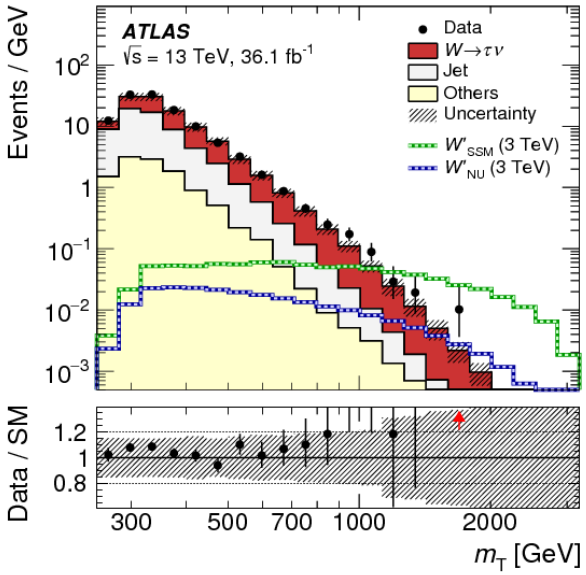


Figure 5.4: Transverse mass distribution obtained in Ref. [183] for the process $pp \to \tau\nu$.

involved in the process. In this sense, it is less general. Since one is exploring energies larger than the Higgs mass, the EFT counting gets slightly modified and those operators that enter the process as $E^2$ are enhanced compared to those entering as $v^2$. Even with poorer experimental precision, that enhancement makes the LHC able to set more powerful constraints for some of those operators.

In order to illustrate that, in Tab. 5.1 we show our results based on a recast of the transverse mass $m_T$ distribution of $\tau\nu$ events in $\sqrt{s} = 13$ TeV LHC collisions recently measured by ATLAS [183]. The impact of the Wilson coefficients on the $\frac{d\sigma(pp\to\tau\nu)}{dm_T}$ cross section (Fig. 5.4) is estimated using the `Madgraph` [184]/`Pythia 8` [185]/`Delphes` [186] simulation chain. The SM predictions is taken from [183], and their quoted uncertainties in each bin are treated as independent nuisance parameters.

We find that the LHC bounds are comparable for the chirality-violating operators to those from hadronic tau decays. However, a word of caution should be put for these constraints. They do not interfere with the SM and thus they, enter into the calculation at the same level as $D = 8$ operators. In this sense, these results are not model-independent.

| Coefficient | ATLAS $\tau\nu$ | Hadronic $\tau$ decays |
|---|---|---|
| $[w_{\ell q}^{(3)}]_{\tau\tau 11}$ | $[0.0, 1.6]$ | $[-12.7, 0.2]$ |
| $[w_{\ell equ}]_{\tau\tau 11}$ | $[-5.6, 5.6]$ | $[-9.7, 4.4]$ |
| $[w_{\ell edq}]_{\tau\tau 11}$ | $[-5.6, 5.6]$ | $[-3.6, 10.5]$ |
| $[w_{\ell equ}^{(3)}]_{\tau\tau 11}$ | $[-3.3, 3.3]$ | $[-12.6, -0.5]$ |

Table 5.1: 95% CL intervals (in $10^{-3}$ units) for the Wilson coefficients at $\mu = 1$ TeV that yield quadratically enhanced corrections to the high-energy tail of $\tau\nu$ production at the LHC. To obtain these results we assume only one Wilson coefficient is present at a time.

On the other hand, for the chirality-conserving coefficient $[w_{\ell q}^{(3)}]_{\tau\tau 11}$ the LHC bounds are one order of magnitude stronger thanks to the fact that the corresponding operator interferes with the SM $q\bar{q}' \to \tau\nu$ amplitude, which makes this bound model independent. We observe an $\mathcal{O}(2\sigma)$ preference for a non-zero value of $[w_{\ell q}^{(3)}]_{\tau\tau 11}$ due to a small excess over the SM prediction observed by ATLAS in several bins of the $m_T$ distribution.

$[w_{\ell q}^{(3)}]_{\tau\tau 11}$ is constrained by the LHC at an $\mathcal{O}(10^{-3})$ level, and similar conclusions can be drawn with regard to $[w_{\ell q}^{(3)}]_{ee11}$ [158,187]. Then hadronic tau decays effectively become a new probe of the vertex correction $\epsilon_L^\tau - \epsilon_L^e \approx [w_{\varphi l}^{(3)}]_{\tau\tau-ee}$, complementing the information from previous low-energy EWPO [162]. Previously, EWPO displayed an $\mathcal{O}(2\sigma)$ preference for a non-zero $[w_{\varphi l}^{(3)}]_{\tau\tau-ee}$, which came from the lepton flavor universality violation observed in $W \to \ell\nu$ decays in LEP2 [188,189]. Including the input from hadronic tau decays reduces both the uncertainty and the best fit value:

$$[w_{\varphi l}^{(3)}]_{\tau\tau-ee} = 0.0150 \pm 0.0085, \tag{5.87}$$

but the disagreement with the SM remains at $\sim 2\sigma$, due to the tension in the $\pi\pi$ channel (Eq. 5.41).

## 5.6 An exploratory study of the potential of the strange sector

The formalism of the strange sector is exactly the same with the change $d \to s$. Unfortunately, less precise data and limitations in the QCD knowledge makes, in principle, not possible to obtain constraints for all the $\epsilon$.

### 5.6.1 One-kaon decay

The most powerful constraint comes from the one kaon decay. Applying the same procedure as in the pion decay one has:

$$\epsilon_L^{s\tau} - \epsilon_L^{se} - \epsilon_R^{s\tau} - \epsilon_R^{se} - \frac{m_K^2}{m_\tau(m_u+m_s)}\epsilon_P^{s\tau} = -(5.1 \pm 10.0)\cdot 10^{-3}\,, \tag{5.88}$$

where uncertainties are dominated by the experimental ones.

### 5.6.2 Inclusive constraint

Unfortunately the separation of channels in $V$ and $A$ ones using symmetry considerations is not possible in the strange sector. In principle one can only relate the experimental data to spectral functions through the total normalized invariant mass distribution,

$$\begin{aligned}\frac{dN_\tau^{V+A}}{N_\tau ds} = 12\pi|V_{us}|^2\, B_e\, S_{ew}\left(1-\frac{s}{m_\tau^2}\right)^2 \cdot \Bigg[ & \left(1+\frac{2s}{m_\tau^2}\right)(1+2\epsilon_{L+R}^{s\tau})\,\mathrm{Im}\,\Pi_{VV}^{(1+0)}(s) \\ & - \frac{2s}{m_\tau^2}\left(1+2\epsilon_{L+R}^{s\tau} - \epsilon_S^{s\tau}\frac{m_\tau}{m_s-m_u}\right)\mathrm{Im}\,\Pi_{VV}^{(0)}(s) + 12\epsilon_T^{s\tau}\frac{\mathrm{Im}\,\Pi_{VT}(s)}{m_\tau^2} \\ & + \left(1+\frac{2s}{m_\tau^2}\right)(1+2\epsilon_{L-R}^{s\tau})\,\mathrm{Im}\,\Pi_{AA}^{(1+0)}(s) \\ & - \frac{2s}{m_\tau^2}\left(1+2\epsilon_{L-R}^{s\tau} + \epsilon_P^{s\tau}\frac{m_\tau}{m_u+m_s}\right)\mathrm{Im}\,\Pi_{AA}^{(0)}(s)\Bigg]\,,\end{aligned} \tag{5.89}$$

where now $\Pi_i(s)$ are referred to the currents with the strange quark. Because of the Cabibbo suppression ($|V_{us}|^2$), experimental uncertainties are typically larger in this sector. In fact, the only inclusive observable available to us is the total strange cross section. Integrating the previous distribution, and then using the analyticity of the correlators to equate the integral of the spectral function to $\frac{i}{2}$

times the integral along the complex circumference, one has:

$$\begin{aligned}
\frac{B_s}{3B_e'|V_{us}|^2 S_{ew}} &= 2\pi i \oint \frac{ds}{m_\tau^2}\left(1-\frac{s}{m_\tau^2}\right)^2\left(1+\frac{2s}{m_\tau^2}\right)\Pi_{VV+AA}^{(1+0)}(s) \\
&- 2\pi i \oint \frac{ds}{m_\tau^2}\left(1-\frac{s}{m_\tau^2}\right)^2\left(\frac{2s}{m_\tau^2}\right)\Pi_{VV+AA}^{(0)}(s) \\
&+ 2\pi i(\epsilon_{L+R}^{s\tau}+\epsilon_{L-R}^{s\tau})\oint \frac{ds}{m_\tau^2}\left(1-\frac{s}{m_\tau^2}\right)^2\left(1+\frac{2s}{m_\tau^2}\right)\Pi_{VV+AA}^{(1+0)}(s) \\
&- 2\pi i\,\epsilon_P^{s\tau}\frac{m_\tau}{m_u+m_s}\oint \frac{ds}{m_\tau^2}\left(1-\frac{s}{m_\tau^2}\right)^2\left(\frac{2s}{m_\tau^2}\right)\Pi_{AA}^{(0)}(s) \\
&+ 2\pi i\,\epsilon_S^{s\tau}\frac{m_\tau}{m_s-m_u}\oint \frac{ds}{m_\tau^2}\left(1-\frac{s}{m_\tau^2}\right)^2\left(\frac{2s}{m_\tau^2}\right)\Pi_{VV}^{(0)}(s) \\
&+ 24\pi i\epsilon_T^{s\tau}\oint \frac{ds}{m_\tau^2}\left(1-\frac{s}{m_\tau^2}\right)^2\frac{\Pi_{VT}(s)}{m_\tau} \\
&\equiv 1+\delta_P+\delta_{m_s}+\delta_{D>2}^{OPE}+\delta_L \\
&+ \alpha_L(\epsilon_{L+R}^{s\tau}+\epsilon_{L-R}^{s\tau})+\alpha_P\epsilon_P^{s\tau}+\alpha_T\epsilon_T^{s\tau}\,. \qquad (5.90)
\end{aligned}$$

where $B_e'$ is defined as in the non-strange discussion.

Since we do not need so much precision for the $\alpha_i$ coefficients, we have made several approximations. We have used that the vectorial and axial $L{+}T(=(0{+}1))$ contributions are very close. This is because they are strongly dominated by the perturbative contribution, which respects chiral symmetry. We have also safely neglected the tiny term proportional to $\epsilon_{L+R}^{s\tau}$ and $\epsilon_{L-R}^{s\tau}$ coming from the longitudinal part $(=(0))$ of the correlators.

At this stage, we can use again the OPE of the correlator along the circumference to make a theoretical prediction of the different integrals. Since the different integrals associated to the total cross section are doubly pinched, *i.e.*, contain a kinematic function proportional to $\left(1-\frac{s}{m_\tau^2}\right)^2$, DVs are very suppressed and the OPE becomes very precise.

In previous works [48, 190–193], $|V_{us}|^2$ has been extracted comparing $R_{\tau,\,s}$ which $R_{\tau,\,ns}$, which allows one to remove perturbative uncertainties and some non-perturbative ones. Since we do not want contaminations from BSM contributions coming from the non-strange sector, we will directly compare $R_{\tau,\,s}$ with the QCD predicted value.[§] Nevertheless, we will take advantage of some of the results

[§]In fact, given the bounds we obtained for the non-strange constraints, it may be worth it doing the study in the traditional way. We will explore this possibility in the near future.

found in those references in order to obtain some of the contributions needed. Typically a contribution $i$ is given in the form:

$$\delta R_\tau^i \equiv \frac{R_{\tau,ns}^i}{|V_{ud}|^2} - \frac{R_{\tau,s}^i}{|V_{us}|^2} = 3S_{ew}(\delta_{ns}^i - \delta_s^i)\,, \tag{5.91}$$

so that, since we have already calculated the non-strange contributions, we can just take

$$\delta_s^i = \delta_{ns}^i - \frac{\delta R_\tau^i}{3S_{ew}}\,. \tag{5.92}$$

In the following sections we detail how to extract values for the different terms.

#### 5.6.2.1 Experimental values

Taking the following numerical inputs [166, 181, 194]:

$$\tilde{B}_e = 0.17778 \pm 0.00031\,, \tag{5.93}$$
$$|\tilde{V}_{us}| = 0.22408 \pm 0.00087\,, \tag{5.94}$$
$$B_s = 0.02909 \pm 0.00048\,, \tag{5.95}$$
$$S_{ew} = 1.0201 \pm 0.0003\,, \tag{5.96}$$

one obtains

$$\frac{B_S}{3B_e'|V_{us}|^2 S_{ew}} = (1.065 \pm 0.019)(1 + 2\epsilon_R^{se} + 2\epsilon_L^{se})\,. \tag{5.97}$$

We will reabsorb the $\epsilon_{L+R}^{se}$ into the $\epsilon_{L+R}^{s\tau}$ as we did in the non strange analysis (this can be done here because, as we mentioned above, we are neglecting the very suppressed new physics $\epsilon_{L+R}^{s\tau}$ and $\epsilon_{L-R}^{s\tau}$ contribution coming from the longitudinal part).

#### 5.6.2.2 L+T integral

The dominant contribution by far is the perturbative one. This calculation is identical to the one already made in the non-strange sector. We obtain:

$$\begin{aligned}\delta_P &= 2\pi i \oint \frac{ds}{m_\tau^2}\left(1 - \frac{s}{m_\tau^2}\right)^2\left(1 + \frac{2s}{m_\tau^2}\right)\Pi_{VV+AA}^{(1+0)}(s) - 1 \\ &= 0.1916 \pm 0.009_{FO-CI} \pm 0.007_{\alpha_s} \pm 0.005_{\text{pert}} = 0.192 \pm 0.012\,.\end{aligned} \tag{5.98}$$

The perturbative series associated to the strange mass are not very well behaved. Taking $\delta R_\tau^{m_s}$ from [192]:

$$\delta R_\tau^{m_s} = (9.3 \pm 3.4)\, m_s^2 \,. \tag{5.99}$$

Since quark masses $m_u$ and $m_d$ are negligible, one can neglect $\delta_{ns}^{m_s}$ (see Eq. 5.92) to obtain:

$$\delta^{m_s} = -\frac{\delta R_\tau^{m_s}}{S_{ew}\, N_c} = -0.0266 \pm 0.0097 \,. \tag{5.100}$$

Repeating the same argument as in the non-strange sector we obtain:

$$\delta_{D>2}^{OPE} = 0 \pm 12\,\pi^2\,\Gamma(3)\,\frac{\Lambda^6}{m_\tau^6} = 0.000 \pm 0.031 \,. \tag{5.101}$$

This uncertainty will be the dominant one.

#### 5.6.2.3 Longitudinal contribution

Here we recall Eq. (5.92) for the longitudinal case:

$$\delta_L = \delta_{L,\,ns} - \frac{\delta R_\tau^L}{3 S_{ew}} \,. \tag{5.102}$$

As we argued in the non strange analysis, $\Pi_{ns}^{(0)}(s)$ is fully dominated by the pion pole:

$$\Pi_{ns}^{(0)}(s) = -\frac{2 f_\pi^2}{s - m_\pi^2} \,, \tag{5.103}$$

so that

$$\delta_{L,\,ns} = \delta_L^\pi = -8\pi^2 \frac{f_\pi^2}{m_\tau^2} \frac{2 m_\pi^2}{m_\tau^2} \left(1 - \frac{m_\pi^2}{m_\tau^2}\right)^2 = -(0.00258 \pm 0.0003) \,. \tag{5.104}$$

The calculation within QCD of $\delta R_\tau^L$ [191] contains a 30% of uncertainty. A more phenomenological approach to extract $\delta R_\tau^L$ is done in the same reference and allows for a much better precision. Let us see how possible new physics effects in that analysis are probably small. The point is that $\delta R_\tau^L$ is going to be dominated by the kaon pole:

$$\delta_L = \delta_L^K + \delta_L^{rem} \,, \tag{5.105}$$

where:¶

$$\delta_L^K = -8\pi^2 \frac{f_K^2}{m_\tau^2} \frac{2m_K^2}{m_\tau^2} \left(1 - \frac{m_K^2}{m_\tau^2}\right)^2 = -(0.0396 \pm 0.0005)\,. \tag{5.106}$$

$\delta_{rem}$ was obtained in Ref. [191] by calculating the contribution coming from the scalar spectral function and $K(1460)$, $K(1800)$ in different fits. Since they give $\delta R_\tau^L = 0.1544 \pm 0.0003$, one has:

$$\delta_{rem} = (-0.0134 \pm 0.0012)(1 + a_i \epsilon_i)\,, \tag{5.107}$$

assuming that $\epsilon_i$ are not strongly enhanced,‖ new physics corrections can be neglected and then:

$$\delta_L = -0.0530 \pm 0.0012\,. \tag{5.108}$$

#### 5.6.2.4 $\epsilon_L^{s\tau}$, $\epsilon_P^{s\tau}$, $\epsilon_S^{s\tau}$ and $\epsilon_T^{s\tau}$ parts

We do not need too much precision for the $\alpha$ coefficients. For $\alpha_L$, we can take conservatively the average between Eq. (5.97) and Eq. (5.98):

$$\alpha_L \equiv \oint \frac{ds}{m_\tau^2} \left(1 - \frac{s}{m_\tau^2}\right)^2 \left(1 + \frac{2s}{m_\tau^2}\right) \Pi_{VV+AA}^{(1+0)}(s) = 1.13 \pm 0.06\,. \tag{5.109}$$

The $\frac{m_\tau}{m_s}$ enhancement makes the $\epsilon_P$ and $\epsilon_S$ part not negligible. Using the results of Ref. [48], one has:

$$\alpha_P = \frac{m_\tau}{m_u + m_s} \delta_L^V = -0.79 \pm 0.02\,, \tag{5.110}$$

$$\alpha_S = -\frac{m_\tau}{m_s - m_u} \delta_L^A = +0.17 \pm 0.02\,. \tag{5.111}$$

In order to estimate this part we can make use of the OPE of the VT correlator [177]. The correlator was computed for light quark masses. In principle the expression would be the same, changing $m_d \to m_s$. The problem is that the

¶Probably Ref. [192] took an experimental value for $f_K$, which could bring NP contaminations to $\delta R_\tau^L$, but since we know there is an excellent agreement with the lattice value and the uncertainty due to $f_K$ in Eq. (5.106) is completely negligible, they can be neglected. Exactly the same argument can be applied with $f_\pi$ in Eq. (5.104).

‖This might not be totally safe for the decay constants of the strange resonances, because they are using similar sum rules to fit them (new physics might compete with the very small corrections which they represent). However, it would be enough that the order of magnitude of $f_{K(1460)}$ is correct. We assume that.

computation was made in the isospin limit $m_u = m_d$, so that we are missing mass contributions of the same order $(m_s - m_u)$ than the ones taken into account. Fortunately, the mass contribution does not dominate. Using Eq. (5.60), we obtain:

$$\alpha_T = 2.6 \pm 0.4\,, \tag{5.112}$$

where we have used as estimates of uncertainties associated to $m_s$ corrections $|\alpha_{T,(m_s-m_u)}| \lesssim |\alpha_{T,(m_s+m_u)}| = 0.17$.

#### 5.6.2.5 Putting everything together

We obtain:

$$\begin{aligned} -0.042 \pm 0.039 = (1.13 \pm 0.06)(\epsilon_{L+R}^{s\tau-se} + \epsilon_{L-R}^{s\tau-se}) + (2.6 \pm 0.4)\epsilon_T^{s\tau} \\ - (0.79 \pm 0.02)\epsilon_P^{s\tau} + (0.17 \pm 0.02)\epsilon_S^{s\tau}\,, \end{aligned} \tag{5.113}$$

where uncertainties are dominated by our conservative estimate of the power corrections.

# Conclusions

In this thesis, we have focused on the phenomenology of some of the more predictive approaches involving hadronic tau decays. Inclusive observables have played a central role.

We have started with an updated study of the inclusive $V-A$ spectral functions. They provide a window to study non-perturbative physics. We have used well-known dispersion relations, which allow us to extract information from the resonance spectrum with a description where the degrees of freedom are quarks and gluons, to obtain some updated values for low-energy constants and vacuum condensates. We have made a careful estimate of Duality Violations, concluding that they are not dominating uncertainties at $s_0 \sim m_\tau^2$ for most of the weight functions and that pinch weight functions efficiently reduce them. However, they have a significant role for the determination of the vacuum condensates, both because their associated weight functions are especially sensitive to Duality Violations and because experimental resolution enforce a determination of them at lower energies. Working at $\mathcal{O}(p^6)$ we have obtained:

$$L_{10}^r(M_\rho) \quad = -(4.1 \pm 0.4) \cdot 10^{-3}\,, \quad C_{87}(M_\rho) \quad = (5.10 \pm 0.22)\,\mathrm{GeV}^{-2}\,. \quad (5.114)$$

Then, we have made a comprehensive analysis of the strong coupling determination from hadronic tau decays. Different approaches, aimed to deal with the non-perturbative contributions, have been studied. The cleanest determination comes from the inclusive non-strange $V+A$ spectral function, where all the approaches and tests, which make use of different assumptions, are in very good agreement. We quote our final number as:

$$\alpha_s(m_\tau^2) = 0.328 \pm 0.013\,, \quad (5.115)$$

which translates, after running from $\mu^2 = m_\tau^2$ to $\mu^2 = M_Z^2$, into

$$\alpha_s(M_z) = 0.1197 \pm 0.015\,, \quad (5.116)$$

in excellent agreement with the global average [195].

In the chiral limit, there are known relations between $K \to \pi\pi$ matrix elements and vacuum condensates. The latter can be found in the $D = 6$ contribution of the OPE of the correlator $\Pi_{V-A}(s)$. We have made a preliminary updated study of the phenomenological implications of those relations. Using hadronic tau-decay data, we have obtained an updated value for $\langle \mathcal{Q}_8 \rangle_\mu$ in the chiral limit. We have explored the possibility of taking $\langle \mathcal{Q}_7 \rangle_\mu$ and $\langle \mathcal{Q}_8 \rangle_\mu$ from the lattice to use it as a new short-distance constraint in the tau sector. This allows, for example, for a determination of $f_\pi$ with a precision below the per-cent level without making use of information on $\tau \to \pi\nu_\tau$ data.

Finally, we have performed a novel and preliminary analysis on the potential of hadronic tau decays to constrain new physics in a model-independent fashion, using the Standard Model Effective Field Theory framework. Combining both inclusive and exclusive observables, we have been able to find bounds on all the couplings involved, typically with a precision below the percent level. Some of them give not only stringent, but also unique low-energy bounds. Combining with LHC data, one can obtain bounds on two $W$ vertex corrections, which are competitive or even more stringent than previous bounds coming from other precise EWPO.

Improved data sets, which could come from collaborations as Belle-2, would translate into improved determinations of the parameters obtained with the different tools we have used. Since we are close to their limit of applicability, it is not easy to quantify the reach of that improvement. If a very fast convergence to quark-hadron duality near the tau mass, where current experimental uncertainties are too large, happened to be observed, there would be a significant reduction of systematic uncertainties.

The strong coupling has been obtained at the tau mass, where the convergence of the perturbative series is slow and where we may be close to the asymptotic region. An improvement in the knowledge of higher-order perturbative corrections would significantly help to reduce perturbative uncertainties. Efforts made in rigorous calculations of higher-loops coefficients and in methods aimed to resum the whole series could shed some light on tau-based determinations of $\alpha_s$.

Finally, some improvements are expected in the phenomenological study of the new physics sensitivity of hadronic tau decays. First, improvement in the lattice input for $f_\pi$ would translate into a better one-pion constraint. On the other hand, a more careful analysis of the two-pion constraint, where one could directly study the invariant mass distribution, or of the inclusive strange ones, could improve the bounds of hadronic tau decays on new physics couplings.

# Appendix A

# Low-energy expansion of the left-right correlation function

At low energies, the correlator $\Pi(s)$ can be expanded in powers of momenta over the chiral symmetry-breaking scale. The series expansion has been calculated to $\mathcal{O}(p^6)$ in $\chi$PT [25, 64, 66]:

$$\begin{aligned}
\Pi(s) &= \frac{2f_\pi^2}{s-m_\pi^2} - 8L_{10}^r - 8B_V^{\pi\pi}(s) - 4B_V^{KK}(s) \\
&+ 16\,C_{87}^r\,s \; - 32\,m_\pi^2\,(C_{61}^r - C_{12}^r - C_{80}^r) \\
&- 32\,(m_\pi^2 + 2m_K^2)\,(C_{62}^r - C_{13}^r - C_{81}^r) \\
&+ 16\left((2\mu_\pi + \mu_K)(L_9^r + 2L_{10}^r) - \left[2B_V^{\pi\pi}(s) + B_V^{KK}(s)\right]\,L_9^r\,\frac{s}{f_\pi^2}\right) \\
&- 8\,G_{2L}(s)\;, \qquad\qquad (A.1)
\end{aligned}$$

where

$$B_V^{ii}(s) \equiv -\frac{1}{192\pi^2}\left(\sigma_i^2\left[\sigma_i\,\log\left(\frac{\sigma_i-1}{\sigma_i+1}\right)+2\right] - \log\left(\frac{m_i^2}{\mu^2}\right) - \frac{1}{3}\right)\;, \qquad (A.2)$$

$$\sigma_i = \sqrt{1-\frac{4m_i^2}{s}}\;, \qquad (A.3)$$

$$\mu_i \equiv m_i^2\log(m_i/\mu)/(16\pi^2 f_\pi^2)\;, \qquad (A.4)$$

and $G_{2L}(s)$ is the two-loop contribution. The analytic expression of $G_{2L}(s)$ is too large to be given here, even in the $s \to 0$ limit; it can be extracted from Ref. [66]. For $\mu = M_\rho$, the numerical values for its contribution and its derivative at $s = 0$ are [9]:

$$G_{2L}(0) = -0.53 \cdot 10^{-3} \,, \tag{A.5}$$

$$G'_{2L}(0) = -0.28 \cdot 10^{-3} \text{ GeV}^{-2} \,. \tag{A.6}$$

# Appendix B

# Relation between matrix elements in the chiral limit

Effective Lagrangians, built with total generality for the low-energy degrees of freedom by imposing that the chiral symmetry transformations properties are the same as the known short-distance version of it, can be used as a tool to relate matrix elements between meson states at first order in $\chi$PT ($\mathcal{O}(p^0)$). Playing with that one can successfully relate (see [196]) $K \to \pi\pi$ matrix elements to $K \to \pi$. However, in order to relate matrix elements among mesons and vacuum condensates, one has, to the best of our knowledge, to invoke the soft-meson theorem [197, 198] in order to remove at least the last meson.

## B.1 The soft-meson theorem

We follow here the derivation of Ref. [198] with our convention for $\gamma_5$ ($P_L = \frac{1-\gamma_5}{2}$) and trivially extending it from $SU(2)$ to $SU(3)$. The theorem states that,

$$\lim_{q\to 0} \langle \phi^k(q)\beta | \, \mathcal{O}(0) \, |\alpha\rangle = \frac{i}{F} \, \langle \beta | \, [Q_5^k, \mathcal{O}(0)] \, |\alpha\rangle \ , \tag{B.1}$$

where $\phi^k$, $k = 1, ..., 8$ are the Goldstone bosons, usually parametrized as $U(x) = e^{i\frac{\lambda_a \phi_a(x)}{F}}$, $Q_5^k$ is the associated chiral charge $Q_5^k = \bar{q}\frac{\lambda_k}{2}\gamma_5 q$ and $\alpha$ and $\beta$ are generic states.

The starting point of the proof is the LSZ reduction formula,

$$\langle \phi^k(q)\beta | \, \mathcal{O}(0) \, |\alpha\rangle = -i \int d^4x \, e^{iqx} (q^2 - m_\phi^2) \, \langle \beta | \, T(\phi^k(x)\mathcal{O}(0)) \, |\alpha\rangle \, |_{q^2=m_\phi^2} \, . \tag{B.2}$$

Now, using that at lowest (non-trivial) order in $\chi PT$

$$\partial_\mu A^{\mu k}(x) = -F m_\phi^2 \phi^k(x)\,, \tag{B.3}$$

one obtains

$$\langle \phi^k(q)\beta|\,\mathcal{O}(0)\,|\alpha\rangle = i \lim_{q^2\to m_\phi^2} \frac{q^2-m_\phi^2}{F m_\phi^2} \int d^4x\, e^{iqx}\,\langle\beta|\,T(\partial_\mu A^{\mu k}(x)\mathcal{O}(0))\,|\alpha\rangle\ . \tag{B.4}$$

Expanding the T-product in terms of the Heaviside function and integrating by parts one gets

$$\langle \phi^k(q)\beta|\,\mathcal{O}(0)\,|\alpha\rangle = i \lim_{q^2\to m_\phi^2} \frac{q^2-m_\phi^2}{F m_\phi^2} \int d^4x\, e^{iqx}[\langle\beta|\,\partial_\mu T(A^{\mu k}(x)\mathcal{O}(0))\,|\alpha\rangle - \delta(x_0)\,\langle\beta|\,[A^{0k}(x),\mathcal{O}(0)]\,|\alpha\rangle]\,. \tag{B.5}$$

Integrating by parts again the first term and defining $\bar{A}^\mu(x) \equiv A^{\mu k}(x)_{x_0=0}$

$$\langle \phi^k(q)\beta|\,\mathcal{O}(0)\,|\alpha\rangle = i \lim_{q^2\to m_\phi^2} \frac{q^2-m_\phi^2}{F m_\phi^2}(-iq_\mu \underbrace{\int d^4x\, e^{iqx}\,\langle\beta|\,T(A^{\mu k}(x)\mathcal{O})\,|\alpha\rangle}_{R^{k\mu}(q)} - \langle\beta|\,[\int d^3x\, e^{-i\vec{q}\cdot\vec{x}}\bar{A}^{0k}(x),\mathcal{O}(0)]\,|\alpha\rangle) \equiv i \lim_{q^2\to m_\phi^2} F(q)\,. \tag{B.6}$$

Assuming now that $F(q)$ admit a Taylor expansion so that

$$F(q) = F(0) + F'(0)\frac{q^2}{\Lambda_\chi^2} + ...\,, \tag{B.7}$$

then it is obvious that

$$\langle \phi^k(q)\beta|\,\mathcal{O}(0)\,|\alpha\rangle \approx i(F(0) + F'(0)\frac{m_\phi^2}{\Lambda_\chi^2} + ...) = iF(0) + \mathcal{O}(\frac{m_\phi^2}{\Lambda_\chi^2}) = i \lim_{q\to 0} F(q)\,. \tag{B.8}$$

If, additionally, one assumes $R^{\mu k}(q)$ does not have any singularities in 0 and performs the limit, one finally recovers Eq. (B.1).

## B.2 Application of the soft meson limit to our matrix elements

Applying it iteratively to $\mathcal{O}(0) = Q_{abcd}$ defined as:

$$Q_{abcd} \equiv \bar{s}_a \Gamma_L^\mu d_b (\bar{u}_c \Gamma_\mu^R u_d - \frac{1}{2} \bar{d}_c \Gamma_\mu^R d_d - \frac{1}{2} \bar{s}_c \Gamma_\mu^R s_d) \,, \tag{B.9}$$

where we $a$, $b$, $c$ and $d$ denote color indices and $\Gamma_\mu^{R(L)} \equiv \gamma_\mu (1 \pm \gamma_5)$, one gets:*

$$\lim_{p,q,k\to 0} \langle \phi^a(p) \phi^b(q) | Q_{abcd} | \phi^c(k) \rangle = \frac{i}{F^3} \langle 0 | \Big[ \Big[ Q_5^a, [Q_5^b, Q_{abcd}] \Big], Q_5^c \Big] | 0 \rangle \,. \tag{B.10}$$

Rewriting $\langle (\pi\pi)_{I=2} |$ and $|K^0\rangle$ in terms of the Goldstones:

$$\begin{aligned} \langle \pi\pi |_{I=2} &= \frac{\sqrt{2} i}{3} (\langle \pi_0 \pi_0 | - \langle \pi^+ \pi^- |) \\ &= \frac{\sqrt{2} i}{3} (\langle \phi_3 \phi_3 | - \frac{1}{\sqrt{2}} \langle \phi_1 \phi_1 | - \frac{1}{\sqrt{2}} \langle \phi_2 \phi_2 |) \,, \end{aligned} \tag{B.11}$$

$$|K^0\rangle = \frac{1}{\sqrt{2}} |\phi_6\rangle + i |\phi_7\rangle \,, \tag{B.12}$$

and rearranging $Q_{abcd}$ as the sum of products of $SU(3)$ octet flavor currents $J_L^{i\,\mu\,ab} J_{j\,\mu\,cd}^R$ where $J_L^{i\,\mu\,ab} = \bar{q}_a \frac{\lambda_i}{2} \Gamma_{L(R)}^\mu q_b$, so that one can use the trivial commutation relations:

$$[Q_5^i, J_{L(R)}^{j\,\mu\,ab}] = \mp i f^{ijk} J_{L(R)}^{k\,\mu\,ab} \,, \tag{B.13}$$

one gets a relation of the form:

$$\lim_{k,p,q\to 0} \langle (\pi\pi)_{I=2} | Q_{abcd} | K^0 \rangle = \frac{1}{F^3} \sum_{i,j} c_{ij} \langle 0 | \, \bar{q}_a \Gamma_\mu^L \frac{\lambda_i}{2} q_b \, \bar{q}_c \Gamma_R^\mu \frac{\lambda_j}{2} q_d | 0 \rangle \,, \tag{B.14}$$

where the exact unphysical $c_{ij}$ one obtains depend on the ordering followed when the commutation relations are applied.

*Notice one can obtain different expressions by applying the commutation relations in a different ordering. However, at the order the equality is valid ($\mathcal{O}(p^0)$) one can use that vacuum is $SU(3)_V$ invariant to trivially relate vacuum condensates (only $SU(3)_V$ singlets survive) and check that the different expressions are indeed equivalent.

## B.3 Equivalences among vacuum condensates in the chiral limit

The possible four-quark operators whose $SU(3)_V$ structure is $8(\in \bar{3}\otimes 3)\otimes 8(\in \bar{3}\otimes 3)$ can be written in two different orthonormal basis vectors connected by a unitary basis [199], the reducible $8\otimes 8$ one, which can be parametrized by the Gell-Mann matrices as in Eq. (B.14) and which more generically and symbolically would be, for a general $8\otimes 8$ operator with some fixed Dirac and color structure:

$$\vec{C} = \sum_{i=1,j=1}^{8} C_{ij}\, \frac{\lambda^i}{2}\vec{\otimes}\frac{\lambda^j}{2}\,, \tag{B.15}$$

and the decomposition in irreducible ones, whose basis $\vec{I}_i$ is made of orthonormal states of $27\oplus 10\oplus 10^*\oplus 8_1\oplus 8_2\oplus 1$. The $64\times 64$ change of basis matrix can be obtained from isoscalar form factors plus Clebsch-Gordan coefficients of Ref. [199]. Indeed the singlet part is obviously:

$$\vec{I}_S = \frac{1}{2\sqrt{2}}\sum_i \frac{\lambda^i}{2}\vec{\otimes}\frac{\lambda^i}{2}\,, \tag{B.16}$$

from which the projection of an operator $\vec{C}$ to the singlet is just:

$$C_S = \vec{C}\cdot\vec{I}_S = \frac{1}{2\sqrt{2}}\sum_i C_{ii}\,, \tag{B.17}$$

but when contracting with vacuum only the singlet survive:

$$\langle 0|\vec{C}|0\rangle = \langle 0|\sum C_i\vec{I}_i|0\rangle = \frac{\sum C_{ii}}{2\sqrt{2}}\langle 0|\vec{I}_S|0\rangle\,, \tag{B.18}$$

so that for a different operator $\vec{B}$ with the same color $a,b,c,d$ and Dirac $\Gamma_1\otimes\Gamma_2$ structure:

$$\langle 0|\vec{B}|0\rangle = \frac{\sum B_{ii}}{\sum C_{ii}}\langle 0|\vec{C}|0\rangle. \tag{B.19}$$

## B.4 Applying the equivalences to get the final matrix elements relations

Independently on the ordering, one gets in Eq. (B.14) $\sum c_{ii} = -2$, so that using Eq. (B.19) one can rewrite Eq. (B.14) as:

$$\lim_{k,p,q\to 0} \langle (\pi\pi)_{I=2} | Q_{abcd} | K^0 \rangle = -\frac{1}{F_0^3} (\bar{d}_a \Gamma_\mu^L u_b \, \bar{u}_c \Gamma_R^\mu d_d) \,. \tag{B.20}$$

Multiplying by $\delta^{ab}\delta^{cd}$ one gets:

$$\lim_{k,p,q\to 0} \langle (\pi\pi)_{I=2} | Q_7 | K^0 \rangle = -\frac{1}{F_0^3} (\bar{d}_a \Gamma_\mu^L u_a \, \bar{u}_b \Gamma_R^\mu d_b) \equiv -\frac{2}{F_0^3} \langle \mathcal{O}_1 \rangle_\mu \,. \tag{B.21}$$

Multiplying instead by $\delta^{ac}\delta^{bd} = \frac{1}{2}\lambda^i_{ab}\lambda^i_{cd} + \frac{1}{N_c}\delta_{ab}\delta_{cd}$:

$$\begin{aligned} \lim_{k,p,q\to 0} \langle (\pi\pi)_{I=2} | Q_8 | K^0 \rangle &= -\frac{1}{F_0^3} \left( \frac{1}{2} \bar{d} \lambda^i \Gamma_\mu^L u \, \bar{u} \lambda^i \Gamma_R^\mu d + \frac{1}{N_c} \bar{d} \Gamma_\mu^L u \, \bar{u} \Gamma_R^\mu d \right) \\ &\equiv -\frac{2}{F_0^3} \left( \frac{1}{2} \langle \mathcal{O}_8 \rangle_\mu + \frac{1}{N_c} \langle \mathcal{O}_1 \rangle_\mu \right) . \end{aligned} \tag{B.22}$$

# Appendix C

# The tensor form factor involved in $\tau \to \pi\pi\nu_\tau$ in R$\chi$T

The tensor form factor we want to get is given by (Eq. 5.31):

$$\langle \pi^- \pi^0 | \bar{d} \sigma^{\mu\nu} u | 0 \rangle = -i(p_-^\mu p_0^\nu - p_-^\nu p_0^\mu) F_T^{\pi\pi}(s)\,, \tag{C.1}$$

where $s \equiv p_n^2 \equiv (p_- + p_0)^2$.

In order to translate the current to the level of pions, we could use $\chi$PT. However, we know that it is not valid in the resonance region. Instead, a far better approximation of it is given (as it can be explicitly checked for the vector form factor [200]) by Resonance Chiral Theory (R$\chi$T) [95]. In this framework, one adds resonances $R$ to the $\chi$PT Lagrangian whose transformation is given under local $SU(3)_L \times SU(3)_R$ symmetry as

$$R \to h R h^\dagger\,, \tag{C.2}$$

where $h(x)$ is the compensating $V$ transformation. Then R$\chi$T assumes, supported by phenomenology, that, for a normalization scale $\mu \sim M_\rho$, the low-energy constants of $\chi$PT at $\mathcal{O}(p^4)$ are fully dominated by the contribution of those resonances when integrating them out. Since inserting spurions associated to tensor sources give no contribution to $\chi$PT at $\mathcal{O}(p^2)$ owing to the counting made in Ref [201], the leading contribution in R$\chi$T comes from the generalization of the formalism of that reference in the presence of resonances [172].

## C.1 Obtaining the long-distance version of the quark-tensor current

Fortunately, when introducing the tensor external fields in the short-distance Lagrangian [201]:

$$\mathcal{L} = \mathcal{L}^0_{QCD} + \bar{q}\sigma^{\mu\nu}\bar{t}_{\mu\nu}q + \text{other sources}\,, \tag{C.3}$$

one can only construct chiral low-energy Lagrangians involving tensor fields with the following building blocks [201]:

$$t^{\mu\nu}_{\pm} = u^\dagger t^{\mu\nu} u^\dagger \pm u t^{\dagger\mu\nu} u\,, \tag{C.4}$$

with $t^{\mu\nu} = P_L^{\mu\nu\lambda\rho}\bar{t}_{\lambda\rho}$, so that $t^{\mu\nu}_{\pm}$ transform as $t^{\mu\nu}_{\pm} \to h t^{\mu\nu}_{\pm} h^\dagger$ ($u^2 = U$).

The most general Lagrangian in the presence of vector resonances and tensor sources which can contribute to the process $\tau \to \pi\pi\nu_\tau$ at the lowest order, following the counting of Ref. [201], is then [172]:

$$\mathcal{L} = C_T \langle V_{\mu\nu} t^{\mu\nu}_+ \rangle\,, \tag{C.5}$$

where $C_T$ is a low-energy constant, in principle unknown.

Now that we have the short and long-distance Lagrangian, we can compute the current at the lowest order by making use that at that order the functional derivative of the action with respect the external tensor field must be the same in both frameworks:

$$\bar{d}\sigma_{\mu\nu}u = \frac{\delta S}{\delta \bar{t}^{\mu\nu}_{21}} = C_T V^{12}_{\mu\nu} = C_T \rho^\dagger_{\mu\nu}\,. \tag{C.6}$$

## C.2 Computing the tensor form factor

Now we have all ingredients we needed. Inserting the current in the presence of interactions (needed for the $\rho \to \pi\pi$ part), one has

$$(2\pi)^4\delta^4(q-p_n)\langle\pi^-\pi^0|\bar{d}\sigma^{\mu\nu}u|0\rangle = \int d^4x\, e^{-iqx}\langle\pi^-\pi^0|C_T\rho^{\dagger\,\mu\nu}(x)e^{i\int d^4x\,\mathcal{L}_I}|0\rangle\,. \tag{C.7}$$

The relevant part of the interaction Lagrangian for the $\rho \to \pi\pi$ decay reads:

$$\mathcal{L}_I = i\frac{G_V}{F^2}(\partial_\mu\pi^0\partial_\nu\pi^+ - \partial_\nu\pi^0\partial_\mu\pi^+)\rho^{-\,\mu\nu}\,, \tag{C.8}$$

from which

$$
\begin{aligned}
&(2\pi)^4\delta^4(q-p_n)\langle\pi^-\pi^0|\bar{d}\sigma^{\mu\nu}u|0\rangle \\
&= -\frac{C_T G_V}{F^2}\int d^4x\, d^4y \\
&\cdot e^{-iqx}\langle\pi^-\pi^0|\rho^{\dagger\,\mu\nu}(x)(\partial_\alpha\pi^0(y)\partial_\beta\pi^+(y)-\partial_\alpha\pi^+(y)\partial_\beta\pi^0(y))\rho^{-\alpha\beta}(y)|0\rangle \\
&= \frac{C_T G_V}{F^2}\int d^4x\, d^4y\, e^{i(-qx+p_n y)}(p^0_\alpha p^-_\beta - p^-_\alpha p^0_\beta) \\
&\qquad \cdot iM_\rho^{-2}\int\frac{d^4k}{(2\pi)^4}\frac{e^{-ik(x-y)}}{M_\rho^2-k^2}[g_{\mu\alpha}g_{\nu\beta}(M_\rho^2-k^2)+g_{\mu\alpha}k_\nu k_\beta - g_{\mu\beta}k_\nu k_\alpha - (\mu\leftrightarrow\nu)] \\
&= \frac{iC_T G_V}{M_\rho^2 F^2}(2\pi)^4\delta^4(q-p_n)\frac{1}{M_\rho^2-k^2}(p_{0\alpha}p_{-\beta}-p_{-\alpha}p_{o\beta}) \\
&\qquad \cdot [g_{\mu\alpha}g_{\nu\beta}(M_\rho^2-k^2)+g_{\mu\alpha}k_\nu k_\beta - g_{\mu\beta}k_\nu k_\alpha - (\mu\leftrightarrow\nu)] \\
&= (2\pi)^4\delta^4(q-p_n)\frac{iC_T G_V}{M_\rho^2 F^2}\frac{1}{M_\rho^2-q^2}2M_\rho^2(p_0^\mu p_-^\nu - p_0^\nu p_-^\mu)\,, \qquad \text{(C.9)}
\end{aligned}
$$

where in the second equality we have inserted the spin 1 propagator as defined in Ref. [95]. Then, we get:

$$F_T(s) = \frac{2C_T G_V}{F^2}\frac{1}{M_\rho^2-s} = \frac{2C_T G_V}{F^2 M_\rho^2}F_V(s) = F_T(0)F_V(s)\,. \qquad \text{(C.10)}$$

## C.3 Computation in pure $\chi$PT and comparison between LECs integrating out the $\rho$.

Even when we do not need it, because all we need is taking $F_T(0) \approx 2\sqrt{2}\,0.663\,\text{GeV}^{-1}$ from the lattice [174], we can compute $F_T(0)$ in pure $\chi$PT in terms of $\chi$PT LECs. Here the Lagrangian is directly given in Ref. [201]. One gets, for the relevant part of the process:

$$\bar{d}\sigma_{\mu\nu}u = \frac{\delta S}{\delta t_{21}^{\mu\nu\,\dagger}} + \frac{\delta S}{\delta t_{21}^{\mu\nu}} = -\frac{i\sqrt{2}\Lambda_2}{F^2}(\partial_\mu\pi^0\partial_\nu\pi^+ - \partial_\mu\pi^+\partial_\nu\pi^0) + \ldots\,, \qquad \text{(C.11)}$$

from which:

$$F_T^{\chi\text{PT}} = \frac{\sqrt{2}\Lambda_2}{F^2}\,, \qquad \text{(C.12)}$$

which is in agreement with the calculation made in Ref. [160]. Then, integrating out the $\rho$, one has:

$$C_T = \frac{M_\rho^2}{2G_V\sqrt{2}\Lambda_2}\,. \tag{C.13}$$

The lattice determination of Ref. [174] can then be re-interpreted as a determination of $\Lambda_2$,

$$\Lambda_2 = \frac{F^2}{\sqrt{2}} F_T(0) \approx 11\,\text{MeV}\,, \tag{C.14}$$

and then, of $|C_T|$:

$$|C_T| \approx 280\,. \tag{C.15}$$

# Resumen de la Tesis

## Introducción

En esta tesis hemos realizado un estudio exhaustivo de observables asociados a desintegraciones hadrónicas de taus que permiten estudios de alta precisión, no sólo en lo referido a la precisión experimental sino también en cuanto a la capacidad de la teoría para predecir los resultados de dichos experimentos.

### El Modelo Estándar de Física de Partículas

Dado el rotundo éxito del Modelo Estándar de Física de Partículas a la hora de dar una descripción muy precisa de todos los observables de altas energías estudiados hasta la fecha, dicho modelo es el mejor marco teórico posible como punto de partida para el estudio de dichas desintegraciones.

El formalismo matemático del Modelo Estándar es la Teoría Cuántica de Campos, que es el más exitoso hasta la fecha a la hora de describir una física de altas energías descrita por partículas relativistas, fermiones y bosones, que pueden dar lugar a otras cuando interaccionan localmente.

El Modelo Estándar fue formulado en un intento de acomodar en dicho formalismo, de la forma más simple posible, toda la información de los datos experimentales a las energías exploradas en la época. Se exige que el Lagrangiano del Universo, que podría considerarse como el punto de partida desde el cual uno asume que subyace todo lo demás, debe respetar cierta simetría local, $SU(3)_C \times SU(2)_L \times U(1)_Y$, y que dicha simetría queda espontáneamente rota a $SU(3)_C \times U(1)_{\mathrm{em}}$ a través de un mecanismo en el que se elige un valor particular entre aquellos que minimizan el potencial de un campo bosónico escalar. La masa del resto de partículas son consecuencia de la interacción de las mismas con dicho campo escalar. Las partículas del Modelo Estándar son:

- Bosones Gauge. En el formalismo de Teoría Cuántica de Campos necesariamente aparecen como consecuencia de imponer invariancia bajo las

distintas simetrías locales. Así, los gluones son los bosones asociados a las interacciones fuertes ($SU(3)_C$) y los fotones y bosones $W^-$ y $Z$ a las electrodébiles ($SU(2)_L \times U(1)_Y$).

- Leptones. Son los bloques de materia fermiónica que no interaccionan (localmente) a través de interacciones fuertes. Se trata de los electrones y neutrinos electrónicos más dos copias idénticas más pesadas, muones y taus junto con sus correspondientes neutrinos.

- Quarks. Son los bloques de materia fermiónica que sí interaccionan localmente a través de interacciones fuertes. Como consecuencia, la dinámica subyacente resulta ser mucho más compleja. A bajas energías, como aquellas en las que nos movemos en nuestro día a día, no pueden viajar libremente (confinamiento de color), sino que forman partículas más complejas. De nuevo, los podemos agrupar en tres parejas, conocidas como familias. En el Modelo Estándar, dichas familias van a poder interaccionar entre ellas a través de la matriz de Cabibbo-Kobayashi-Maskawa (CKM).

- Bosones Escalares. Se trata de otro de los tipos de partículas permitidos por Teoría Cuántica de Campos. Sólo interaccionan a través de interacciones electrodébiles. Empleando una determinada transformación local de la simetría asociada tras la rotura espontánea de la simetría, sólo una nueva partícula física sobrevive: el bosón de Higgs.

Además, cada partícula tiene asociada una antipartícula, idéntica pero con cargas opuestas. El Lagrangiano del Modelo Estándar no es más que el más genérico (renormalizable) posible dados esos bloques de materia y dichas simetrías. Una vez fijados con datos experimentales los parámetros libres de la teoría, que son las masas de las partículas, los elementos de la matriz CKM y los acoplamientos fuerte ($\alpha_s$) y electrodébil ($e$), su éxito ha ido más allá de predecir correctamente medidas experimentales cada vez más precisas a las energías en el que éste fue formulado. Todas las medidas realizadas hasta la fecha a energías notablemente mayores, llegando hasta el LHC, están también en buen acuerdo con sus predicciones teóricas, que incluían la aparición de nuevas partículas, como el bosón de Higgs, que aún no habían sido descubiertas.

## Motivación

El éxito sin precedentes del Modelo Estándar a la hora de describir las medidas experimentales del LHC no deja de ser sorprendente. Hasta ahora cada vez que

se habían explorado nuevas escalas, se había descubierto nueva física que no quedaba completamente descrita por los modelos previos. De hecho, dicha nueva física había arrojado luz sobre las diferentes incógnitas abiertas por las teorías previas.

El Modelo Estándar podría dar una descripción precisa de la naturaleza, salvo por la materia oscura, hasta escalas cercanas a la longitud de Planck, donde se conoce que la gravedad, no descrita por el mismo, es relevante. Sin embargo, desde un punto de vista puramente teórico no tenemos ninguna razón fundamental para pensar que exactamente las simetrías y los bloques de materia que gobiernan las escalas a las que el Modelo Estándar fue construido, describan todas las escalas mayores. Precisamente ese hecho motiva seguir buscando nueva física que nos permita seguir entendiendo, asumiendo que no es fruto del azar, por qué los bloques de materia siguen esos patrones con esas simetrías.

Para tratar de vislumbrar dicha nueva física, uno puede tomar varios caminos. Uno de ellos consiste en mejorar la precisión experimental y las predicciones teóricas del Modelo Estándar para una serie de observables que dependan de los mismos parámetros teóricos desconocidos. En el caso en el que se encontrara que los valores experimentales que se obtienen para dichos parámetros teóricos en distintos experimentos son incompatibles, habría que concluir que el Modelo Estándar no es capaz de ofrecer una descripción correcta de dichos procesos, lo que nos forzaría a introducir nueva física. Las extracciones de parámetros realizadas en los capítulos 2, 3 y 4 pueden utilizarse para dichas comparativas.

Por otro lado, uno puede buscar nueva física utilizando modelos concretos. En su lugar, en el capítulo 5 realizamos un análisis en el marco del Modelo Estándar como Teoría de Campos Efectiva, que agrupa muchos de ellos.

Independientemente de la estructura de nueva física a muy altas energías, el Modelo Estándar no es un simple algoritmo en el que uno introduce valores numéricos para los distintos parámetros teóricos desconocidos y recibe una predicción teórica exacta para el observable que uno desee. En ese sentido, el Modelo Estándar actúa como un marco teórico desde el que se pueden desarrollar diferentes herramientas para entender la física de un proceso. La fenomenología del Modelo Estándar no es más que el desarrollo y la aplicación de dichas herramientas para entender la compleja dinámica que emerge de dicho modelo a las distintas energías.

En este trabajo nos hemos centrado en la desintegración hadrónica del tau. El tau es el único leptón lo suficientemente pesado como para desintegrarse en hadrones, que son las partículas que forman los quarks cuando confinan. El tau se desintegra emitiendo un neutrino tauónico y un bosón $W$ "off shell" que rápi-

damente decae a quarks que hadronizan. Las energías son lo suficientemente bajas como para que dicha desintegración quede precisamente descrita por una interacción local efectiva entre una corriente débil leptónica y una de quarks, conocida como Teoría de Fermi. Esto permite un estudio exhaustivo tanto de las interacciones electrodébiles responsables de dicha desintegración como de las fuertes, responsables de la producción de un contínuo hadrónico* a través de la corriente de quarks, en un régimen de energía no perturbativo en el que realizar predicciones precisas resulta ser un desafío. En esta tesis hemos estudiado algunos de los observables cuya predicción teórica es más precisa con las técnicas disponibles en la actualidad, junto con las consecuencias fenomenológicas de la comparación de las mismas con los datos experimentales.

## Metodología

La naturaleza electrodébil de la desintegración del tau a hadrones permite un cálculo perturbativo de la distribución diferencial de dicha desintegración, salvo por elementos de matrices hadrónicos producidos a través de la corriente de quarks. A bajas energías, dichos elementos pueden ser rigurosamente calculados en la teoría efectiva que da una descripción precisa de las interacciones fuertes a bajas energías, la Teoría Quiral de Perturbaciones.

La Teoría Quiral de Perturbaciones es una expansión en potencias de momentos, masas de mesones, los hadrones más ligeros, y otras fuentes externas (como los fotones o los bosones $W$ y $Z$) que explota la simetría (aproximada) de sabor $(SU(3)_L \times SU(3)_R)$ formada por los tres quarks ligeros ($u$, $d$ y $s$). Dicha simetría aproximada se rompe espontáneamente a $SU(3)_V$ a través del condensado de quarks, cuya existencia es consecuencia de un vacío a bajas energías que ya no puede entenderse como un vacío sin quarks ni gluones. La rotura espontánea de la simetría aproximada da lugar a 8 mesones ligeros (su masa distinta de cero es el resultado de la rotura explícita de simetría debida a que las masas de los quarks no son exactamente 0, haciendo que la simetría sea sólo aproximada), que son las únicas partículas que interaccionan directamente a través de interacciones fuertes a bajas energías.

Ésto permite dar una descripción precisa, por ejemplo, de la desintegración del tau al pion, el más ligero de los mesones. Sin embargo, dicha teoría funciona peor y acaba dejando de ser válida cuando nos vamos a energías mayores o cuando exigimos una precisión demasiado alta. En dichos casos podemos utilizar alguna

*El neutrino puede llevarse una fracción arbitraria de la energía inicial del tau, de modo que la restante irá al estado hadrónico final.

extensión de la misma con algunas asunciones extra, como puede ser la Teoría Quiral de Resonancias. Sin embargo, dicha teoría está lejos de dar una descripción teórica a la precisión experimental actual basada en primeros principios y libre de ambigüedades.

Probablemente los métodos con mayor capacidad predictiva desarrollados hasta la fecha en el sector son los métodos dispersivos, que utilizan propiedades conocidas de objetos matemáticos de la teoría para establecer relaciones entre diversas cantidades. Con ellos, uno puede dar una descripción muy precisa de observables inclusivos, es decir, de sumas sobre distintos canales de desintegración hadrónicos. El punto de partida consiste en la relación directa existente entre la probabilidad de desintegración a determinadas sumas de hadrones a una energía dada con las partes imaginarias de funciones de correlación entre corrientes de quarks.

Dichas funciones de correlación pueden calcularse a energías lo suficientemente altas en términos de quarks y gluones a través de la Expansión en Producto de Operadores. En dicha expansión, uno separa las contribuciones a distancias cortas, calculables mediante métodos puramente perturbativos y contribuciones de largas distancias, que quedan en función de condensados de operadores de quarks y gluones en el vacío. Un sencillo análisis dimensional nos enseña que aquellos condensados de dimensión más baja van a dominar la contribución teórica de los observables. Mientras sean distintos de 0 y la expansión esté bien definida, la contribución puramente perturbativa (asociada al operador identidad) será la dominante.

Sin embargo, dicha expansión está definida en el eje Euclídeo para energías altas y su extensión analítica no funciona en el eje Minkowskiano, especialmente a las energías relevantes en el espectro hadrónico. No obstante, utilizando la conocida estructura analítica de dichas funciones de correlación, uno puede obtener relaciones dispersivas entre las integrales experimentales sobre dicho espectro e integrales a lo largo de la circunferencia compleja, donde las energías son lo suficientemente altas como para que la expansión en términos de quarks y hadrones funcione, salvo por pequeñas correcciones conocidas como violaciones de dualidad quark-hadrón. Dichas violaciones serán menores a mayores energías, para los canales más inclusivos y para aquellos observables que minimicen las contribuciones de las integrales cercanas al eje Minkowskiano. Las integrales experimentales han sido calculadas utilizando los datos obtenidos por la colaboración ALEPH, asociada a un detector del colisionador LEP con el mismo nombre. Afortunadamente, dicha colaboración ha hecho públicas las distribuciones de masa in-

variante, junto con las matrices de correlación, para las diferentes distribuciones inclusivas utilizadas en esta tesis.

## Relaciones de dispersión quirales

En el primer estudio fenomenológico de esta tesis, hemos realizado un estudio actualizado de las relaciones de dispersión asociadas a los correladores (1+0) no extraños vectorial menos axial. Dado que la contribución perturbativa cancela a todos los órdenes en teoría de perturbaciones en el límite quiral (masas de quarks nulas) y que las correcciones de masa son despreciables, la primera contribución de su Expansión en Producto de Operadores es la de dimensión 6. Este hecho permite obtener rigurosamente las relaciones conocidas como reglas de suma de Weinberg. Incluso cuando a nivel de quarks uno no puede describir el espectro experimental de resonancias, sabemos el valor de dos integrales con diferentes pesos de dicho espectro, salvo por correcciones logarítmicas muy pequeñas y por violaciones de dualidad.

Introduciendo relaciones de dispersión con integrales pesadas por funciones con singularidades en el origen, uno puede obtener información sobre el correlador y sus derivadas a energía 0. Por otro lado, introduciendo en las integrales pesos más sensibles a la parte de alta energía del espectro, se accede a los condensados dimensionales del correlador estudiado. Sin embargo, las violaciones de dualidad quark-hadrón son especialmente importantes en estas últimas relaciones y las incertidumbres asociadas a las mismas han de ser tenidas en cuenta. Ésto puede comprobarse observando que la dependendencia en el límite superior de la integral involucrando datos experimentales no es la predicha por la Expansión en Producto de Operadores al nivel de precisión necesario para obtener los condensados.

Aunando el potencial de las relaciones dispersivas conocidas con todo lo que sabemos sobre violaciones de dualidad, se realiza un análisis minucioso a la hora de minimizar y estimar su rol. Para ello, nos apoyamos en una parametrización que incorpora alguno de los aspectos conocidos de dichas violaciones, teniendo en cuenta que no es esperable que dicha parametrización ofrezca una descripción exacta de las mismas. Se ha obtenido

$$L_{10}^{\rm eff} = (-6.48 \pm 0.05) \cdot 10^{-3}\,, \tag{C.16}$$

$$C_{87}^{\rm eff} = (8.40 \pm 0.18) \cdot 10^{-3}\ {\rm GeV}^{-2}\,, \tag{C.17}$$

$$\mathcal{O}_6 = (-3.6\,^{+\,1.0}_{-\,0.9}) \cdot 10^{-3}\ {\rm GeV}^{6}\,, \tag{C.18}$$

$$\mathcal{O}_8 = (-1.0 \pm 0.5) \cdot 10^{-2}\ {\rm GeV}^{8}\,, \tag{C.19}$$

donde $L_{10}^{\rm eff}$ y $C_{87}^{\rm eff}$ están trivialmente relacionados con el correlador y su derivada en el origen. Su definición está relacionada con los acoplamientos que describen dicho correlador en Teoría Quiral de Perturbaciones. En efecto, nos encontramos en la región de validez de dicha teoría y, por tanto, hemos podido combinar los cálculos existentes con el resultado anterior para obtener un valor válido hasta $\mathcal{O}(p^6)$ de dichos acoplamientos:

$$L_{10}^r(M_\rho) = -(4.1 \pm 0.4) \cdot 10^{-3}\,, \tag{C.20}$$
$$C_{87}^r(M_\rho) = (5.10 \pm 0.22) \cdot 10^{-3}\,\text{GeV}^{-2}\,. \tag{C.21}$$

Encontramos que dichos resultados están en buen acuerdo con otras determinaciones.

## Determinación de la constante de acoplamiento fuerte

Uno de los parámetros libres del Modelo Estándar de Física de Partículas es la constante de acoplamiento fuerte. Es bien sabido que el valor de dicho acoplamiento depende de la energía tratada. Afortunadamente, dicha dependencia puede calcularse en teoría de perturbaciones y, por tanto, una vez conocida a una energía puede conocerse a todas (al menos mientras teoría de perturbaciones sea válida). Mientras que a bajas energías dicho acoplamiento diverge, de modo que la región de confinamiento de color aparece más allá de la Cromodinámica Cuántica (teoría de interacciones fuertes) perturbativa, a muy altas energías se da el fenómeno de libertad asintótica, de modo que a infinita energía los quarks pueden viajar como estados libres.

En este estudio, abordamos la determinación dispersiva de la constante de acoplamiento fuerte a través de desintegraciones hadrónicas de taus, que permite la determinación de dicha constante a la escala energética de dicha partícula. En este caso, uno trabaja con el correlador $V + A$. La contribución puramente perturbativa, la cual domina la predicción teórica de la Expansión en Producto de Operadores, es conocida a 4 loops. La alta sensibilidad de la misma a una constante de acoplamiento fuerte cuyo valor se acerca al límite de validez de teoría de perturbaciones, permite una determinación muy precisa, que puede compararse a otras determinaciones a otras escalas, ofreciendo una comprobación experimental de la dependencia en energía predicha por el Modelo Estándar.

Al nivel de precisión actual, se hace necesario un estudio exhaustivo de la contribución no perturbativa, el cual es posible gracias a las distribuciones invariantes de masas obtenidas por la colaboración ALEPH. En este trabajo se

ha realizado un análisis crítico de las diferentes determinaciones que se pueden encontrar en la literatura, explorando sus posibles debilidades, realizando tests para comprobar su solidez e implementando nuevos procedimientos para intentar reducir dichas debilidades. Diferentes procedimientos y comprobaciones han dado lugar a valores en total acuerdo para la constante de acoplamiento fuerte. Los diversos observables estudiados se han encontrado compatibles con una dualidad quark-hadrón que para los canales más inclusivos funcionan en muy buena aproximación desde energías menores que la asociada a la masa del tau y con un contaje no divergente en los primeros términos de la Expansión en Producto de Operadores. El valor final obtenido es:

$$\alpha_s(m_\tau^2) = 0.328 \pm 0.013\,, \tag{C.22}$$

que se traduce, a la escala de la masa del $Z$, típicamente utilizada para comparar con otras determinaciones, en:

$$\alpha_s(M_z) = 0.1197 \pm 0.015\,. \tag{C.23}$$

Dicha determinación está en total acuerdo con el valor obtenido en el ajuste global del PDG.

## Relaciones entre elementos de matriz en el límite quiral

En el límite quiral, pueden obtenerse dos relaciones entre elementos de matriz asociados a la desintegración de kaones a dos piones a través de los llamados pingüinos electrodébiles, uno de los posibles modos de desintegración de dicho proceso, y los condensados de cuatro quarks que aparecen en la Expansión en Producto de Operadores del correlador $V - A$.

En esta tesis se ha utilizado la actualización de las funciones espectrales de ALEPH anteriormente mencionadas para realizar un estudio preliminar de las consecuencias fenomenológicas de dichas relaciones. En primer lugar, se puede obtener, empleando datos experimentales de desintegraciones hadrónicas, uno de los elementos de matriz más relevantes a la hora de estudiar violación de CP ($\frac{\epsilon'}{\epsilon}$) en desintegraciones no leptónicas de kaones:

$$\langle(\pi\pi)_{I=2}|\mathcal{Q}_8|K^0\rangle_{2\,\mathrm{GeV}} = (1.14 \pm 0.49)\ \mathrm{GeV}^3\,. \tag{C.24}$$

Ciertas aproximaciones en los pasos intermedios, como la extrapolación de las relaciones más allá del límite quiral, limitan la precisión de dicha predicción.

Dado que hoy en día, mediante simulaciones en redes discretizadas, se pueden obtener valores precisos para los elementos de matriz kaónicos, hemos explorado la posibilidad de tomar el camino inverso. Utilizando dichas relaciones, tenemos acceso a la contribución dominante (dimensión 6) de la Expansión en Producto de Operadores del correlador $V - A$. Definiendo relaciones de dispersión que explotan el conocimiento del correlador a cortas distancias salvo por correcciones de dimensión 8, uno puede obtener valores precisos de otras constantes que aparecen en dichas relaciones de dispersión, como la constante de desintegración del pion:

$$\sqrt{2} f_\pi = (131.6 \pm 1.0)\,\text{MeV}\,, \tag{C.25}$$

donde comprobamos que las relaciones de dispersión son capaces de dar predicciones muy precisas para observables cuyas contribuciones están dominadas por las resonancias $\rho$ y $a_1$, de modo que no pueden ser descritos ni por teoría de perturbaciones a nivel de quarks ni por Teoría Quiral de Perturbaciones. Adicionalmente, hemos obtenido para el condensado de dimensión 8,

$$a_4 = -(0.7 \pm 0.6)\,\cdot 10^{-2}\,\text{GeV}^8\,. \tag{C.26}$$

## Nueva física en desintegraciones hadrónicas de taus

Dada la alta precisión que es capaz de ofrecer el sector de desintegraciones hadrónicas de taus, resulta natural preguntarse si las determinaciones anteriores pueden verse afectadas por nueva física o incluso si pueden dar pistas sobre hacia dónde no buscarla, dado el buen acuerdo con el resto de determinaciones.

Si, como se espera, la escala de nueva física se encuentra a escalas mucho mayores que la masa del Higgs, la sensibilidad de los observables a una determinada escala está suprimida por dos potencias de dicha escala. Sin embargo, la alta precisión alcanzada en los datos experimentales y en la descripción teórica de los mismos, unida a la supresión del proceso en el Modelo Estándar, que sólo ocurre a través de la interacción de corrientes electrodébiles, hacen de las desintegraciones hadrónicas de taus una interesante ventana a posible nueva física.

Empleando la extensión del Lagrangiano efectivo más general posible de dimensión 6 que da cuenta de la desintegración del tau a hadrones, se pueden estudiar observables tanto exclusivos como inclusivos en función de nuevos acoplamientos, de forma independiente de modelo. Se ha realizado un estudio exhaustivo, que se encuentra en estado preliminar, del potencial de los mismos.

En el caso exclusivo, la principal limitación existente en la mayoría de canales es la incertidumbre teórica debida a los elementos de matriz hadrónicos. Para las

desintegraciones a un mesón, dependientes de un único parámetro que puede obtenerse de simulaciones en redes discretizadas y, tras tener en cuenta correcciones radiativas, se obtienen, como es bien conocido, fuertes restricciones a nueva física. También se han encontrado fuertes restricciones para desintegraciones a dos hadrones. El canal $\tau \to \eta\pi\nu_\tau$ está suprimido en el Modelo Estándar, lo cual permite obtener una restricción a nueva física interesante. Hemos utilizado los valores obtenidos en un análisis reciente. Para el canal $\tau \to \pi\pi\nu_\tau$, hemos empleado como factor de forma vectorial de referencia (insensible a correcciones de nueva física) el obtenido en el proceso $e^+e^- \to \pi\pi$ que, salvo por pequeñas correcciones de isospín, es idéntico al obtenible de $\tau \to \pi\pi\nu_\tau$. Esta comparativa da como resultado una fuerte restricción a nueva física.

Para los canales inclusivos se han empleado dos integrales en el caso del canal $V + A$ y otras dos en el $V - A$, asignando de forma conservadora incertidumbres para los efectos no perturbativos. Aunque las violaciones de dualidad son notablemente menores en el canal $V + A$, el mejor conocimiento de la Expansión en Producto de Operadores en el $V - A$ hace que ambos canales tengan una sensibilidad a nueva física similar. De hecho, La restricción inclusiva más fuerte proviene del mismo momento que nos permitió obtener un valor de la constante de desintegración del pion. En este caso, tomamos el valor de dicha constante, al igual que el elemento de matriz de kaon a dos piones, de simulaciones en redes discretizadas.

Combinando las diferentes restricciones, hemos obtenido de forma preliminar para los diferentes acoplamientos que parametrizan la física más allá del modelo estándar:

$$\begin{pmatrix} \epsilon_L^\tau - \epsilon_L^e + \epsilon_R^\tau - \epsilon_R^e \\ \epsilon_R^\tau \\ \epsilon_S^\tau \\ \epsilon_P^\tau \\ \epsilon_T^\tau \end{pmatrix} = \begin{pmatrix} 1.0 \pm 1.5 \\ 0.2 \pm 1.6 \\ -0.6 \pm 1.5 \\ 0.6 \pm 1.4 \\ -0.06 \pm 0.75 \end{pmatrix} \times 10^{-2} \ . \tag{C.27}$$

Se ha comparado en el marco del Modelo Estándar como Teoría de Campos Efectiva con otras restricciones provenientes de otros observables electrodébiles de precisión y con observables en el LHC y se ha comprobado que en dicho marco general, estas restricciones son competitivas y complementarias a las demás.

## Conclusiones

Los desintegraciones hadrónicas de taus constituyen una ventana para el estudio de interacciones electrodébiles y fuertes. En esta tesis se ha realizado un análisis fenomenológico de algunas de las aplicaciones de dichas desintegraciones con mayor capacidad predictiva.

Los métodos dispersivos asociados a observables inclusivos proveen a día de hoy algunas de las herramientas más potentes a la hora de obtener predicciones teóricas y juegan un papel central en el desarrollo de ésta tesis. En primer lugar, se han aplicado para realizar un cuidadoso análisis de la física no perturbativa que gobierna la física del correlador quiral. Gracias a ello, se han obtenido, entre otros resultados, dos constantes de bajas energías de Teoría Quiral de Perturbaciones:

$$L_{10}^r(M_\rho) = -(4.1 \pm 0.4) \cdot 10^{-3}\,, \tag{C.28}$$
$$C_{87}^r(M_\rho) = (5.10 \pm 0.22) \cdot 10^{-3}\,\mathrm{GeV}^{-2}\,. \tag{C.29}$$

El estudio de la constante de acoplamiento fuerte a partir de los datos inclusivos no extraños ha sido la siguiente aplicación de los métodos dispersivos. Tras un cuidadoso análisis de las incertidumbres no perturbativas, uno obtiene

$$\alpha_s(m_\tau^2) = 0.328 \pm 0.013\,. \tag{C.30}$$

Explotando relaciones en el límite quiral entre elementos de matrices de kaon a dos piones y condensados de cuatro quarks que aparecen en el correlador quiral, se pueden obtener medidas de los primeros utilizando datos de desintegraciones de taus. Alternativamente, se puede mejorar la determinación de otros parámetros obtenibles con taus empleando resultados de simulaciones en redes discretizadas para los valores de los elementos de matrices de kaon a dos piones para mejorar nuestro conocimiento sobre dicho correlador. Ambos procedimientos han sido estudiados y se ha obtenido una determinación puramente inclusiva de la constante de desintegración del pion con una precisión mayor que un 1%.

Por último, se ha realizado un análisis sobre la sensibilidad de las desintegraciones hadrónicas de taus a diferentes observables tanto exclusivos como inclusivos, en el marco del Modelo Estándar como Teoría Efectiva, el cual extiende el modelo estándar bajo ciertas asunciones de una manera independiente del modelo. Se han obtenido una serie de restricciones a nueva física complementarias con restricciones provenientes de observables de bajas energías y de observables provenientes del LHC.

Sin lugar a dudas, una mejora de los datos experimentales utilizados, que podría venir de colaboraciones experimentales como Belle-2, supondría una mejora en la determinación de los diferentes parámetros. Dado que estamos cerca del límite de aplicabilidad de dichas relaciones dispersivas, cuantificar esa mejora de forma creíble no es trivial. Las incertidumbres sistemáticas, dominantes en muchos de los observables estudiados, podrían disminuir si se confirmara que en la zona cercana a la masa del tau, que actualmente presenta grandes incertidumbres experimentales, hay una disminución quantitativa de las violaciones de quark-hadrón. Por supuesto, mejoras de éstos métodos dispersivos desde un punto de vista teórico, serían también bienvenidas.

Dada la lenta convergencia de las series perturbativas a la masa del tau, donde nos acercamos al límite de aplicabilidad de teoría de perturbaciones, un cálculo de los siguientes órdenes desconocidos en teoría de perturbaciones, así como el desarrollo de métodos de resumación de las series perturbativas libres de ambigüedades, podrían suponer una mejora en la determinación de la constante fuerte basada en desintegraciones de taus.

Mientras tanto, pequeñas mejoras en algunos de los estudios fenomenológicos pueden ser estudiadas. Por ejemplo, en el estudio de nueva física, se puede plantear para un futuro un estudio más exhaustivo de algunos de los canales exclusivos, como el canal a dos piones (en el que posiblemente una comparativa directa de las distribuciones energéticas dé lugar a mejores restricciones), las restricciones provenientes del espectro extraño e incluso posibles aplicaciones a modelos específicos de nueva física.

# Acknowledgements

Me resulta difícil dar las gracias en unas líneas a todas las personas que han hecho posible esta tesis. No me gusta dar nombres porque seguro que me dejo gente fuera. Sin embargo, sería injusto quedarme en un agradecimiento genérico.

En primer lugar, me gustaría dar las gracias a mis padres, Ángeles y Antonio. Si he llegado hasta aquí es en una buena parte por ellos. Además de estar siempre ahí para apoyarme cuando hace falta, sin su interés a la hora de crearme curiosidad sobre lo que me rodea, tal vez hubiera seguido otro camino.

Por supuesto, también tengo que dar las gracias a Jesús. Hasta cierto punto, el que acabara estudiando física debió estar influido por mi curiosidad sobre qué narices estudiaba mi hermano cuando yo aún era un niño. Gracias también por su ayuda para que pudiera acabar esta tesis. Sin aquellas carreritas por Madrid con el pasaporte, mi estancia en Los Alamos no hubiera sido posible.

Tengo que hacer un agradecimiento especial a Toni. Si no hubiera apostado por darme garantías de financiación en un momento en el que la economía estaba pasando por un momento delicado, muy probablemente no habría podido realizar la tesis en Valencia. Gracias también por su orientación durante todo el doctorado y por su paciencia a la hora de explicarme conceptos clave para la realización de mi tesis y por darme tiempo y espacio para entenderlos. Por último, quiero darle las gracias por la rápida revisión de esta tesis.

Tampoco puedo dejar de darle las gracias a Martín. Su papel en esta tesis es fundamental, tanto en el primer trabajo como a la hora de liderar el proyecto de nueva física llevado a cabo en mi estancia en los Alamos. Sin su empeño, no habría salido adelante. Gracias también por la agradable estancia en el CERN y, claro, por la cuidadosa revisión de mi tesis.

I would like to thank Vincenzo for accepting me for the research stay in Los Alamos and for his hospitality and guidance during it, which allowed for a, in my humble opinion, fruitful collaboration. Also, thanks to Adam for being part of it and to the Seets and Sean for making my stay enjoyable.

También tengo que darle las gracias a Pablo y Laura por aguantarme un millón de horas tanto en el piso como en el IFIC. Estoy seguro de que no hubiera disfrutado tanto mi doctorado sin ellos. También tengo que dar las gracias al resto de la gente del IFIC con la que he pasado tiempo en el día a día, como Javi y Marija en los primeros años y un buen grupo de doctorandos en los últimos. Les deseo que les vaya bien en el resto de su doctorado. Entre ellos tengo que dar las gracias en particular a Héctor por ayudar siempre que ha hecho falta y por colaborar en algún proyecto del que seguro que acaba saliendo algo. Gracias también al resto de gente del grupo y del despacho, de los que merece la pena mencionar a Alberto y Miguel, el primero por estar ahí desde que llegué y el segundo por estar también en el máster y echarme un cable con los papeles del depósito.

Hay mucha gente que ha puesto su granito de arena para que llegue a hacer la tesis. Por supuesto, doy las gracias al resto de mi familia por estar siempre ahí si hace falta. Lo mismo puedo decir de mis amigos de Morón, Ivan, Juandi, Paco y Cristian. Esa sensación de volver al pueblo y echar un buen rato sin importar el tiempo que haya pasado es muy agradable.

Tengo que agradecer también a los compañeros de piso que he tenido a lo largo de los años, por hacer de la experiencia de compartir piso, desagradable para algunos, una bonita experiencia desde la que seguir adelante. Gracias otra vez a Iván, Juandi, Pablo y Laura y también a Okan, Juma, Nico, Jose. Al primero y al último, además de al resto de habituales, les doy también las gracias por esas noches de videojuegos, también repetidas a lo largo del doctorado, siempre útiles para desconectar un poco.

De mis años estudiando en Sevilla, doy las gracias a todos los que hicieron posible que fuera una buena experiencia. En particular, tengo que destacar a los compañeros de clase que me acompañaron durante los 5 años, de los que guardo muy buenos recuerdos, Esaú, Inma, Jose, Luis, y también Carmen, a la que adoptamos un poco más tarde. También a los profesores que me permitieron una buena formación y a aquellos que despertaron mi curiosidad por el mundo de las partículas. Sin ellos, el salto a Valencia nunca hubiera sido posible.

Del año de máster, tengo que agradecer a mis compañeros por hacer de ese año una nueva experiencia agradable y a los diferentes profesores por hacer del máster un año de formación de alta calidad. Sin muchos de los conceptos aprendidos en el mismo, mi tesis no hubiera sido posible. También tengo que dar las gracias a Pedro por dirigirme el trabajo de fin de máster en un tiempo récord.

Gracias a todos.

# Bibliography


[1] S. L. Glashow. Partial Symmetries of Weak Interactions. *Nucl. Phys.*, 22:579–588, 1961.

[2] Steven Weinberg. A Model of Leptons. *Phys. Rev. Lett.*, 19:1264–1266, 1967.

[3] Abdus Salam. Weak and Electromagnetic Interactions. *Conf. Proc.*, C680519:367–377, 1968.

[4] S. L. Glashow, J. Iliopoulos, and L. Maiani. Weak Interactions with Lepton-Hadron Symmetry. *Phys. Rev.*, D2:1285–1292, 1970.

[5] Antonio Pich. Aspects of quantum chromodynamics. In *Proceedings, Summer School in Particle Physics: Trieste, Italy, June 21-July 9, 1999*, pages 53–102, 1999.

[6] Antonio Pich. The Standard Model of Electroweak Interactions. In *Proceedings, High-energy Physics. Proceedings, 18th European School (ESHEP 2010): Raseborg, Finland, June 20 - July 3, 2010*, pages 1–50, 2012. [,1(2012)].

[7] Antonio Pich. Precision Tau Physics. *Prog. Part. Nucl. Phys.*, 75:41–85, 2014.

[8] Eduardo de Rafael. An Introduction to sum rules in QCD: Course. In *Probing the standard model of particle interactions. Proceedings, Summer School in Theoretical Physics, NATO Advanced Study Institute, 68th session, Les Houches, France, July 28-September 5, 1997. Pt. 1, 2*, pages 1171–1218, 1997.

[9] Martin Gonzalez-Alonso. *Low-energy tests of the Standard Model*. PhD thesis, Valencia U., IFIC, 2010.

[10] Steven Weinberg. *The quantum theory of fields. Vol. 2: Modern applications*. Cambridge University Press, 2013.

[11] Kenneth G. Wilson. Nonlagrangian models of current algebra. *Phys. Rev.*, 179:1499–1512, 1969.

[12] Wolfhart Zimmermann. Normal products and the short distance expansion in the perturbation theory of renormalizable interactions. *Annals Phys.*, 77:570–601, 1973. [Lect. Notes Phys.558,278(2000)].

[13] David B. Kaplan. Effective field theories. In *Beyond the standard model 5. Proceedings, 5th Conference, Balholm, Norway, April 29-May 4, 1997*, 1995.

[14] Antonio Pich. Effective field theory: Course. In *Probing the standard model of particle interactions. Proceedings, Summer School in Theoretical Physics, NATO Advanced Study Institute, 68th session, Les Houches, France, July 28-September 5, 1997. Pt. 1, 2*, pages 949–1049, 1998.

[15] U. Mosel. *Path integrals in field theory: An introduction*. 2004.

[16] Andrzej J. Buras. Weak Hamiltonian, CP violation and rare decays. In *Probing the standard model of particle interactions. Proceedings, Summer School in Theoretical Physics, NATO Advanced Study Institute, 68th session, Les Houches, France, July 28-September 5, 1997. Pt. 1, 2*, pages 281–539, 1998.

[17] Francisco J. Yndurain. *The Theory of Quark and Gluon Interactions*. Theoretical and Mathematical Physics. Springer, Berlin, Germany, 2006.

[18] P. Pascual and R. Tarrach. QCD: Renormalization for the practitioner. *Lect. Notes Phys.*, 194:1–277, 1984.

[19] Mikhail A. Shifman, A. I. Vainshtein, and Valentin I. Zakharov. QCD and Resonance Physics. Theoretical Foundations. *Nucl. Phys.*, B147:385–447, 1979.

[20] Aneesh V. Manohar. Effective field theories. In *Quarks and colliders. Proceedings, 10th Winter Institute, Lake Louise, Canada, February 19-25, 1995*, pages 274–315, 1995.

[21] Aneesh V. Manohar. Introduction to Effective Field Theories. In *Les Houches summer school: EFT in Particle Physics and Cosmology Les Houches, Chamonix Valley, France, July 3-28, 2017*, 2018.

[22] Curtis G. Callan, Jr., Sidney R. Coleman, J. Wess, and Bruno Zumino. Structure of phenomenological Lagrangians. 2. *Phys. Rev.*, 177:2247–2250, 1969.

[23] A. Pich. Chiral perturbation theory. *Rept. Prog. Phys.*, 58:563–610, 1995.

[24] Antonio Pich. Effective Field Theory with Nambu-Goldstone Modes. In *Les Houches summer school: EFT in Particle Physics and Cosmology Les Houches, Chamonix Valley, France, July 3-28, 2017*, 2018.

[25] J. Gasser and H. Leutwyler. Chiral Perturbation Theory: Expansions in the Mass of the Strange Quark. *Nucl. Phys.*, B250:465–516, 1985.

[26] Johan Bijnens, Gilberto Colangelo, and Gerhard Ecker. The Mesonic chiral Lagrangian of order $p^6$. *JHEP*, 02:020, 1999.

[27] Antonio Pich and Joaquim Prades. Perturbative quark mass corrections to the tau hadronic width. *JHEP*, 06:013, 1998.

[28] John F. Donoghue and Eugene Golowich. Chiral sum rules and their phenomenology. *Phys. Rev.*, D49:1513–1525, 1994.

[29] M. Davier, L. Girlanda, Andreas Hocker, and J. Stern. Finite energy chiral sum rules and tau spectral functions. *Phys. Rev.*, D58:096014, 1998.

[30] S. Peris, B. Phily, and E. de Rafael. Tests of large $N_c$ QCD from hadronic tau decay. *Phys. Rev. Lett.*, 86:14–17, 2001.

[31] Johan Bijnens, Elvira Gamiz, and Joaquim Prades. Matching the electroweak penguins $Q_7$, $Q_8$ and spectral correlators. *JHEP*, 10:009, 2001.

[32] Vincenzo Cirigliano, Eugene Golowich, and Kim Maltman. QCD condensates for the light quark V-A correlator. *Phys. Rev.*, D68:054013, 2003.

[33] C. A. Dominguez and K. Schilcher. Finite energy chiral sum rules in QCD. *Phys. Lett.*, B581:193–198, 2004.

[34] Stephan Narison. V-A hadronic tau decays: A Laboratory for the QCD vacuum. *Phys. Lett.*, B624:223–232, 2005.

[35] Jose Bordes, Cesareo A. Dominguez, Jose Penarrocha, and Karl Schilcher. Chiral condensates from tau decay: A Critical reappraisal. *JHEP*, 02:037, 2006.

[36] A. A. Almasy, K. Schilcher, and H. Spiesberger. QCD condensates of dimension D=6 and D=8 from hadronic tau-decays. *Phys. Lett.*, B650:179–184, 2007.

[37] A. A. Almasy, K. Schilcher, and H. Spiesberger. Determination of QCD condensates from tau-decay data. *Eur. Phys. J.*, C55:237–248, 2008.

[38] Martin Gonzalez-Alonso, Antonio Pich, and Joaquim Prades. Determination of the Chiral Couplings $L_{10}$ and $C_{87}$ from Semileptonic Tau Decays. *Phys. Rev.*, D78:116012, 2008.

[39] Martin Gonzalez-Alonso, Antonio Pich, and Joaquim Prades. Violation of Quark-Hadron Duality and Spectral Chiral Moments in QCD. *Phys. Rev.*, D81:074007, 2010.

[40] Martin Gonzalez-Alonso, Antonio Pich, and Joaquim Prades. Pinched weights and Duality Violation in QCD Sum Rules: a critical analysis. *Phys. Rev.*, D82:014019, 2010.

[41] Diogo Boito, Maarten Golterman, Matthias Jamin, Kim Maltman, and Santiago Peris. Low-energy constants and condensates from the $\tau$ hadronic spectral functions. *Phys. Rev.*, D87(9):094008, 2013.

[42] C. A. Dominguez, L. A. Hernandez, K. Schilcher, and H. Spiesberger. Chiral sum rules and vacuum condensates from tau-lepton decay data. *JHEP*, 03:053, 2015.

[43] Diogo Boito, Anthony Francis, Maarten Golterman, Renwick Hudspith, Randy Lewis, Kim Maltman, and Santiago Peris. Low-energy constants and condensates from ALEPH hadronic $\tau$ decay data. *Phys. Rev.*, D92(11):114501, 2015.

[44] S. Schael et al. Branching ratios and spectral functions of tau decays: Final ALEPH measurements and physics implications. *Phys. Rept.*, 421:191–284, 2005.

[45] Martin González-Alonso, Antonio Pich, and Antonio Rodríguez-Sánchez. Updated determination of chiral couplings and vacuum condensates from hadronic $\tau$ decay data. *Phys. Rev.*, D94(1):014017, 2016.

[46] Michel Davier, Andreas Höcker, Bogdan Malaescu, Chang-Zheng Yuan, and Zhiqing Zhang. Update of the ALEPH non-strange spectral functions from hadronic $\tau$ decays. *Eur. Phys. J.*, C74(3):2803, 2014.

[47] D. M. Asner et al. Hadronic structure in the decay $\tau \to \nu_\tau \pi^- \pi^0 \pi^0$ and the sign of the tau-neutrino helicity. *Phys. Rev.*, D61:012002, 2000.

[48] E. Gamiz, M. Jamin, A. Pich, J. Prades, and F. Schwab. Determination of $m_s$ and $|V_{us}|$ from hadronic tau decays. *JHEP*, 01:060, 2003.

[49] P. A. Boyle, L. Del Debbio, N. Garron, R. J. Hudspith, E. Kerrane, K. Maltman, and J. M. Zanotti. Some continuum physics results from the lattice V-A correlator. *PoS*, LATTICE2012:156, 2012.

[50] Stephan Narison. Improved light quark masses from pseudoscalar sum rules. *Phys. Lett.*, B738:346–360, 2014.

[51] D. R. Boito, O. Cata, M. Golterman, M. Jamin, K. Maltman, J. Osborne, and S. Peris. Duality violations in tau hadronic spectral moments. *Nucl. Phys. Proc. Suppl.*, 218:104–109, 2011.

[52] E. Braaten, Stephan Narison, and A. Pich. QCD analysis of the tau hadronic width. *Nucl. Phys.*, B373:581–612, 1992.

[53] Vincenzo Cirigliano, John F. Donoghue, Eugene Golowich, and Kim Maltman. Determination of $\langle(\pi\pi)_{I=2}|Q_{7,8}|K_0\rangle$ in the chiral limit. *Phys. Lett.*, B522:245–256, 2001.

[54] F. Le Diberder and A. Pich. The perturbative QCD prediction to R(tau) revisited. *Phys. Lett.*, B286:147–152, 1992.

[55] Boris Chibisov, R. David Dikeman, Mikhail A. Shifman, and N. Uraltsev. Operator product expansion, heavy quarks, QCD duality and its violations. *Int. J. Mod. Phys.*, A12:2075–2133, 1997.

[56] Mikhail A. Shifman. Quark hadron duality. In *At the frontier of particle physics. Handbook of QCD. Vol. 1-3*, pages 1447–1494, Singapore, 2001. World Scientific, World Scientific. [3,1447(2000)].

[57] B. Blok, Mikhail A. Shifman, and Da-Xin Zhang. An Illustrative example of how quark hadron duality might work. *Phys. Rev.*, D57:2691–2700, 1998. [Erratum: Phys. Rev.D59,019901(1999)].

[58] Mikhail A. Shifman. Snapshots of hadrons or the story of how the vacuum medium determines the properties of the classical mesons which are produced, live and die in the QCD vacuum. *Prog. Theor. Phys. Suppl.*, 131:1–71, 1998.

[59] O. Cata, M. Golterman, and S. Peris. Duality violations and spectral sum rules. *JHEP*, 08:076, 2005.

[60] Oscar Cata, Maarten Golterman, and Santiago Peris. Possible duality violations in tau decay and their impact on the determination of $\alpha_s$. *Phys. Rev.*, D79:053002, 2009.

[61] Steven Weinberg. Precise relations between the spectra of vector and axial vector mesons. *Phys. Rev. Lett.*, 18:507–509, 1967.

[62] Claude W. Bernard, Anthony Duncan, John LoSecco, and Steven Weinberg. Exact Spectral Function Sum Rules. *Phys. Rev.*, D12:792, 1975.

[63] Steven Weinberg. Phenomenological Lagrangians. *Physica*, A96:327–340, 1979.

[64] J. Gasser and H. Leutwyler. Low-Energy Expansion of Meson Form-Factors. *Nucl. Phys.*, B250:517–538, 1985.

[65] G. Ecker. Chiral perturbation theory. *Prog. Part. Nucl. Phys.*, 35:1–80, 1995.

[66] Gabriel Amoros, Johan Bijnens, and P. Talavera. Two point functions at two loops in three flavor chiral perturbation theory. *Nucl. Phys.*, B568:319–363, 2000.

[67] C. A. Dominguez, L. A. Hernandez, K. Schilcher, and H. Spiesberger. Tau-decay hadronic spectral functions: probing quark-hadron duality. 2016.

[68] T. Das, G. S. Guralnik, V. S. Mathur, F. E. Low, and J. E. Young. Electromagnetic mass difference of pions. *Phys. Rev. Lett.*, 18:759–761, 1967.

[69] Sinya Aoki et al. Review of lattice results concerning low-energy particle physics. *Eur. Phys. J.*, C74:2890, 2014.

[70] K. Ackerstaff et al. Measurement of the strong coupling constant alpha(s) and the vector and axial vector spectral functions in hadronic tau decays. *Eur. Phys. J.*, C7:571–593, 1999.

[71] Samuel Friot, David Greynat, and Eduardo de Rafael. Chiral condensates, $Q_7$ and $Q_8$ matrix elements and large-$N_c$ QCD. *JHEP*, 10:043, 2004.

[72] Pere Masjuan and Santiago Peris. A Rational approach to resonance saturation in large-N(c) QCD. *JHEP*, 05:040, 2007.

[73] A. Pich, I. Rosell, and J. J. Sanz-Cillero. Form-factors and current correlators: Chiral couplings $L^r_{10}(\mu)$ and $C^r_{87}(\mu)$ at NLO in $1/N_c$. *JHEP*, 07:014, 2008.

[74] Vincenzo Cirigliano, John F. Donoghue, Eugene Golowich, and Kim Maltman. Improved determination of the electroweak penguin contribution to epsilon-prime / epsilon in the chiral limit. *Phys. Lett.*, B555:71–82, 2003.

[75] R. Barate et al. Measurement of the spectral functions of axial - vector hadronic tau decays and determination of $\alpha_s(M^2_\tau)$. *Eur. Phys. J.*, C4:409–431, 1998.

[76] B. L. Ioffe and K. N. Zyablyuk. The V - A sum rules and the operator product expansion in complex $q^2$ - plane from tau decay data. *Nucl. Phys.*, A687:437–453, 2001.

[77] B. V. Geshkenbein, B. L. Ioffe, and K. N. Zyablyuk. The Check of QCD based on the tau - decay data analysis in the complex $q^2$ - plane. *Phys. Rev.*, D64:093009, 2001.

[78] K. N. Zyablyuk. V-A sum rules with D=10 operators. *Eur. Phys. J.*, C38:215–223, 2004.

[79] Joan Rojo and Jose I. Latorre. Neural network parametrization of spectral functions from hadronic tau decays and determination of QCD vacuum condensates. *JHEP*, 01:055, 2004.

[80] Johan Bijnens and P. Talavera. Pion and kaon electromagnetic form-factors. *JHEP*, 03:046, 2002.

[81] Stephan Durr and Joachim Kambor. Two point function of strangeness carrying vector currents in two loop chiral perturbation theory. *Phys. Rev.*, D61:114025, 2000.

[82] Matthias Jamin, Jose Antonio Oller, and Antonio Pich. Order $p^6$ chiral couplings from the scalar $K\pi$ form-factor. *JHEP*, 02:047, 2004.

[83] Karol Kampf and Bachir Moussallam. Tests of the naturalness of the coupling constants in ChPT at order $p^6$. *Eur. Phys. J.*, C47:723–736, 2006.

[84] Maarten Golterman, Kim Maltman, and Santiago Peris. NNLO low-energy constants from flavor-breaking chiral sum rules based on hadronic $\tau$-decay data. *Phys. Rev.*, D89(5):054036, 2014.

[85] Rene Unterdorfer and Hannes Pichl. On the Radiative Pion Decay. *Eur. Phys. J.*, C55:273–283, 2008.

[86] P. A. Boyle, L. Del Debbio, N. Garron, R. J. Hudspith, E. Kerrane, K. Maltman, and J. M. Zanotti. Combined NNLO lattice-continuum determination of $L^r_{10}$. *Phys. Rev.*, D89(9):094510, 2014.

[87] R. J. Dowdall, C. T. H. Davies, G. P. Lepage, and C. McNeile. Vus from pi and K decay constants in full lattice QCD with physical u, d, s and c quarks. *Phys. Rev.*, D88:074504, 2013.

[88] Marc Knecht and Andreas Nyffeler. Resonance estimates of $O(p^6)$ low-energy constants and QCD short distance constraints. *Eur. Phys. J.*, C21:659–678, 2001.

[89] V. Cirigliano, G. Ecker, M. Eidemuller, Roland Kaiser, A. Pich, and J. Portoles. Towards a consistent estimate of the chiral low-energy constants. *Nucl. Phys.*, B753:139–177, 2006.

[90] V. Cirigliano, G. Ecker, M. Eidemuller, A. Pich, and J. Portoles. The $<$ VAP $>$ Green function in the resonance region. *Phys. Lett.*, B596:96–106, 2004.

[91] A. Pich. Colorless mesons in a polychromatic world. In *Phenomenology of large-$N_c$ QCD. Proceedings, Tempe, USA, January 9-11, 2002*, pages 239–258, 2002.

[92] Johan Bijnens and Gerhard Ecker. Mesonic low-energy constants. *Ann. Rev. Nucl. Part. Sci.*, 64:149–174, 2014.

[93] Pere Masjuan and Santiago Peris. A Rational approximation to $<$ VV-AA $>$ and its O($p^6$) low-energy constant. *Phys. Lett.*, B663:61–65, 2008.

[94] G. Ecker, J. Gasser, H. Leutwyler, A. Pich, and E. de Rafael. Chiral Lagrangians for Massive Spin 1 Fields. *Phys. Lett.*, B223:425–432, 1989.

[95] G. Ecker, J. Gasser, A. Pich, and E. de Rafael. The Role of Resonances in Chiral Perturbation Theory. *Nucl. Phys.*, B321:311–342, 1989.

[96] Peter A. Boyle, Luigi Del Debbio, Jan Wennekers, and James M. Zanotti. The S Parameter in QCD from Domain Wall Fermions. *Phys. Rev.*, D81:014504, 2010.

[97] E. Shintani, S. Aoki, H. Fukaya, S. Hashimoto, T. Kaneko, H. Matsufuru, T. Onogi, and N. Yamada. S-parameter and pseudo-Nambu-Goldstone boson mass from lattice QCD. *Phys. Rev. Lett.*, 101:242001, 2008.

[98] P. A. Baikov, K. G. Chetyrkin, and Johann H. Kuhn. Order $\alpha^4(s)$ QCD Corrections to Z and tau Decays. *Phys. Rev. Lett.*, 101:012002, 2008.

[99] A. A. Pivovarov. Renormalization group analysis of the tau lepton decay within QCD. *Z. Phys.*, C53:461–464, 1992. [Yad. Fiz.54,1114(1991)].

[100] Antoni Pich. $\alpha_s$ from hadronic $\tau$ decays. In *Proceedings, High-Precision $\alpha_s$ Measurements from LHC to FCC-ee: Geneva, Switzerland, October 2-13, 2015*, pages 37–40, 2015.

[101] David d'Enterria and Peter Z. Skands, editors. *Proceedings, High-Precision $\alpha_s$ Measurements from LHC to FCC-ee*, Geneva, 2015. CERN, CERN.

[102] K. A. Olive et al. Review of Particle Physics. *Chin. Phys.*, C38:090001, 2014.

[103] Antonio Pich. Review of $\alpha_s$ determinations. 2013. [PoSConfinementX,022(2012)].

[104] Alexandre Deur, Stanley J. Brodsky, and Guy F. de Teramond. The QCD Running Coupling. *Prog. Part. Nucl. Phys.*, 90:1–74, 2016.

[105] David J. Gross and Frank Wilczek. Ultraviolet Behavior of Nonabelian Gauge Theories. *Phys. Rev. Lett.*, 30:1343–1346, 1973. [,271(1973)].

[106] H. David Politzer. Reliable Perturbative Results for Strong Interactions? *Phys. Rev. Lett.*, 30:1346–1349, 1973. [,274(1973)].

[107] Sidney R. Coleman and David J. Gross. Price of asymptotic freedom. *Phys. Rev. Lett.*, 31:851–854, 1973.

[108] Antonio Pich. Tau Decay Determination of the QCD Coupling. In *Workshop on Precision Measurements of alphas*, 2011.

[109] M. Davier, S. Descotes-Genon, Andreas Hocker, B. Malaescu, and Z. Zhang. The Determination of $\alpha_s$ from Tau Decays Revisited. *Eur. Phys. J.*, C56:305–322, 2008.

[110] Michel Davier, Andreas Hocker, and Zhiqing Zhang. The Physics of hadronic tau decays. *Rev. Mod. Phys.*, 78:1043–1109, 2006.

[111] D. Buskulic et al. Measurement of the strong coupling constant using tau decays. *Phys. Lett.*, B307:209–220, 1993.

[112] T. Coan et al. Measurement of alpha-s from tau decays. *Phys. Lett.*, B356:580–588, 1995.

[113] Diogo Boito, Oscar Cata, Maarten Golterman, Matthias Jamin, Kim Maltman, James Osborne, and Santiago Peris. A new determination of $\alpha_s$ from hadronic $\tau$ decays. *Phys. Rev.*, D84:113006, 2011.

[114] Diogo Boito, Maarten Golterman, Matthias Jamin, Andisheh Mahdavi, Kim Maltman, James Osborne, and Santiago Peris. An Updated determination of $\alpha_s$ from $\tau$ decays. *Phys. Rev.*, D85:093015, 2012.

[115] Diogo Boito, Maarten Golterman, Kim Maltman, James Osborne, and Santiago Peris. Strong coupling from the revised ALEPH data for hadronic $\tau$ decays. *Phys. Rev.*, D91(3):034003, 2015.

[116] Oscar Cata, Maarten Golterman, and Santi Peris. Unraveling duality violations in hadronic tau decays. *Phys. Rev.*, D77:093006, 2008.

[117] Antonio Pich and Antonio Rodríguez-Sánchez. Determination of the QCD coupling from ALEPH $\tau$ decay data. *Phys. Rev.*, D94(3):034027, 2016.

[118] E. C. Poggio, Helen R. Quinn, and Steven Weinberg. Smearing the Quark Model. *Phys. Rev.*, D13:1958, 1976.

[119] F. Le Diberder and A. Pich. Testing QCD with tau decays. *Phys. Lett.*, B289:165–175, 1992.

[120] Diogo Boito, Maarten Golterman, Kim Maltman, and Santiago Peris. Strong coupling from hadronic $\tau$ decays: A critical appraisal. *Phys. Rev.*, D95(3):034024, 2017.

[121] Stephen L. Adler. Some Simple Vacuum Polarization Phenomenology: $e^+e^- \to$ Hadrons: The $\mu$ - Mesic Atom x-Ray Discrepancy and ${g_\mu}^{-2}$. *Phys. Rev.*, D10:3714, 1974. [,445(1974)].

[122] S. G. Gorishnii, A. L. Kataev, and S. A. Larin. The $O(\alpha_s^3)$-corrections to $\sigma_{tot}(e^+e^- \to hadrons)$ and $\Gamma(\tau^- \to \nu_\tau + hadrons)$ in QCD. *Phys. Lett.*, B259:144–150, 1991.

[123] Levan R. Surguladze and Mark A. Samuel. Total hadronic cross-section in e+ e- annihilation at the four loop level of perturbative QCD. *Phys. Rev. Lett.*, 66:560–563, 1991. [Erratum: Phys. Rev. Lett.66,2416(1991)].

[124] K. G. Chetyrkin, A. L. Kataev, and F. V. Tkachov. Higher Order Corrections to Sigma-t (e+ e- —> Hadrons) in Quantum Chromodynamics. *Phys. Lett.*, 85B:277–279, 1979.

[125] Michael Dine and J. R. Sapirstein. Higher Order QCD Corrections in e+ e- Annihilation. *Phys. Rev. Lett.*, 43:668, 1979.

[126] William Celmaster and Richard J. Gonsalves. An Analytic Calculation of Higher Order Quantum Chromodynamic Corrections in e+ e- Annihilation. *Phys. Rev. Lett.*, 44:560, 1980.

[127] Antonio Pich and Joaquim Prades. Strange quark mass determination from Cabibbo suppressed tau decays. *JHEP*, 10:004, 1999.

[128] Antonio Pich. $\alpha_s$ Determination from Tau Decays: Theoretical Status. *Acta Phys. Polon. Supp.*, 3:165–170, 2010.

[129] Patricia Ball, M. Beneke, and Vladimir M. Braun. Resummation of (beta0 alpha-s)**n corrections in QCD: Techniques and applications to the tau hadronic width and the heavy quark pole mass. *Nucl. Phys.*, B452:563–625, 1995.

[130] Matthias Neubert. QCD analysis of hadronic tau decays revisited. *Nucl. Phys.*, B463:511–546, 1996.

[131] G Altarelli, P. Nason, and G. Ridolfi. A Study of ultraviolet renormalon ambiguities in the determination of alpha-s from tau decay. *Z. Phys.*, C68:257–268, 1995.

[132] Martin Beneke and Matthias Jamin. $\alpha_s$ and the tau hadronic width: fixed-order, contour-improved and higher-order perturbation theory. *JHEP*, 09:044, 2008.

[133] Martin Beneke, Diogo Boito, and Matthias Jamin. Perturbative expansion of tau hadronic spectral function moments and $\alpha_s$ extractions. *JHEP*, 01:125, 2013.

[134] S. Descotes-Genon and B. Malaescu. A Note on Renormalon Models for the Determination of $\alpha_s(M_\tau)$. 2010.

[135] Matthias Jamin. Contour-improved versus fixed-order perturbation theory in hadronic tau decays. *JHEP*, 09:058, 2005.

[136] Irinel Caprini and Jan Fischer. $\alpha_s$ from tau decays: Contour-improved versus fixed-order summation in a new QCD perturbation expansion. *Eur. Phys. J.*, C64:35–45, 2009.

[137] Irinel Caprini and Jan Fischer. Expansion functions in perturbative QCD and the determination of $\alpha_s(M_\tau^2)$. *Phys. Rev.*, D84:054019, 2011.

[138] Gauhar Abbas, B. Ananthanarayan, Irinel Caprini, and Jan Fischer. Perturbative expansion of the QCD Adler function improved by renormalization-group summation and analytic continuation in the Borel plane. *Phys. Rev.*, D87(1):014008, 2013.

[139] Gauhar Abbas, B. Ananthanarayan, and Irinel Caprini. Determination of $\alpha_s(M_\tau^2)$ from Improved Fixed Order Perturbation Theory. *Phys. Rev.*, D85:094018, 2012.

[140] Gauhar Abbas, B. Ananthanarayan, Irinel Caprini, and Jan Fischer. Expansions of $\tau$ hadronic spectral function moments in a nonpower QCD perturbation theory with tamed large order behavior. *Phys. Rev.*, D88(3):034026, 2013.

[141] Murray Gell-Mann, R. J. Oakes, and B. Renner. Behavior of current divergences under SU(3) x SU(3). *Phys. Rev.*, 175:2195–2199, 1968.

[142] Stephan Narison. Withdrawn: QCD as a theory of hadrons from partons to confinement. 2002.

[143] B. Holdom. Massless QCD has vacuum energy? *New J. Phys.*, 10:053040, 2008.

[144] Stephan Narison. Power corrections to $\alpha_s(M_\tau)$,$|V_{us}|$ and anti-$m_s$. *Phys. Lett.*, B673:30–36, 2009.

[145] Stephan Narison and A. Pich. Semiinclusive tau decays involving the vector or axial - vector hadronic currents. *Phys. Lett.*, B304:359–365, 1993.

[146] Maria Girone and Matthias Neubert. Test of the running of $\alpha_s$ in tau decays. *Phys. Rev. Lett.*, 76:3061–3064, 1996.

[147] Tomasz Korzec. Determination of the Strong Coupling Constant by the ALPHA Collaboration. *EPJ Web Conf.*, 175:01018, 2018.

[148] Mattia Bruno, Mattia Dalla Brida, Patrick Fritzsch, Tomasz Korzec, Alberto Ramos, Stefan Schaefer, Hubert Simma, Stefan Sint, and Rainer Sommer. QCD Coupling from a Nonperturbative Determination of the Three-Flavor $\Lambda$ Parameter. *Phys. Rev. Lett.*, 119(10):102001, 2017.

[149] S. Alekhin, J. Blümlein, S. Moch, and R. Placakyte. Parton distribution functions, $\alpha_s$, and heavy-quark masses for LHC Run II. *Phys. Rev.*, D96(1):014011, 2017.

[150] André H. Hoang, Daniel W. Kolodrubetz, Vicent Mateu, and Iain W. Stewart. Precise determination of $\alpha_s$ from the $C$-parameter distribution. *Phys. Rev.*, D91(9):094018, 2015.

[151] John F. Donoghue and Eugene Golowich. Dispersive calculation of $B_7^{3/2}$ and $B_8^{3/2}$ in the chiral limit. *Phys. Lett.*, B478:172–184, 2000.

[152] Diogo Boito, Irinel Caprini, Maarten Golterman, Kim Maltman, and Santiago Peris. Hyperasymptotics and quark-hadron duality violations in QCD. *Phys. Rev.*, D97(5):054007, 2018.

[153] Antonio Pich and Antonio Rodríguez-Sánchez. Relations between $K \to \pi\pi$ matrix elements and vacuum condensates. *In preparation*, 2018.

[154] Bachir Moussallam. Reanalysis of the Das et al. sum rule and application to chiral $O(p^4)$ parameters. *Eur. Phys. J.*, C6:681–691, 1999.

[155] Philippe Boucaud, Vicent Gimenez, C. J. David Lin, Vittorio Lubicz, Guido Martinelli, Mauro Papinutto, and Chris T. Sachrajda. An Exploratory lattice study of Delta I = 3/2 $K \to \pi\pi$ decays at next-to-leading order in the chiral expansion. *Nucl. Phys.*, B721:175–211, 2005.

[156] T. Blum et al. Lattice determination of the $K \to (\pi\pi)_{I=2}$ Decay Amplitude $A_2$. *Phys. Rev.*, D86:074513, 2012.

[157] Vincenzo Cirigliano, Adam Falkowski, Martín González-Alonso, and Antonio Rodríguez-Sánchez. Hadronic tau decays as New Physics probes in the LHC era. *In preparation*, 2018.

[158] Vincenzo Cirigliano, James Jenkins, and Martin Gonzalez-Alonso. Semileptonic decays of light quarks beyond the Standard Model. *Nucl. Phys.*, B830:95–115, 2010.

[159] Tanmoy Bhattacharya, Vincenzo Cirigliano, Saul D. Cohen, Alberto Filipuzzi, Martin Gonzalez-Alonso, Michael L. Graesser, Rajan Gupta, and Huey-Wen Lin. Probing Novel Scalar and Tensor Interactions from (Ultra)Cold Neutrons to the LHC. *Phys. Rev.*, D85:054512, 2012.

[160] E. A. Garcés, M. Hernández Villanueva, G. López Castro, and P. Roig. Effective-field theory analysis of the $\tau^- \to \eta^{(\prime)}\pi^-\nu_\tau$ decays. *JHEP*, 12:027, 2017.

[161] Veronique Bernard, Micaela Oertel, Emilie Passemar, and Jan Stern. Tests of non-standard electroweak couplings of right-handed quarks. *JHEP*, 01:015, 2008.

[162] Adam Falkowski, Martín González-Alonso, and Kin Mimouni. Compilation of low-energy constraints on 4-fermion operators in the SMEFT. *JHEP*, 08:123, 2017.

[163] B. Grzadkowski, M. Iskrzynski, M. Misiak, and J. Rosiek. Dimension-Six Terms in the Standard Model Lagrangian. *JHEP*, 10:085, 2010.

[164] Martín González-Alonso, Jorge Martin Camalich, and Kin Mimouni. Renormalization-group evolution of new physics contributions to (semi)leptonic meson decays. *Phys. Lett.*, B772:777–785, 2017.

[165] J. P. Lees et al. Study of the process $e^+e^- \to \pi^+\pi^-\eta$ using initial state radiation. *Phys. Rev.*, D97:052007, 2018.

[166] Martín González-Alonso and Jorge Martin Camalich. Global Effective-Field-Theory analysis of New-Physics effects in (semi)leptonic kaon decays. *JHEP*, 12:052, 2016.

[167] Roger Decker and Markus Finkemeier. Short and long distance effects in the decay tau —> pi tau-neutrino (gamma). *Nucl. Phys.*, B438:17–53, 1995.

[168] Vincenzo Cirigliano and Ignasi Rosell. Two-loop effective theory analysis of $\pi(K) \to e\bar{\nu}_e[\gamma]$ branching ratios. *Phys. Rev. Lett.*, 99:231801, 2007.

[169] Rafel Escribano, Sergi Gonzalez-Solis, and Pablo Roig. Predictions on the second-class current decays $\tau^- \to \pi^-\eta^{(\prime)}\nu_\tau$. *Phys. Rev.*, D94(3):034008, 2016.

[170] V. Cirigliano, G. Ecker, and H. Neufeld. Radiative tau decay and the magnetic moment of the muon. *JHEP*, 08:002, 2002.

[171] Vincenzo Cirigliano, Andreas Crivellin, and Martin Hoferichter. No-go theorem for nonstandard explanations of the $\tau \to K_S\pi\nu_\tau$ CP asymmetry. *Phys. Rev. Lett.*, 120(14):141803, 2018.

[172] V. Mateu and J. Portoles. Form-factors in radiative pion decay. *Eur. Phys. J.*, C52:325–338, 2007.

[173] Oscar Cata and Vicent Mateu. Novel patterns for vector mesons from the large-N(c) limit. *Phys. Rev.*, D77:116009, 2008.

[174] I. Baum, V. Lubicz, G. Martinelli, L. Orifici, and S. Simula. Matrix elements of the electromagnetic operator between kaon and pion states. *Phys. Rev.*, D84:074503, 2011.

[175] J. A. Miranda and P. Roig. Effective-field theory analysis of the $\tau^- \to \pi^-\pi^0\nu_\tau$ decays. 2018.

[176] Michel Davier, Andreas Hoecker, Bogdan Malaescu, and Zhiqing Zhang. Reevaluation of the hadronic vacuum polarisation contributions to the Standard Model predictions of the muon $g-2$ and $\alpha(m_Z^2)$ using newest hadronic cross-section data. *Eur. Phys. J.*, C77(12):827, 2017.

[177] N. S. Craigie and J. Stern. Sum Rules for the Spontaneous Chiral Symmetry Breaking Parameters of QCD. *Phys. Rev.*, D26:2430, 1982.

[178] Matthias Jamin and Vicent Mateu. OPE-R(chi)T matching at order alpha(s): Hard gluonic corrections to three-point Green functions. *JHEP*, 04:040, 2008.

[179] S. Aoki et al. Review of lattice results concerning low-energy particle physics. *Eur. Phys. J.*, C77(2):112, 2017.

[180] Matthias Jamin. Flavor symmetry breaking of the quark condensate and chiral corrections to the Gell-Mann-Oakes-Renner relation. *Phys. Lett.*, B538:71–76, 2002.

[181] Y. Amhis et al. Averages of $b$-hadron, $c$-hadron, and $\tau$-lepton properties as of summer 2016. *Eur. Phys. J.*, C77(12):895, 2017.

[182] M. González-Alonso, O. Naviliat-Cuncic, and N. Severijns. New physics searches in nuclear and neutron $\beta$ decay. 2018.

[183] Morad Aaboud et al. Search for High-Mass Resonances Decaying to $\tau\nu$ in pp Collisions at $\sqrt{s}$=13 TeV with the ATLAS Detector. *Phys. Rev. Lett.*, 120(16):161802, 2018.

[184] J. Alwall, R. Frederix, S. Frixione, V. Hirschi, F. Maltoni, O. Mattelaer, H. S. Shao, T. Stelzer, P. Torrielli, and M. Zaro. The automated computation of tree-level and next-to-leading order differential cross sections, and their matching to parton shower simulations. *JHEP*, 07:079, 2014.

[185] Torbjörn Sjöstrand, Stefan Ask, Jesper R. Christiansen, Richard Corke, Nishita Desai, Philip Ilten, Stephen Mrenna, Stefan Prestel, Christine O. Rasmussen, and Peter Z. Skands. An Introduction to PYTHIA 8.2. *Comput. Phys. Commun.*, 191:159–177, 2015.

[186] J. de Favereau, C. Delaere, P. Demin, A. Giammanco, V. Lemaître, A. Mertens, and M. Selvaggi. DELPHES 3, A modular framework for fast simulation of a generic collider experiment. *JHEP*, 02:057, 2014.

[187] Admir Greljo and David Marzocca. High-$p_T$ dilepton tails and flavor physics. *Eur. Phys. J.*, C77(8):548, 2017.

[188] C. Patrignani et al. Review of Particle Physics. *Chin. Phys.*, C40(10):100001, 2016.

[189] Alberto Filipuzzi, Jorge Portoles, and Martin Gonzalez-Alonso. $U(2)^5$ flavor symmetry and lepton universality violation in $W \to \tau\nu_\tau$. *Phys. Rev.*, D85:116010, 2012.

[190] Elvira Gamiz, Matthias Jamin, Antonio Pich, Joaquim Prades, and Felix Schwab. $V_{us}$ and $m_s$ from hadronic tau decays. *Phys. Rev. Lett.*, 94:011803, 2005.

[191] Elvira Gamiz, Matthias Jamin, Antonio Pich, Joaquim Prades, and Felix Schwab. Theoretical progress on the $V_{us}$ determination from tau decays. *PoS*, KAON:008, 2008.

[192] Elvira Gamiz. $|V_{us}|$ from hadronic $\tau$ decays. In *7th International Workshop on the CKM Unitarity Triangle (CKM 2012) Cincinnati, Ohio, USA, September 28-October 2, 2012*, 2013.

[193] Renwick J. Hudspith, Randy Lewis, Kim Maltman, and James Zanotti. A resolution of the inclusive flavor-breaking $\tau$ $|V_{us}|$ puzzle. *Phys. Lett.*, B781:206–212, 2018.

[194] Jens Erler. Electroweak radiative corrections to semileptonic tau decays. *Rev. Mex. Fis.*, 50:200–202, 2004.

[195] Gavin P. Salam. The strong coupling: a theoretical perspective. 2017.

[196] Marc Knecht, Santiago Peris, and Eduardo de Rafael. A critical reassessment of $Q_7$ and $Q_8$ matrix elements. *Phys. Lett.*, B508:117–126, 2001.

[197] Ken Kawarabayashi and Mahiko Suzuki. Partially conserved axial vector current and the decays of vector mesons. *Phys. Rev. Lett.*, 16:255, 1966.

[198] J. F. Donoghue, E. Golowich, and Barry R. Holstein. Dynamics of the standard model. *Camb. Monogr. Part. Phys. Nucl. Phys. Cosmol.*, 2:1–540, 1992. [Camb. Monogr. Part. Phys. Nucl. Phys. Cosmol.35(2014)].

[199] J. J. de Swart. The Octet model and its Clebsch-Gordan coefficients. *Rev. Mod. Phys.*, 35:916–939, 1963. [Erratum: Rev. Mod. Phys.37,326(1965)].

[200] Francisco Guerrero and Antonio Pich. Effective field theory description of the pion form-factor. *Phys. Lett.*, B412:382–388, 1997.

[201] O. Cata and V. Mateu. Chiral perturbation theory with tensor sources. *JHEP*, 09:078, 2007.